2021-06

Mathematical models for the infectiology and cost-effectiveness of the control strategies for brucellosis

Nyerere, Nkuba

NM-AIST

https://doi.org/10.58694/20.500.12479/1371

MATHEMATICAL MODELS FOR THE INFECTIOLOGY AND COST-EFFECTIVENESS OF THE CONTROL STRATEGIES FOR BRUCELLOSIS

Nkuba Nyerere

A Thesis Submitted in Partial Fulfillment of the Requirements for the Degree of Doctor of Philosophy in Mathematical and Computer Sciences and Engineering of the Nelson Mandela African Institution of Science and Technology

Arusha, Tanzania

June, 2021

ABSTRACT

Brucellosis is a contagious zoonotic infection caused by Gram-negative bacteria of family *Brucellaceae* and genus *Brucella* that affects humans and animals. The disease is of economic significance, veterinary interest and a public health concern in most developing countries. Direct interaction among vulnerable and infectious animals or their tainted products represent the two substantial pathways for the infection conveyance. This study aimed at developing and analyzing deterministic mathematical models for the infectiology and cost-effectiveness of Brucellosis control measures. The control mechanisms that were taken into consideration are vaccination of livestock, culling of seropositive animals by slaughtering, personal protection, and proper environmental hygiene and sanitation. Both analytical and numerical simulations are presented. Sensitivity analysis of the effective reproductive number revealed that the rates of livestock mortality, recruitment, livestock to livestock transmission, vaccination and disease-driven culling are the most sensitive parameters and should be targeted in designing of the control strategies for the disease. Optimal control and cost-effectiveness analysis of the model disclosed that merging of personal protection, environmental hygiene and sanitation, progressive slaughtering of seropositive livestock, and livestock vaccination significantly reduces infection spread in both humans and livestock at a lower cost. Additionally, seasonal weather variations have great impact on Brucellosis transmission dynamics in human, livestock and wild animals. Therefore, for the disease to be controlled or eradicated, this study recommends the timely implementation of control measures pursuant to fluctuations in disease transmission.

DECLARATION

I, **Nkuba Nyerere** do hereby declare to the Senate of Nelson Mandela African Institution of Science and Technology that this thesis is my original work and to the best of my knowledge has not been submitted or presented to any other institution for similar or different award.

Nkuba Nyerere Mnyerere. 20/07/2021

Name and signature of the candidate **Date**

The above declaration is confirmed

Prof. Livingstone L. S. Luboobi 21st June 2021

Name and signature of supervisor 1 **Date**

Dr. Saul C. Mpeshe 21st June 2021

Name and signature of supervisor 2 **Date**

Prof. Gabriel M. Shirima 20/07/2021

Name and signature of supervisor 3 **Date**

COPYRIGHT

CERTIFICATION

The undersigned certify that they have read and hereby recommend for acceptance by the Nelson Mandela African Institution of Science and Technology a research report entitled: ***Mathematical Models for the Infectiology and Cost-Effectiveness of the Control Strategies for Brucellosis***, in partial fulfillment of the requirements for the degree of Doctor of Philosophy in Mathematical and Computer Sciences and Engineering of the Nelson Mandela African Institution of Science and Technology.

Prof. Livingstone L. S. Luboobi — 21st June 2021

Name and signature of supervisor 1 — **Date**

Dr. Saul C. Mpeshe — 21st June 2021

Name and signature of supervisor 2 — **Date**

Prof. Gabriel M. Shirima — 20/07/2021

Name and signature of supervisor 3 — **Date**

ACKNOWLEDGMENTS

I would like to thank my refuge, strength, an ever-present help in trouble, Almighty God for His love, care, protection, kindness, counsel and loving eye on me during my studies. Whenever hard pushed, I wept to my creator; He drove me into a capacious place. God is the source of my knowledge, skills, wisdom, strength, faith and health that enabled me to complete this study successfully.

Special and heartfelt appreciation goes to my inspirational supervisors; Prof. Livingstone Serwadda Luboobi, Dr. Saul Chilongola Mpeshe and Prof. Gabriel Mkilema Shirima for their tireless efforts, encouragements, and mentorship that turned my mind to this work and made timely progresses. May the Almighty God bless abundantly.

I desire to manifest my deep thankfulness to the African Development Bank for sponsoring my studies, and Sokoine University of Agriculture for bestowing me with a study leave to accomplish this study. My sincerest gratitude to Mr. Julius Lenguyana, Ms. Victoria Ndossi, Mr. Japhet Laizer and Mr. Humphrey Robert; the NMI-AIST project team for their spontaneous outpouring of support and cooperation.

I also register my special appreciation to my parents Joseph Mbeho and Elizabeth Bukwimba, my beloved sisters Sabina and Abiana, brothers Malongo and Nsesso for their prayers.

Special thanks to Becky Aloo, a colleague and special friend from the School of Life Sciences who despite her tight schedule and the demands of PhD life and family issues, still made time to review my write-ups and help me produce better drafts. I also thank Prof. Abba Gumel, Prof. Farai Nyabadza, Prof. Edward Lungu and Prof. Julius Tumwiine for their invaluable support, mentorship and suggestions that helped me to improve my work. Since it is not possible to mention everybody who has contributed to this work, allow me express my heartfelt appreciation to everybody who stretched mind or hand towards the accomplishment of this study.

DEDICATION

This research work is dedicated to my loving and caring wife, Sophia, my son Daniel and my daughters Dorcas, Elizabeth and Edith who has been constantly a source of encouragement and support in the midst of my graduate study difficulties. I am very obliged and proud of them. This study is also dedicated to my grandfather, Marko Bukwimba Nginya, who loves me unconditionally and whose proverbs inspired me to work hard for things I yearn to accomplish.

TABLE OF CONTENTS

LIST OF ABBREVIATIONS

CDC	Centers for Disease Control and Prevention.
CFSPH	Center for Food Security and Public Health.
FAO	Food and Agriculture Organization
ICER	Incremental Cost-Effectiveness Ratio.
OIE	World Organization for Animal Health (Office International des Epizooties).
SEI	Susceptible-Exposed-Infectious.
SEIR	Susceptible-Exposed-Infectious-Recovered.
SEIRS	Susceptible-Exposed-Infectious-Recovered-Susceptible.
SEIRV	Susceptible-Exposed-Infectious-Recovered-Quantity of Brucella in the Environment.
SEIS	Susceptible-Exposed-Infectious-Susceptible.
SEIV	Susceptible-Exposed-Infectious-Quantity of Brucella in the Environment.
SI	Susceptible-Infectious.
SIR	Susceptible-Infectious-Recovered.
SIRS	Susceptible-Infectious-Recovered-Susceptible.
SIS	Susceptible-Infectious-Susceptible.
USA	United States of America.
WHO	World Health Organization.

LIST OF TABLES

LIST OF FIGURES

LIST OF APPENDICES

CHAPTER ONE

INTRODUCTION

This Chapter depicts the comprehensive insights allied with current research. It primarily concentrates on Brucellosis disease baseline information, illustrates the problem statement, objectives and explains the significance of addressing the study problem.

1.1 Background

1.1.1 Disease and Etiology

Brucellosis, which has been also known as Crimean fever, Rock fever, Malta fever, Bang's disease, Maltese fever, Mediterranean fever, Undulant fever, Gibraltar fever, or Gastric remittent, is a neglected zoonotic bacterial infection that can be acquired by humans from infected animals' meat, urine, body fluids, aborted materials, unpasteurized milk and milk based products (Zhang *et al*., 2014). It is caused by Gram-negative bacteria of the genus *Brucella* that comprises of ten species in which four of these namely; *B. abortus*, *B. melitensis*, *B. canis*, and *B. suis* causes human Brucellosis (CFSPH, 2018; Li, Sun, Zhang, Jin *et al*., 2014; Poester *et al*., 2013; WHO, 2006).

World international organizations such as the Food and Agriculture Organisation (FAO), World Organization for Animal Health (Office International des Epizooties (OIE)), and the World Health Organisation (WHO) consider Brucellosis amongst the world most prevalent zoonoses alongside rabies and bovine tuberculosis (Schelling *et al*., 2003). The history of Brucellosis goes beyond the isolation and identification of *Brucella melitensis* and extends back to people's initial contact with animals (Akpinar, 2016; Greenfield *et al*., 2002). Wyatt (2016) disclosed that the disease was first detected in Malta after the Crimean War in the 1850s but anthropologists and archaeologists confirmed the presence of *Brucella* in the earliest periods of humankind (Mutolo *et al*., 2012). The disease was described by Manuel Rodriguez Caramazana as Malta fever in Minorca and later, Jeffery Allen Marston who did not know its exact cause described it for the first time in 1860 as gastric remittent (Marston, 1861). The name of the disease honor the contribution of a Sottish physician, Sir David Bruce, who in 1887 isolated the causative Gram-negative *coccobacili* from the livers, kidney and spleens of five British solders who died in Malta (Bruce, 2011; Zhang *et al*., 2015). The name of the aetiologic agent was derived

from the word "melita" which means 'Malta' in Latin (*Micrococcus melitensis*, now renamed *Brucella melitensis*) due to the fact that the disease was first seen in Malta (Vassallo, 1996).

A study by a Danish veterinarian Bernard Lauritz Frederik Bang in 1895 isolated *Brucella abortus* from aborted cattle in Denmark. It was noted that the pathogen could also infect sheep, horses and goats. To honor his contribution, the disease was called Bang's disease (El-Sayed & Awad, 2018). Wright and Smith (1897) discovered that the disease was zoonotic after detecting specific antibodies of *Brucella melitensis* in human and animal serum-agglutination tests. In 1905, a Greek physician working with Bruce, Themistokles Zammit revealed that Maltese goats with no clinical signs of the disease carried the aetiologic agent and could transmit the disease to humans through the ingestion of unpasteurized milk (Ainseba *et al*., 2010; Wyatt, 2013). In 1914, Jacob Traum discovered *Brucella suis* from prematurely-born piglets' stomachs, livers and kidneys in Indiana, the United States (Mantur & Amarnath, 2008).

In 1918, Alice Evans revealed that the causative agents of Bang's disease and Malta fever belong to the genus *Brucella* and a connection between human and animal Brucellosis was exposed following the isolation of the organism from humans aborted foetus which closely resembled Bruces's organism (Young *et al*., 2009). The discrimination of bovine, swine, and caprine forms of the undulant fever invoked by *B. abortus*, *B. suis*, and *B. melitensis* respectively became possible by 1938. The infection remains common and continually re-emerging zoonosis worldwide since 1884, being accountable for at least 500 000 human new cases every year (Godfroid *et al*., 2005). Low infectious doses (10-100 bacterial cells), rapid transmission through different pathways, persistence in the environment, and treatment difficulties with antibiotics makes *Brucella* a possible 'bioterrorism' agent (El-Sayed & Awad, 2018). At present, the identified species of *Brucella* are ten, which have been given names based on either the places of identification, infection features or the source animal. Four species have been described as zoonotic pathogens namely; *B. melitensis* (highest pathogenicity) named after the place Malta, *B. suis* (high pathogenicity) named after the source animal (swine), *B. abortus* named after the feature of infection, and *B. canis* (moderate pathogenicity) named after the source animal (canine) (Medscape, 2018; N Xavier *et al*., 2010; Zinsstag *et al*., 2005).

1.1.2 Economic Importance and Transmission

Brucellosis is endemic in developing countries and it causes overwhelming losses to the livestock industry especially small-holder livestock farmers by obstructing their access to interna-

tional markets and limiting economic growth (Franc *et al*., 2018). The disease causes financial losses associated with veterinary fees and animal replacement costs. Ingestion of contaminated products such as licking discharges or suckling milk from the infected animals/individuals are the two sources of direct spread of Brucellosis in susceptible animals. The bacteria are transferred to humans through ingestion of contaminated dairy products such as unpasteurized milk, raw blood and meat. In addition, Brucellosis may be transmitted to humans following direct interaction with pathogenic animals' vaginal discharges or aborted fetuses as well as through occupational hazards such as handling of infected animals during birth or abortion, laboratory manipulation and injection of oneself with a needle during mass vaccination. In this regard, livestock farmers, abattoir workers, veterinarians, and laboratory technologists are at immense risk of contracting the infection. Ducrotoy *et al.* (2017) uphold that epidemiologically, there are circumstances where small ruminants contact infected cattle and get contaminated with *B. abortus* in the absence of *B. melitensis* and vice-versa.

1.1.3 Symptoms and Clinical Signs

The symptoms displayed by infected animals have some economic implication to stakeholders. These symptoms include; poor weight gain, reduced fertility, abortion, substantial decrease in milk production, and lost draught power (Franc *et al*., 2018; Yilma *et al*., 2016). Clinical signs in human include: intermittent or continuous fever, profuse sweat, weakness, headache, weight loss, chills, joint pains, aches and distressing complications in pregnant women. Testicular or bone abscesses formation, neurological complications, and endocarditis can also occur in chronic stage (CDC, 2018; Dean *et al*., 2012). If not treated, the infection can persist for months or years causing debilitating conditions to individuals. Clinical signs of Brucellosis in humans resemble those of febrile illness such as malaria, relapsing fever, rheumatic fever, typhoid fever and joint diseases and hence the confusion presents diagnostic challenges.

1.1.4 Control and Treatment

Brucellosis in humans is a devastating disease and needs lengthened treatments with a mixture of antibiotics (John *et al*., 2010). Treatment of Brucellosis is given to cure, reduce the duration of symptoms, avert relapses, or avoid complications such as encephalitis, spondylitis, arthritis, endocarditis, sacroiliitis, epididymoorchitis, and abortion (Pappas *et al*., 2006). Rigorous vaccination and milk pasteurization in the US has successfully reduced the number of infected cases to 100 per year. The current human Brucellosis cases which account to almost 60% in USA

mainly Texas and California result from the uptake of unauthorized unpasteurised dairy based products from Mexico (Pappas *et al*., 2006). In Africa, especially the Sub-Shabaran African region, there is poor understanding and unclear prevalence rates of Brucellosis due to varied countries geographical factors (Tumwine *et al*., 2015). Scholars uphold that there are poor socio-economic conditions in most African countries, where people live by and with their domestic animals, with limited health networks and non-existence of surveillance and vaccination programmes (Pappas *et al*., 2006).

In Tanzania, regardless of the limited data on its distribution, affected host species and impact, livestock Brucellosis has a high prevalence in many parts of the country. The disease was first reported in Tanzania specifically in Arusha in 1927 (Kitaly, 1984). Studies have established the existence of the infection in livestock across various regions, zones and production systems in the country with seroprevalence at an individual animal level varying from 1 to 30% as compared to human with an average prevalence of 1 to 5% (Swai & Schoonman, 2009). A study by Carugati *et al*. (2018) demonstrate a moderate Brucellosis incidence in Northern Tanzania and maintain that the disease is endemic in the area and poses serious human health problems. However, previous studies also reported the existence of human cases in different zones of Tanzania including northern, eastern and lake zones with seroprevalence ranging from 0.7 to 20.5% (Shirima, 2005; Swai & Schoonman, 2009).

1.2 Problem Statement

Despite the efforts and intervention by FOA, WHO and OIE, Brucellosis has continued to pose economic challenges not only to livelihood but also to food security among countries, both developed and developing across generations. Several control options have been implemented but none successfully controls the disease. This therefore necessitates the need to evaluate the current strategies used to control the disease and their effectiveness for a proper prevention or eradication of the disease. A few studies (Lolika *et al*., 2018; Nannyonga *et al*., 2015; Roth *et al*., 2003) have composed and analyzed the spread and dynamics of the disease in heterogeneous/homogeneous populations. Nevertheless, little have been done on the mathematical technique of optimal control and cost-effectiveness in lowering or eliminating the infection in cattle, human and small ruminant classes. Holistic approach in evaluating the control scenarios for Brucellosis in an environment where wildlife, cattle, small ruminants and humans do interact had never been done using mathematical models. Similarly, cost-effectiveness in con-

trolling the disease in such ecosystems is required. With the aid of mathematical models, this work aimed at studying the dynamics and cost-effectiveness of Brucellosis control measures, and further explored the impact of wild animals and variations in seasonal weather attributes on the disease infectiology.

1.3 Rationale

Brucellosis costs sub-Saharan African region and the world millions of dollars per year due to abortion, animal replacement costs, declining milk production, reduced work efficiency in humans among others. It is one of the major economic threats to animal holders and especially the small scale farmers. Although different studies have been done on the identification and characterization of the *Brucella* bacteria, disease transmission, distribution, prevention and control, little have been done on the mathematical modelling aspect, especially in the complex interaction of individuals. It is against this background, the study at hand was geared towards formulating and analysing mathematical models for dynamics and cost-effectiveness of control options for Brucellosis in a complex ecosystem where wildlife, cattle, small ruminants and humans interacts. The study further investigated the impacts of variations in seasonal weather attributes on the disease spread.

1.4 Objectives

1.4.1 General Objective

The goal of this research was to establish and analyze the mathematical models for the conveyance and cost-effectiveness of control options for Brucellosis in a complex ecosystem where wildlife, cattle, small ruminants and humans interacts.

1.4.2 Specific Objectives

The study was piloted by the succeeding specific objectives:

(i) To formulate and analyze the mathematical models for the dynamics and controls for Brucellosis spread.

(ii) To determine the optimal combination of the controls for Brucellosis eradication.

(iii) To analyze the cost-effectiveness of the Brucellosis control measures.

1.5 Research Questions

The study intended to address the following questions:

(i) What basic assumptions and parameters to use in formulation of the models for Brucellosis?

(ii) What is the optimal combination of the controls for the formulated model?

(iii) What is the cost-effectiveness of Brucellosis control measures?

1.6 Significance of the Study

The findings of this study provides: (a) an insight into the epidemiology of Brucellosis; (b) awareness on the economic impacts and cost-effectiveness of the optimal controls by advising veterinarians, farmers, public health workers and policy makers on the long term social and economic effects of Brucellosis in the community; (c) an environment to assess how interventions may change the disease dynamics and how benefits may be attained from the interventions; (d) a guide to the design of control strategies by identifying the critical intervention points for minimizing the disease burden; and a platform for further research on the dynamics of Brucellosis in Tanzania and the world at large.

1.7 Delimination of the Study

The main focus of this study was to formulate and analyze mathematical models for transmission dynamics and cost-effectiveness of the control strategies for Brucellosis. Secondary data for five years (2012-2017) used in estimation of some parameters of the model were conveniently collected in collaboration with Afrique One-ASPIRE (African Science Partnership for Intervention Research Excellence) and Zoonosis in emerging livestock systems (ZELS) projects from Manyara and Arusha regions.

CHAPTER TWO

LITERATURE REVIEW

2.1 History of Mathematical Models in Health Application

A mathematical model refers to an illustration of a system using mathematical language and concepts; it is an essential tool for evaluating the propagation and control of transmittable diseases. Mathematical models are therefore used to investigate and predict how transmittable diseases advance to demonstrate the possible outcomes of an outbreak and advise on public health interventions. Such models employ a number of presumptions and mathematics to identify the parameters for various infectious diseases and gauge the effects of different interventions such as mass vaccination and education campaign programmes. They can also assist in decision-making on when and which intervention(s) should be implemented and to what extent. Modeling of communicable infections is a means which had been exploited to probe diseases spread, prediction of outbreaks and appraise the curbing strategies of an epidemic.

In 1766, a trained physician by the name Daniel Bernoulli performed the earliest mathematical modeling study in the transmission of diseases and established a mathematical model to study fatality from smallpox in England. The model was used to evince that universal immunization at birth against the disease could increase lifespan by 3 years and 2 months (Bernoulli & Blower, 2004). In 1772, Lambert and Laplace followed up Bernoulli's work by expanding the model to include age-dependent factors. Nevertheless, their research focus was not systematically developed until 1911 when a benchmark study by Ross established the modern mathematical epidemiology (Siettos & Russo, 2013). The law of mass action in modern epidemiology was then applied by William Hamer and Ronald Ross to explain the epidemic behavior of measles and malaria respectively. The Kermack-McKendrick and the Reed-Frost epidemic models of 1927 and 1928 respectively both described the association between immune, infected, and susceptible individuals in a population and successfully predicted the behaviour of epidemics analogous to recorded observations of various outbreaks (Brauer & Castillo-Chavez, 2013).

The study by Ross, McKendrick and Kermack addressed the use of mass-action incidence in the spread of infections, and established that the probability for a susceptible individual to be septic corresponds to the number of its interactions with infective ones. Their work also established the compartmental deterministic epidemic modeling and predicted the critical fraction of

susceptible individuals that should be surpassed in the population for an outbreak to increase depending on the transmission potential of an infection. Fourty five years later, the reports by MacDonald furthered Ross's model to clarify the malaria transmission and proposed techniques for eliminating it at operational level. The significant contribution of MacDonald and Ross to the field made mathematical models for the spread and control of pathogens transmitted by mosquito to be branded as Ross-MacDonald models (Smith *et al*., 2004). Generally, there have been several different models with compartment structures depending on the type of disease. Some of the possible classes of compartmental models are; susceptible-infectious (SI), susceptible-infectious-susceptible (SIS), susceptible-exposed-infectious (SEI), susceptible-exposed-infectious-susceptible (SEIS), susceptible-infectious-recovered (SIR), susceptible-infectious-recovered-susceptible (SIRS), susceptible-exposed-infectious-recovered (SEIR) and susceptible-exposed-infectious-recovered-susceptible (SEIRS) (Hethcote, 1994).

2.2 Brucellosis Mathematical Models

Ainseba *et al*. (2010) constructed and analysed a susceptible-infected mathematical model for Brucellosis in the ovine population. In this model, both indirect and direct forms of Brucellosis conveyance were considered and it was established that susceptible individuals could directly contract Brucellosis from infected individuals through contact or indirectly due to the existence of venomous creatures in the surroundings. The net reproductive number was reckoned and utilized in the analysis of global asymptotic behavior of the model. Numerical simulations took place to explore the influence of a slaughtering policy and the findings suggested that, as a means to better comprehend about the spread of infections in sheep or any other animal population, the incorporation of infection age and/or the chronological age is needed. However, the formulated model was too elementary to generalize the complex dynamics of Brucellosis which involves wild animals, livestock, human and the environment.

Hou and Sun (2016) used Changling County of Jilin Province Brucellosis infection characteristics monitoring data to formulate a multi-stage model for conveyance of the disease in sheep. Appertaining to the assumption that *Brucella* spread primarily causes disease in adult sheep and that young sheep infectivity is negligible, the sheep population was classified into young susceptible, susceptible adult or sexually mature, vaccinated, exposed and infectious classes. The basic reproductive number computation was done and the model dynamic properties were discussed. In regard to the embedded parameters, sensitivity examination of the basic reproduc-

tive number was performed and it was found that the sheep birth, vaccination, and elimination rates for infectious sheep were important players in limiting transmission of the disease. Further investigation and comparison of the effects of sheep vaccination and culling strategies revealed that the two controls were efficient and feasible in limiting of Brucellosis in the region, however, the latter was more effective than the former. Nonetheless, the model did not consider the impact of contaminated environment and within human transmission in the dynamics of the infection.

Amaku *et al*. (2009) established a mathematical model to simulate Brucellosis conveyance in herds of female bovines and analyzed the effects of different vaccination strategies. The model was based on statistics from some states of Brazil where surveys on serology were carried out and detected a prevalence rate higher than 2%. The findings showed that in areas with low immunization coverage of approximately 30%, the time required to lower the prevalence rate to 2% which is embraced as a standard was nearly twice time observed for higher coverage of approximately 90%. The study further predicted that if the model parameters remain unchanged, it would take a decade to reduce Brucellosis prevalence to 1% or 2% which is the adequate phase for disease eradication. The intensification of female cattle vaccination efforts was recommended to achieve high coverage in this study.

Dobson and Meagher (1996) developed a mathematical model for Brucellosis spread in Yellow stone National Park, USA. Their study maintained that it was pertinent to understand communicable disease dynamics in the management and safeguarding of both domestic and wild ungulate species within and nearby the nature reserves and national parks.

Zhang *et al*. (2014) set up a SEIV model to excavate the spread of Brucellosis in Zhejiang Province of China. The formulated model fitted the real disease situation and predicted Brucellosis tendency of the region. The evaluation of the efficiency of the control schemes were done in dairy cows. The careful analysis of the model gave quantitative result as follows: the introduction of dairy cows from the northern areas limited disease extinction due to large variations in the number of infectious dairy cows, the spread rate of *Brucella* from the surroundings to dairy cattle was greater than from infective dairy cattle to vulnerable cattle, Brucellosis control strategies required a consideration of seasonal parameters due to its periodic nature under certain circumstances, and the combination of birth rate management and disinfection twice a week in infected regions best controlled the disease in cows.

Kadelka (2015) employed a mathematical model in analyzing the immunological data collected from vaccination with strain RB51 or strain 19 of *Brucella*. The measures taken allowed for the separation of the subjects into good and bad responses was designed, followed by an investigation of the differences in the immune responses after vaccination with two *Brucella* strains. The immune response mathematical model that describes the formation of antagonistic anti and pro-inflammatory and memory cells was developed. The findings from this study showed that the activity and number of memory cells obtained after vaccination are affected by different characteristics of pro-inflammatory cells development.

Huo *et al*. (2013) formulated a sheep-human Brucellosis transmission model that involved the human and sheep population and *Brucella* in Inner Mongolia, China. The model divided the sheep population into vulnerable, exposed and infectious, while the human group was classified into susceptible, acute infection and chronic infection. The average *Brucella* load enough to cause infection in the hosts was defined as the infectious unit. The computation of the threshold number used in the determination of the presence and stability of the equilibria was done. Numerical simulations and sensitivity analysis of the reproductive number were performed using reported human Brucellosis data from the region. The findings showed that the disease could not be eliminated even if disinfection and immunization rates of adult sheep were 100%. The study further investigated and compared the effects of immunization, disinfection and elimination strategies. The findings showed that the vaccination and disinfection of both adult and young sheep were effective and appropriate control strategies for controlling Brucellosis in the Inner Mongolia. However, the assumption that the exposed and infectious sheep had the same infectivity and shedding rate of *Brucella* into the environment by abortions or secretions made the exposed class redundant. Similarly, the inadequacy of data for human to human conveyance was not a sufficient condition for this particular transmission route to be ignored.

Racloz *et al*. (2013) performed a formal mathematical analysis of the Mongolia model by Zinsstag *et al*. (2005) to examine different settings where stability state is attained by latently parasitized, infective or pathological animals. Although the need for more data was evident to have better estimation of the entrance denseness for the conveyance of Brucellosis in diverse parts of the world, the employed system of differential equations and the equilibria for the model were found to be reasonably robust. Demographic determinants of livestock were found to be the important parameter for Brucellosis persistence. The study further depicted that despite

the varying control efforts in pastoral areas, Brucellosis remains largely persistent worldwide. The study recommended ecological considerations like sustaining ecosystem services when planning for infection control strategies in the pastoral settings. Improved governance, land reforms, placing limitations on livestock stocking density and integrated social and economic development should be part and parcel of the plan. However, wild animals and the seasonal interaction between wild and domestic animals were not taken into account in the model.

Li, Sun, Zhang, Jin *et al*. (2014) presented a mathematical model to examine the efficacious control and preventive efforts for Brucellosis transmission dynamics in Hinggan League. The formulated model described the sheep to humans and sheep-to-sheep spread of Brucellosis. The sheep flock at any time was classified into basic ewes and other sheep, and each of the classes was further divided into susceptible, recessive infected, quarantined seropositive infected and vaccinated subgroups whereas the human class was partitioned into susceptible, acute infections and chronic infections. The study showed that the susceptible sheep and human could acquire infections from polluted environment and the recessive infected sheep. Numerical simulations of the study agreed with the 2001 to 2011 records on human Brucellosis incidences, and the trend of human Brucellosis incidences was given. The disease control reproduction number for the region was estimated to be 1.9789. The study also demonstrated that combination of detection and elimination, vaccination, and banning of blended pasture amongst basic ewes and other sheep are valuable in restricting human Brucellosis in Hinggan League. However, the model does not fit to the sub-Saharan Africa countries where small ruminants and cattle share grazing areas. An assumption that recessive infected and quarantined seropositive infected sheep release the equal amount of *Brucella* into the surroundings per unit time makes the quarantined class redundant. Thus, there is a need of combining the recessive infected and quarantined seropositive infected classes.

Li, Sun, Wu *et al*. (2014) proposed SEIRV multi-group model incorporating two-way transmissions among sheep and cattle in public farms. The influence of bidirectional infection resulting from the mixed feeding of the two groups was investigated. Investigation and confirmation of the uniform existence of a unique positive equilibrium was done using the computed basic reproduction number. The Brucellosis persistence equilibrium for the model was proved to be uniformly attracting if the basic reproductive number is >1. Sensitivity analysis of the contagious flocks with distinct systems in terms of some parameters was also performed. Findings

revealed that Brucellosis cannot be eradicated if there is a two-way transmission between cattle and sheep and the reproductive number being < 1 is not an adequate condition for elimination of the disease in the community. The study recommended that mixed feeding prohibition is the best control measure for Brucellosis elimination. However, the assumption that individuals at latent stage and infectious stage have the same transmission rate makes the exposed class redundant. In addition, the model did not incorporate the human population yet the disease is of public health concern.

Kang *et al*. (2014) developed a model to simulate the conveyance of Brucellosis within the cattle population in India. The model was used to estimate the impact of test-and-slaughter, reduction of the transmission rate, and mass vaccination in disease spread control. The epidemiological benefits of different rates of vaccination and decreased transmission were analyzed. The findings showed that test-and-slaughter is an effective strategy for eliminating and eradicating Brucellosis. However, socio-cultural restrictions prevent the culling of cattle in India. This model further revealed that reduction of Brucellosis transmission rates correspondingly lowered the stability and endemic levels of its prevalence. Pulse vaccination initially lowered the prevalence rates but this increased with the inflow of susceptible births. However, the limitations in surveillance data acted as the major constraint of this study. On the other hand, the model formulation was dictated by the available data and not the biology of the disease, and so did not incorporate small ruminants, human population and the indirect route of disease transmission through contaminated environment.

Nie *et al*. (2014) described dairy cattle Brucellosis spread in Jilin Province, China using a mathematical model. The cattle population was classified into susceptible, exposed, and infected while the virus compartment was included to capture the outside transferred amount of *Brucella*. The basic reproductive number was computed and accustomed in proving for the existence and uniform attraction of the equilibrium points. The parameter values for the system and prediction of infection number with time were estimated using 20-years Jilin province Brucellosis data. The results from the study disclosed that the disease would still persist in the Province for the next 30 years even if the existing measures were taken into account. Moreover, the combination of culling through test and slaughter, disinfection and minimization of the number of outer importing is the best control strategy for dairy cattle Brucellosis. However, the model did not consider the impact of small ruminants and weather variations on the disease

spread.

De Souza *et al*. (2016) developed a model with the purpose of measuring the impact of a combination of S19 and RB51 vaccines in reducing Brucellosis prevalence. The model divided the cattle herd into seven classes namely: susceptible, vaccinated with the RB51 strain, primiparous latent carriers, vaccinated with the S19 strain, multiparous latent carriers, primiparous infectious cows, and multiparous infectious cows. The study concluded that the adoption of RB51 vaccination as a complement to S19 vaccination significantly reduced bovine Brucellosis prevalence in a short time. However, ignoring the contribution of small ruminants, wild animals, contaminated environment and the aspect of seasonality limits the model application.

Hou and Sun (2016) used Changling County of Jilin Province Brucellosis infection characteristics monitoring data in formulating a multi-stage model for the disease spread in sheep. Appertaining to the assumption that *Brucella* spread primarily causes disease in adult sheep and that infectivity of young sheep is negligible, the sheep population was classified into young susceptible, susceptible adult or sexually mature, vaccinated, exposed and infectious classes. The basic reproductive number computation was done and the model dynamic properties were discussed. With respect to the embedded parameters, the basic reproductive number's sensitivity analysis was performed and it was discovered that sheep birth, vaccination, and elimination rates for infectious sheep were important players in Brucellosis transmission. Further investigation and comparison of the effects of sheep vaccination and culling strategies revealed that the two controls are efficient and feasible in limiting Brucellosis in the region. However, the latter was more effective than the former. Nonetheless, the model did not consider the impact of contaminated environment and human to human transmission in the dynamics of Brucellosis.

Lou *et al*. (2016) described a susceptible-exposed-infected-vaccinated model with periodicity in the rates of Brucellosis transmission. The impacts of seasonal disease transmission in livestock and human populations of Bayingolin Mongol Autonomous Prefecture of Xinjiang were investigated. The basic reproductive number was evaluated and estimated to be 2.5524. Sensitivity examination of the reproductive number and human Brucellosis cases for the model parameters demonstrated that reduced livestock birth rate, increased slaughter rate of seropositive livestock, increased immunization rates for susceptible livestock, and decreased loss in rates of immunization efficacy were effective strategies for controlling the epidemic. The study predicted a continuous growth in the number of newly acute Brucellosis in humans and its max-

imum value was estimated to be 15 325 that would be reached around the summer of 2023. However, this study did not consider the contribution of contaminated environment in the Brucellosis transmission dynamics.

Li, Sun, Zhang and Jin (2017) formulated a sheep and human Brucellosis dynamics model with direct and indirect transmission routes. The sheep population was grouped into basic ewes and other sheep, and further divided into susceptible, recessive infected, quarantined seropositive infected and vaccinated subgroups while the human population was classified into susceptible, acute infections and chronic infections. Recessive infected sheep and contaminated environment were the two main sources of contagion for the susceptible sheep and humans. The study proved that Brucellosis extinction and persistence equilibrium points are globally attracting if $R_0 < 1$ and $R_0 > 1$ respectively. Nevertheless, this model did not consider the goats and cattle populations.

Li, Guo *et al.* (2017) presented a mathematical model incorporating the indirect transmission route to evaluate the effect of infected livestock culling, vaccination of vulnerable livestock, and environmental disinfection control strategies. The study used the national human data from eleven China provinces that had a high number of Brucellosis cases and compared results from three different models. The potential possible disease outbreaks were investigated using the model with best fit and standard incidence. It was found that the country's average reproduction number was relatively less than that of the province with high Brucellosis incidence, suggesting that the indirect transmission of the disease was a more common route compared to direct transmission. The study concluded that, Brucellosis in China could be controlled if the elimination of infected animals, environmental disinfection, and animal vaccination were increased. The finding further suggested that a combination of all these three control measures were necessary to ensure cost-effective control. However, the important aspects for Brucellosis control like personal protection in humans, and impacts of seasonal weather variations were not captured in the model.

Alhamada *et al.* (2017) investigated the elements of jeopardy connected with *Brucella* seropositivity in small ruminants in Duhok province in Iraq and found that sheep flock size, animal age, mixed grazing of goats and sheep, districts from which animals were raised, and goats' twelve months abortion history on farm were autonomously affiliated to huge Brucellosis prevalence.

Tumwiine and Robert (2017) presented a mathematical model depicting the conveyance of Brucellosis in cattle herds. The model analysis was carried out to gain and establish the stability of the equilibria. A boundary parameter categorized as the basic reproduction number R_0 was calculated and the conditions under which bovine Brucellosis can be cleared in the cattle population were established. It was found out that if $R_0 < 1$, Brucellosis can be eradicated in the cattle herd or it persists if $R_0 > 1$. Lyapunov function and Poincair´e-Bendixson theory were respectively used to prove that the Brucellosis-free and Brucellosis persistence equilibria are uniformly asymptotically stable. Numerical simulation revealed that an increase in magnitude of treatment rate for infected cattle, and the reduction of contact rate between infectious cattle and susceptible or recovered cattle controlled the disease. However, the model can be improved by incorporating small ruminants and the aspect of seasonality that captures cattle calving season, temperature, humidity, soil salinity, and exposure of the bacteria to sunlight.

Zhou *et al*. (2018) established a multi-group model to explore the key factors, probable effects, to characterize Brucellosis transmission, and prioritize control measures in Inner Mongolia, China. Direct Lyapunov method and asymptotic autonomous systems theory were used to characterize the global threshold dynamics of the disease. The weighted sum method was used in the formulation of a multi-objective optimisation problem and it was converted to a scalar optimisation problem of total control cost reduction. The existence and characterization of an optimal control problem were established using a Pontragin's maximum principle. Model parameterization and computation of optimal control scheme was done. The effects of health education, sheep recruitment, culling of infected sheep, and sheep vaccination to the dynamics and control of Brucellosis were explored. The study revealed that Brucellosis would continue to increase in the area because the controls were not working well. The study recommended the use of health education, sheep vaccination and restriction of unregulated sheep breeding controls. However, the model did not consider the contribution of other ruminants and the impact of seasonal weather variations on the disease transmission.

Nepomuceno *et al*. (2018) presented a network-type individual-based modeling as an alternative approach to compartmental models which are used in controlling bovine Brucellosis. Spatial aspects like migration between herds, heterogeneous populations, and control actions designated as pulse interventions were considered and implemented in the model. It was shown that the mean field behavior of a compartmental model may be reproduced by an equivalent

individual-based model. To enable the replication of the presented results, details of this process and flowcharts were provided. Real parameters from São Paulo state of Brazil herds were used to investigate three numerical examples in situations which explored meta-population, pulsed and continuous vaccination and eradication effects. Analysis from this study depicted results which are in agreement with the expected disease behavior.

Abatih *et al*. (2015) presented a mathematical approach to analyze Brucellosis spread among bison. Quantitative and qualitative analysis were used to show that the infection would disappear from the herd if $R_0 < 1$ or would persist otherwise. The results from Sobol method for global sensitivity analysis showed that the recovery rate and loss of resistance rate were accountable for high inconsistency in the infectious bison number expected. Partial ranked correlation coefficients computation revealed that transmission coefficient, recovery rate, mortality rate, and density-dependent reduction in birth correlated negatively with the infective bison number while the calving rate and resistance loss rate highly correlated positively with the infectious bison number. Thus, measures to control Brucellosis in bison should target at increasing the size of mortality rate, recovery rate and birth reduction density dependent rate as well as decreasing calving rate and loss of resistance. To raise the correctness of the infectious bison number expected, precise estimate of the recovery rate and loss of resistance from experimental studies are needed.

Lolika *et al*. (2018) introduced a framework for Brucellosis mathematical modeling that aimed at improving the quantitative understanding of the disease dynamics. In particular, the introduced model framework was a prolongation of Abatih *et al*. (2015) model that was used to examine the influence of culling and chronic individuals on the disease conveyance in a periodic or non-periodic environment. The model was analyzed to get insights on the epidemic and endemic behavior of the disease using threshold dynamics described by the basic reproduction number. Culling at optimal level in a periodic and non-periodic environment was explored using the optimal control theory. However, this study did not incorporate domestic ruminants and indirect transmission of the disease in bison population.

Mathematical models give insights into the epidemiology of communicable diseases and the architecture of control measures (Keeling & Danon, 2009). They can well be utilized in directing the identification of vital intercession points designed at minimizing disease-induced deaths. Additionally, they may serve as a means of cost, magnitude, and duration quantification

of disease epidemics (Garner & Beckett, 2005). Mathematical models also offer a platform to evaluate how interventions can alter infection dynamics and how benefits can accumulate from interventions (Giraldo & Palacio, 2008). Thus, incorporating these models benefits the design for Brucellosis control measures.

The mathematical models presented by Ainseba *et al.* (2010), and Hou and Sun (2016) studied the spread of Brucellosis in a sheep population and those presented by Amaku *et al.* (2009), Kang *et al.* (2014), Nie *et al.* (2014), Zhang *et al.* (2014), De Souza *et al.* (2016), and Tumwiine and Robert (2017) focused on the disease conveyance in cattle populations only. These models missed important aspects of the disease behavior and the population of humans cannot be ignored when studying its dynamics. On the other hand, the study by Lolika *et al.* (2018) which adopted the model by Abatih *et al.* (2015) explored the impacts of various parameters accountable for infection spread in a bison class. This study was more theoretical as it considered a single population and did not show the effect of bison Brucellosis on other populations or the environment.

The mathematical models by Hou *et al.* (2016), Li, Sun, Zhang and Jin (2017), and Li, Sun, Zhang, Jin *et al.* (2014) were formulated to explore the influence of different Brucellosis control scenarios on sheep and human populations. The inclusion of humans, sheep and contaminated environment in the model and the incorporated control strategies provide a better understanding of Brucellosis dynamics compared to models with one or two populations. Nevertheless, the models can be improved by incorporating other ruminant populations and seasonality in the transmission of the disease. A mathematical model by Li, Sun, Wu *et al.* (2014) takes into consideration cattle and sheep populations and investigates the impact of mixed feeding and bidirectional infection between the two populations. This mathematical model is better but it can be improved by including the human population and other domestic ruminants like goats so as to fit in most of the pastoral communities. Seasonal weather variation parameters and wild animals also can be incorporated so as to create a more realistic model. The mathematical model by Zinsstag *et al.* (2005) which was adopted by Racloz *et al.* (2013) is also good as it includes sheep, goat and human populations, and it provides a greater comprehension of the disease dynamics as it incorporates most of the transmission key parameters. However, the model can also be improved by incorporating the indirect route of transmission, seasonal weather parameters for disease dynamics and wild animals.

In terms of control strategies six of the mathematical models (Ainseba *et al*., 2010; Amaku *et al*., 2009; De Souza *et al*., 2016; Li, Su, Wu *et al*., 2014; Nepomuceno *et al*., 2018; Zhang *et al*., 2014) examined the utilization of one control measure, five (Hou *et al*., 2013; Hou & Sun, 2016; Kang *et al*., 2014; Lou *et al*., 2016; Zhang *et al*., 2014) explored the impact of a combination of two control measures, while four studies (Li, Sun, Zhang, Jin *et al*., 2014; Li, Guo *et al*., 2017; Nie *et al*., 2014; Zhou *et al*., 2018) examined the influence of merging of three control parameters in minimizing or eradicating the disease. The remaining studies aimed at providing potential information for Brucellosis spread. Based on the model structure and control strategies incorporated, the model by Li, Guo *et al*. (2017) fits in areas with mixed farming systems. However, it can be improved by considering personal protection in humans, wild animals, and seasonality. In addition, the models proposed by Hou *et al*. (2013), and Hou and Sun (2016) are recommended for studying the disease in a single animal population but can also be improved by incorporating controls like personal protection, and environmental hygiene and sanitation.

2.3 Conclusion

Generally, a few mathematical studies have analyzed Brucellosis infection transmission in homogeneous/heterogeneous populations. Nevertheless, limited studies thought about the mathematical aspect of optimal control and cost-effectiveness in containing the infection in human, cattle, and small ruminant sub-populations. The goal of this work was to explore the impacts of control measures and their cost-effectiveness on controlling Brucellosis using mathematical models. The study also aimed at investigating the impact of wildlife and seasonal weather variations to the disease infectiology.

CHAPTER THREE

MATHEMATICAL MODEL FOR BRUCELLOSIS TRANSMISSION DYNAMICS IN LIVESTOCK AND HUMAN POPULATIONS

In this chapter we present an establishment and analysis of a mathematical model for Brucellosis spread. The transmission routes considered in this model are infected livestock to human, between humans, and contaminated surroundings to both livestock and human forms of transmission. We present an investigation on the implications of livestock vaccination, environmental hygiene and sanitation, human treatment, and the gradual culling of infected animals through test and slaughter that control of Brucellosis transmission in livestock and human populations. Analytical solutions and numerical simulations are also presented. The chapter is organized into five sections, namely: model formulation, model properties, model analysis, numerical simulations, and conclusion.

3.1 Model Formulation

3.1.1 Dynamics of Brucellosis

In this sub-section we formulate and present a mathematical model for the conveyance of Brucellosis in cattle, humans, and small ruminants (sheep and goats) groups. In this model, direct conveyance of Brucellosis within humans, between cattle, small ruminants (sheep and goats), and out of livestock to human, and indirect transmission from the surroundings to humans and livestock are considered. Interpersonal spread of Brucellosis is possible as signposted in El-Sayed & Awad (2018), Corbel (2006), Meltzer *et al*. (2010), Mesner *et al*. (2007) and Palanduz *et al*. (2000). There are several means of human to human transmission of Brucellosis that includes breastfeeding, transplancental, blood transfusion, sexual intercourse, and organ transplantation (Tuon *et al*., 2017).

Moreover, some animals like domestic ruminants remain vulnerable unless if immunized at certain times (pulse vaccination). In regard to the epidemiological state of individuals, the bovine herd at a given time t is grouped into susceptible $S_c(t)$, vaccinated $V_c(t)$, and infectious $I_c(t)$ subgroups. Likewise, the small ruminant group at all times t is classified into susceptible $S_s(t)$, vaccinated $V_s(t)$, and infective $I_s(t)$ subgroups whereas the total human population, $N_h(t)$ at

any time t is clustered into susceptible, $S_h(t)$, infected, $I_h(t)$ and recovered, $R_h(t)$ subgroups. Vulnerable bovine may acquire the disease when in direct contact with diseased bovine at a rate of β_c or indirectly by contacting tainted environment at a rate α_c. On the other hand, small ruminants are prone to the disease and contract infection once they directly interact with infective small ruminants at a rate β_s or indirectly when in contact with contaminated surroundings at a rate α_s. In addition, vulnerable humans are infected by what can be termed as summative contributions of conveyance namely infective small ruminants, cattle, humans, and contaminated surroundings. Taking into an account that determining the quantity of *Brucella* in surroundings is very difficult; we establish a contagious unit, let $B(t)$ signify the number of contagious units within the surroundings; an average number of *Brucella* enough to infect the susceptible host. It is further maintained that, detection of incubation period for Brucellosis is hard, however, the rate of transmission for individuals at this stage and that of infectious individuals is the same and release equal amount of *Brucella* into the surroundings per unit time (Hou *et al.*, 2013). Based on this background, we assume that the infective class hosts both individuals in the latent and infectious periods. More importantly, contacts within occupational groups namely farmers, laboratory assistants, veterinary surgeons, and breeders are vulnerable to the pathogen.

3.1.2 Model Assumptions

The model was formulated under the following presumptions:

(i) Each population is homogeneously mixed;

(ii) The cross transmission between ruminants is negligible;

(iii) The environment is contaminated by *Brucella* from infected animals;

(iv) Livestock testing positive for *Brucella* pathogens (seropositivity) is permanent;

(v) Vaccinated individuals may be infected in case their immunity wanes;

(vi) The natural mortality rate is constant in every specie; and

(vii) Natural death rate for each class is not more than the birth rate.

Table 1 gives the description of the model variables whereas Table 2 summarizes the model parameters and their descriptions.

Table 1: Model Variables

Variable	Description
$S_h(t)$	Number of susceptible humans at time t
$I_h(t)$	Number of infected human at time t
$R_h(t)$	Number of recovered humans at time t
$S_c(t)$	Number of susceptible cattle at time t
$I_c(t)$	Number of infected cattle at time t
$V_c(t)$	Number of vaccinated cattle at time t
$S_s(t)$	Number of susceptible small ruminants at time t
$I_s(t)$	Number of infected small ruminants at time t
$V_s(t)$	Number of vaccinated small ruminants at time t
$B(t)$	Number of *Brucella* bacteria per unit volume in the environment at time t

3.1.3 Brucellosis Dynamics Compartmental Flow Diagram

Figure 1 illustrates the interaction between human population, cattle, *Brucella* contagious environment, sheep and goats.

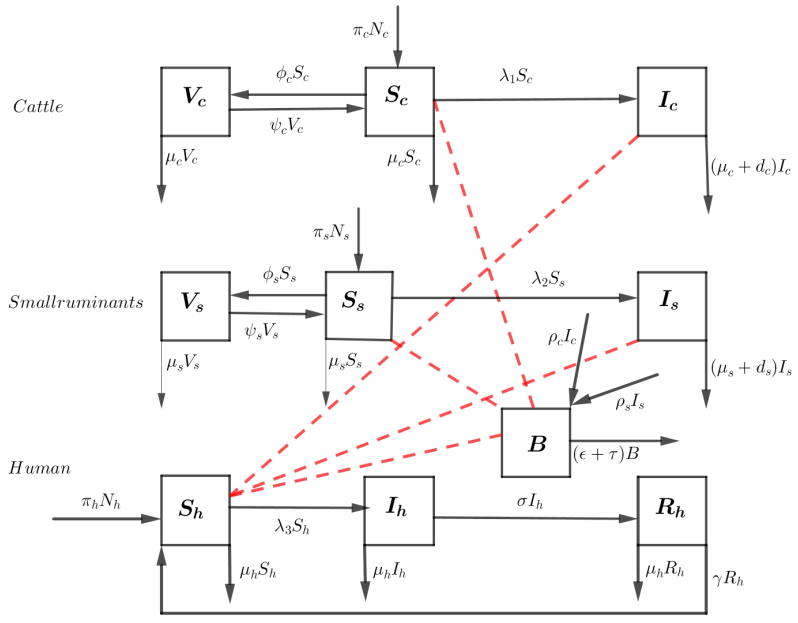

Figure 1: A geometric representation of the direct and indirect spread of Brucellosis in livestock and humans. An inter-relation between individuals from one subpopulation to another is represented by solid arrows while interactions leading to infections are shown by dotted lines.

Table 2: Description of the model parameters

Parameter	Description
π_c	Per capita cattle birth rate
ϕ_c	Immunization rate in cattle
π_h	Per capita human birth rate
σ	The rate of recovery in humans
μ_h	Per capita natural mortality rate in humans
ψ_c	Waning rate of vaccine efficacy in cattle
β_c	Transmission rate within cattle
d_c	Culling rate of seropositive bovine
μ_c	Per individual natural mortality rate in cattle
α_c	Transmission rate of the environmental *Brucella* to cattle
α_s	Transmission rate of the environmental *Brucella* to small ruminants
α_h	Transmission rate of the environmental *Brucella* to human
ρ_c	Infected cattle shedding rate of *Brucella*
ρ_s	Infected small ruminants shedding rate of *Brucella*
β_{ch}	Cattle to humans spread rate
β_{sh}	Small ruminants to humans spread rate
ϵ	Decay rate of the environmental *Brucella*
τ	Rate of environmental sanitation
π_s	Per capita small ruminants birth rate
ϕ_s	Rate of immunization of small ruminants
ψ_s	Waning rate of vaccine efficacy in small ruminants
β_s	Disease spread ratio among small ruminants
d_s	Slaughtering rate of infective small ruminants
μ_s	Per capita small ruminants rate of natural deaths

3.1.4 Model Equations

Guided by the presumptions, the interaction between variables and the parameters illustrated in Fig. 1, the Brucellosis conveyance is summarized by the succeeding differential equations:

$$\begin{aligned}
\frac{dV_c}{dt} &= \phi_c S_c - (\psi_c + \mu_c)V_c \\
\frac{dS_c}{dt} &= \pi_c N_c + \psi_c V_c - (\lambda_1 + \phi_c + \mu_c)S_c \\
\frac{dI_c}{dt} &= \lambda_1 S_c - (\mu_c + d_c)I_c \\
\frac{dV_s}{dt} &= \phi_s S_s - (\mu_s + \psi_s)V_s \\
\frac{dS_s}{dt} &= \pi_s N_s + \psi_s V_s - (\lambda_2 + \phi_s + \mu_s)S_s \\
\frac{dI_s}{dt} &= \lambda_2 S_s - (\mu_s + d_s)I_s \\
\frac{dB}{dt} &= \rho_c I_c + \rho_s I_s - (\epsilon + \tau)B \\
\frac{dS_h}{dt} &= \pi_h N_h + \gamma R_h - (\lambda_3 + \mu_h)S_h \\
\frac{dI_h}{dt} &= \lambda_3 S_h - (\sigma + \mu_h + d_h)I_h \\
\frac{dR_h}{dt} &= \sigma I_h - (\gamma + \mu_h)R_h
\end{aligned} \tag{3.1}$$

where the force of infection functions λ_1, λ_2, and λ_3 are defined by:

$$\lambda_1 = \beta_c I_c + \alpha_c B. \tag{3.2}$$

$$\lambda_2 = \beta_s I_s + \alpha_s B. \tag{3.3}$$

and

$$\lambda_3 = \beta_{hc} I_c + \beta_{hh} I_h + \beta_{hs} I_s + \alpha_h B. \tag{3.4}$$

3.2 Model Properties

3.2.1 Invariant Region

This subsection presents an assessment on the well-posedness of model system (3.1). The assessment was done by investigating the existence and viability of its solution. This means the investigation looked at how the solutions are well-posed mathematically (there exists a bounded solution at any time t) and epidemiologically (variables have biological meaning). That is,

solutions of the system whose initial values are greater or equal to zero maintain their behaviour for all time $t \geq 0$. The compact form below expresses the model system (3.1):

$$\frac{dX}{dt} = AX + G$$

where,

$$A = \begin{bmatrix}
-(\mu_c + \psi_c) & \phi_c & 0 & 0 & 0 & 0 & 0 & 0 & 0 & 0 \\
\psi_c & -d_0 & 0 & 0 & 0 & 0 & 0 & 0 & 0 & 0 \\
0 & \lambda_1 & -(\mu_c + d_c) & 0 & 0 & 0 & 0 & 0 & 0 & 0 \\
0 & 0 & 0 & -(\mu_s + \psi_s) & \phi_s & 0 & 0 & 0 & 0 & 0 \\
0 & 0 & 0 & \psi_s & -d_1 & 0 & 0 & 0 & 0 & 0 \\
0 & 0 & 0 & 0 & \lambda_2 & -(\mu_s + d_s) & 0 & 0 & 0 & 0 \\
0 & 0 & 0 & 0 & 0 & 0 & -d_2 & 0 & \gamma & 0 \\
0 & 0 & 0 & 0 & 0 & 0 & \lambda_3 & -d_3 & 0 & 0 \\
0 & 0 & \rho_c & 0 & 0 & 0 & 0 & \sigma & -(\gamma + \mu_h) & 0 \\
0 & 0 & \rho_c & 0 & 0 & \rho_s & 0 & 0 & 0 & -(\epsilon + \tau)
\end{bmatrix}$$

with,

$$d_0 = (\lambda_1 + \phi_c + \mu_c), \;\; d_1 = (\lambda_2 + \phi_s + \mu_s),$$

$$d_2 = (\lambda_3 + \mu_h), \;\; d_3 = (\sigma + \mu_h + d_h),$$

$$X = (V_c, S_c, I_c, V_s, S_s, I_s, S_h, I_h, R_h, B),$$

and G is a column vector denoted by

$$G = (0, \pi_c N_c^0, 0, 0, \pi_s N_s^0, 0, \pi_h N_h^0, 0, 0, 0)^T.$$

It is noticeable that A is Meltzer matrix because its entire off-diagonal elements are non-negative for every $X \in \mathbb{R}_+^{10}$. Thus, given that $G > 0$, the model system (3.1) is positively invariant in $\mathbb{R}_+^{10}$, it implies that, arbitrary trajectories of the system with initial points in $\mathbb{R}_+^{10}$ stays in $\mathbb{R}_+^{10}$ endlessly. Also, G is Lipschitz continuous. Hence, there exists a distinctive supreme solution and consequently:

$$\Omega = \{(V_c, S_c, I_c, V_s, S_s, I_s, S_h, I_h, R_h, B) \geq 0\} \in \mathbb{R}_+^{10}.$$

is the viable region for the model (3.1). So, with regard to epidemiology and mathematics, the model (3.1) is well-posed in the region Ω.

Alternatively, positivity of solutions can be shown using integration as in the following subsection.

3.2.2 Positiveness of Solutions

For the sake of Brucellosis model (3.1) to be mathematically meaningful, it is essential to verify that each of its state variable is non-negative for time $t > 0$.

Theorem 3.1

Let the baseline data set be $\{V_c(0), S_c(0), I_c(0), V_s(0), S_s(0), I_s(0), S_h(0), I_h(0), R_h(0), B(0)\} \in \mathbb{R}_+^{10}$, then the set of solutions $\{V_c(t), S_c(t), I_c(t), V_s(t), S_s(t), I_s(t), S_h(t), I_h(t), R_h(t), B(t)\}$ of model (3.1) is positive for $t > 0$.

Proof. From the first equation of model system (3.1) we have:

$$\frac{dV_c}{dt} = \phi_c S_c - (\mu_c + \psi_c)V_c \geq -(\mu_c + \psi_c)V_c,$$

Integrating both sides we have:

$$\int_0^t \frac{dV_c}{dt} ds \geq \int_0^t -(\mu_c + \psi_c)V_c ds.$$

$$V_c(t) \geq V_c(0)e^{-(\mu_c+\psi_c)ds},$$

since

$$(\mu_c + \psi_c) > 0.$$

If we let the baseline data $V_c(0) > 0$, then $V_c(t) > 0$. Similar manner can be applied in proving that each state variable is greater than zero for time $t > 0$. That is:

$$S_c(t) \geq S_c(0)e^{-(\lambda_1+\mu_c+\phi_c)ds}.$$

$$I_c(t) \geq I_c(0)e^{-(\mu_c+d_c)ds}.$$

$$V_s(t) \geq V_s(0)e^{-(\mu_s+\psi_s)ds}.$$

$$S_s(t) \geq S_s(0)e^{-(\lambda_2+\mu_s+\phi_s)ds}.$$

$$I_s(t) \geq I_s(0)e^{-(\mu_s+d_s)ds}.$$

$$S_h(t) \geq S_h(0)e^{-(\lambda_3+\mu_h)ds}.$$

$$I_h(t) \geq I_h(0)e^{-(\sigma+\mu_h+d_h)ds}.$$

$$R_h(t) \geq R_h(0)e^{-(\gamma+\mu_h)ds}.$$

$$B(t) \geq B(0)e^{-(\epsilon+\tau)ds}.$$

□

3.2.3 Steady State Solutions

Derivation of the conditions for existence of equilibrium points within the animal population was done in this subsection. The consideration for the animal population emanates from the fact that the first seven equations of system (3.1) do not depend on the last three equations, and that equations for the human population depends on the equations for livestock and *Brucella*. Furthermore, the equilibria are derived by setting to zero the right-hand side of model system (3.1). Let $E^*(V_c^*, S_c^*, I_c^*, V_s^*, S_s^*, I_s^*, B^*)$ serve as the point of equilibrium for the animal population in model system (3.1), the solution for each state variable in terms of I_c^* and I_s^* at steady state is:

$$S_c^* = \frac{(\epsilon+\tau)(\psi_c+\mu_c)\pi_c N_c^0}{(\psi_c+\mu_c)(((\epsilon+\tau)\beta_c+\alpha_c\rho_c)I_c^*+\alpha_c\rho_s I_s^*)+\mu_c(\epsilon+\tau)(\phi_c+\psi_c+\mu_c)}, \tag{3.5}$$

$$V_c^* = \frac{\phi_c(\epsilon+\tau)\pi_c N_c^0}{(\psi_c+\mu_c)(((\epsilon+\tau)\beta_c+\alpha_c\rho_c)I_c^*+\alpha_c\rho_s I_s^*)+\mu_c(\epsilon+\tau)(\phi_c+\psi_c+\mu_c)},$$

$$S_s^* = \frac{(\epsilon+\tau)(\psi_s+\mu_s)\pi_s N_s^0}{(\psi_s+\mu_s)(((\epsilon+\tau)\beta_s+\alpha_s\rho_s)I_s^*+\alpha_s\rho_c I_c^*)+\mu_s(\epsilon+\tau)(\phi_s+\psi_s+\mu_s)}, \tag{3.6}$$

$$V_s^* = \frac{\phi_s(\epsilon+\tau)\pi_s N_s^0}{(\psi_s+\mu_s)(((\epsilon+\tau)\beta_s+\alpha_s\rho_s)I_s^*+\alpha_s\rho_c I_c^*)+\mu_s(\epsilon+\tau)(\phi_s+\psi_s+\mu_s)},$$

$$B^* = \frac{\rho_c I_c^* + \rho_s I_s^*}{\epsilon+\tau}, \tag{3.7}$$

$$I_c^* = \frac{\lambda_1^* S_c^*}{\mu_c+d_c}, \tag{3.8}$$

and

$$I_s^* = \frac{\lambda_2^* S_s^*}{\mu_s+d_s}. \tag{3.9}$$

where,

$$\lambda_1^* = \beta_c I_c^* + \alpha_c B^* \tag{3.10}$$

and

$$\lambda_2^* = \beta_s I_s^* + \alpha_s B^*. \tag{3.11}$$

Substituting equation (3.5) and (3.10) in (3.8) and simplifying, we have:

$$(A_1 I_c^* + A_0(1-R_{ec}))I_c^* + (\psi_c+\mu_c)\alpha_c\rho_s I_s^*((\mu_c+d_c)I_c^* - \pi_c N_c^0) = 0 \tag{3.12}$$

where,

$$R_{ec} = \frac{(\beta_c(\epsilon+\tau)+\alpha_c\rho_c)(\psi_c+\mu_c)\pi_c N_c^0}{\mu_c(\epsilon+\tau)(\mu_c+d_c)(\phi_c+\psi_c+\mu_c)}$$

$A_1 = (\mu_c + d_c)(\psi_c + \mu_c)((\epsilon + n\tau)\beta_c + \alpha_c\rho_c)$ and $A_0 = \mu_c(\epsilon + \tau)(\phi_c + \psi_c + \mu_c)$.

It can be noticed from (3.12) that, the Brucellosis free equilibrium point occurs if and only if $I_c^* = I_s^* = 0$. Based on the fact that co-infections by two distinct *Brucellae* are quite improbable due to the development of resistance in an existing infection (Ducrotoy *et al*., 2017), an endemic equilibrium point in cattle exists if $I_c \neq 0$ and $I_s = 0$, that is:

$$(A_1 I_c^* + A_0(1 - R_{ec}))I_c^* = 0. \tag{3.13}$$

The solutions for polynomial (3.13) are $I_c^* = 0$ and $A_1 I_c^* + A_0(1 - R_{ec}) = 0$, whereby $I_c^* = 0$ and $A_1 I_c^* + A_0(1 - R_{ec}) = 0$ respectively correspond to the existence of Brucellosis free and unique disease persistence equilibrium points. Furthermore, $A_0(1 - R_{ec})$ is positive if $R_{ec} < 1$ and negative if $R_{ec} > 1$. This proves that a transcritical bifurcation exists at $R_{ec} = 1$.

Theorem 3.2

The cattle Brucellosis transmission model has a distinctive disease persistence equilibrium point if and only if $R_{ec} > 1$.

Similarity, if (3.6) and (3.11) are substituted in (3.9) we have:

$$(A_3 I_s^* + A_2(1 - R_{es}))I_s^* + (\psi_s + \mu_s)\alpha_s\rho_c I_c^*((\mu_s + d_s)I_s^* - \pi_s N_s^0) = 0 \tag{3.14}$$

where,

$$R_{es} = \frac{(\beta_s(\epsilon + \tau) + \alpha_s\rho_s)(\psi_s + \mu_s)\pi_s N_s^0}{\mu_s(\epsilon + \tau)(\mu_s + d_s)(\phi_s + \psi_s + \mu_s)}$$

$A_3 = (\mu_s + d_s)(\psi_s + \mu_s)((\epsilon + \tau)\beta_s + \alpha_s\rho_s)$ and $A_2 = \mu_s(\epsilon + \tau)(\phi_s + \psi_s + \mu_s)$

$$A_2(1 - R_{es}) = A_2\left(1 - \frac{(\beta_s(\epsilon + \tau) + \alpha_s\rho_s)(\psi_s + \mu_s)\pi_s N_s^0}{\mu_s(\epsilon + \tau)(\mu_s + d_s)(\phi_s + \psi_s + \mu_s)}\right) \tag{3.15}$$

Again, A_2 is negative if $R_{es} > 1$ and positive if $R_{es} < 1$ suggesting for the existence of a transcritical bifurcation at $R_{es} = 1$. Hence the following Theorem holds:

Theorem 3.3

A distinctive Brucellosis persistence equilibrium point exists in the small ruminants population if and only if $R_{es} > 1$.

3.3 Analysis of the Model

3.3.1 Brucellosis-free State

To secure a Brucellosis-free equilibrium point, the right side of equations in model system (3.1) is set to zero, simply put:

$$\frac{dS_c}{dt} = \frac{dV_c}{dt} = \frac{dI_c}{dt} = \frac{dS_s}{dt} = \frac{dV_s}{dt} = \frac{dI_s}{dt} = \frac{dS_h}{dt} = \frac{dI_h}{dt} = \frac{dB}{dt} = \frac{dR_h}{dt} = 0.$$

We denote the Brucellosis-free point of equilibrium for the model by E^0. In the absence of disease, $I_c = I_s = I_h = B = 0$. This means, the summation of vulnerable and immunized populations is the same to entire population. The Brucellosis-free equilibrium point $E^0 = (V_c^0, S_c^0, 0, V_s^0, S_s^0, 0, S_h^0, 0, 0, 0)$ for model system (3.1) exists where:

$$V_c^0 = \frac{\phi_c \pi_c N_c^0}{\mu_c(\phi_c + \psi_c + \mu_c)}, S_c^0 = \frac{(\mu_c + \psi_c)\pi_c N_c^0}{\mu_c(\phi_c + \psi_c + \mu_c)}, V_s^0 = \frac{\phi_s \pi_s N_s^0}{\mu_s(\phi_s + \psi_s + \mu_s)}, \; S_s^0 = \frac{(\mu_s + \psi_s)\pi_s N_s^0}{\mu_s(\phi_s + \psi_s + \mu_s)},$$

and

$$S_h^0 = \frac{\pi_h N_h^0}{\mu_h}.$$

3.3.2 The Reproduction Number

In this subsection we use the benchmark technique of the next generation operator established in Diekmann *et al.* (1990, 2010) to ascertain the effective or control reproductive number, R_e for model system (3.1). The control reproductive number is pigeonholed as the measure of the average infections number caused by one transmitting individual imposed in a population which mediation strategies are administered (Okuonghae & Korobeinikov, 2007). The chance of an outbreak and the imperative effort to curb its communicability is indicated by the magnitude of effective or net reproductive number. In the absence of interventions or controls, basic reproduction number, R_0, is described as the number of secondary afflictions triggered by one diseased individual in the course of its whole infectivity time. Besides, the native record of some taints suggests that communicability is well measured by the effective reproductive number as distinguished from the basic reproductive number (Cintrón-Arias *et al.*, 2009).
Considering a system for the infective variables:

$$\begin{aligned}
\frac{dI_c}{dt} &= (\beta_c I_c + \alpha_c B)S_c - (\mu_c + d_c)I_c \\
\frac{dI_s}{dt} &= (\beta_s I_s + \alpha_s B)S_s - (\mu_s + d_s)I_s \\
\frac{dI_h}{dt} &= (\beta_{hc} I_c + \beta_{hs} I_s + \beta_{hh} I_h + \alpha_h B)S_h - (\mu_h + d_h)I_h \\
\frac{dB}{dt} &= \rho_c I_c + \rho_s I_s - (\epsilon + \tau)B
\end{aligned} \tag{3.16}$$

The effective reproductive number is found by picking up the spectral radius of the next generation matrix:

$$FV^{-1} = \left[\frac{\partial \mathcal{F}_i(E^0)}{\partial t}\right]\left[\frac{\partial \mathcal{V}_i(E^0)}{\partial t}\right]^{-1}$$

whereby E^0 is the Brucellosis free steady state, the vector $\mathcal{F}_i$ refers to new infection appearance rate in compartment i while vector $\mathcal{V}_i$ is the transfer of infections out of compartment i to another, such that:

$$\mathcal{F}_i = \begin{bmatrix} (\beta_c I_c + \alpha_c B)S_c \\ (\beta_s I_s + \alpha_s B)S_s \\ (\beta_{hc} I_c + \beta_{hs} I_s + \beta_{hh} I_h + \alpha_h B)S_h \\ 0 \end{bmatrix}$$

$$\mathcal{V}_i = \begin{bmatrix} (\mu_c + d_c)I_c \\ (\mu_s + d_s)I_s \\ (\sigma + \mu_h + d_h)I_h \\ -\rho_c I_c - \rho_s I_s + (\epsilon + \tau)B \end{bmatrix}$$

It is important to note that $\mathcal{V}_i$ is a resultant vector of: $\mathcal{V}_i^+$, which is the individuals transfer rate into compartment i by any other agencies (e.g immigration and births); and $\mathcal{V}_i^-$, described as the individuals transfer rate out of compartment i (e.g emigration, deaths, and recovery). That is:

$$\mathcal{V}_i = \mathcal{V}_i^- - \mathcal{V}_i^+,\ i = \{1, 2, 3, 4\}$$

The Variational matrices V of $\mathcal{V}_i$ and F of $\mathcal{F}_i$ calculated at E^0 are respectively:

$$V = \begin{bmatrix} \mu_c + d_c & 0 & 0 & 0 \\ 0 & \mu_s + d_s & 0 & 0 \\ 0 & 0 & \sigma + \mu_h + d_h & 0 \\ -\rho_c & -\rho_s & 0 & (\epsilon + \tau) \end{bmatrix}$$

and

$$F = \begin{bmatrix} \beta_c S_c^0 & 0 & 0 & \alpha_c S_c^0 \\ 0 & \beta_s S_s^0 & 0 & \alpha_s S_s^0 \\ \beta_{hc} S_h & \beta_{hs} S_h & \beta_{hh} S_h & \alpha_h B \\ 0 & 0 & 0 & 0 \end{bmatrix}$$

The indices i and j, for $i, j \in [1, 2, 3, 4]$, refer to rates of infected states, the entry F_{ij} is the rate of septic individuals in tainted class j offer raise or generate new afflictions to individuals in tainted class i, in the linearised system. For this reason, in the inexistence of new disease instances generated in tainted class i by an individual in tainted state j instantly after affliction, we get $F_{ij} = 0$. The inverse of V become apparent:

$$V^{-1} = \begin{bmatrix} \frac{1}{\mu_c + d_c} & 0 & 0 & 0 \\ 0 & \frac{1}{\mu_s + d_s} & 0 & 0 \\ 0 & 0 & \frac{1}{\sigma + \mu_h + d_h} & 0 \\ \frac{\rho_c}{(\mu_c + d_c)(\epsilon + \tau)} & \frac{\rho_s}{(\mu_s + d_s)(\epsilon + \tau)} & 0 & \frac{1}{\epsilon + \tau} \end{bmatrix}$$

The entry $(V^{-1})_{ij}$ refers septic individuals average time spent in compartment j throughout their longevity once imposed into the class i of Brucellosis-free steady state, with a presumption that the population continues to be near the Brucellosis-free state and restraining reinfection. Concretely, $\frac{1}{\mu_c + d_c}$, refers to the average time contagious cattle remain contagious, $\frac{1}{\mu_s + d_s}$ is the average time small ruminant spends in the state of being infective while $\frac{1}{\sigma + \mu_h + d_h}$ is average time a contagious human remain contagious, and $\frac{1}{\epsilon + \tau}$ is the mean time *Brucella* last in the surroundings. Besides, cattle *Brucella* spends $\frac{\rho_c}{\mu_c + d_c} \times \frac{1}{\epsilon + \tau}$ time in the surroundings whereas, $\frac{\rho_c}{\mu_c + d_c}$ is the likelihood that a contagious cattle will release *Brucella* to the surroundings. On another note, *Brucella* discharged by small ruminants will use $\frac{\rho_s}{\mu_s + d_s} \times \frac{1}{\epsilon + \tau}$ time in the environment where, $\frac{\rho_s}{\mu_s + d_s}$ is the likelihood that an infected small ruminant will release

Brucella on the surroundings. Thus, the Next Generation Matrix is calculated to be:

$$FV^{-1} = \begin{bmatrix} R_{11} & R_{12} & 0 & \frac{\alpha_c S_c^0}{\epsilon+\tau} \\ R_{21} & R_{22} & 0 & \frac{\alpha_s S_s^0}{\epsilon+\tau} \\ R_{31} & R_{32} & R_{33} & \frac{\alpha_h S_h^0}{\epsilon+\tau} \\ 0 & 0 & 0 & 0 \end{bmatrix} \tag{3.17}$$

where,

$$\begin{aligned}
R_{11} =& \frac{\beta_c S_c^0}{\mu_c + d_c} + \frac{\alpha_c \rho_c S_c^0}{(\mu_c + d_c)(\epsilon+\tau)}, \\
R_{12} =& \frac{\alpha_c \rho_s S_c^0}{(\mu_s + d_s)(\epsilon+\tau)}, \\
R_{21} =& \frac{\alpha_s \rho_c S_s^0}{(\mu_c + d_c)(\epsilon+\tau)}, \\
R_{22} =& \frac{\beta_s S_s^0}{\mu_s + d_s} + \frac{\alpha_s \rho_s S_s^0}{(\mu_s + d_s)(\epsilon+\tau)}, \\
R_{31} =& \frac{\beta_{hc} S_h^0}{\mu_c + d_c} + \frac{\alpha_h \rho_c S_h^0}{(\mu_c + d_c)(\epsilon+\tau)}, \\
R_{32} =& \frac{\beta_{hs} S_h^0}{\mu_s + d_s} + \frac{\alpha_h \rho_s S_h^0}{(\mu_c + d_c)(\epsilon+\tau)}, \\
R_{33} =& \frac{\beta_{hh} S_h^0}{(\sigma + \mu_h + d_h)}.
\end{aligned}$$

The (i, k) entry of the Next Generation Matrix FV^{-1}, is number of secondary cases anticipated in compartment i as a result of individuals initially in compartment k when the individual's environment remains the same for its entire duration of infection (Van den Driessche & Watmough, 2002). Specifically; R_{11} represents infected cattle number expected to be generated by a single contagious cattle, R_{12} is the number of infected cattle expected as a result of one contagious small ruminant via ingestion of environmental ***Brucella***, R_{21} is the infected small ruminants number expected from one infective cattle, R_{22} is the number of infected small ruminants expected from the direct interaction with one infective small ruminant, R_{31} is the number of infected people expected from one contagious cattle, R_{32} is the anticipated number of infected humans as a consequence of linkages with small ruminants ***Brucella***, R_{33} denotes the number of infected people expected from one contagious person, and R_{34} is the expected number of infected humans produced through direct contact with environmental *Brucella*. Further, it should be borne in mind that, matrix FV^{-1} is non-negative and thus, has a non-negative eigenvalue. The non-negative eigenvalue is related to non-negative eigenvector

that indicates the apportionment of infective individuals with the largest number secondary infections R_e per generation (Padmanabhan *et al.*, 2017). Thus, the largest eigenvalue of the Next Generation Matrix is exhibited by:

$$\rho(FV^{-1}) = R_e = max \begin{cases} \dfrac{R_{11} + R_{22} + \sqrt{(R_{22} - R_{11})^2 + 4R_{12}R_{21}}}{2} \\ \dfrac{\beta_{hh}\pi_h N_h^0}{\mu_h(\sigma + \mu_h + d_h)} \end{cases} \tag{3.18}$$

where,

$$\begin{aligned} R_{11} =& \frac{(\beta_c(\epsilon+\tau) + \alpha_c\rho_c)(\psi_c + \mu_c)\pi_c N_c^0}{\mu_c(\mu_c + d_c)(\epsilon+\tau)(\phi_c + \psi_c + \mu_c)}, \\ R_{12} =& \frac{(\psi_c + \mu_c)\alpha_c\rho_s\pi_c N_c^0}{\mu_c(\mu_s + d_s)(\epsilon+\tau)(\phi_c + \psi_c + \mu_c)}, \\ R_{22} =& \frac{(\beta_s(\epsilon+\tau) + \alpha_s\rho_s)(\psi_s + \mu_s)\pi_s N_s^0}{\mu_s(\mu_s + d_s)(\epsilon+\tau)(\phi_s + \psi_s + \mu_s)}, \\ R_{21} =& \frac{(\psi_s + \mu_s)\alpha_s\rho_c\pi_s N_s^0}{\mu_s(\mu_c + d_c)(\epsilon+\tau)(\phi_s + \psi_s + \mu_s)}. \end{aligned}$$

In equation (3.18) the first case demonstrates the effective reproduction numbers in livestock while the second case represents the human population. As illustrated, there is independence among the cases thus allow a for separate analysis.

When there is no livestock vaccination: $\psi_c = \psi_s = \phi_c = \phi_s = 0$ and

$$R_{11} = \frac{(\beta_c(\epsilon+\tau) + \alpha_c\rho_c)\pi_c N_c^0}{\mu_c(\mu_c + d_c)(\epsilon + n\tau)}, R_{22} = \frac{(\beta_s(\epsilon+\tau) + \alpha_s\rho_s)\pi_s N_s^0}{\mu_s(\mu_s + d_s)(\epsilon+\tau)},$$
$$R_{12} = \frac{\alpha_c\rho_s\pi_c N_c^0}{\mu_c(\mu_s + d_s)(\epsilon+\tau)}, \text{ and } R_{21} = \frac{\alpha_s\rho_c\pi_s N_s^0}{\mu_s(\mu_c + d_c)(\epsilon+\tau)}$$

When there is no intervention in the livestock population: $\psi_c = \psi_s = \phi_c = \phi_s = \tau = 0$, the control reproduction number turns to a basic reproduction number:

$$R_0 = \frac{R_{11}^0 + R_{22}^0 + \sqrt{(R_{22}^0 - R_{11}^0)^2 + 4R_{12}^0 R_{21}^0}}{2} \tag{3.19}$$

where,

$$R_{11}^0 = \frac{(\beta_c\epsilon + \alpha_c\rho_c)\pi_c N_c^0}{\mu_c(\mu_c + d_c)\epsilon}, R_{22}^0 = \frac{(\beta_s\epsilon + \alpha_s\rho_s)\pi_s N_s^0}{\mu_s(\mu_s + d_s)\epsilon}, R_{12}^0 = \frac{\alpha_c\rho_s\pi_c N_c^0}{\mu_c(\mu_s + d_s)\epsilon}, \text{ and}$$

$$R_{21}^0 = \frac{\alpha_s\rho_c\pi_s N_s^0}{\mu_s(\mu_c + d_c)\epsilon}.$$

On the other hand, the average number of afflictions in the wake of one infectious human introduced in a human population whereupon control measures are taken is found to be:

$$R_{eh} = \frac{\beta_{hh}\pi_h N_h^0}{\mu_h(\sigma + \mu_h + d_h)}$$

In absence of treatment, $\sigma = 0$, the basic reproductive within human population is conveyed by:

$$R_{0h} = \frac{\beta_{hh}\pi_h N_h^0}{\mu_h(\mu_h + d_h)}$$

Further, Brucellosis is a zoonosis; ruminants spread it to humans, with reference to a specific case in the Neforms of transmission included in the Generation Matrix (3.17), cattle to humans effective reproduction number is denoted by:

$$R_{hc} = R_{31} = \frac{(\beta_{hc}(\epsilon + \tau) + \alpha_h\rho_c)\pi_h N_h^0}{(\mu_c + d_c)(\epsilon + \tau)}$$

Moreover, the control reproductive number from the small ruminants to human is given by:

$$R_{hs} = R_{32} = \frac{(\beta_{hs}(\epsilon + \tau) + \alpha_h\rho_s)\pi_h N_h^0}{(\mu_s + d_s)(\epsilon + \tau)}$$

Besides, equation (3.4) illustrates the presence of Brucellosis in humans might have resulted from the interaction between susceptible humans and contagious human or contagious ruminants or environment. Therefore, a simultaneous introduction of one infected human, one tainted bovine, and one tainted small ruminant in the human population necessitate that the effective reproductive number in human be instinctively given by:

$$R_h = \frac{\beta_{hh}\pi_h N_h^0}{\mu_h(\sigma + \mu_h + d_h)} + \frac{(\beta_{hc}(\epsilon + \tau) + \alpha_h\rho_c)\pi_h N_h^0}{(\mu_c + d_c)(\epsilon + \tau)} + \frac{(\beta_{hs}(\epsilon + \tau) + \alpha_h\rho_s)\pi_h N_h^0}{(\mu_s + d_s)(\epsilon + \tau)} \quad (3.20)$$

3.3.3 Local Stability of the Brucellosis Free Equilibrium

An investigation of the local stability of the Brucellosis-free equilibrium point was done by employing trace-determinant method as presented in this subsection.

Theorem 3.4

The Brucellosis-free equilibrium model system (3.1) is locally asymptotically stable if $R_0 < 1$ and unstable if $R_0 > 1$.

Proof. We show that the Jacobian matrix $J(E_0)$ of the Brucellosis model at DFE has a positive determinant and negative trace. The variational matrix for system (3.1) is denoted by:

$$J(E_0) = \begin{bmatrix} -a_1 & \phi_c & 0 & 0 & 0 & 0 & 0 & 0 & 0 & 0 \\ \psi_c & -a_2 & a_3 & 0 & 0 & 0 & 0 & 0 & 0 & -\alpha_c S_c^0 \\ 0 & 0 & a & 0 & 0 & 0 & 0 & 0 & 0 & \alpha_c S_c^0 \\ 0 & 0 & 0 & -b_1 & \phi_s & 0 & 0 & 0 & 0 & 0 \\ 0 & 0 & 0 & \psi_s & b_2 & b_3 & 0 & 0 & 0 & -\alpha_s S_s^0 \\ 0 & 0 & 0 & 0 & 0 & b & 0 & 0 & 0 & \alpha_s S_s^0 \\ 0 & 0 & -\beta_{hc} S_h & 0 & 0 & -\beta_{hs} S_h & -\mu_h & -c_1 & \gamma & -\alpha_h S_h^0 \\ 0 & 0 & \beta_{hc} S_h & 0 & 0 & \beta_{hs} S_h & 0 & c & 0 & \alpha_h S_h^0 \\ 0 & 0 & 0 & 0 & 0 & 0 & 0 & \sigma & -(\gamma + \mu_h) & 0 \\ 0 & 0 & \rho_c & 0 & 0 & \rho_s & 0 & 0 & 0 & -(\epsilon + \tau) \end{bmatrix}$$

where,

$$a_1 = \mu_c + \psi_c, \;\; a_2 = (\phi_c + \mu_c) \;\; , a_3 = -\beta_c S_c^0,$$

$$b_1 = \mu_s + \psi_s, \;\; b_2 = -(\phi_s + \mu_s) \;\; , b_3 = -\beta_s S_s^0,$$

$$c_1 = \beta_{hh} S_h^0, \quad , c = \beta_{hh} S_h^0 - (\sigma + \mu_h + d_h),$$

$$a = \beta_c S_c^0 - (\mu_c + d_c),$$

and

$$b = \beta_s S_s^0 - (\mu_s + d_s).$$

The trace of the Variational matrix $J(E_0)$ is exposed to view by:

$$\begin{aligned} Tr(J(E_0)) = & -(\mu_c + d_c)\left(1 - \frac{\beta_c S_c^0}{\mu_c + d_c}\right) - (\mu_s + d_s)\left(1 - \frac{\beta_s S_s^0}{\mu_s + d_s}\right) \\ & -(\sigma + \mu_h + d_h)\left(1 - \frac{\beta_{hh} S_h^0}{\sigma + \mu_h + d_h}\right) - (\phi_c + \psi_c + 2\mu_c) \\ & -(\phi_s + \psi_s + 2\mu_s) - (\gamma + 2\mu_h) - (\epsilon + \tau) \end{aligned}$$

So, the trace of the variational matrix is less than zero, simply put $Tr(J(E_0)) < 0$ provided:

$$\frac{\beta_c S_c^0}{\mu_c + d_c} < 1, \quad \frac{\beta_s S_s^0}{\mu_c + d_s} < 1 \quad \text{and} \quad \frac{\beta_{hh} S_h^0}{\sigma + \mu_h + d_h} < 1.$$

Moreover, using Maple 16 Software, the computation of the determinant of matrix $J(E_0)$ was found to be:

$$Det(J(E_0)) = a_0\,(1-R_h)\left((1-R_c)\,(1-R_{ec}) - \frac{\rho_c\alpha_c S_c^0}{(\mu_c+d_c)(\epsilon+\tau)}\,(1-R_s)\right).$$

where,

$$R_h = \frac{\beta_{hh}S_h^0}{\sigma+\mu_h+d_h}, \quad R_s = \frac{\beta_s S_s^0}{\mu_s+d_s}, \quad R_c = \frac{\beta_c S_c^0}{\mu_c+d_c}, \quad R_{es} = \frac{(\epsilon+\tau)\beta_s S_s^0}{(\epsilon+\tau)(\mu_s+d_s)},$$

and

$$a_0 = (\phi_c+\psi_c+\mu_c)(\phi_s+\psi_s+\mu_s)(\gamma+\mu_h)(\sigma+\mu_h+d_h)(\mu_c+d_c)(\mu_s+d_s)(\epsilon+\tau)\mu_c\mu_s\mu_h.$$

The determinant of the variational matrix, $J(E_0)$ is positive as long as:

$$R_c < 1, \quad R_{es} < 1, \quad R_s < 1, \quad \text{and} \quad (1-R_c)\,(1-R_{ec}) > \frac{\rho_c\alpha_c S_c^0}{(\mu_c+d_c)(\epsilon+\tau)}\,(1-R_s).$$

Furthermore, while R_h, and R_s, refer to the average number of secondary human infections due to physical interaction between vulnerable and infected humans, and vulnerable and infected small ruminants respectively, R_c, indicates the mean number of secondary infections in humans triggered by direct contact between vulnerable and infected cattle and R_v shows the mean number of secondary afflictions resulting from direct or indirect contact with one tainted small ruminant across the susceptible livestock population. So, each population's Brucellosis-free equilibrium is stable asymptotically at the local level if $R_e < 1$. This result is similar to that found by Theorem 6.13 of Diekmann and Heesterbeek (2000) and Theorem 2 of Van den Driessche and Watmough (2002). □

3.3.4 Global Stability of the Brucellosis-Free Equilibrium

An analysis for the global stability of the Brucellosis-free equilibrium point was done in this subsection by using Castillo-Chavez *et al*. (2002) approach. Model system (3.1) can be expressed as:

$$\begin{cases} \dfrac{dX_s}{dt} = A(X_s - X_{DFE,S}) + A_1 X_i \\ \dfrac{dX_i}{dt} = A_2 X_i \end{cases} \tag{3.21}$$

where X_s is the vector representing the compartments that do not transmit the disease and X_i symbolize the Brucellosis-transmitting vector components. In case A_2 is a Metzler matrix (i.e. the out-diagonal entries of A_2 are nonnegative) and A has real negative eigenvalues, the

Brucellosis-free equilibrium is globally stable asymptotically. On the basis of model system (3.1) we get:

$$X_i = (I_c, I_s, I_h, B)^T, X_s = (V_c, S_c, V_s, S_s, S_h, R_h)^T,$$

$$X_s - X_{DFE,s} = \begin{bmatrix} V_c - \dfrac{\phi_c \Lambda_c}{\mu_c(\psi_c + \phi_c + \mu_c)} \\ S_c - \dfrac{(\phi_c + \mu_c)\Lambda_c}{\mu_c(\psi_c + \phi_c + \mu_c)} \\ V_s - \dfrac{\phi_s \Lambda_s}{\mu_s(\psi_s + \phi_s + \mu_s)} \\ S_s - \dfrac{(\phi_s + \mu_s)\Lambda_s}{\mu_s(\psi_s + \phi_s + \mu_s)} \\ S_h - \dfrac{\Lambda_h}{\mu_h} \\ R_h \end{bmatrix}$$

and

$$A_1 = \begin{bmatrix} 0 & 0 & 0 & 0 \\ -\beta_c S_c & 0 & 0 & -\alpha_c S_c \\ 0 & 0 & 0 & 0 \\ 0 & -\beta_s S_s & 0 & -\alpha_s S_s \\ -\beta_{hc} S_h & -\beta_{hs} S_h & -\beta_{hc} S_h & -\alpha_h S_h \\ 0 & 0 & \sigma & 0 \end{bmatrix}$$

Verification on whether A_2 is a Metzler matrix and that A, a matrix for non-spreading classes have real negative eigenvalues is needed. So, the equations for non-spreading classes in (3.1) gives the matrix:

$$A = \begin{bmatrix} -(\psi_c + \mu_c) & \phi_c & 0 & 0 & 0 & 0 \\ \psi_c & -(\phi_c + \mu_c) & 0 & 0 & 0 & 0 \\ 0 & 0 & -(\psi_s + \mu_s) & \phi_s & 0 & 0 \\ 0 & 0 & \psi_s & -(\phi_s + \mu_s) & 0 & 0 \\ 0 & 0 & 0 & 0 & -\mu_h & \gamma \\ 0 & 0 & 0 & 0 & 0 & -(\gamma + \mu_h) \end{bmatrix}$$

with eigenvalues $\lambda_1 = -\mu_s, \lambda_2 = -(\psi_s + \phi_s + \mu_s), \lambda_3 = -\mu_c, \lambda_4 = -(\psi_c + \phi_c + \mu_c)$ and

$$A_2 = \begin{bmatrix} \beta_c S_c^0 - (\mu_c + d_c) & 0 & 0 & \alpha_c S_c^0 \\ 0 & \beta_s S_s^0 - (\mu_s + d_s) & 0 & \alpha_s S_s^0 \\ \beta_{hc} S_h & \beta_{hs} S_h^0 & \beta_{hh} S_h - (\mu_h + d_h) & \alpha_h S_h^0 \\ \rho_c & \rho_s & 0 & -(\epsilon + \tau) \end{bmatrix}$$

It can be seen that, A have real negative eigenvalues and that A_2 is a Metzler matrix. This entails that a globally stable asymptotically Brucellosis-free equilibrium for the model system (3.1) exists.

3.3.5 Global Stability of a Brucellosis Persistence Equilibrium

The local stability for the Brucellosis-free equilibrium proposes that the disease persistence equilibrium in the reversed condition is also locally stable. This subsection presents the global behaviour of the Brucellosis persistence equilibrium, E^* of the model system (3.1).

Theorem 3.5

The Brucellosis model system (3.1) of the Brucellosis persistence equilibrium point is globally asymptotically stable on Ω if $R_0 > 1$.

Proof. A well-defined Lyapunov function of model system (3.1) is constructed by employing a useful and most sophisticated approach of compartmental epidemiological models as described in Korobeinikov and Wake (2002), Korobeinikov (2004), McCluskey (2006), Korobeinikov (2007) and Bowong *et al*. (2011). Through the approach, a Lyapunov function is constructed with a structure:

$$V = \sum a_i (x_i - x_i^* \ln x)$$

where a_i refers to a properly chosen positive constant, x_i denotes the population of the i^{th} compartment and x_i^* represents the level of an equilibrium. The Lyapunov function nominee V for model system (3.1) is defined by:

$$\begin{aligned} L =&(S_c - S_c^* \ln S_c) + A_1(V_c - V_c^* \ln V_c) + A_2(I_c - I_c^* \ln I_c) + (S_s - S_s^* \ln S_s) \\ &+ A_3(V_s - V_s^* \ln V_s) + A_4(I_s - I_s^* \ln I_s) + (S_h - S_h^* \ln S_h) + A_5(I_h - I_h^* \ln I_h) \\ &+ A_6(R_h - R_h^* + A_7(B - B^* \ln B)). \end{aligned} \tag{3.22}$$

where $A_1, A_2, A_3, A_4, A_5, A_6$ and A_7 are positive constants. The derivative of the Lyapunov function L with respect to time is put on view by:

$$\begin{aligned} \frac{dL}{dt} =& \left(1 - \frac{S_c^*}{S_c}\right)\frac{dS_c}{dt} + A_1\left(1 - \frac{V_c^*}{V_c}\right)\frac{dV_c}{dt} + A_2\left(1 - \frac{I_c^*}{I_c}\right)\frac{dI_c}{dt} + \left(1 - \frac{S_s^*}{S_s}\right)\frac{dS_s}{dt} \\ &+ A_3\left(1 - \frac{V_s^*}{V_s}\right)\frac{dV_s}{dt} + A_4\left(1 - \frac{I_s^*}{I_s}\right)\frac{dI_s}{dt} + \left(1 - \frac{S_h^*}{S_h}\right)\frac{dS_h}{dt} + A_5\left(1 - \frac{I_h^*}{I_h}\right)\frac{dI_h}{dt} \\ &A_6\left(1 - \frac{R_h^*}{R_h}\right)\frac{dR_h}{dt} + A_7\left(1 - \frac{B^*}{B}\right)\frac{dB}{dt}. \end{aligned} \tag{3.23}$$

Considering model system (3.1) at E^* we have:

$$\pi_h N_h = -\gamma R_h^* + (\beta_{hc} I_c^* + \beta_{hs} I_s^* + \beta_{hh} I_h^* + \alpha_h B^*) S_h^*,$$

$$\sigma + \mu_h + d_h = (\beta_{hc} I_c^* + \beta_{hs} I_s^* + \beta_{hh} I_h^* + \alpha_h B^*)\frac{S_h^*}{I_h^*},$$

$$\pi_s N_s = (\beta_s I_s^* + \alpha_s B^* + \phi_s + \mu_s) S_s^* - \psi_s V_s^*,$$

$$\pi_c N_c = (\beta_c I_c^* + \alpha_c B^* + \phi_c + \mu_c) S_c^* - \psi_c V_c^*,$$

$$\mu_c + d_c = \frac{(\beta_c I_c^* + \alpha_c B^*) S_c^*}{I_c^*},$$

$$\mu_s + d_s = \frac{(\beta_s I_s^* + \alpha_s B^*) S_s^*}{I_s^*},$$

$$(\epsilon + \tau) = \frac{\rho_c I_c^* + \rho_s I_s^*}{B^*},$$

$$\phi_c = \frac{(\psi_c + \mu_c) V_c^*}{S_c^*},$$

$$\phi_s = \frac{(\psi_s + \mu_s) V_s^*}{S_s^*},$$

$$\sigma = \frac{(\gamma + \mu_h) R_h^*}{I_h^*}.$$

Then, equation (3.23) may be re-written as:

$$\begin{aligned}\frac{dL}{dt} =& -(\phi_c+\mu_c)S_c\left(1-\frac{S_c^*}{S_c}\right)^2-(\phi_s+\mu_s)S_s\left(1-\frac{S_s^*}{S_s}\right)^2-\mu_hS_h\left(1-\frac{S_h^*}{S_h}\right)^2\\
&-\left(1-\frac{S_c^*}{S_c}\right)\left(\beta_cI_cS_c\left(1-\frac{I_c^*S_c^*}{I_cS_c}\right)+\alpha_cBS_c\left(1-\frac{B^*S_c^*}{BS_c}\right)+\psi_cV_c\left(\frac{V_c^*}{V_c}-1\right)\right)\\
&-\left(1-\frac{S_s^*}{S_s}\right)\left(\beta_sI_sS_s\left(1-\frac{I_s^*S_s^*}{I_sS_s}\right)+\alpha_sBS_s\left(1-\frac{B^*S_s^*}{BS_s}\right)+\psi_sV_s\left(\frac{V_s^*}{V_s}-1\right)\right)\\
&-a_1\left(1-\frac{V_c^*}{V_c}\right)\left(1-\frac{V_c^*S_c}{V_cS_c^*}\right)-(\psi_s+\mu_s)BV_sA_3\left(1-\frac{V_s^*}{V_s}\right)\left(1-\frac{V_s^*S_s}{V_sS_s^*}\right)\\
&+A_2\left(1-\frac{I_c^*}{I_c}\right)\left(\beta_cI_cS_c\left(1-\frac{S_c^*}{S_c}\right)+\alpha_cBS_c\left(1-\frac{B^*S_c^*I_c}{BS_cI_c^*}\right)\right)\\
&+A_4\left(1-\frac{I_s^*}{I_s}\right)\left(\beta_sI_sS_s\left(1-\frac{S_s^*}{S_s}\right)+\alpha_sBS_s\left(1-\frac{B^*S_s^*I_s}{BS_sI_s^*}\right)\right)\\
&-A_5\left(1-\frac{S_h^*}{S_h}\right)\left(a_2\left(\frac{R_h^*}{R_h}-1\right)+a\left(1-\frac{I_c^*S_h^*}{I_cS_h}\right)+b\left(1-\frac{I_s^*S_h^*}{I_sS_h}\right)+c\left(1-\frac{B^*S_h^*}{BS_h}\right)\right)\\
&+A_6\left(1-\frac{I_h^*}{I_h}\right)\left(\beta_{hc}I_cS_h\left(1-\frac{I_c^*S_h^*I_h}{I_cS_hI_h^*}\right)+\beta_{hs}I_sS_h\left(1-\frac{I_s^*S_h^*I_h}{I_sS_hI_h^*}\right)\right)\\
&+A_6\left(1-\frac{I_h^*}{I_h}\right)\left(\beta_{hh}I_hS_h\left(1-\frac{I_h^*S_h^*I_h}{I_hS_hI_h^*}\right)+\alpha_hBS_h\left(1-\frac{B^*S_h^*I_h}{BS_hI_h^*}\right)\right)\\
&-A_7(\gamma+\mu_h)R_h\left(1-\frac{R_h^*}{R_h}\right)\left(1-\frac{I_hR_h^*}{I_h^*R_h}\right)\\
&+A_8\left(1-\frac{B^*}{B}\right)\left(\rho_cI_c\left(1-\frac{BI_c^*}{B^*I_c}\right)+\rho_sI_s\left(1-\frac{BI_s^*}{B^*I_s}\right)\right). \qquad (3.24)\end{aligned}$$

where,

$$a_1=(\psi_c+\mu_c)BV_cA_1,\ \ a_2=\gamma R_h,$$

$$a=\beta_{hc}I_cS_h,\quad b=\beta_{hs}I_sS_h,\ \ c=\alpha_hBS_h.$$

Equation (3.24) can be written as:

$$\begin{aligned}\frac{dL}{dt} =& -\left((\phi_c+\mu_c)S_c\left(1-\frac{S_c^*}{S_c}\right)^2+(\phi_s+\mu_s)S_s\left(1-\frac{S_s^*}{S_s}\right)^2+\mu_hS_h\left(1-\frac{S_h^*}{S_h}\right)^2\right)\\
&+F(S_c,V_c,I_c,S_s,V_s,I_s,B).\end{aligned}$$

whereby F offsets the right-hand terms of the equation (3.24). In accordance to the technique portrayed in Korobeinikov and Wake (2002), Korobeinikov (2004), McCluskey (2006), Korobeinikov (2007), Bowong *et al.* (2011) and Li, Guo *et al.* (2017), F is a non-positive function for $S_c,V_c,I_c,S_s,V_s,I_s,S_h,I_h,B,R_h>0$. Thus, $\frac{dL}{dt}<0$ for $S_c,V_c,I_c,S_s,V_s,I_s,S_h,I_h,R_h,B>0$ albeit zero incase $S_c=S_c^*,V_c=V_c^*,I_c=I_c^*,S_s=S_s^*,V_s=V_s^*,I_s=I_s^*,S_h=S_h^*,I_h=I^*,R_h=R_h^*$, and $B=B^*$. Consequently, when $R_e>1$,

model system (3.1) has a globally asymptotically stable and unique Brucellosis persistence equilibrium point E^*. □

3.4 Sensitivity Analysis

In this section, we investigate the relative importance of the parameters featuring in the effective reproductive number for the livestock population. Brucellosis incidences and prevalences can best be reduced or eradicated if the parameters with significant impact in the conveyance of the disease are taken into consideration when planning for and implementing intervention strategies. Sensitivity analysis is widely utilized in measuring the soundness of model projections to values of embedded parameters, considering there are customarily uncertainties in information collection and supposed values of parameters. Sensitivity indices provide details on how important each parameter is to infection spread and prevalence, and permits the measuring of relative variations in a state variable once a parameter varies. Accordingly, sensitivity analysis is accustomed to identify parameters that bear higher influence on the reproduction number, R_e and that need to be in sight for intervention schemes. It is common knowledge that initial disease conveyance is directly-related to R_e, for this reason sensitivity indices for R_e attributes for model (3.1) are computed. The explicit expression of R_e for livestock is given by the first case of equation (3.18). Since R_e is dependent on only twenty parameters, an analytical expression of sensitivity index of each parameter is reckoned taking advantage of the normalized forward sensitivity index (Chitnis *et al.*, 2008; Van de Driessche, 2017) as follows:

$$\Upsilon_{\mu_c}^{R_e} = \frac{\partial R_e}{\partial \mu_c} \times \frac{\mu_c}{R_e} = -0.84$$

$$\Upsilon_{\pi_c}^{R_e} = \frac{\partial R_e}{\partial \pi_c} \times \frac{\pi_c}{R_e} = +0.69$$

In a similar fashion, we compute the sensitivity indices for all parameters used in the first case of equation (3.18) and present the results in Table 3. The parameter values (given in units per year) used in the computation are mainly from Li, Sun, Zhang, Jin *et al.* (2014).

Table 3: Sensitivity indices for R_e parameters

Parameter	Value	Sensitivity Index
Λ_c	0.3	0.69
β_c	0.0011	0.54
ϕ_c	0.7	-0.36
ψ_c	0.4	0.22
μ_c	0.25	-0.84
d_c	0.35	-0.40
α_c	0.00035	0.15
ρ_c	10	0.15
ϵ	8	-0.10
τ	12	-0.16
Λ_s	0.4	0.31
β_s	0.001	0.20
ϕ_s	0.8	-0.15
ψ_s	0.5	0.09
μ_s	0.35	-0.39
d_s	0.4	-0.16
α_s	0.00032	0.11
ρ_s	15	0.11

Table 3 signifies that the most sensitive parameters of the effective reproductive number in each population are rates of natural death, birth, transmission, disease-induced deaths and vaccination. The positive sign in the sensitivity index suggests that increasing the magnitude of that parameter drives an increase in R_e and vise-versa. For instance, an increase or decrease of cattle birth rate by 10% leads to an increase or decrease of R_e by 6.9%. On the other hand, the negative sign in the sensitivity index of a parameter signifies that an increase in magnitude of a parameter value leads to a decrease in R_e and vice versa. For example, an increase in cattle natural mortality rate by 10% results in a 8.4% decrease of the effective reproductive number. This implies that culling in large livestock flocks is inevitable if we want to control Brucellosis transmissions.

3.5 Numerical Simulations

To verify plurality of the analytical results, numerical simulations for model system (3.1) is given in the this section. Our computations utilized the parameter values (given in units per year) presented in Li, Sun, Zhang, Jin *et al*. (2014) work. Table 4 contains the parameter values and Figure 2 illustrates how livestock, human and *Brucella* sub-populations varies in relation to time.

Table 4: Brucellosis Model Parameter Values

Parameter	Value	Unit
Λ_c	0.3	$year^{-1}$
β_c	0.0011	$year^{-1}$
ϕ_c	0.7	$year^{-1}$
ψ_c	0.4	$year^{-1}$
μ_c	0.25	$year^{-1}$
d_c	0.35	$year^{-1}$
α_c	0.00035	$year^{-1}$
ρ_c	10	$year^{-1}$
ϕ_h	0.03	$year^{-1}$
β_h	0.0002	$year^{-1}$
σ_h	0.9	$year^{-1}$
μ_h	0.00005	$year^{-1}$
d_h	0.000002	$year^{-1}$
α_h	0.002	$year^{-1}$
β_{hc}	0.000158	$year^{-1}$
β_{hs}	0.000158	$year^{-1}$
γ	0.5	$year^{-1}$
ϵ	8	$year^{-1}$
τ	12	$year^{-1}$
Λ_s	0.4	$year^{-1}$
β_s	0.001	$year^{-1}$
ϕ_s	0.8	$year^{-1}$
ψ_s	0.5	$year^{-1}$
μ_s	0.35	$year^{-1}$
d_s	0.4	$year^{-1}$
α_s	0.00032	$year^{-1}$
ρ_s	15	$year^{-1}$

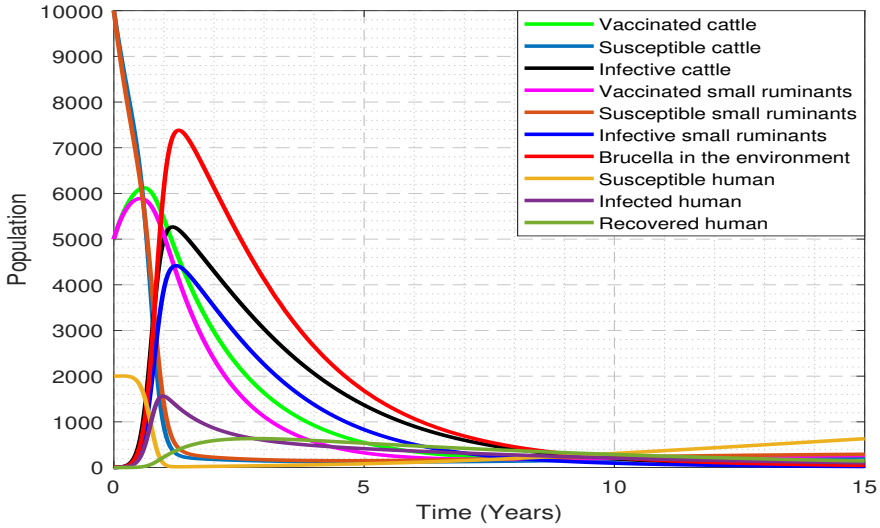

Figure 2: Variations in model sub-populations in relation to time

Figure 2 demonstrates the rapid decrease of human vulnerability with an increases in time as a consequence of natural death rate and Brucellosis infections. It further shows that at first there is increased number of diseased humans with time because of the large number of vulnerable individuals that acquire infection but this later decreases as a result of decreased susceptibility due to increased immunization in animals and treatment rate in humans. Thus, enhancing effective treatment among diseased humans increases the population recovered .

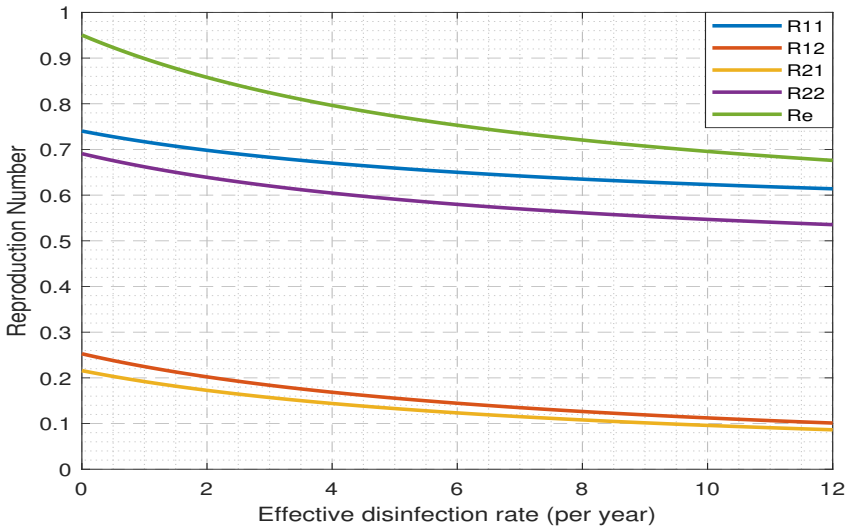

Figure 3: Effective disinfection rate

As illustrated in Fig. 3, the frequency of effective disinfection plays a big role in limiting the number of secondary Brucellosis afflictions in populations of cattle and small ruminants. For instance, the effective reproduction number R_e decreases from 0.95 to 0.79 when disinfection

is applied monthly in a year given that all other controls under consideration are kept constant. This means it is possible to eliminate the disease in the population if testing and slaughtering eliminates at least 35% and 40% of the infected cattle and small ruminants respectively.

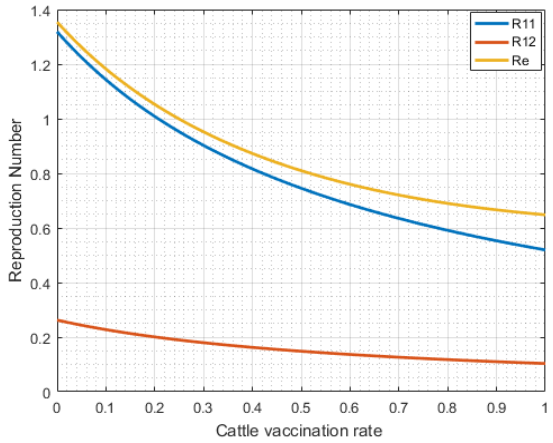

(a) Cattle vaccination rate

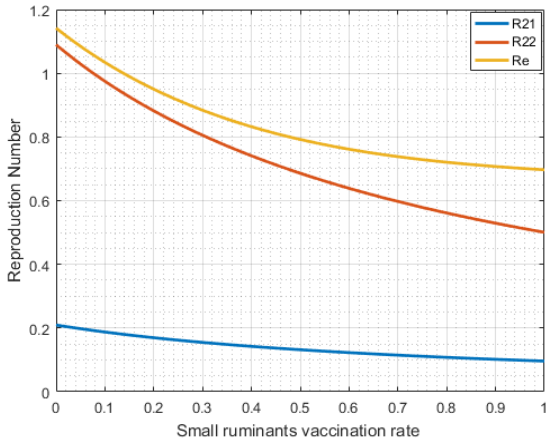

(b) Small ruminants vaccination rate

Figure 4: The impact of ruminants vaccination on the effective reproductive number

Furthermore, as illustrated in Fig. 4a, the effective reproduction number decreases as cattle vaccination rate increases. For instance, a 70% vaccination rate results in the reduction of the effective number from 1.3 to 0.72. This implies that cattle vaccination plays a significant contribution in the reduction or elimination of Brucellosis transmission if and only if it is implemented in combination with other controls like test-and-slaughter and environmental disinfection. Figure 4a further shows that the cattle population attains its disease-free equilibrium at a 20% vaccination rate. A similar trend is observed in Fig. 4b where vaccination of small ruminants significantly reduces their secondary Brucellosis infections and the small ruminants Brucellosis-free state is attained at a 16% vaccination rate. Moreover, if other control parameters are kept constant and disease-induced rate varied, the Brucellosis-free equilibrium ($R_e < 1$) is obtained at 10% and 12.5% disease induced elimination rates for small ruminants and cattle respectively (Fig. 5a and Fig. 5b).

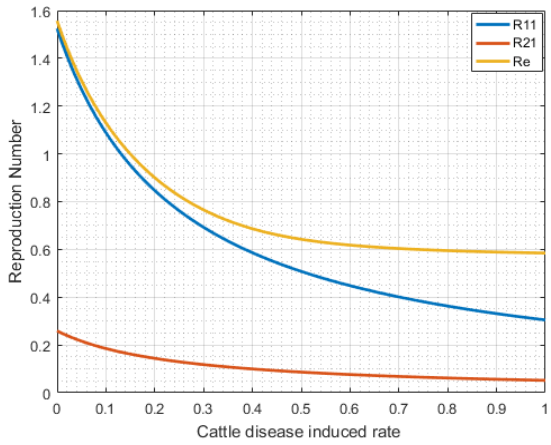

(a) Cattle Brucellosis culling rate

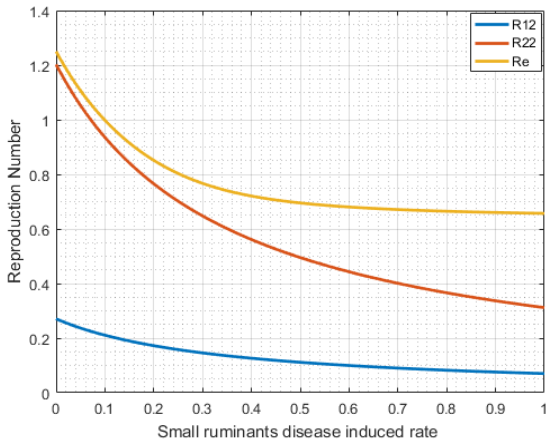

(b) Small ruminants Brucellosis culling rate

Figure 5: The impact of culling infective ruminant on the effective reproductive number

In line with this, Shirima *et al.* (2014) conducted Brucellosis screening in the period 2005 to 2010 at the National Livestock Research Institute headquarters, Mpwapwa-Tanzania and found that the usage of S19 vaccine, step by step culling of seropositive livestock by slaughtering, correct disposal of aborted foetuses and placentas, solitude and detention of pregnant cows close to calving, and restricted introduction of new animals plays a great role in disease elimination.

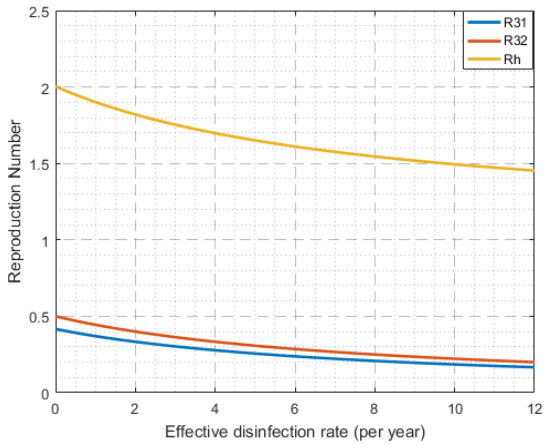

(a) Variations in R_e with respect to changes in environmental sanitation

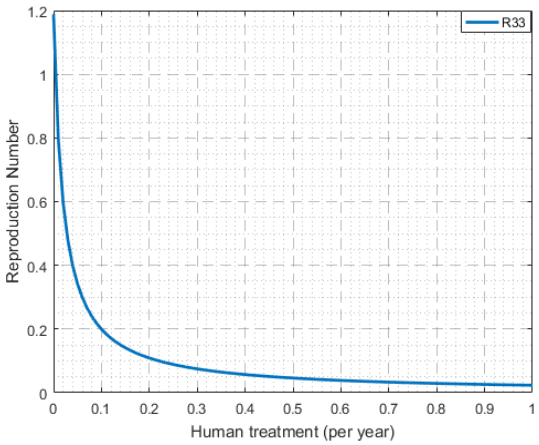

(b) Variations in R_e in relation to alteration in human treatment

Figure 6: Influence of environmental hygiene and human treatment on the effective reproduction number

Similarly, Fig. 6a illustrates that the spread of Brucellosis from tainted surroundings to humans is effectively controlled by maintaining environmental hygiene and sanitation. However, the direct interaction between septic small ruminants or bovine is ineffectively restricted because

the ruminants to human effective reproductive number cannot be reduced to less than one. This affirms the fact that reduction in the number of infective humans is due to increased human treatment. Furthermore, Fig. 6b indicates the significant contribution of human treatments to the lessening or elimination of the spread of Brucellosis between humans. This is affirms the fact that reduction in the number of infective humans limits human to human transmission but eradication of human Brucellosis requires control of livestock to humans and human treatment.

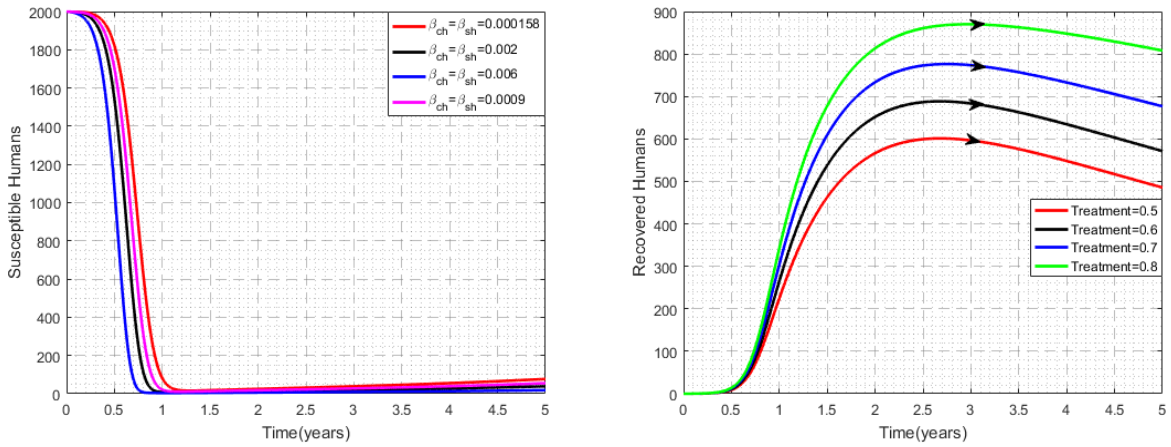

(a) Variations in Susceptible Humans

(b) Variations in Recovered Humans

Figure 7: Respective Variations in susceptible and recovered humans due to changes in transmission and human treatment rates.

Figure 7a illustrates significant decrease in the susceptible humans number due to the interaction with infective domestic ruminants in a period of one year. In addition, Fig. 7b demonstrates that an increase in the rate of treatments increases the number of recovered humans. That is, to minimize or eliminate Brucellosis prevalence within the human population, efforts must be invested to control animal Brucellosis alongside with treatment of Brucellosis in humans.

3.6 Conclusion

This chapter intended at formulating and analyzing a mathematical model that investigates various control parameters' impact on the conveyance of Brucellosis in livestock and humans. The focus was on livestock vaccination; human treatment; gradual culling of animals through slaughter; and environmental hygiene and sanitation. Both numerical simulations and analytical solutions demonstrate that Brucellosis is a perfect zoonosis; the disease in humans does not affect the livestock population. This is due to the fact that the transmission in human solely depends on ruminants Brucellosis; that is human Brucellosis can be eliminated only if ruminant

Brucellosis is eliminated. Given the fact that effective control of human Brucellosis entirely depends on the controls vested on livestock, effective control of the disease needs collaboration between public health and animal health sectors.

CHAPTER FOUR

OPTIMAL CONTROL STRATEGIES FOR THE INFECTIOLOGY OF BRUCELLOSIS

In this chapter we investigate and present the effects of various combinations of personal protection, gradual slaughtering of seropositive domestic ruminants, sanitation of the surroundings, and livestock vaccination in controlling of Brucellosis conveyance dynamics. We formulate and derive the necessary conditions governing the optimal control problem using the method of Pontryagin's Maximum Principle. The primary objective is to reduce Brucellosis conveyance in humans and livestock along with the costs of the control schemes. Incremental Cost-effectiveness Ratio (ICER) is employed to obtain the control strategy with high impact in disease control while minimizing the cost of its implementation. The sections under this chapter include: model formulation, characterization of the optimal control problem, numerical simulations, cost-effective investigation, as well as the chapter conclusion.

4.1 Optimal Control Model Formulation

In this section we construct a Brucellosis conveyance model embedding the time-dependent controls on some attributes. The most relevant rationale for adopting the precautionary and control mechanisms against Brucellosis is to lower its prevalence, and possibly eliminate it from the community. Specifically, preventive mechanism reduces vulnerability of healthy subpopulation whilst a variety of pathogenic folks in the population is minimized through control strategies. We use a time dependent control variable u_1 to represent livestock vaccination which aims at minimizing their vulnerability and subsequently lower the infection spread to the immunization coverage failure rate $(1-u_1(t))\lambda_1$. That is to say, $u_1(t)$ measures the efficacy of $Rev1$ and $S19$ vaccines for small ruminants and cattle respectively, and $(1-u_1(t))\lambda_1$ is the failure rate in vaccination coverage for livestock. In the case of 100% vaccination coverage, zero Brucellosis incidence is logged in that specific area. For this reason, $u_1(t)$ targets at lowering the vulnerability level of healthy livestock in conjunction with the disease spread rate. By virtue of the fact that there is neither treatment of infected ruminants nor disease-induced deaths, the time-dependent variable $u_2(t)$ is introduced as the control effort that appraises the effectiveness of progressive infective livestock culling, d_s and d_c for the infective small ruminants and cattle respectively. Additionally, the progressive slaughtering of infective livestock focuses on

restricting their population and subsequently decrease the disease spread rate to $u_2(t)d_s$ and $u_2(t)d_c$ in small ruminants and cattle respectively. To lower bacterial load from the surroundings, a control parameter $u_3(t)$ is proposed, measuring the effectiveness of sanitation τ of the surroundings. Specifically, the hygiene and sanitation of the surroundings concerns appropriate disposal of aborted foetuses and placentas. A time dependent control parameter $u_4(t)$ that measures the efficiency of personal protection is introduced in the model so that $(1 - u_4(t))\lambda_2$ becomes the inefficaciousness rate of the control scheme. Personal protection in this sense connotes environmental protection, personal hygiene, food safety, and adopting risk-free working conducts. Further, risk-free working conduct refers to the use of safety equipments - masks, gloves, eye-wear and closed footwear - at manipulating possibly contaminated materials like placentas, gravid uterus, and aborted foetuses. Built on the premise that human Brucellosis treatment lowers the disease in humans only and that it has extremely small or negligible spread obstructing outcome in livestock, the time-dependent control over this attribute shall not be introduced in the model. The Pontryagin's Maximum Principle is employed in determination of the required conditions for optimal control and identification the best combination. The main purpose is to restrict or inhibit the spread of Brucellosis and minimize the cost of administering these controls.

4.1.1 Model Presumptions

The optimal control model was formulated in accordance with the following assumptions:

(i) There is homogeneity in the interaction of individuals in every subpopulation;

(ii) The spread of Brucellosis between small ruminants and cattle is negligible;

(iii) The environment is contaminated by *Brucella* pathogens from infected animals;

(iv) Seropositivity in animals is for life;

(v) Immunized livestock can get illness in case their resilience against the disease fades;

(vi) Natural death rate in every breed is constant;

(vii) Natural death in each breed is less than the birth rate.

The flow diagram that incorporates time-dependent control parameters is displayed in Fig. 8 whilst Table 5 summarize the variables and Table 6 the model parameters.

Table 5: Model Variables

Variable	Description
$S_h(t)$	Number of susceptible humans at time t
$I_h(t)$	Number of infected human at time t
$R_h(t)$	Number of recovered humans at time t
$S_c(t)$	Number of susceptible cattle at time t
$I_c(t)$	Number of infected cattle at time t
$S_s(t)$	Number of susceptible small ruminants at time t
$I_s(t)$	Number of infected small ruminants at time t
$B(t)$	Number of brucella bacteria load per unit volume in the environment at time t

4.1.2 The Optimal Control Problem

Figure 8 illustrates the linkages between human, environment, cattle, and small ruminants groups. The model developed is displayed in form of a system of differential equations (4.1).

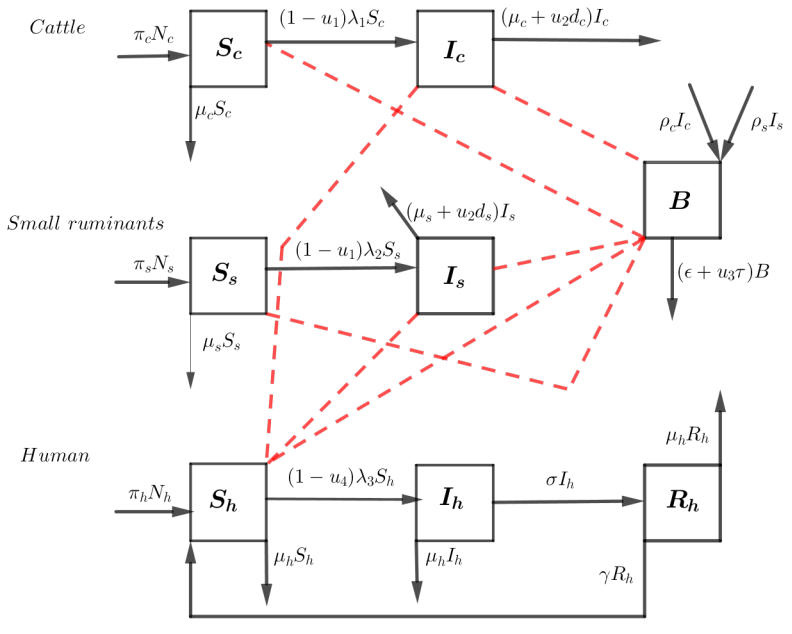

Figure 8: An illustration of Brucellosis transmission in humans and animals. Solid arrows indicate individual movement from one class to another and dotted lines indicate contacts leading to contagion.

Table 6: Model parameters and their description

Parameter	Description
π_c	Per capita cattle birth rate
π_h	Per capita human birth rate
σ	Human recovery rate
μ_h	Per capita human natural death rate
β_c	Within cattle transmission rate
α_c	Brucella from the environment to cattle transmission rate
α_s	Brucella from the environment to small ruminants transmission rate
α_h	Brucella from the environment to human transmission rate
β_{ch}	Cattle to human transmission rate
β_{sh}	Small ruminants to human transmission rate
π_s	Small ruminants per capita birth rate
β_s	Within small ruminants transmission rate
μ_s	Per capita small ruminants natural death rate
τ	Environmental hygiene and sanitation rate
ϵ	Decaying rate of brucella in the environment
d_c	Culling rate of seropositive cattle
d_s	Culling rate of seropositive small ruminants

$$
\begin{aligned}
\frac{dS_c}{dt} &= \pi_c N_c^0 - ((1-u_1(t))(\beta_c I_c + \alpha_c B) + \mu_c) S_c \\
\frac{dI_c}{dt} &= (1-u_1(t))(\beta_c I_c + \alpha_c B) S_c - (\mu_c + u_2(t) d_c) I_c \\
\frac{dS_s}{dt} &= \pi_s N_s^0 - ((1-u_1(t))(\beta_s I_s + \alpha_s B) + \mu_s) S_s \\
\frac{dI_s}{dt} &= (1-u_1(t))(\beta_s I_s + \alpha_s B) S_s - (\mu_s + u_2(t) d_s) I_s \\
\frac{dS_h}{dt} &= \pi_h N_h^0 + \gamma R_h - ((1-u_4(t))(\beta_{hc}(t) I_c + \beta_{hs} I_s + \beta_{hh}(t) I_h + \alpha_h B) + \mu_h) S_h \\
\frac{dI_h}{dt} &= (1-u_4(t))(\beta_{hc} I_c + \beta_{hs} I_s + \beta_{hh} I_h + \alpha_h B) S_h - (\sigma + \mu_h + d_h) I_h \\
\frac{dR_h}{dt} &= \sigma I_h - (\gamma + \mu_h) R_h \\
\frac{dB}{dt} &= \rho_c I_c + \rho_s I_s - (\epsilon + u_3(t)\tau) B
\end{aligned}
\tag{4.1}
$$

In determination of the optimal efforts, an objective functional J is formulated and minimized subject to the number of human and livestock infections along with the cost of implementing the controls:

$$
J = \int_0^{t_f} \left(A_1 I_c + A_2 I_s + A_3 B + A_4 I_h + \frac{B_1 u_1^2}{2} + \frac{B_2 u_2^2}{2} + \frac{B_3 u_3^2}{2} + \frac{B_4 u_4^2}{2} \right) dt \tag{4.2}
$$

where, A_1, A_2, A_3, and A_4, are positive constant weights for tainted bovine, tainted small ruminants, *Brucella* within the surroundings and septic human sub-populations respectively. Besides, B_1, B_2, B_3, and B_4 are respectively the positive constant weights balancing the cost elements attached to the control parameters u_1, u_2, u_3, and u_4. Importantly, the cost associated to any control scenario is presumed to be non-linear and takes a quadratic form which is: $\frac{B_1 u_1^2}{2}$ refers to the cost of control tactics related to ruminants vaccination, $\frac{B_2 u_2^2}{2}$ stands for the cost attached to the gradual culling of tainted livestock scheme, $\frac{B_3 u_3^2}{2}$ represents the cost connected to hygiene and sanitation of the surroundings, and $\frac{B_4 u_4^2}{2}$ portrays the cost attached to personal protection.

In light of the objective functional $J(u_1, u_2, u_3, u_4)$, the intention is to reduce the number of tainted humans and livestock alongside the minimization of the cost for controls, $u_1(t), u_2(t), u_3(t)$, and $u_4(t)$. We search the the optimal control solutions $u_1^*(t), u_2^*(t), u_3^*(t)$, and $u_4^*(t)$ such that:

$$
J(u_1^*, u_2^*, u_3^*, u_4^*) = min\{J(u_1, u_2, u_3, u_4) | u_1, u_2, u_3, u_4 \in u\}. \tag{4.3}
$$

where,

$\mathbf{u} = \{u_1, u_2, u_3, u_4\}$ so that u_1, u_2, u_3, and u_4 are measurable with: $0 \leq u_1 \leq 1$, $0 \leq u_2 \leq 1$, $0 \leq u_3 \leq 1$, and $0 \leq u_4 \leq 1$, for $t \in [0, \ t_f]$ is a control set.

4.2 Existence of an Optimal Control

Theorem 4.1

An optimal control set $(u_1^*, u_2^*, u_3^*, u_4^*) \in \mathbf{u}$ with corresponding non-negative states $(S_c, I_c, S_s, I_s, S_h, I_h, R_h)$ that minimizes the objective functional $J(u_1(t), u_2(t), u_3(t), u_4(t))$ exists.

Proof. The positiveness and consistent boundedness of the state variables alongside the controls on $[0, t_f]$ suggests the existence of a minimizing sequence

$$J(u_1^n(t), u_2^n(t), u_3^n(t), u_4^n(t))$$

such that

$$\lim_{n\to\infty} J(u_1^n(t), u_2^n(t), u_3^n(t), u_4^n(t)) = \inf_{(u_1^n(t), u_2^n(t), u_3^n(t), u_4^n(t)) \in u} J(u_1^n(t), u_2^n(t), u_3^n(t), u_4^n(t)).$$

The boundedness of all the state and control parameters insinuates that all derivatives of the state variables are bounded as well. Supposing the respective sequence of the state variables be denoted by $(S_c, I_c, S_s, I_s, S_h, I_h, R_h, B)$, subsequently all state variables are Lipschitz continuous with the same Lipschitz constant. This means that the sequence $(S_c, I_c, S_s, I_s, S_h, I_h, R_h)$ is consistently equicontinuous in $[0, t_f]$. In accordance with the method by Lukes and DL (1982), the state sequence has a subsequence that converges steadily to $(S_c, I_c, S_s, I_s, S_h, I_h, R_h, B)$ in $[0, t_f]$. In addition, it can be established that the control sequence $u^n = (S_c^n, I_c^n, S_s^n, I_s^n, S_h^n, I_h^n, R_h^n, B^n)$ has a subsequence that converges weakly in $L^2(0, t_f)$. Let $(u_1^*, u_2^*, u_3^*, u_4^*) \in u$ be designed that $u_i^n \to u_i^*$ weakly in $L^2(0, t_f)$ for $i = 1, 2, 3, 4$. Implementing the lower semi-continuity of norms in weak L^2, we have:

$$\|u_i^*\|_{L^2}^2 \leq \lim_{n\to\infty} \inf \|u_i^n(t)\|_{L^2}^2, \ i = 1, 2, 3, 4.$$

This means that,

$$J(u_1^*, u_2^*, u_3^*, u_4^*) \leq \lim_{n\to\infty} \int_0^{t_f} (A_1 I_c^n + A_2 I_s^2 + A_3 I_h^n + A_4 B_4^n + \frac{B_1 u_1^n}{2} + \frac{B_2 u_2^n}{2} + \frac{B_3 u_3^n}{2} + \frac{B_4 u_4^n}{2}) dt$$

Therefore, the controls set $(u_1^*, u_2^*, u_3^*, u_4^*)$ that minimizes the objective functional $J(u_1, u_2, u_3, u_4)$ exists. □

4.3 Optimal Control Characterization

We derives the conditions required for an optimal control and formulates the optimality system that uses lower and upper bound approach to describe the formulated optimal control problem. The essential requirement is that the control problem should satisfy Pontryagin's maximum principle (Pontryagin *et al*., 1962). Such a principle transposes system (4.1) and equation (4.2) to a point-wise minimization problem of a Hamiltonian H, with respect to $u_1, u_2, u_3,$ and u_4 designated by:

$$\begin{aligned} H =& A_1 I_c + A_2 I_s + A_3 B + A_4 I_h + \frac{B_1 u_1^2}{2} + \frac{B_2 u_2^2}{2} + \frac{B_3 u_3^2}{2} + \frac{B_4 u_4^2}{2} \\ &+ \lambda_{S_c}(\pi_c N_c^0 - ((1-u_1)(\beta_c I_c + \alpha_c B) + \mu_c) S_c) \\ &+ \lambda_{I_c}((1-u_1)(\beta_c I_c + \alpha_c B) S_c - (\mu_c + u_2) I_c) \\ &+ \lambda_{S_s}(\pi_s N_s^0 - ((1-u_1)(\beta_s I_s + \alpha_s B) + \mu_s) S_s) \\ &+ \lambda_{I_s}((1-u_1)(\beta_s I_s + \alpha_s B) S_s - (\mu_s + u_2) I_s) \\ &+ \lambda_B(\rho_c I_c + \rho_s I_s - (\epsilon + u_3 \tau) B) \\ &+ \lambda_{S_h}(\pi_h N_h^0 + \gamma R_h - ((1-u_4)(\beta_{hc} I_c + \beta_{hs} I_s + \beta_{hh} I_h + \alpha_h B) + \mu_h) S_h) \\ &+ \lambda_{I_h}((1-u_4)(\beta_{hc} I_c + \beta_{hs} I_s + \beta_{hh} I_h + \alpha_h B) S_h - (\sigma + \mu_h + d_h) I_h) \\ &+ \lambda_{R_h}(\sigma I_h - (\gamma + \mu_h + d_h) R_h) \end{aligned} \tag{4.4}$$

where λ_{S_c}, λ_{I_c}, λ_{S_s}, λ_{I_s}, λ_B, λ_{S_h}, λ_{I_h}, and λ_{R_h}, are the adjoint or co-state variables.
Implementing Pontryagin's maximum principle and the existence result for the optimal control described in Fleming and Rishel (2012), we secure:

Theorem 4.2

For optimal tetra controls u_1^*, u_2^*, u_3^* and u_4^* that minimizes $J(u_1, u_2, u_3, u_4)$ over u, there exist adjoint variables λ_{S_c}, λ_{I_c}, λ_{S_s}, λ_{I_s}, λ_B, λ_{S_h}, λ_{I_h}, and λ_{R_h}, satisfying:

$$
\begin{aligned}
\frac{d\lambda_{S_c}}{dt} &= (1-u_1)(\beta_c I_c + \alpha_c B)(\lambda_{S_c} - \lambda_{I_c}) + \mu_c \lambda_{S_c} \\
\frac{d\lambda_{I_c}}{dt} &= -A_1 + (1-u_1)\left(\lambda_{S_c} - \lambda_{I_c}\right)\beta_c S_c + \lambda_{I_c}(\mu_c + u_2 d_c) \\
&\quad + (1-u_4)\left(\lambda_{S_h} - \lambda_{I_h}\right)\beta_{hc} S_h - \rho_c \lambda_B \\
\frac{d\lambda_{S_s}}{dt} &= (1-u_1)(\beta_s I_s + \alpha_s B)(\lambda_{S_s} - \lambda_{I_s}) + \mu_s \lambda_{S_s} \\
\frac{d\lambda_{I_s}}{dt} &= -A_2 + (1-u_1)\left(\lambda_{S_s} - \lambda_{I_s}\right)\beta_s S_s + \lambda_{I_s}(\mu_s + u_2 d_s) \\
&\quad + (1-u_4)\left(\lambda_{S_h} - \lambda_{I_h}\right)\beta_{hs} S_h - \lambda_B \rho_s \\
\frac{d\lambda_{S_h}}{dt} &= (1-u_4)(\beta_{hc} I_c + \beta_{hs} I_s + \beta_{hh} I_h + \alpha_h B)\left(\lambda_{S_h} - \lambda_{I_h}\right) + \mu_h \lambda_{S_h} \\
\frac{d\lambda_{I_h}}{dt} &= -A_4 + (1-u_4)\left(\lambda_{S_h} - \lambda_{I_h}\right)\beta_{hh} S_h + \lambda_{I_h}(\sigma + \mu_h + d_h) - \sigma \lambda_{R_h} \\
\frac{d\lambda_{R_h}}{dt} &= \gamma\left(\lambda_{R_h} - \lambda_{S_h}\right) + \mu_h \lambda_{R_h} \\
\frac{d\lambda_B}{dt} &= -A_3 + (1-u_1)(\lambda_{S_c} - \lambda_{I_c})\alpha_c S_c + (1-u_1)(\lambda_{S_s} - \lambda_{I_s})\alpha_s S_s \\
&\quad + (1-u_4)(\lambda_{S_h} - \lambda_{I_h})\alpha_h S_h + \lambda_B(\epsilon + u_3 \tau)
\end{aligned}
\tag{4.5}
$$

with transversality conditions:

$$
\lambda_{S_c}(t_f) = \lambda_{I_c}(t_f) = \lambda_{S_s}(t_f) = \lambda_{I_s}(t_f) = \lambda_B(t_f) = \lambda_{S_h}(t_f) = \lambda_{I_h}(t_f) = \lambda_{R_h}(t_f) = 0. \tag{4.6}
$$

The following characterization holds on the interior of the control set u

$$
\begin{aligned}
u_1^* &= max\left\{0, min\left(1, \frac{1}{B_1}\left(\left(\beta_c I_c + \alpha_c B\right)\left(\lambda_{I_c} - \lambda_{S_c}\right)S_c + \left(\beta_s I_s + \alpha_s B\right)\left(\lambda_{I_s} - \lambda_{S_s}\right)S_s\right)\right)\right\} \\
u_2^* &= max\left\{0, min\left(1, \frac{1}{B_2}\left(d_c I_c \lambda_{I_c} + d_s I_s \lambda_{I_s}\right) S_c\right)\right\} \\
u_3^* &= max\left\{0, min\left(1, \frac{1}{B_3}\lambda_B B\right)\right\} \\
u_4^* &= max\left\{0, min\left(1, \frac{1}{B_4}\left(\beta_{hc} I_c + \beta_{hs} I_s + \beta_{hh} I_h + \alpha_h B\right)\left(\lambda_{I_h} - \lambda_{S_h}\right)S_h\right)\right\}
\end{aligned}
\tag{4.7}
$$

where λ_{S_c}, λ_{I_c}, λ_{S_s}, λ_{I_s}, λ_B, λ_{S_h}, λ_{I_h}, and λ_{R_h}, are solutions to equation (4.6).

Proof. The form of adjoint (or costate) system (4.5) and transversality conditions (4.6) are standard outcomes from Pontryagin's Maximum Principle (Pontryagin *et al.*, 1962). To get the costate system (4.5), the partial derivatives of the Hamiltonian (H) (4.4) with respect to each

state variable are computed as follows:

$$\begin{aligned}
\frac{d\lambda_{S_c}}{dt} &= -\frac{\partial H}{\partial S_c}; \lambda_{S_c}(t_f) = 0 \\
&\vdots \\
\frac{d\lambda_{R_h}}{dt} &= -\frac{\partial H}{\partial R_h}; \lambda_{R_h}(t_f) = 0
\end{aligned} \tag{4.8}$$

The optimality equations (4.7) are deduced by computing the partial derivative of the Hamiltonian equation (4.4) with respect to every control parameter and solve for the optimal values of u_i^* where the derivative vanishes. That is to say: $\frac{\partial H}{\partial u_i} = 0$ for $0 \leq u_i \leq 1$ and $i = 1, 2, 3, 4$.
For instance:

$$\frac{\partial H}{\partial u_1} = B_1 u_1 + (\lambda_{S_c} - \lambda_{I_c})(\beta_c I_c + \alpha_c B)S_c + (\lambda_{S_s} - \lambda_{I_s})(\beta_s I_s + \alpha_s B)S_s$$

which gives,

$$u_1^* = \frac{1}{B_1} = (\lambda_{I_c} - \lambda_{S_c})(\beta_c I_c + \alpha_c B)S_c + (\lambda_{I_s} - \lambda_{S_s})(\beta_s I_s + \alpha_s B)S_s$$

The characterization equation (4.7) is deduced through solving for u_i^* subject to the constraints. The numerical solutions of the optimality system and the respective results of varying the optimal controls u_1, u_2, u_3 and u_4,, choice of parameter options plus interpretation from diverse instances are discussed in the next subsection. □

4.4 Numerical Simulations

The numerical analysis of the Brucellosis optimal control model system (4.4) is described in this subsection. Personal protection, vaccination of susceptible livestock, environmental hygiene and sanitation, and the gradual culling of seropositive ruminants are the controls of interest. The optimal control solution is found through solving the optimality system that comprises of the adjoint system (4.5) and the state system (4.1). The Fourth-order Runge–Kutta iterative scheme method is employed in solving the state equations with an initial estimate for the controls over the simulated time. The backward fourth-order Runge–Kutta scheme was used in solving the adjoint equations by utilizing the existing iteration solutions of the state equations due to the transversality conditions (4.8). Besides, the convex combination of the prior controls and the value from the characterizations (4.7) are applied in updating the controls. The procedure is reiterated and the iterations are obstructed once the values of unknowns at the preceding iterations are so close to the ones at the existing iteration (Lenhart & Workman, 2007). By

virtue of the fact that Brucellosis is endemic in many sub-Saharan Africa region countries and that a single control measure cannot prevent the infection, an investigation on the impacts of merging a minimum of three control parameters over a six-years period is done. Furthermore, the estimation of the objective functional's real weights is extremely demanding and requires a bunch of information. In that regard, the objective function weights are chosen on a theoretical basis as; $A_1 = 15$, $A_3 = 5$, $A_2 = 20$, $A_4 = 10$, $B_1 = 15$, $B_2 = 10$, $B_3 = 10$, $B_4 = 10$ just to grant the control parameters proposed in the paper, and the initial state variables are chosen as; $S_c(0) = 200, I_c(0) = 10, S_s(0) = 200, I_s(0) = 5, S_h(0) = 50, I_h(0) = 10,$ and $R_h(0) = 5, B(0) = 100$ while the parameter values used are in Table 7.

The parameter values adopted in computations are predominantly from Li, Sun, Zhang, Jin *et al*. (2014).

Table 7: Model parameter values

Parameter	Value	Unit
Λ_c	0.3	$year^{-1}$
β_c	0.0011	$year^{-1}$
μ_c	0.25	$year^{-1}$
d_c	0.35	$year^{-1}$
α_c	0.00035	$year^{-1}$
ρ_c	10	$year^{-1}$
ϵ	8	$year^{-1}$
τ	12	$year^{-1}$
Λ_s	0.4	$year^{-1}$
β_s	0.001	$year^{-1}$
μ_s	0.35	$year^{-1}$
d_s	0.4	$year^{-1}$
α_s	0.00032	$year^{-1}$
ρ_s	15	$year^{-1}$

4.4.1 Strategy A: Environmental Sanitation, Gradual Culling and Vaccination

In this control scenario, the effectiveness of livestock immunization u_1, gradual culling of seropositive livestock, u_2 and environmental hygiene and sanitation, u_3 are utilized in the min-

imization of the objective functional J whilst personal protection control u_4, is not practiced. Figure 9 depicts the patterns observed in infectious compartments.

.

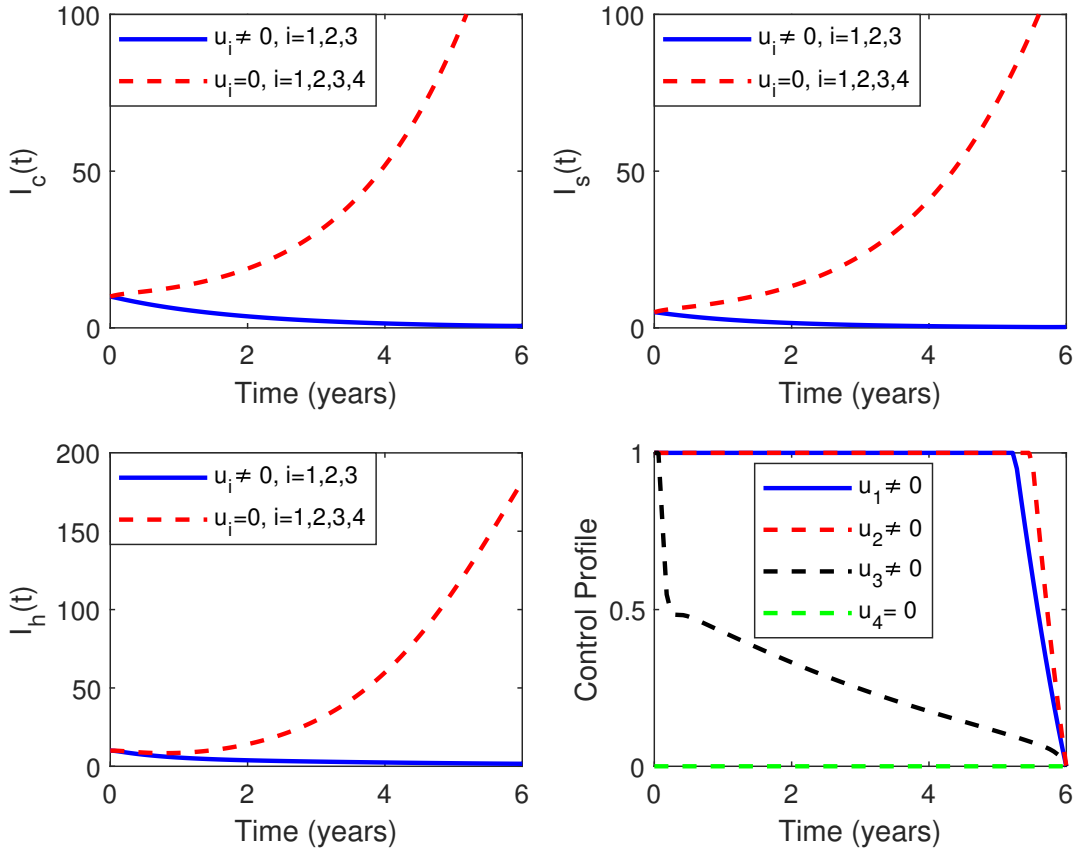

Figure 9: Brucellosis dynamics under culling of ruminants, vaccination, and environmental hygiene.

Figure 9 indicates that a concurrent implementation of the three control tactics in four consecutive years leads to Brucellosis eradication in cattle, and small ruminants in two years while 2-3 years are required for eradication of the disease in humans. In the case of no controls, the infectious classes grow exponentially.

4.4.2 Strategy B: Personal Protection, Vaccination and Gradual Culling

Under this scheme, personal protection, u_4, vaccination of livestock u_1, and the gradual culling of seropositive ruminants, u_2 are applied in the objective function J optimization whereas surroundings hygiene sanitation control, u_3 is not implemented. Figure 10 exemplifies the alterations in the infectious compartments.

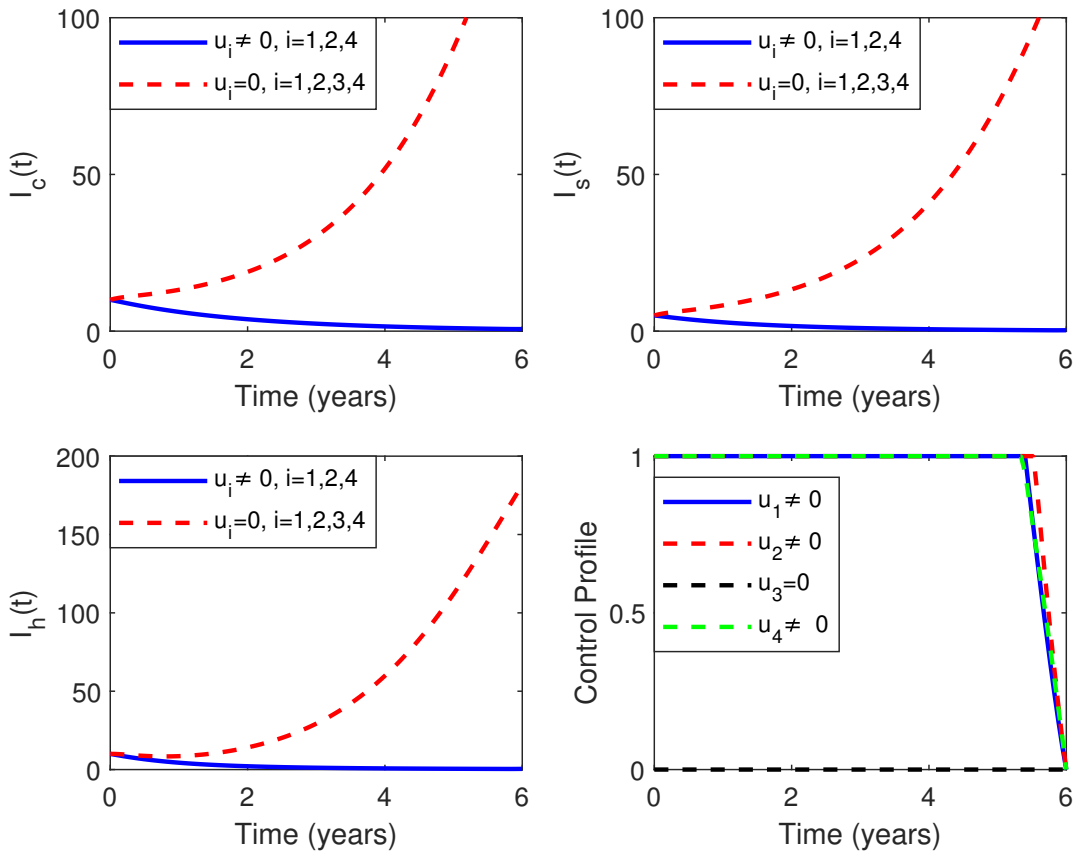

Figure 10: Livestock and human Brucellosis dynamics under personal protection, vaccination, and the gradual culling of seropositive ruminants controls.

Figure 10 demonstrates that the bovine population achieves its Brucellosis-free equilibrium less than 4 years period while eradication of the disease in humans and small ruminants is possible in less than 2 years provided the three controls is jointly employed. In the event of missing controls, the tainted classes grow at rapid pace.

4.4.3 Strategy C: Personal Protection, Environmental Hygiene and Vaccination

In this scenario, personal protection, u_4, livestock vaccination control u_1, and environmental sanitation, u_3 are utilized in the optimization of the objective functional J whereas gradual culling of seropostive livestock control u_2, remains unexploited. Figure 11 depicts the trends in the tainted classes.

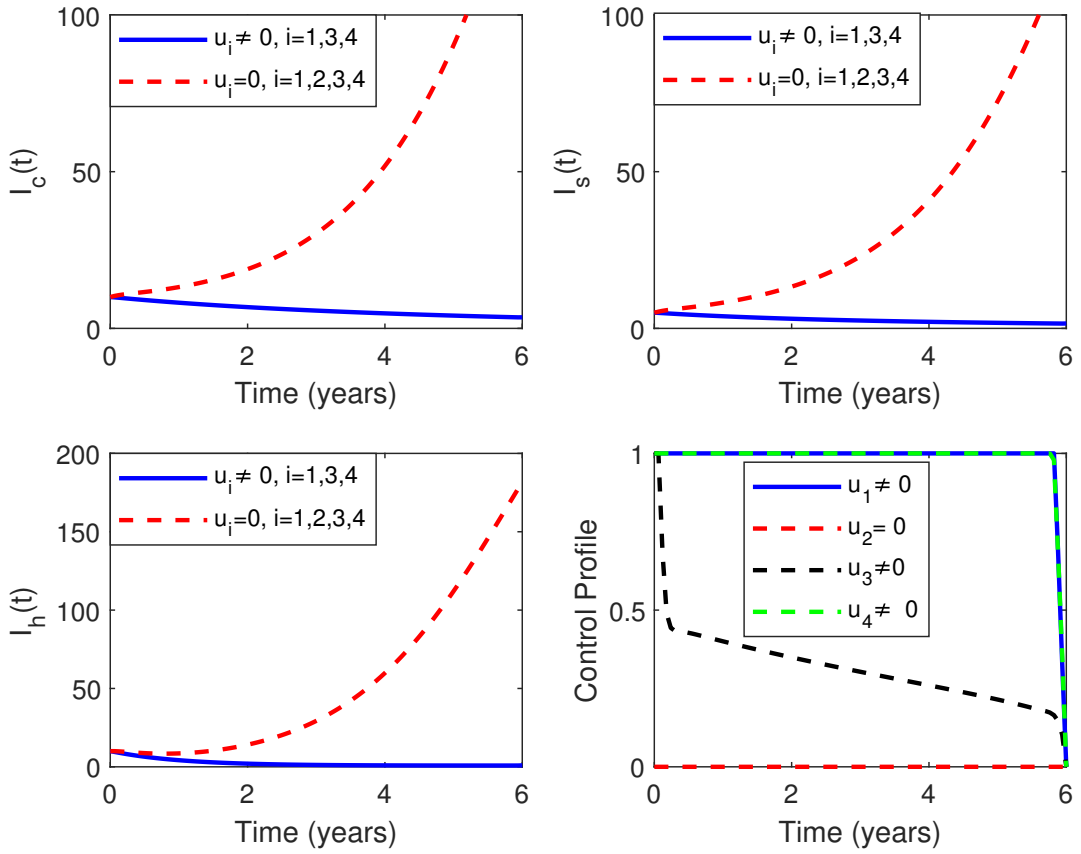

Figure 11: Brucellosis dynamics under optimal personal protection, vaccination, and environmental hygiene controls.

Figure 11 portrays that a combination of the three control tactics gives rise to eradication of the infectious humans and consequently the Brucellosis-free equilibrium is achieved in a two years. Additionally, the small ruminant group reaches its Brucellosis-free equilibrium point within five years whilst that of bovine attains disease equilibrium point is at least six year. In the absence of controls, the number of individuals in the infective classes increases.

4.4.4 Strategy D: Gradual Culling, Personal Protection and Environmental Hygiene

In this strategy, environmental hygiene and sanitation, u_3, personal protection, u_4, and gradual culling of infective ruminants u_2, are utilized in the minimization of the objective functional J whilst vaccination of ruminants u_1, is not taken into account. Figure 12 demonstrates the alteration in infectious human and livestock.

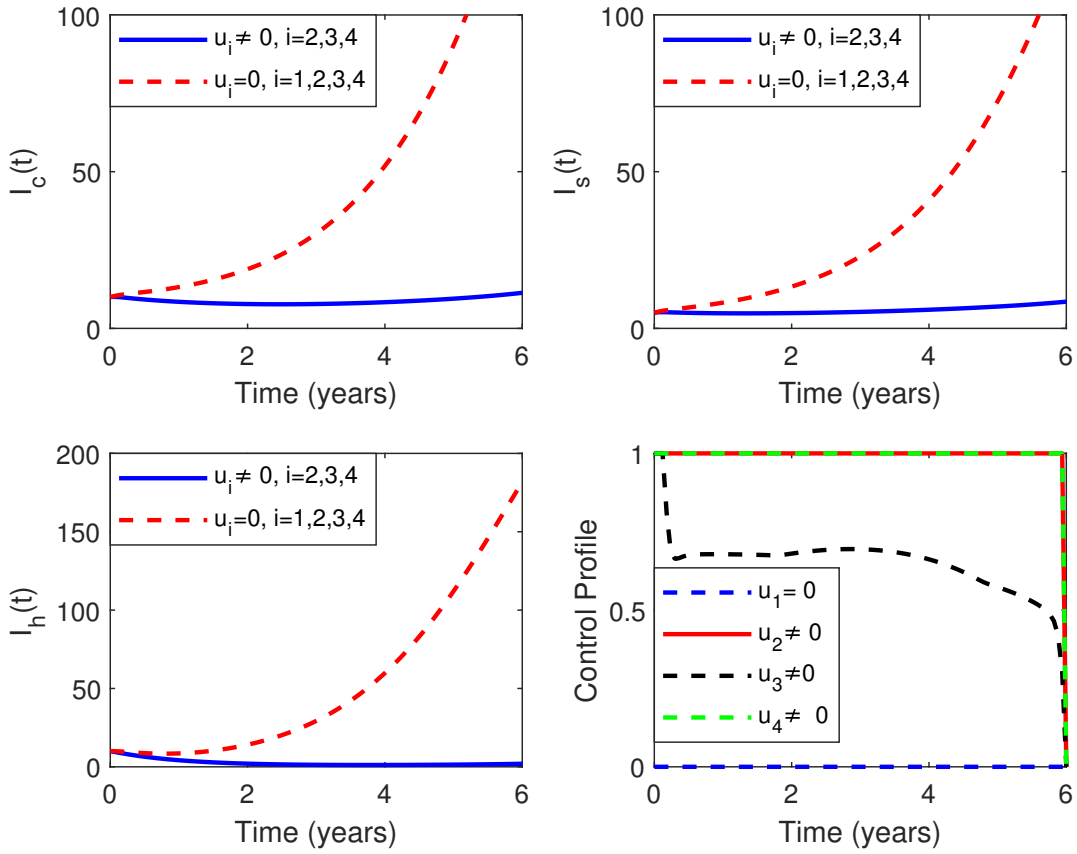

Figure 12: Brucellosis dynamics under optimal personal protection, environmental sanitation and gradual culling of seropostive ruminants controls

Figure 12 reveals that the optimal enforcement of personal protection, environmental hygiene and gradual culling of tainted ruminants reduces the number of septic human to zero in a duration less than two years while tainted ruminants fails to extinct for more than six years. This would mean that implementing a combination of the three control schemes may fail to lead to Brucella-free equilibria in the ruminant classes. Therefore, the tactic is mathematically not advisable.

4.4.5 Strategy E: Personal Protection, Vaccination, Gradual Culling and Environmental Sanitation

Under this scheme, four control strategies; personal protection, u_4, ruminants vaccination, u_1, environmental hygiene and sanitation, u_3 , and the gradual culling of seropositive ruminants, u_2, are concurrently applied in optimizing the objective function J. Figure 13 demonstrates the changes in the tainted subpopulations.

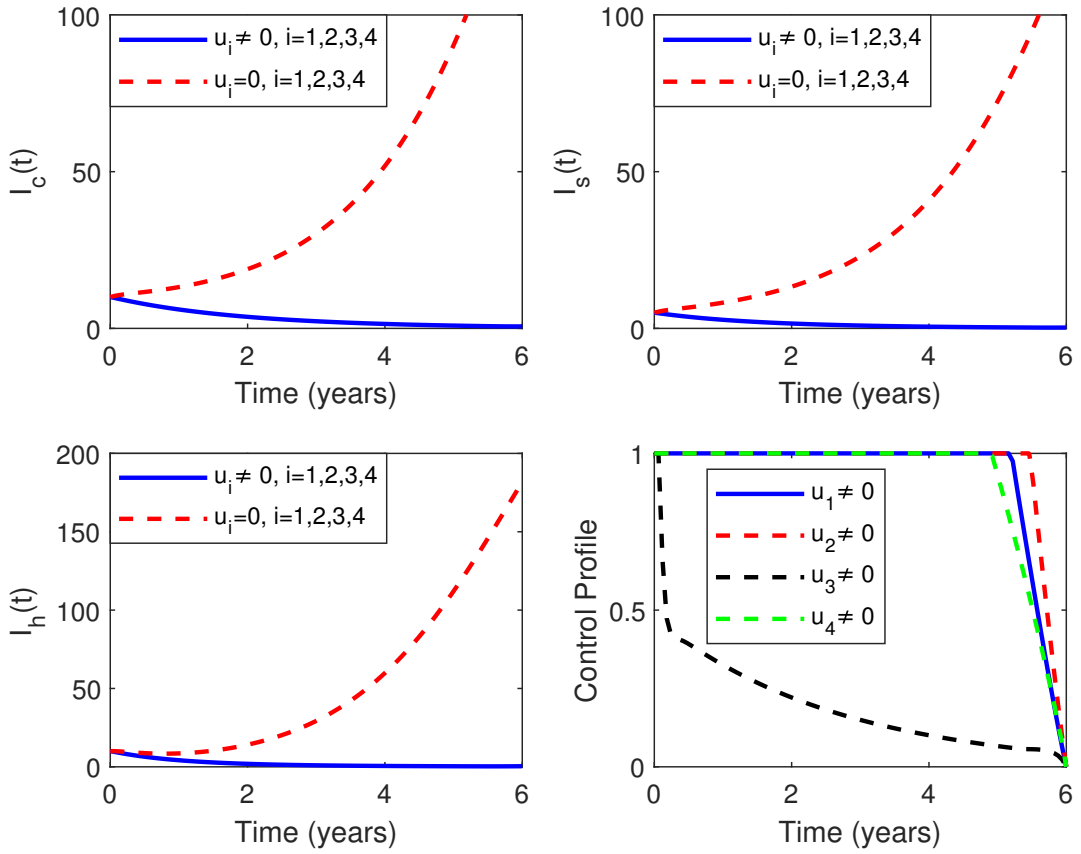

Figure 13: Brucellosis spread personal protection, vaccination, environmental sanitation, and gradual culling of seropositive ruminants controls.

Figure 13 outlines that a combination of the four control tactics have a great impact on the spread of Brucellosis. For instance, the number of tainted small ruminants and human becomes zero in not more than 2 years whereas tainted bovine decrease to zero in not more than 4 years period of time. When the controls are absent, the number of infectious classes grow at exponential rates. Pursuant to this, Shirima *et al.* (2014) stress that the gradual slaughtering of tainted animals, solitude and confinement of pregnant bovines near calving, the use of $S19$ vaccine, proper disposal of placentas and aborted foetuses, and the restricted introduction of new animals leads to Brucellosis eradication.

4.5 Cost-Effectiveness Analysis

This section employed ICER as outlined in Hartwell *et al.* (2011), Klok and Postma (2004), McFarlane and Bayoumi (2004) and Okosun *et al.* (2013) to compute cost-effectiveness of the control scenarios A, B, C, D and E. The selection of this method was based on the fact that, it permits the comparison of the cost-effectiveness among combinations of at least two control

methods. Specifically, a comparison is done amongst two competing control tactics incrementally; one intervention in comparison to the next-less efficient option. ICER is identified as the ratio of disparity in cost amongst two feasible interventions over the disparity in their respective effect provided the competition is on the same resources. Mathematically:

$$ICER \text{ for } X = \frac{\text{Cost of Strategy } X - \text{Cost of Strategy } Y}{\text{Effect of Strategy } X - \text{Effect of Strategy } Y}$$

whereby X and Y correspond to the strategic interventions being compared in the present case, and the benefits or loss in state of health has to be measured in respect to the quality-adjusted life years (QALYs) lost or acquired. That is, the number of infections averted was estimated as the total number of infectious individuals without control minus the total number of individuals with controls According to this method, control options which are much exorbitant and less efficacious are ruled out. In accordance to the numerical simulation results of model (4.1), the five control tactics can be ranked in order of increasing efficacy rated as total afflictions deflected, and the ICER for each two competitive control schemes is computed and displayed in Table 8.

Table 8: ICER for A, B, C, D and E control strategies

Strategy	Total infections averted	Total cost ($)	ICER
Strategy A	12953	4795.7	0.3702
Strategy B	19789	4368	-0.0625
Strategy D	20346	45535	73.9075
Strategy C	21409	13169	-30.4478
Strategy E	24832	4047	-2.6649

According to the presented results in Table 8 strategy D is more costly and under-achieving control scheme. As such, it is discarded from the batch of options so that it does not utilize scarce resources. The recomputed ICER for other four possibilities are therein Table 9.

Table 9: ICER for A, B, C and E control strategies

Strategy	Total infections averted	Total cost ($)	ICER
Strategy A	12953	4795.7	0.3702
Strategy B	19789	4368	-0.0625
Strategy C	21409	13169	5.4324
Strategy E	24832	4047	-2.6649

Table 9 indicates that control tactics C is more costly and an under-achieving strategy, so it is discarded from the set of electable schemes as it fails to utilize scarce resources. Table 10 illustrates the estimated ICER for the other three control options.

Table 10: ICER for A, B, and E control strategies

Strategy	Total infections averted	Total cost ($)	ICER
Strategy A	12953	4795.7	0.3702
Strategy B	19789	4368	-0.0625
Strategy E	24832	4047	-0.0638

The comparative analysis between A and B strategies demonstrates that strategy B saved a cost of $0.0625 than strategy A. As indicated in strategy B's lower ICER, strategy A is strongly dominated; implying that it is an expensive and ineffective as compared to the former. Thus, strategy A is excluded from alternatives set for proper utilization of the scarce resource available. The estimated ICER are displayed in Table 11.

Table 11: ICER for A and E control strategies

Strategy	Total infections averted	Total cost ($)	ICER
Strategy B	19789	4368	0.2208
Strategy E	24832	4047	-0.0638

Besides, Table 11 demonstrates that control tactic E rescued a cost of $0.0638 over strategy B. In this case, the additional expense is negative while the incremental impact is positive (south-east quadrant of the cost-effectiveness plane), the intervention is unambiguously cost-effective (dominant and attaining better performance at a lowest cost) (Hartwell *et al*., 2011; Klok & Postma, 2004; McFarlane & Bayoumi, 2004). The lower ICER of control scheme E demonstrates that strategy B is exorbitant and ineffective as compared to strategy E; that is to say that, strategy E is more efficient and makes more saving than strategy B. Consequently, strategy B is discarded from the set of control options as it fails to utilize scarce resources. Therefore, strategy E which is the combination of livestock immunization, progressive killing of seropositive small ruminants and bovine through slaughtering, surroundings sanitation and personal protection presents the lowest ICER and it is more cost-effective strategy than all other control options.

4.6 Conclusion

The aim of this chapter was to devise and evaluate a mathematical model for assessing the impacts of Brucellosis transmission dynamics control measures. The focus was on human protection; livestock vaccination; hygiene and sanitation of surroundings; and the progressive culling of tainted ruminants through slaughtering. The Pontryagin's Maximum Principle and incremental cost-effectiveness ratio were respectively employed in analyzing the optimal control problem and cost-effectiveness of the control tactics. The results from both optimal control and cost-effectiveness analysis disclosed that merging of livestock immunization, progressive culling of septic small ruminants and bovine, personal protection, and hygiene of the surroundings is the best control scheme since it creates a high impact with lower cost. It was additionally established that control scenario B; the combination of livestock immunization, personal protection, and the progressive slaughtering of tainted small ruminants and bovine by slaughtering is the second most cost-effective strategy after strategy A; the combination of environmental hygiene, livestock vaccination, and progressive culling of diseased small ruminants and bovine. Moreover, control strategy C signifying the combination of livestock immunization, personal protection, surroundings hygiene and sanitation is the subsequent efficient in disease control whereas strategy D is the most inefficient of the control options and it is not advisable for enforcement since it has minor effects and larger cost. An essential examination of the four control schemes have shown that the immunization of ruminants and the progressive slaughtering of seropostive bovine and small ruminants are pre-requisites in designing Brucellosis control strategies. This study advocates that for the efficient control of Brucellosis spread, a combination of livestock immunization, progressive culling of disease bovine and small ruminants, personal protection in humans, and environmental hygiene need to be enacted.

CHAPTER FIVE

MODELING THE IMPACT OF SEASONAL WEATHER VARIATIONS ON THE INFECTIOLOGY OF BRUCELLOSIS

In this chapter we formulate and analyze a mathematical model for the transmission dynamics of Brucellosis that explores the impact of seasonal weather variations on direct and indirect transmission parameters for wild animals, domestic ruminants and human populations. Both analytical solutions and numerical simulations are presented. The chapter is organized into introduction, model formulation and analysis, and numerical simulations.

5.1 Introduction

Seasonal weather variation plays considerable functions in changing the dynamic character of some infectious diseases. For instance, they can influence host-pathogen interactions thereby enabling the parameters of the basic reproduction ratio that establish the rate at which septic hosts are generated (Altizer *et al*., 2006). The seasonal variation of infectious disease incidences is mainly caused by the survival of pathogens outside the host that depends on the attributes of the surroundings (exposure to sunlight, humidity, temperature and soil salinity), host behaviour, host immune function, and the abundance of non-human hosts and vectors (Grassly & Fraser, 2006).

Mathematical models can give an insight on how the sturdiness and mechanisms of seasonal fluctuations can change the persistence and spread of infections. In this view, understanding the timing and aetiology of seasonal fluctuations can provide crucial intuitions on how parasite-host schemes work, when and how parasite control efforts need to be employed, and how risks of the disease will respond to varied patterns of seasonality and anthropogenic climate change. Brucellosis incidences in either developed or developing countries exhibit seasonal fluctuations with high incidences in certain months of the year. According to WHO (2006), there is a notable seasonality in the Brucellosis incidences in countries with temperate or cold climates, with most cases occurring in the summer and spring. This concurs with the climax period for parturition and abortion in animals which consequently results in higher exposure level to people attending animals and consuming their products. Furthermore, seasonality in the transmission dynamics of the disease is mostly attributed to seasonal livestock movements due

to availability of water and grasslands. This is the common practice in sub-Saharan African region countries, for instance majority of the cattle owners (83.1%) in Northern Tanzania move cattle away from homes during dry seasons (Kimaro *et al*., 2018). This changes the dynamics of the disease as a high concentration of animals is expected near water bodies and wildlife parks hence an increase in the contact rate between healthy and diseased animals. Besides, the survival of the pathogens in the environment that depends largely on temperature, humidity, exposure to ultra violent light, soil pH and salinity (Grassly & Fraser, 2006) significantly affect the dynamics of the disease in both domestic animals and humans. Moreover, in ideal environments, the survival of *Brucella spp.* is reported to last up to 135 days (Aune *et al*., 2012). In this view, there is a need to assess the impact of seasonal weather variations in the transmission dynamics of Brucellosis in both human and domestic ruminants using mathematical models.

5.2 Model Formulation

A deterministic model that illustrates the dynamics of Brucellosis in humans and animals is formulated and analysed under this section. More importantly, incorporating the parameters for seasonal weather in the disease transmission routes follows the approach presented in Lolika *et al*. (2018) and Ngeleja *et al*. (2017, 2018). The stimulus of seasonal variations on the direct transmission of Brucellosis in domestic ruminants, humans and wild animals are respectively modeled by the periodic continuous functions $\beta_a(t) = b_1(1 + a_1 \sin \omega t)$, $\beta_h(t) = b_2(1 + a_2 \sin \omega t)$ and $\beta_w(t) = b_3(1 + a_3 \sin \omega t)$ while the indirect transmission in the three populations is captured by $\alpha_a(t) = c_1(1 + r_1 \sin \omega t)$, $\alpha_h(t) = c_2(1 + r_2 \sin \omega t)$ and $\alpha_w(t) = c_3(1 + r_3 \sin \omega t)$ respectively.

Furthermore, we consider the pathogen shedding rate by the infective livestock and wild animals to represented by the periodic functions of the form, $\rho(t) = \rho_0(1 + \rho_1 \sin \omega t)$ and $\rho_w(t) = \rho_2(1 + \rho_3 \sin \omega t)$ respectively. The decaying rate of the pathogens in the environment is also represented by periodic continuous function $\epsilon(t) = \epsilon_0(1 + \epsilon_1 \sin \omega t)$. The constants; $b_1, b_2, b_3, c_1, c_2, c_3, \rho_0, \rho_2$ and ϵ_0 are the baseline values of the parameters $\beta_a, \beta_h, \beta_w, \alpha_a, \alpha_h$, α_w, ρ_a, ρ_w and ϵ respectively, whereas $0 < a_1, a_2, a_3, r_1, r_2, r_3, \rho_1, \rho_3, \epsilon_1 < 1$ are the strength of seasonal forcing in transmission (amplitudes of seasonal variations) for each seasonal parameter, and $\omega = \dfrac{\pi}{6}$, corresponds to one month period of time.

5.2.1 Model Presumptions

The following presumptions were considered in formulation of the Brucellosis model:

(i) Each population is homogeneously mixed;

(ii) Infectious animals shed *Brucella* to the environment;

(iii) Infectiousness of ruminants is life-long;

(iv) Vaccinations do not provide permanent immunity;

(v) The natural mortality rate is constant and less than birth rate in each of the species.

The variables and parameter values per year incorporated in this model are summarized in Table 13 and Table 14, respectively.

Table 13: Model Variables

Variable	Description
$S_h(t)$	Number of susceptible humans at time t
$I_h(t)$	Number of infected human at time t
$R_h(t)$	Number of recovered humans at time t
$S_a(t)$	Number of susceptible animals at time t
$I_a(t)$	Number of infected animals at time t
$V_a(t)$	Number of vaccinated animals at time t
$B(t)$	Number of *brucella* bacteria load per unit volume in the environment at time t

The interactions between humans, domestic animals as well as the pathogens in the environment are shown in Fig. 14 and the resulting model system is as by equations (5.1).

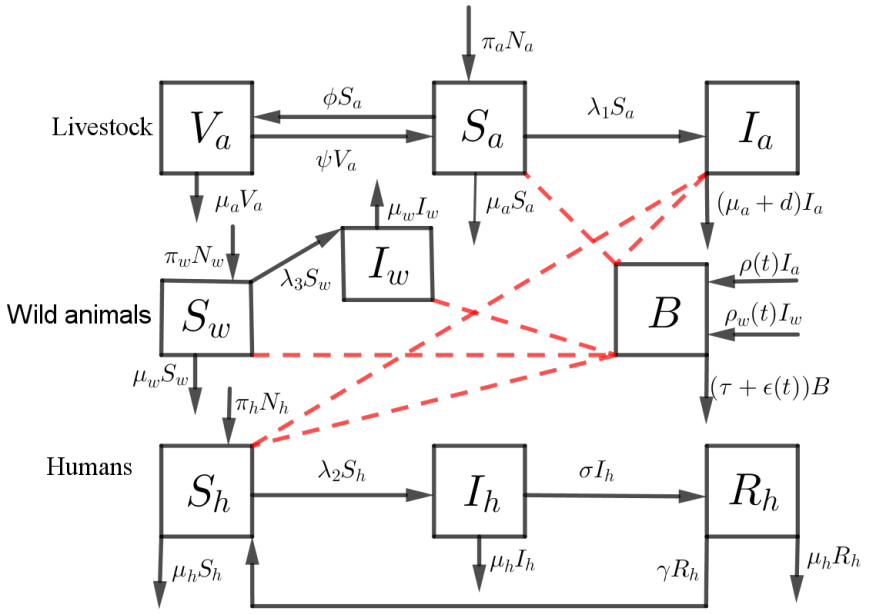

.

Figure 14: Flow diagram for Brucellosis dynamics in wild animals, domestic ruminants and humans.

$$
\begin{cases}
\frac{dV_a}{dt} &= \phi S_a - (\psi + \mu_a) V_a \\
\frac{dS_a}{dt} &= \pi_a N_a + \psi V_a - (\beta_a(t) I_a + \alpha_a(t) B + \phi + \mu_a) S_a \\
\frac{dI_a}{dt} &= (\beta_a(t) I_a + \alpha_a(t) B) S_a - (\mu_a + d) I_a \\
\frac{dS_h}{dt} &= \pi_h N_h + \gamma R_h - (\beta_h(t) I_a + \beta_h I_h + \alpha_h(t) B + \mu_h) S_h \\
\frac{dI_h}{dt} &= (\beta_h(t) I_a + \alpha_h(t) B) S_h - (\sigma + \mu_h) I_h \\
\frac{dR_h}{dt} &= \sigma I_h - (\gamma + \mu_h) R_h \\
\frac{dS_w}{dt} &= \pi_w N_w - (\beta_w(t) I_w + \alpha_w(t) B + \mu_w) S_w \\
\frac{dI_w}{dt} &= (\beta_w I_w + \alpha_w(t) B) - \mu_w I_w \\
\frac{dB}{dt} &= \rho(t) I_a + \rho_w(t) I_w - (\tau + \epsilon(t)) B
\end{cases}
\tag{5.1}
$$

5.2.2 Model Properties

In this subsection the Box Invariance method proposed by Abate *et al.* (2009) was used to assess the well-posedness (existence and feasibility of its solution) of the model (5.1). That is, an investigation into whether the solutions of system (5.1) that has non-negative initial values remain non-negative is presented for $t \geq 0$. Furthermore, the compact form of system (5.1) can

Table 14: Parameters of the model and their description

Parameter	Description	Value	Source
Λ_a	Livestock per recruitment rate	0.1	Nyerere *et al*. (2019)
ϕ_a	Livestock vaccination rate	0.7	Nyerere *et al*. (2019)
Λ_h	Human recruitment rate	0.02	Nyerere *et al*. (2019)
σ	Human recovery rate	0.25	Nyerere *et al*. (2019)
μ_h	Per capita human natural death rate	0.02	Nyerere *et al*. (2019)
ψ	Livestock vaccine efficacy waning rate	0.4	Li *et al*. (2017)
β_a	Within livestock transmission rate	0.0011	Li *et al*. (2017)
d	Gradual culling of seropositive livestock	0.35	Li *et al*. (2017)
μ_a	Per capita livestock natural mortality rate	0.25	Li *et al*. (2017)
Λ_w	Wild animals recruitment rate	0.08	Abatih *et al*. (2015)
β_w	Within wild animals transmission rate	0.05	Abatih *et al*. (2015)
α_w	*Brucella* from B to wild animals transmission rate	0.00035	Li *et al*. (2017)
μ_w	Per capita wild animals natural death rate	0.07	Abatih *et al*. (2015)
α	*Brucella* from B to livestock transmission rate	0.00035	Li *et al*. (2017)
α_h	*Brucella* from the B to human transmission rate	0.002	Nyerere *et al*. (2019)
ρ	*Brucella* shedding rate of infected livestock	0.5	Nyerere *et al*. (2019)
ρ_w	*Brucella* shedding rate of infected wild animals	15	Hou *et al*. (2013)
β_h	Livestock to human transmission rate	0.0002	Nyerere *et al*. (2019)
ϵ	Decaying rate of brucella in the environment	8	Li *et al*. (2019)
τ	Environmental hygiene and sanitation rate	12	Li *et al*. (2019)

be expressed as:

$$\frac{dX}{dt} = AX + F$$

where, $X = (V_a, S_a, I_a, S_h, I_h, R_h, S_w, I_w, B)$, F is a column vector given by

$$F = (0, \pi_a N_a, 0, \pi_h N_h, 0, 0, \pi_w N_w, 0, 0)^T$$

and

$$A = \begin{bmatrix} -(\psi+\mu_a) & \phi & 0 & 0 & 0 & 0 & 0 & 0 & 0 \\ \psi & -\lambda_1 & 0 & 0 & 0 & 0 & 0 & 0 & 0 \\ 0 & \lambda_1 & -(\mu_a+d(t)) & 0 & 0 & 0 & 0 & 0 & 0 \\ 0 & 0 & 0 & \lambda_2+\mu_h & 0 & \gamma & 0 & 0 & 0 \\ 0 & 0 & 0 & \lambda_1 & -(\sigma+\mu_h) & 0 & 0 & 0 & 0 \\ 0 & 0 & 0 & 0 & \sigma & -(\gamma+\mu_h) & 0 & 0 & 0 \\ 0 & 0 & 0 & 0 & 0 & 0 & -(\lambda_3+\mu_w) & 0 & 0 \\ 0 & 0 & 0 & 0 & 0 & 0 & \lambda_3 & -\mu_w & 0 \\ 0 & 0 & \rho & 0 & 0 & 0 & 0 & \rho_w & -\lambda \end{bmatrix}$$

where,

$$\lambda_1 = \beta_a(t)I_a + \alpha(t)B + \phi + \mu_a,$$

$$\lambda_2 = \beta_h(t)I_a + \beta_h(t)I_h + \alpha_h B,$$

$$\lambda_3 = \beta_w(t)I_w + \alpha_w(t)B,$$

and

$$\lambda = \tau + \epsilon(t).$$

Noting that A is Meltzer matrix for all $X \in \mathbb{R}^9_+$. Therefore, based on the fact that $F \geq 0$, model (5.1) is positively invariant in $\mathbb{R}^9_+$, this implies that an arbitrary trajectory of the system starting in $\mathbb{R}^9_+$ forever remains in $\mathbb{R}^9_+$. In addition, F is Lipschitz continuous. Thus, a unique maximal solution exists and so:

$$\mathcal{D} = \{(V_a, S_a, I_a, S_h, I_h, R_h, S_w, I_w, B) \geq 0\} \subseteq \mathbb{R}^9_+$$

is the feasible region for the model (5.1). Thus, model (5.1) is epidemiologically and mathematically well-posed in the region $\mathcal{D}$.

5.2.3 Brucellosis-Free Equilibrium

The Brucellosis-free equilibrium solution for system (5.1) is computed and found to be:

$$(V_a^0, S_a^0, I_a^0, S_h^0, I_h^0, R_h^0, S_w^0, I_w^0, B^0) = \left(\frac{\phi\pi_a N_a^0}{\mu_a(\phi+\psi+\mu_a)}, \frac{(\psi+\mu_a)\pi_a N_a^0}{\mu_a(\phi+\psi+\mu_a)}, 0, \frac{\pi_h N_h^0}{\mu_h}, 0, 0, \frac{pi_w N_w^0}{\mu_w}, 0, 0\right) \tag{5.2}$$

5.2.4 The Reproduction Number

A heterogeneous population with individuals which can be grouped into n homogeneous compartments is considered in this subsection. Let $x = (x_1, ..., x_n)^T$, with $x_i \geq 0$, be the state

of individuals in each compartment. It is assumed that the compartments can be divided into; infected designated as $i = 1, ..., m$, and uninfected designated as $i = m + 1, ..., n$. We also define X_s to be the set of all disease-free states:

$$X_s = \{x \geq 0 : x_i = 0, \forall i = 1, ..., m\}.$$

Let $\mathcal{F}_i(t, x)$ be the rate of new cases entering the i^{th} compartment, $\mathcal{V}_i^+(t, x)$ be the rate of infected cases joining the compartment by other means (for example immigration and births), and $\mathcal{V}_i^-(t, x)$ be the transfer rate of individuals out of compartment i (for example emigrations, recovery and deaths). Henceforth, the Brucellosis transmission model is governed by a non-autonomous ordinary differential system:

$$\frac{dx_i}{dt} = \mathcal{F}_i(t, x) - \mathcal{V}_i(t, x) \triangleq f_i(t, x), i = 1, ..., n, \tag{5.3}$$

where $\mathcal{V}_i(t, x) = \mathcal{V}_i^-(t, x) - \mathcal{V}_i^+(t, x)$.

Following the approach by Van den Driessche and Watmough (2002), and that of Wang and Zhao (2008) for epidemic models, we look at conditions (A1)-(A7) for the Brucellosis model. Given that model system (5.1) is equivalent to a periodic ordinary differential system (5.3), we can easily see that conditions (A1)-(A5) stated below are satisfied.

(A1) For every $1 \leq i \leq n$, the functions $\mathcal{F}_i(t, x)$, $\mathcal{V}_i^+(t, x)$ and $\mathcal{V}_i^-(t, x)$ are continuous and non-negative on $\mathbb{R} \times \mathbb{R}_+^n$ and continuously differentiable with respect to x. This is based on the fact that each function denotes a directed non-negative transfer of individuals.

(A2) There exist a real number $\omega > 0$ such that for each $1 \leq i \leq n$, the functions $\mathcal{F}_i(t, x)$, $\mathcal{V}_i^+(t, x)$ and $\mathcal{V}_i^-(t, x)$ are ω-periodic in t. Biologically this describes a periodic environment by virtue of seasonality.

(A3) If $x_i = 0$, then $\mathcal{V}_i^-(t, x) = 0$. Particularly, if $x \in X_s$ then $\mathcal{V}_i^-(t, x) = 0$ for $i = 1, ..., m$. In other words, there is no transfer of individuals from an empty compartment;

(A4) $\mathcal{F}_i = 0$ for $i > m$. This means that the infection incidences for non-infected classes is zero.

(A5) If $x \in X_s$, then $\mathcal{F}_i = \mathcal{V}_i^+ = 0$ for $i = 1, ..., m$. This implies that if the population is disease free in the beginning, it will remain so.

We know that model system (5.3) has a Brucellosis-free periodic solution, so we define a 5×5 matrix for the non-transmitting compartments as:

$$M(t) = \begin{bmatrix} -(\psi + \mu_a) & \phi & 0 & 0 & 0 \\ \psi & -(\phi + \mu_a) & 0 & 0 & 0 \\ 0 & 0 & -\mu_h & \gamma & 0 \\ 0 & 0 & 0 & -(\gamma + \mu_h) & 0 \\ 0 & 0 & 0 & 0 & -\mu_w \end{bmatrix}$$

Let $\Phi_M(t)$ represent the monodromy matrix of the linear ω-periodic system $\dfrac{dz}{dt} = M(t)z$. Then $\rho(\Phi_M(\omega)) < 1$ implying that $E^0(t)$ is linearly asymptotically stable in the disease-free subspace X_s, that is:

(A6) $\rho(\Phi_M(\omega)) < 1$, whereby $\rho(\Phi_M(\omega))$ is the dominant eigenvalue of $\Phi_M(\omega)$ is satisfied.

For easy presentation of the results and convenience purposes we let C to denote all continuous functions on the real line. If f is a periodic function in C then $\bar{f}$ symbolizes an average value of f on time interval $[0 \;\; T]$ outlined by:

$$\bar{f} = \frac{1}{T} \int_0^T f(t)dt \tag{5.4}$$

for continuous T periodic function $f(t)$. Inspired by the approaches of Van den Driessche and Watmough (2002) and Diekmann *et al*. (2010) we obtain:

$$F = \begin{bmatrix} \dfrac{(\psi + \mu_a)\bar{\beta}_a(t)\pi_a N_a^0}{\mu_a(\phi + \psi + \mu_a)} & 0 & 0 & \dfrac{(\psi + \mu_a)\bar{\alpha}_a(t)\pi_a N_a^0}{\mu_a(\phi + \psi + \mu_a)} \\ \dfrac{\bar{\beta}_h(t)\pi_h N_h^0}{\mu_h} & \dfrac{\bar{\beta}_h(t)\pi_h N_h^0}{\mu_h} & 0 & \dfrac{\bar{\alpha}_h(t)\pi_h N_h^0}{\mu_h} \\ 0 & 0 & \dfrac{\bar{\beta}_w(t)\pi_w N_w^0}{\mu_w} & \dfrac{\bar{\alpha}_w(t)\pi_w N_w^0}{\mu_w} \\ \bar{\rho}_a(t) & 0 & \bar{\rho}_w(t) & 0 \end{bmatrix} \tag{5.5}$$

and

$$V = \begin{bmatrix} \mu_a + d & 0 & 0 & 0 \\ 0 & \sigma + \mu_h & 0 & 0 \\ 0 & 0 & \mu_\omega & 0 \\ 0 & 0 & 0 & (\tau + \bar{\epsilon}(t)) \end{bmatrix} \tag{5.6}$$

and observe that F is non-negative and $(-V)$ is cooperative because its off-diagonal entries are non-negative.

Accordingly, the effective reproductive number of the time-averaged autonomous system is:

$$[R_e] = \frac{R_{11} + R_{33} + \sqrt{(R_{11} - R_{33})^2 + 4R_{13}R_{31}}}{2} \tag{5.7}$$

where,

$$R_{11} = \frac{(\bar{\beta}_a(t)(\tau + \bar{\epsilon}(t)) + \bar{\alpha}_a(t)\bar{\rho}(t))(\psi + \mu_a)\pi_a N_a^0}{\mu_a(\phi + \psi + \mu_a)(\mu_a + d)(\tau + \bar{\epsilon}(t))},$$

$$R_{33} = \frac{(\bar{\beta}_w(t)(\tau + \bar{\epsilon}(t)) + \bar{\alpha}_w(t)\bar{\rho}_w(t))(\psi + \mu_a)\pi_w N_w^0}{\mu_w^2(\tau + \bar{\epsilon}(t))},$$

$$R_{13} = \frac{\bar{\alpha}_a(t)\bar{\rho}_w(t)(\psi + \mu_a)\pi_a N_a^0}{\mu_a\mu_w(\tau + \bar{\epsilon}(t))(\phi + \psi + \mu_a)},$$

and

$$R_{31} = \frac{\bar{\alpha}_w(t)\rho(t)\pi_w N_w^0}{\mu_w(\mu_a + d)(\tau + \bar{\epsilon}(t))}.$$

Generally, the time-averaged control reproductive number computed as the spectral radius of FV^{-1} using Maple package. In this case is found to be:

$$\rho(FV^{-1}) = [R_e] = \frac{1}{T}\int_0^T \frac{R_{11} + R_{33} + \sqrt{(R_{11} - R_{33})^2 + 4R_{13}R_{31}}}{2} dt \tag{5.8}$$

If no interventions are administered, the time-averaged basic reproductive number for model system (5.1) is found to be:

$$[R_0] = \frac{1}{T}\int_0^T \frac{R_{11}^0 + R_{33}^0 + \sqrt{(R_{11}^0 - R_{33}^0)^2 + 4R_{13}^0 R_{31}^0}}{2} dt \tag{5.9}$$

where,

$$R_{11} = \frac{(\bar{\beta}_a(t)\bar{\epsilon}(t) + \bar{\alpha}_a(t)\bar{\rho}(t))\pi_a N_a^0}{\mu_a^2\bar{\epsilon}(t)},$$

$$R_{33} = \frac{(\bar{\beta}_w(t)\bar{\epsilon}(t) + \bar{\alpha}_w(t)\bar{\rho}_w(t)\mu_a)\pi_w N_w^0}{\mu_w^2\bar{\epsilon}(t)},$$

$$R_{13} = \frac{\bar{\alpha}_a(t)\bar{\rho}_w(t)\pi_a N_a^0}{\mu_a\mu_w\bar{\epsilon}(t)},$$

and

$$R_{31} = \frac{\bar{\alpha}_w(t)\rho(t)\pi_w N_w^0}{\mu_w \mu_a \bar{\epsilon}(t)}.$$

$[R_0]$ is interpreted as the average number of secondary cases resulting from the introduction of a single infected individual into a completely susceptible population at a random time of the year. The condition $[R_0] < 1$ is a sufficient and necessary for long-term disease extinction.

Furthermore, let $Y(t,s), t \geq s$, be the evolution operator of the linear ω-periodic system:

$$\frac{dy}{dt} = -V(t)y \tag{5.10}$$

That is, for each $s \in \mathbb{R}$ the 4×4 matrix $Y(t,s)$ satisfies

$$\frac{d}{dt}Y(t,s) = -V(t)Y(t,s), \forall t \geq s, Y(s,s) = I$$

where I is a 4×4 identity matrix. Therefore, the monodromy matrix $\Phi_V(t)$ of (5.10) equals $Y(t,0), t \geq 0$. Thus, condition (A7) below is satisfied.

(A7) The internal evolution of individuals within the infective classes resulting from deaths and movements is dissipative and decays exponentially in many cases. This is due to loss of infective members from natural and disease-induced mortality. Thus, $\rho(\Phi_V(\omega)) < 1$.

In the light of suppositions (A1)-(A7), we analyze the reproduction number for the model system (5.1). For this purpose, we presume that the population is nearby the Brucellosis-free periodic equilibrium $E^0(t)$. In conformity with the standard theory of linear periodic systems (34), there exists $\alpha > 0$ and $K > 0$ such that

$$\|Y(t,s)\| \leq Ke^{-\alpha(t-s)}, \forall t \geq s, s \in \mathbb{R}. \tag{5.11}$$

Consequently:

$$\|Y(t,t-a)F(t-a)\| \leq K\|F(t-a)\|e^{-\alpha a}, \forall t \in \mathbb{R}, a \in [0,\infty). \tag{5.12}$$

Following the method presented by Wang and Zhao (2008) we compute the basic reproduction number of the non-autonomous model system (5.1). Suppose $\Gamma(s)$ is the initial distribution of infective cases in periodic environment, then $F(s)\Gamma(s)$ is the rate of new infectious individuals produced by the infected individuals who were introduced at time s. $Y(t,s)F(s)\Gamma(s)$, represents the distribution of the newly infected at time s, and remain in the infected compartment

at time $t \geq s$. It follows that the cumulative distribution of new infections at t produced by all infected $\Gamma(t)$ individuals introduced at prior to $t = s$ given by:

$$\Psi(t) = \int_{-\infty}^{t} Y(t,s)F(s)\Gamma(s)ds = \int_{0}^{\infty} Y(t,t-a)F(t,t-a)\Gamma(t-a)da, \ \ \forall t \in \mathbb{R}, \ \ \Gamma \in C_\omega \tag{5.13}$$

Let C_ω be the ordered Banach space of all $\omega-$periodic functions from $\mathbb{R}$ to $\mathbb{R}^n$, that is equipped with the maximum norm, $\|.\|_\infty$ and the positive cone $C_\omega^+ = \{\Gamma \in C_\omega \Gamma(t) \geq 0, t \in \mathbb{R}\}$. We define the linear operator $L : C_\omega \to C_\omega$ by

$$(L\Gamma)(t) = \int_{0}^{\infty} Y(t,t-a)F(t,t-a)\Gamma(t-a)da, \ \ \forall t \in \mathbb{R}, \ \ \Gamma \in C_\omega \tag{5.14}$$

where L is the next infection operator. The basic reproductive number is exhibited by:

$$R_\omega = \rho(L) \tag{5.15}$$

where $\rho(L)$ is the dominant eigenvalue of L. By direct calculation, the evolution operator $Y(t,s)$ for the system (5.1) is found to be:

$$Y(t,s) = \begin{bmatrix} e^{-(\mu_a+d)(t-s)} & 0 & 0 & 0 \\ 0 & e^{-(\sigma+\mu_h)(t-s)} & 0 & 0 \\ 0 & 0 & e^{-\mu_\omega(t-s)} & 0 \\ 0 & 0 & 0 & \bar{Y}(t,s) \end{bmatrix} \tag{5.16}$$

with

$$\bar{Y}(t,s) = e^{-(\tau+\epsilon_0)(t-s)+\frac{6\epsilon_0\epsilon_1}{\pi}\left(cos\left(\frac{\pi t}{6}\right)-cos\left(\frac{\pi s}{6}\right)\right)}.$$

Motivated by Posny and Wang (2014), the next infection operator may be evaluated numerically as:

$$\begin{aligned}(L\varphi)(t) &= \int_{0}^{\infty} Y(t,t-a)F(t,t-a)\Gamma(t-a)da \\ &= \int_{0}^{\omega} G(t,a)\Gamma(t-a)da \end{aligned} \tag{5.17}$$

where,

$$\begin{aligned} G(t,s) &\approx \sum_{k=0}^{M} Y(t,t-s-k\omega)F(t-s) \\ &\approx \sum_{k=0}^{M} \begin{bmatrix} m_{11} & 0 & 0 & m_{14} \\ m_{21} & m_{22} & 0 & m_{24} \\ 0 & 0 & m_{33} & m_{33} \\ m_{41} & 0 & m_{43} & 0 \end{bmatrix} \end{aligned}$$

for positive integers M large enough, and

$$\begin{cases} m_{11} = \dfrac{\beta_a(t-s)(\psi+\mu_a)\pi_a N_a^0}{\mu_a(\phi+\psi+\mu_a)} e^{-(\mu_a+d)(t-s)} \\ m_{14} = \dfrac{\alpha_a(t-s)(\psi+\mu_a)\pi_a N_a^0}{\mu_a(\phi+\psi+\mu_a)} e^{-(\mu_a+d)(t-s)} \\ m_{21} = \dfrac{\beta_h(t-s)\pi_h N_h^0}{\mu_h} e^{-(\sigma+\mu_a)(t-s)} \\ m_{22} = \dfrac{\beta_h(t-s)\pi_h N_h^0}{\mu_h} e^{-(\sigma+\mu_a)(t-s)} \\ m_{24} = \dfrac{\alpha_h(t-s)\pi_h N_h^0}{\mu_h} e^{-(\sigma+\mu_a)(t-s)} \\ m_{33} = \dfrac{\beta_w(t-s)\pi_h N_h^0}{\mu_h} e^{-\omega(t-s)} \\ m_{34} = \dfrac{\alpha_w(t-s)\pi_w N_w^0}{\mu_w} e^{-\omega(t-s)} \\ m_{41} = \rho(t-s) e^{-(\tau+\epsilon_0)(t-s)+\frac{6\epsilon_0\epsilon_1}{\pi}\left(cos\left(\frac{\pi t}{6}\right)-cos\left(\frac{\pi s}{6}\right)\right)} \\ m_{43} = \rho_w(t-s) e^{-(\tau+\epsilon_0)(t-s)+\frac{6\epsilon_0\epsilon_1}{\pi}\left(cos\left(\frac{\pi t}{6}\right)-cos\left(\frac{\pi s}{6}\right)\right)} \end{cases} \tag{5.18}$$

5.2.5 Global Stability of the Brucellosis-free Solution

The conditions for global stability of a Brucellosis-free periodic solution are established in this subsection.

Theorem 5.1

The Brucellosis-free periodic solution of system (5.1) is globally asymptotically stable if the basic reproduction number in $\mathcal{D}$ is less than unit.

Proof. Consider the matrix function

$$F(t) - V(t) = \begin{bmatrix} \beta_a(t)S_a^0 - (\mu_a + d) & 0 & 0 & \alpha_a(t)S_a^0 \\ \dfrac{\beta_h(t)\pi_h N_h^0}{\mu_h} & \beta_h(t)S_h^0 - (\sigma+\mu_h) & 0 & \dfrac{\alpha_h(t)\pi_h N_h^0}{\mu_h} \\ 0 & 0 & \beta_w(t)S_w^0 - \mu_w & \dfrac{\alpha_w(t)\pi_w N_w^0}{\mu_w} \\ \rho(t) & 0 & \rho_w(t) & -(\tau+\epsilon(t)) \end{bmatrix} \tag{5.19}$$

We verify that matrix function (5.19) is continuous, irreducible, cooperative, and ω-periodic. Let $\Phi_{(F-V)(.)}(t)$ be the fundamental solution matrix of the linear ordinary differential system:

$$\dot{x} = [F(t) - V(t)]x, \tag{5.20}$$

and $\rho(\Phi_{(F-V)(.)}(\omega))$ signify the dominant eigenvalue of $\Phi_{(F-V)(.)}(\omega)$. Based on Theorem 2.2 of Wang and Zhao (2008) we have $R_0 < 1$ given $\rho(\Phi_{(F-V)(.)}(\omega)) < 1$.

Lemma 5.1

Let $v = 1/\omega ln\rho(\Phi_{(F-V)(.)}(\omega))$. Then there exists a positive ω-periodic function $v(t)$ such that $e^{vt}v(t)$ is a solution to equation (5.20).

From the non-disease transmitting equations of system (5.1), the following are deduced:

$$V_a(t) \leq \frac{\phi\pi_a N_a^0}{\mu_a(\phi+\psi+\mu_a)} \triangleq V_a^0, \qquad S_a(t) \leq \frac{(\psi+\mu_a)\pi_a N_a^0}{\mu_a(\phi+\psi+\mu_a)} \triangleq S_a^0,$$

$$S_h(t) \leq \frac{\pi_h N_h^0}{\mu_h} \triangleq S_h^0, \qquad S_\omega(t) \leq \frac{\pi_w N_w^0}{\mu_w} \triangleq S_w^0.$$

Similarly, the following is computed from the infectious and recovered classes of system (5.1):

$$\frac{d}{dt}\begin{bmatrix} I_a(t) \\ I_h(t) \\ I_w(t) \\ B(t) \end{bmatrix} \leq (F-V)\begin{bmatrix} I_a(t) \\ I_h(t) \\ I_w(t) \\ B(t) \end{bmatrix}$$

In accordance with Lemma 5.1, there exists $v(t)$ such that $x(t) = (\bar{I}_a(t), \bar{I}_h(t), \bar{I}_w(t), \bar{B}(t)) = v(t)e^{vt}$ is a solution to equation (5.20) with $v = 1/\omega ln\rho(\Phi_{(F-V)(.)})$.

Based on the fact that $R_0 < 1$, we have $\rho(\Phi_{(F-V)(.)}) < 1$ and $v < 0$. Thus,

$$(I_a(t), I_h(t), I_w(t), B(t)) \leq (\bar{I}_a(t), \bar{I}_h(t), \bar{I}_w(t), \bar{B}(t))$$

if t is very large would insinuate that

$$\lim_{t\to\infty} I_a(t) = \lim_{t\to\infty} I_h(t) = \lim_{t\to\infty} B(t) = \lim_{t\to\infty} I_w(t) = 0.$$

Moreover, as $t \to \infty$ we have:

$$\frac{d}{dt}(V_a + S_a) \to \pi_a N_a^0 - \mu_a(V_a + S_a)$$

which implies

$$\frac{dV_a}{dt} \to \phi\left(\frac{\pi_a N_a^0}{\mu_a} - V_a\right) - (\psi+\mu_a)V_a = \frac{\psi\pi_a N_a^0}{\mu_a} - (\phi+\psi+\mu_a)V_a$$

or

$$\frac{\phi\pi_a N_a^0}{\mu_a(\phi+\psi+\mu_a)} = V_a^0$$

that leads to:

$$S_a(t) \to \frac{\pi_a N_a^0}{\mu_a} - V_a^0 = \frac{(\psi + \mu_a)\pi_a N_a^0}{\mu_a(\pi + \psi + \mu_a)} = S_a^0$$

Again,

$$\frac{dS_h}{dt} \to \pi_h N_h^0 - \mu_h S_h, \quad \frac{dS_w}{dt} \to \pi_w N_w^0 - \mu_w S_w$$

that gives

$$S_h^0 = \frac{\pi_h N_h^0}{\mu_h}, \quad S_w^0 = \frac{\pi_w N_w^0}{\mu_w}$$

Therefore,

$$\lim_{t\to\infty} x(t) = (V_a^0, S_a^0, 0, S_h^0, 0, 0, S_w^0, 0, 0)$$

for each solution $x(t)$ in the model system (5.1). □

5.2.6 Endemic Equilibrium Solution

In this subsection we aimed at investigating the behaviour of the model system (5.1) when $R_0 > 1$. It is shown that if $R_0 > 1$, Brucellosis infection persists in the animals and human populations; a positive periodic solution exists.

Pursuant to the approach in Zhao (2001) and Zhao *et al.* (2003) we define:

$$X = \mathbb{R}_+^9; X_0 = \mathbb{R}_+^4 \times Int(\mathbb{R}_+)^5; \partial X_0 = X \backslash X_0.$$

Let $L : X \to X$ represent the Poncaré map connected with the model system (5.1) such that $\mathcal{P}(x_0) = u(\omega, x_0)\ \forall x_0 \in X$, where $u(t, x_0)$ designate a unique solution of the system with $u(0, x_0) = x_0$.

Definition 5.1

The solutions of the model system (5.1) are considered to be uniformly persistent in case there exists some $\xi > 0$ so that:

$$\lim_{t\to\infty} InfV_a(t) > \xi, \ \lim_{t\to\infty} InfS_a(t) > \xi, \ \lim_{t\to\infty} InfI_a(t) > \xi,$$

$$\lim_{t\to\infty} InfS_h(t) > \xi, \ \lim_{t\to\infty} InfI_h(t) > \xi, \ \lim_{t\to\infty} InfR_h(t) > \xi,$$

$$\lim_{t\to\infty} InfS_w(t) > \xi, \ \lim_{t\to\infty} InfI_w(t) > \xi, \ \lim_{t\to\infty} InfB(t) > \xi,$$

whenever,

$$V_a(0) > 0, S_a(0) > 0, I_a(0) > 0, S_h(0) > 0, I_h(0) > 0, R_h(0) > 0, S_w(0) > 0, I_w(0) > 0, B(0) > 0.$$

Theorem 5.2

The solutions of the model system (5.1) are uniformly persistent, and the system admits at least one positive ω-periodic solution if $R_0 > 1$.

Proof. We define

$$H_\partial = \{(V_a(0), S_a(0), I_a(0), S_h(0), I_h(0), R_h(0), S_w(0), I_w(0), B(0)) \in \partial\mathcal{X}_0 :$$

$$\mathcal{P}^m(V_a(0), S_a(0), I_a(0), S_h(0), I_h(0), R_h(0), S_w(0), I_w(0), B(0)) \in \partial X_0, \forall m \geq 0\}$$

and

$$\tilde{H}_\partial = \{(V_a(0), S_a(0), 0, S_h(0), 0, 0, S_w(0), 0, 0) : V_a(0) \geq 0, S_a(0) \geq 0, S_h(0) \geq 0, S_w(0) \geq 0\}.$$

It is evident that $\tilde{H}_\partial \subseteq H_\partial$.

We first prove that $H_\partial = \tilde{H}_\partial$. Consider the baseline values

$$(V_a(0), S_a(0), I_a(0), S_h(0), I_h(0), R_h(0), S_w(0), I_w(0), B(0)) \in \partial X_0 \backslash \tilde{H}.$$

If $I_a(0) = 0, I_h(0), I_w(0) = 0$ and $B(0) > 0$, then based on the fact that recruitment rate for vulnerable individuals exists, we have $I_a' > 0$. Similarly, if $I_w(0) = 0, I_h(0), B(0) = 0$ and $I_a(0) > 0$, then $B'(0) > 0$, $I_a(0) = 0, I_h(0), I_w(0) = 0$ and $B(0) > 0$, $I_a(0) = 0, I_h(0), B(0) = 0$ and $I_w(0) > 0$, then $B'(0) > 0$. It follows that $(V_a(t), S_a(t), I_a(t), S_h(t), I_h(t), R_h(t), S_w(t), I_w(t), B(t)) \notin \partial X_0$ for $0 < t \ll 1$. Thus, the positive invariance of X_0 implying that $H_\partial = \tilde{H}_\partial$.

Again, if we consider the fixed point

$$H_0 = \left(\frac{\phi\pi_a N_a^0}{\mu_a(\phi+\psi+\mu_a)}, \frac{(\psi+\mu_a)\pi_a N_a^0}{\mu_a(\phi+\psi+\mu_a)}, 0, \frac{\pi_h N_h^0}{\mu_h}, 0, \frac{\pi_w N_w^0}{\mu_w}, 0, 0\right),$$

we define

$$W^S(H_0) = \{x_0 : L^m(x_0) \to H_0, x \to \infty\}.$$

It can be deduced from system (5.1) that if $I_a = I_h = I_w = B = 0$ and $t \to \infty$,

$$V_a(t) \to V_a^0 = \frac{\phi\pi_a N_a^0}{\mu_a(\phi+\psi+\mu_a)}, \;\; S_a(t) \to S_a^0 \frac{(\psi+\mu_a)\pi_a N_a^0}{\mu_a(\phi+\psi+\mu_a)}$$

$$S_h(t) \to S_h^0 = \frac{\pi_h N_h^0}{\mu_h}, \;\; S_w(t) \to S_w^0 = \frac{\pi_w N_w^0}{\mu_w}$$

We prove that $W^S(H_0) \cap X_0 = \emptyset$.

Let $\|.\|$ represent a norm on $\mathbb{R}^9_+$. In regard to the continuity of solutions with respect to the initial conditions, for each $\epsilon > 0$ however small, there exists $\delta > 0$ such that for all

$$(V_a(0), S_a(0), I_a(0), S_h(0), I_h(0), R_h(0), S_w(0), I_w(0), B(0)) \in \partial X_0$$

with

$$\|(V_a(0), S_a(0), I_a(0), S_h(0), I_h(0), R_h(0), S_w(0), I_w(0), B(0)) - H_0\| \leq \delta,$$

we have

$$\|u(t, (V_a(0), S_a(0), I_a(0), S_h(0), I_h(0), R_h(0), S_w(0), I_w(0), B(0))) - u(t, H_0)\| \leq \epsilon, \forall t \in [0, \omega].$$

So we affirm that

$$\lim_{t\to\infty} sup\|(V_a(0), S_a(0), I_a(0), S_h(0), I_h(0), R_h(0), S_w(0), I_w(0), B(0)) - H_0\| \geq \delta,$$

$$\forall (V_a(0), S_a(0), I_a(0), S_h(0), I_h(0), R_h(0), S_w(0), I_w(0), B(0)) \in X_0$$

and prove by contradiction as follows:

Suppose

$$\lim_{t\to\infty} sup\|(V_a(0), S_a(0), I_a(0), S_h(0), I_h(0), R_h(0), S_w(0), I_w(0), B(0)) - H_0\| < \delta,$$

for some

$$(V_a(0), S_a(0), I_a(0), S_h(0), I_h(0), R_h(0), S_w(0), I_w(0), B(0)) \in X_0.$$

In addition, we assume without loss of generality that

$$\mathcal{P}^m\|(V_a(0), S_a(0), I_a(0), S_h(0), I_h(0), R_h(0), S_w(0), I_w(0), B(0)) - H_0\| < \delta, \forall m \geq 0.$$

Therefore, $\forall t \in [0, \omega], m \geq 0$ we have,

$$\|u(t, (V_a(0), S_a(0), I_a(0), S_h(0), I_h(0), R_h(0), S_w(0), I_w(0), B(0))) - u(t, H_0)\| \leq \epsilon.$$

Furthermore, for any non-negative t, we can write $t = t_0 + n\omega$ with $t_0 \in [0, \omega]$ and n is the greatest integer less than or equal to t/ω. Subsequently we get

$$\|u(t, (V_a(0), S_a(0), I_a(0), S_h(0), I_h(0), R_h(0), S_w(0), I_w(0), B(0))) - u(t, H_0)\|$$

$$= \|u(t_0, (V_a(0), S_a(0), I_a(0), S_h(0), I_h(0), R_h(0), S_w(0), I_w(0), B(0))) - u(t_0, H_0)\| \leq \epsilon$$

for any $t > 0$.

Let

$$(V_a(t), S_a(t), I_a(t), S_h(t), I_h(t), R_h(t), S_w(t), I_w(t), B(t))$$

$$= (V_a(0), S_a(0), I_a(0), S_h(0), I_h(0), R_h(0), S_w(0), I_w(0), B(0))$$

It follows that,

$$\frac{\phi\pi_a N_a^0}{\mu_a(\phi+\psi+\mu_a)} - \epsilon < V_a(t) < \frac{\phi\pi_a N_a^0}{\mu_a(\phi+\psi+\mu_a)} + \epsilon,$$
$$\frac{(\psi+\mu_a)\pi_a N_a^0}{\mu_a(\phi+\psi+\mu_a)} - \epsilon < S_a(t) < \frac{(\psi+\mu_a)\pi_a N_a^0}{\mu_a(\phi+\psi+\mu_a)} + \epsilon,$$
$$\frac{\pi_h N_h^0}{\mu_h} - \epsilon < S_h(t) < \frac{\pi_h N_h^0}{\mu_h} + \epsilon,$$
$$\frac{\pi_w N_w^0}{\mu_w} - \epsilon < S_w(t) < \frac{\pi_w N_w^0}{\mu_w} + \epsilon,$$
$$0 < I_a(t) < \epsilon,$$
$$0 < I_h(t) < \epsilon,$$
$$0 < I_w(t) < \epsilon,$$
$$0 < B(t) < \epsilon.$$

Then we have,

$$\begin{aligned}
\frac{dI_a}{dt} =& (\beta_1(t)I_a + \alpha_1(t)B)S_a - (\mu_a + d)I_a \\
\geq& (\beta_1(t)I_a + \alpha_1(t)B)\left(\frac{(\psi+\mu_a)\pi_a N_a^0}{\mu_a(\phi+\psi+\mu_a)} - \epsilon\right) - (\mu_a + d)I_a \\
=& (\beta_1(t)I_a + \alpha_1(t)B)\left(\frac{(\psi+\mu_a)\pi_a N_a^0}{\mu_a(\phi+\psi+\mu_a)}\right) - (\mu_a + d)I_a - \epsilon(\beta_1(t)I_a + \alpha_1(t)B)
\end{aligned}$$

Similarly,

$$\frac{dI_h}{dt} \geq (\beta_2(t)I_h + \alpha_2(t)B)\left(\frac{\pi_h N_h^0}{\mu_h}\right) - (\sigma + \mu_h)I_h - \epsilon(\beta_2(t)I_h + \alpha_2(t)B)$$

and

$$\frac{dI_w}{dt} \geq (\beta_w(t)I_w + \alpha_w(t)B)\left(\frac{\pi_w N_w^0}{\mu_w}\right) - \mu_w I_w - \epsilon(\beta_w(t)I_w + \alpha_w(t)B)$$

Thus we obtain

$$\frac{d}{dt}\begin{bmatrix} I_a(t) \\ I_h(t) \\ I_w(t) \\ B(t) \end{bmatrix} \geq (F - V - \epsilon K)\begin{bmatrix} I_a(t) \\ I_h(t) \\ I_w(t) \\ B(t) \end{bmatrix}$$

But $R_0 > 1$ if and only if $\rho(\Phi_{(F-V)(.)}) > 1$. Accordingly, for $\epsilon > 0$ however small, we have $\rho(\Phi_{(F-V)(.)}) > 1$. Using Lemma 1 and the comparison principle, we get

$$\lim_{t\to\infty} I_a(t) = \lim_{t\to\infty} B(t) = \lim_{t\to\infty} I_h(t) = \lim_{t\to\infty} I_w(t) = \infty$$

which is a contradiction our original supposition.

Thus, $\mathcal{P}$ is uniformly persistent with respect to $(X_0, \partial X_0)$, and H_0 is not cyclic in H_∂, implying that the solutions for the original system (Zhao *et al*., 2003) are uniformly persistence. Consequently, the Poincaré map p has a fixed point

$$(\bar{V}_a(0), \bar{S}_a(0), \bar{I}_a(0), \bar{S}_h(0), \bar{I}_h(0), \bar{S}_w(0), \bar{I}_w(0), \bar{B}(0)) \in X_0$$

with

$$V_a(0), S_a(0), S_H(0), S_w(0) \neq 0.$$

Thus,

$$(\bar{V}_a(0), \bar{S}_a(0), \bar{I}_a(0), \bar{S}_h(0), \bar{I}_h(0), \bar{S}_w(0), \bar{I}_w(0), \bar{B}(0)) \in Int(\mathbb{R}_+)^9$$

and

$$(\tilde{V}_a(0), \tilde{S}_a(0), \tilde{I}_a(0), \tilde{S}_h(0), \tilde{I}_h(0), \tilde{S}_w(0), \bar{I}_w(0), \tilde{B}(0))$$

$$= u(t, (\tilde{V}_a(0), \tilde{S}_a(0), \tilde{I}_a(0), \tilde{S}_h(0), \tilde{I}_h(0), \tilde{S}_w(0), \bar{I}_w(0), \tilde{B}(0)))$$

is a positive ω-periodic solution of the system. □

5.3 Numerical Simulations

In this section we present verification of some analytical findings that were performed through a numeral simulation for model system (5.1). Our computations were guided by baseline parameter values as used in different literature relevant to this work and unavailable parameter values are assumed for illustration. The parameter, descriptions and values in per year are shown in Table 14. Figures 15, 16, 17 and 18, illustrate the variations in human, wild animals and livestock subpopulations while Fig. 19 shows the existence of a globally attracting disease-free periodic solution. Additionally, Figs. 20, 21 and 22 highlight the impact of temperature variations in the transmission dynamics of Brucellosis.

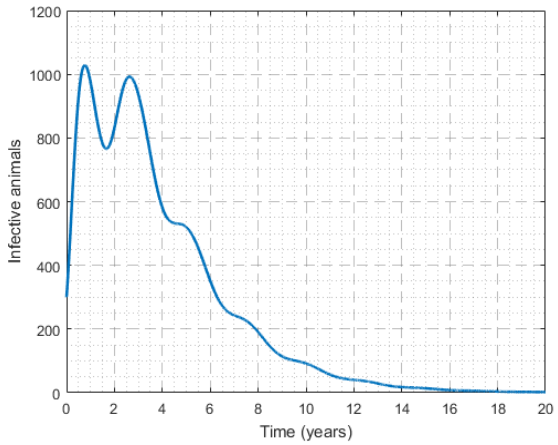

(a)

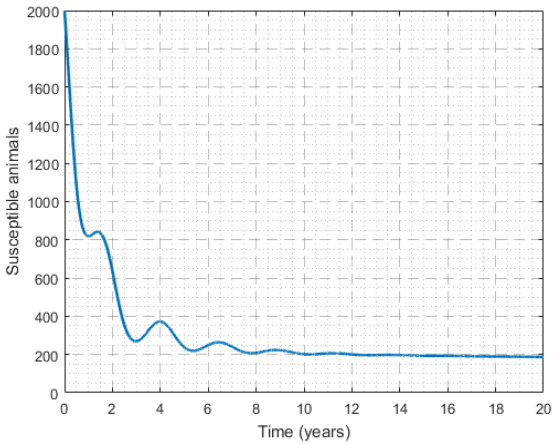

(b)

Figure 15: Seasonal variations in the number of infective and susceptible animals

Figure $15a$ indicates that the number of seropositive livestock decreases seasonally with time while Fig. $15b$ illustrates a decrease in the susceptible animals subpopulation as time increases. The decrease in the number of infective livestock is due to the proper implementation of vaccination and the gradual culling of seropostive animals control strategies. On the other hand, the sharp decrease in the susceptible animals subpopulation can be associated with large number of infective animals and consequently the high transmission rate in less than one year period of time while the gradual decrease in the next two years is due to vaccination programmes and decreased infection rate.

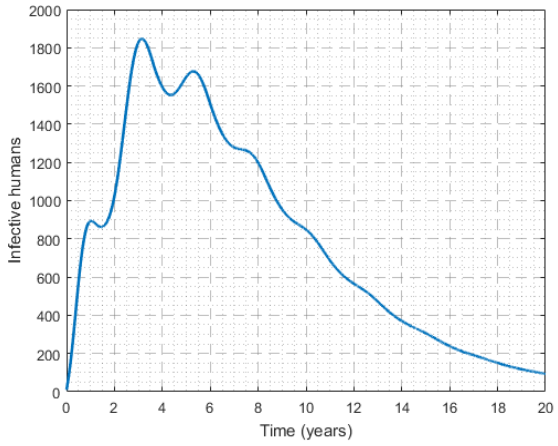

(a)

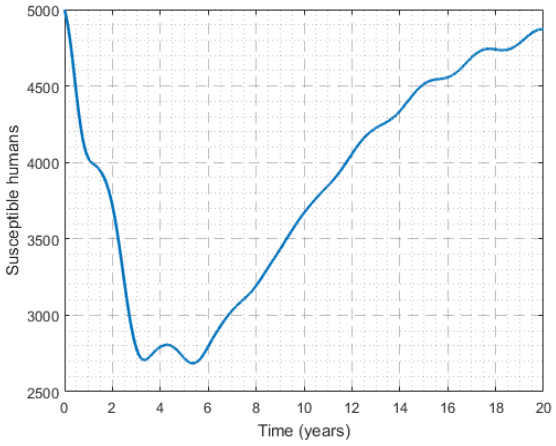

(b)

Figure 16: Seasonal variations in the number of infective and susceptible humans

Figure 16 shows a strong relationship between the number of infective and susceptible humans. For instance, at $t = 0$, $S_a = 5000$ and $I_a = 0$ whilst at $t = 3$, $S_a = 2555$ and $I_a = 1850$. The

seasonal increase in the individuals in Figure $16a$ is associated with low human treatment rate and poor control of the disease from infective livestock as well as contaminated environment. Besides, the decrease of susceptible humans in Fig. $16b$ is due to the high transmission rate both from infective animals and their products while the increase is connected to the proper implementation of the control options such as environmental hygiene, animal vaccination and gradual culling of seropositive animals.

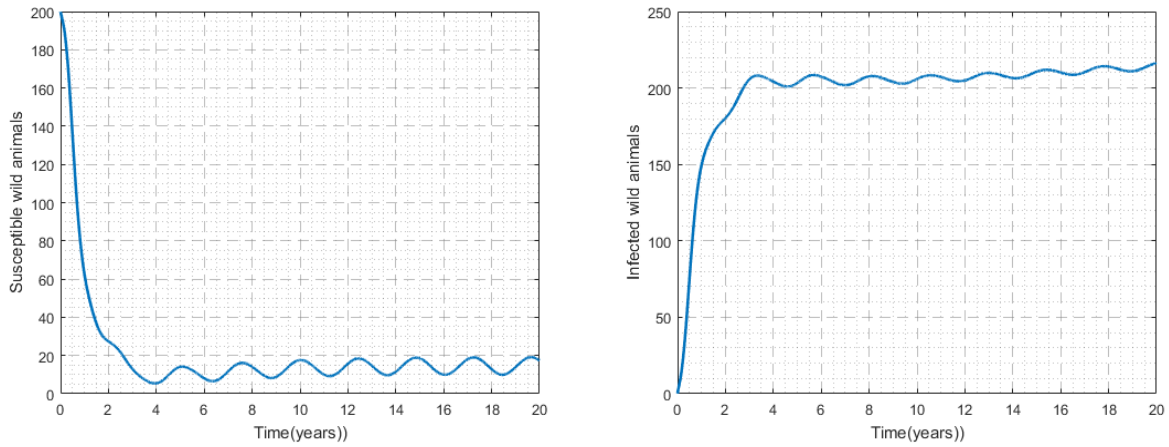

(a) (b)

Figure 17: Seasonal variations in the number of infective and susceptible wild animals

Figure 17 shows that the number of susceptible wild animals decreases with the increase in infective wild animals. In particular, the introduction of 200 susceptible wild animals in the contaminated environment produces more than 200 infective wild animals. This is based on that fact that both infective and susceptible animals have free movements and interactions within their parks. Besides, the lack of wild animal Brucellosis control measures and the fact that the disease does not kill keeps the number of infected wild animals seasonally increasing. Thus, for a better control of Brucellosis transmission dynamics in livestock and humans, the interactions between domestic and wild animals should be restricted.

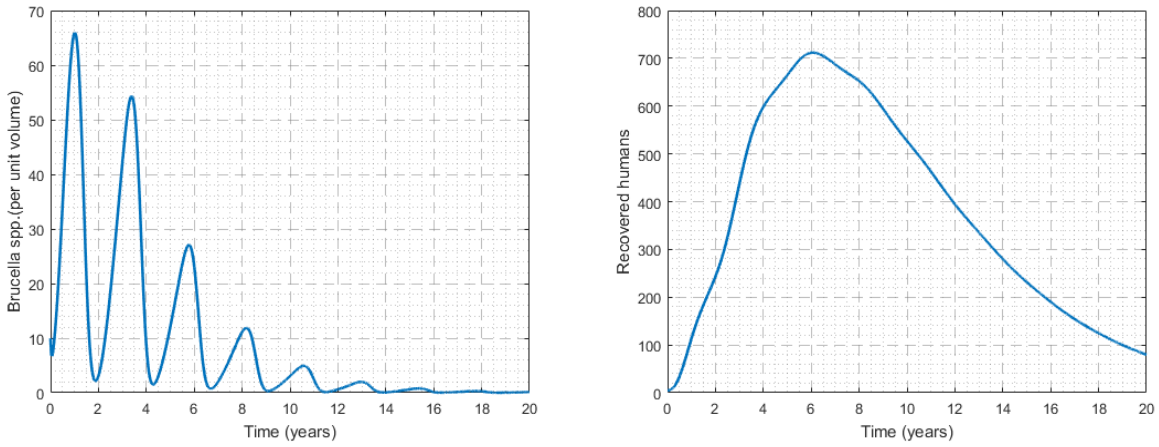

(a) (b)

Figure 18: Effects of variation of environmental hygiene and human treatment to effective reproduction number

Figure 18a shows that the number of *Brucella* in the surroundings decreases seasonally as time increases while Fig. 18b illustrates the variations in the number of recovered humans with respect to increase in time. These variations are associated with the regular implementation of the control strategies like environment hygiene and sanitation, human treatment and gradual culling of infective animals. Furthermore, the recovered human population in the first six years increases due to effective treatment of the infectives and its decrease is associated with the decreased number of infected humans as well as the proper control of the disease from livestock and their products.

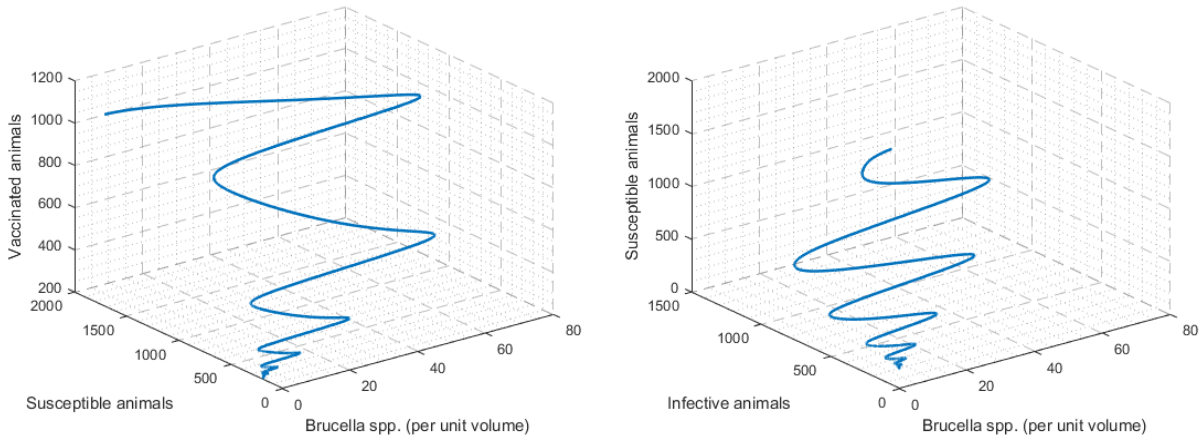

(a) (b)

Figure 19: The effect of *Brucella spp.* to both susceptible and infected animals

Figure 19 shows the existence of a stable periodic solution between the animal subpopulations

and the number of *Brucella* in the environment.

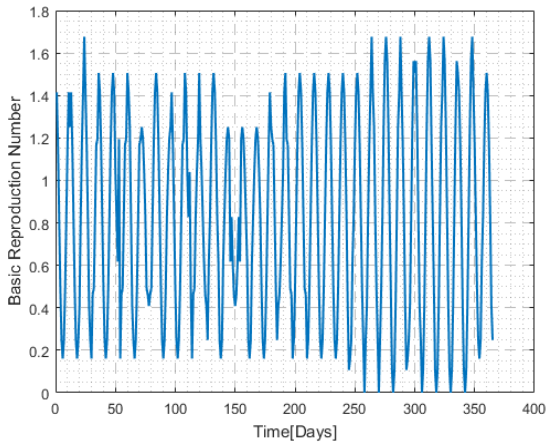

(a) Maximum daily temperature

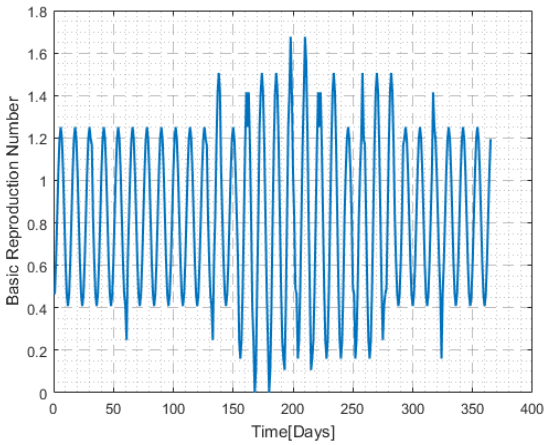

(b) Minimum daily temperature

Figure 20: The effects of extreme temperature variations in the effective reproductive number for the year 1979 in Mpwapwa District Dodoma

Figure $20a$ shows the effective reproductive number variations in season with regard to the maximum daily temperature while Fig. $20b$ illustrates the effective reproduction number changes with regard to seasonal variations of minimum daily temperature.

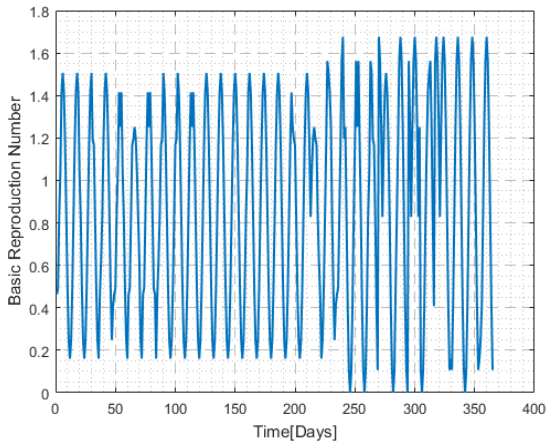

(a) Maximum daily temperature

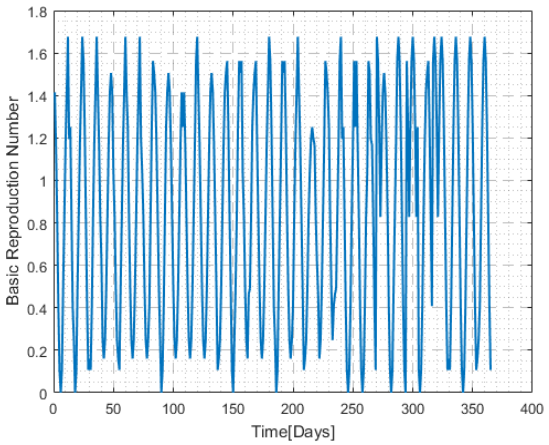

(b) Minimum daily temperature

Figure 21: The effects of extreme temperature variations in the effective reproductive number for the year 2014 in Ngorongoro District Arusha

Figure $21a$ illustrates the variations in effective reproductive number versus the maximum daily temperature while Fig. $21b$ depicts the changes in the effective reproduction number with respect to seasonal variations of the minimum daily temperature.

Figure $21a$ illustrates the variations in effective reproduction number versus the maximum daily temperature while Fig. $21b$ depicts the changes in the effective reproductive number with respect to the seasonal variations of the minimum daily temperature.

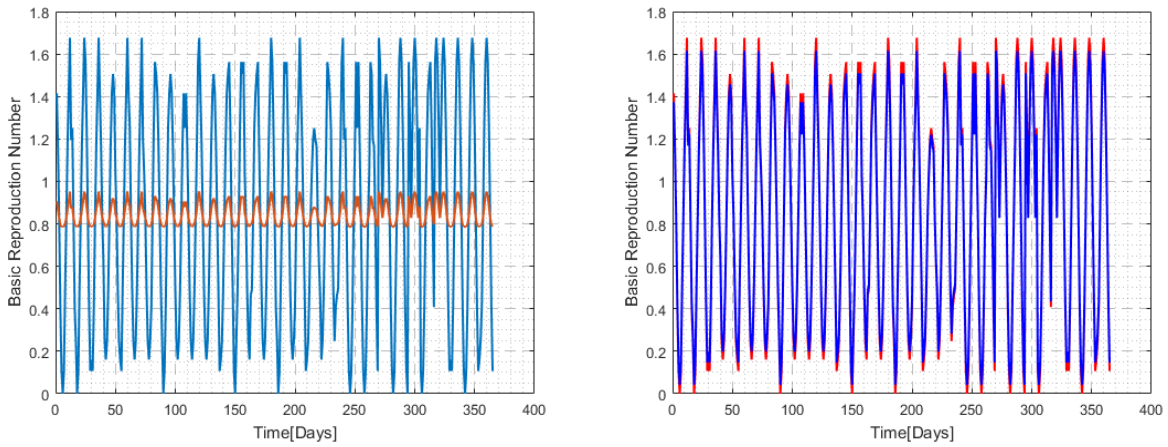

(a) (b)

Figure 22: The effects of temperature variations in the effective reproductive number for the year 2014 in Ngorongoro District Arusha

Figure 22 presents the comparison between direct and indirect routes of Brucellosis transmission. In particular, high strength of seasonal forcing shown in Fig. 22a is due seasonality in both routes of disease transmission while the curve with low amplitude is due to lack of seasonality in the direct disease transmission. Moreover, Fig. 22b indicates that seasonality of direct transmission has a significant contribution to the Brucellosis transmission than indirect transmission; the graph in red is for seasonality in both direct and indirect while the blue is for seasonality in direct transmission route only.

Generally, the findings from this study advocates that as long as the weather patterns favours an increase in the spread rates of Brucellosis in human, livestock, wild animals and environment, there will be a significant increase of incidence of the disease and vice versa. This means that to effectively prevent, control, eliminate or eradicate Brucellosis from the community, measures should be timely taken in accordance with the fluctuation in the disease transmission rates as a result of daily temperature variations. Thus, to avoid underestimation or overestimation of the resources when dealing with Brucellosis, the aspect of seasonal weather variation should be taken into account when planning for prevention, control, elimination or eradication of Brucellosis infections.

CHAPTER SIX

GENERAL DISCUSSION, CONCLUSION AND RECOMMENDATIONS

6.1 General Discussion

This study intended to develop and anlayze mathematical models for the infectiology and cost-effectiveness of Brucellosis control schemes. More importantly, three specific objectives which are: to develop and analyze the mathematical models for the spread and control strategies of Brucellosis, to determine the optimal combination of the controls for Brucellosis eradication, and to analyze the cost-effectiveness of the control strategies among each other, guided the study. The preventive and control measures taken into account were: personal protection, livestock vaccination, slaughtering of seropositive livestock progressively, and hygiene and sanitation of the surroundings. The summary of the findings for each Chapter is presented as follows:

Chapter Two: gives a review of various studies related to this work; it gives the importance and history of mathematical modeling since 1766 and analyzes various Brucellosis compartmental mathematical models. In addition, it establishes the basis for this study by identifying the research gap to be filled.

Chapter Three: A deterministic mathematical model for Brucellosis that incorporates human to human, livestock to human, and contaminated surroundings to both livestock and human routes of disease spread was formulated and analyzed. The impacts of livestock vaccination, environmental hygiene and sanitation, human treatment, and gradual culling of infected animals through slaughtering controls to the disease transmission in livestock and human subpopulations were investigated. A positive invariable region for the model formulated was established and the next generation operator method was used to compute the net reproductive number. It was proved that the Brucellosis-free equilibrium exists, locally and globally asymptotically stable if $R_e < 1$, while the endemic Brucellosis equilibrium point exists, asymptotically stable locally and globally if $R_e > 1$. Sensitivity analysis of the effective reproductive number indicated that natural mortality rate, recruitment rate, ruminant to ruminant transmission rate, vaccination rate, and the gradual culling rate of seropositive ruminants are the most sensitive parameters and should be targeted in designing of the control strategies for the disease. Numerical simulation

showed that human Brucellosis may be cleared only if it can be eliminated in cattle and small ruminants.

Chapter Four: A mathematical model that incorporates time-dependent controls to some parameters was developed and used to explore the influence of livestock in the conveyance of Brucellosis. The controls under consideration were personal protection, the gradual slaughtering of seropositive small ruminants and cattle, vaccination, and environmental hygiene. The Pontryagin's maximum principle was used to derive the essential conditions for an optimal control problem. The main aim was to identify a strategy that downplays the conveyance of Brucellosis along with the costs of implementation. The findings revealed that the efficient usage of a combination of personal protection, gradual slaughtering of seropositive small ruminants and cattle, livestock vaccination, and environmental hygiene has a considerable effect in reducing the disease spread in human and livestock subpopulations at the lowest cost.

In Chapter Five: A deterministic mathematical model for Brucellosis that incorporates seasonality on direct and indirect transmission parameters for domestic ruminants, wild animals, humans and the environment was formulated and analyzed. Both analytical and numerical simulations were presented. The findings showed that the variations in seasonal weather have a great impact on the Brucellosis conveyance in livestock, human and wild animals. Thus, for effective disease control, measures should be timely implemented upon the fluctuation in disease spread.

6.2 Conclusion

This study was geared towards formulating and analyzing mathematical models that investigated different control parameters impact on the Brucellosis spread in animal and human groups. The focus was on human treatment; livestock gradual slaughtering of infective ruminants; vaccination; and environmental hygiene. Both analytical solutions and numerical simulations demonstrates that the infection is a perfect zoonosis; Brucellosis in humans does not affect the livestock population. This is due the fact that the transmission in human is influenced by the existence of the infection in ruminants; that is human Brucellosis can be eliminated only if ruminants Brucellosis is eliminated.

In the analysis of optimal control problem, the Pontryagin's Maximum Principle was used; while incremental cost-effectiveness ratio have been used to analyze the cost-effectiveness of the

control options. The results obtained from both cost-effectiveness and optimal control analyses indicated that a combination of personal protection, gradual slaughtering of infected livestock, livestock vaccination, and environmental sanitation is the best control option as it has higher impact and lower implementation cost. It was further showed that the combination of personal protection, progressive slaughtering of infected livestock, and livestock vaccination is the second most cost-effective scheme whilst the combination of personal protection, environmental hygiene, and progressive culling of seropositive ruminants cost higher with low impact in disease control. Momentous analysis of the control scenarios indicated that the gradual slaughtering of seropostive livestock, and vaccination of susceptible livestock are the pre-requisites for any design of control scheme.

Moreover, the findings from the study advocates the significant increase of incidence of the disease with the increase in the transmission rates of Brucellosis in livestock, human, wild animals and the environment at favourable weather condition. The converse is also true. This means to effectively prevent, control, eliminate or eradicate Brucellosis from the community, measures should be timely taken in accordance to the fluctuation in the disease transmission rates as a result of daily temperature variations. Thus, to avoid underestimation or overestimation of the resources when dealing with Brucellosis, the aspect of seasonal weather variation should be taken into account when planning for prevention, control, elimination or eradication of Brucellosis infections.

6.3 Recommendations

Different measures are in place to fight Brucellosis, but the disease continues to pose significant threat to veterinarians, livestock keepers as well as public health works, the study recommends the following:

(i) The most sensitive parameters like natural mortality rate, recruitment rate, ruminant to ruminant transmission rate, vaccination rate, and disease induced culling rate of the ruminants are mostly sensitive parameters and should be targeted in designing of the disease control schemes.

(ii) Brucellosis transmission may be controlled effectively by adopting the combination of personal protection, culling of infective ruminants, applying livestock vaccination, and environmental hygiene as efficient controls.

(iii) In order to prevent, control, eliminate or eradicate Brucellosis from the community, measures such as personal protection, gradual culling of seropositive livestock, livestock vaccination, and environmental hygiene should be timely taken in accordance to the fluctuation in the disease transmission rates as a result of daily temperature variations.

(iv) The vaccination and culling of seropositive animals are pre-requisities when considering the minimization or elimination of Brucellosis from the community. However, this should be coupled with other control measures.

(v) An investigation for Brucellosis transmission dynamics should be done using a time-delayed mathematical model.

(vi) Mathematical modeling of the spatio-temporal dynamics of Brucellosis should be done using patch models.

REFERENCES

Abate, A., Tiwari, A., & Sastry, S. (2009). Box invariance in biologically-inspired dynamical systems. *Automatica*, 45(7), 1601–1610.

Abatih, E., Ron, L., Speybroeck, N., Williams, B., & Berkvens, D. (2015). Mathematical analysis of the transmission dynamics of brucellosis among bison. *Mathematical Methods in the Applied Sciences*, 38(17), 3818–3832.

Ainseba, B., Benosman, C., & Magal, P. (2010). A model for ovine brucellosis incorporating direct and indirect transmission. *Journal of Biological Dynamics*, 4(1), 2–11.

Akpinar, O. (2016). Historical perspective of brucellosis: a microbiological and epidemiological overview. *Le Infezioni in Medicina*, 24(1), 77–86.

Alhamada, A. G., Habib, I., Barnes, A., & Robertson, I. (2019). Risk factors associated with brucella seropositivity in sheep and goats in Duhok Province, Iraq. *Veterinary Sciences*, 4(65), 1–9.

Altizer, S., Dobson, A., Hosseini, P., Hudson, P., Pascual, M., & Rohani, P. (2006). Seasonality and the dynamics of infectious diseases. *Ecology Letters*, 9(4), 467–484.

Amaku, M., Dias, R., Ferreira Neto, J., & Ferreira, F. (2009). Mathematical modeling of bovine brucellosis control by vaccination. *Arquivo Brasileiro de Medicina Veterinária e Zootecnia*, 61, 135–141.

Aune, K., Rhyan, J. C., Russell, R., Roffe, T. J., & Corso, B. (2012). Environmental persistence of Brucella abortus in the Greater Yellowstone Area. *The Journal of Wildlife Management*, 76(2), 253–261.

Bernoulli, D., & Blower, S. (2004). An attempt at a new analysis of the mortality caused by smallpox and of the advantages of inoculation to prevent it. *Reviews in Medical Virology*, 14(5), 275–288.

Bowong, S., Tewa, J. J., & Kamgang, J. C. (2011). Stability analysis of the transmission dynamics of tuberculosis models. *World Journal of Modelling and Simulation*, 7(2), 83–100.

Brauer, F., & Castillo-Chavez. (Eds.). (2013). *Mathematical Models for Communicable Diseases*. Society of Industrial and Applied Mathematics.

Bruce, D. (2011). Discoverer of brucellosis. *Singapore Medical Journal*, 52(3), 138.

Carugati, M., Biggs, H, M., Maze, M. J., Stoddard, R. A., Cash-Goldwasser, S., Hertz, J. T., Halliday, J. E., Saganda, W., Lwezaula, B. F., Kazwala, R. R., Cleaveland, S., Maro, V. P., Rubach, M. P., & Crump, J. A. (2018). Incidence of human brucellosis in the Kilimanjaro Region of Tanzania in the periods 2007–2008 and 2012–2014. *Transactions of the Royal Society of Tropical Medicine and Hygiene*, 112(3), 136–143.

CDC. Brucellosis Signs and Symptoms, *https://www.cdc.gov/brucellosis/symptoms/index.html*. Accessed 2018-11-07.

CFSPH. Brucellosis:Brucella abortus, *http://cfsph.iastate.edu/Factsheets/pdfs/brucellosis-abortus.pdf*. Accessed 2018-11-07.

Chitnis, N., Hyman, J. M., & Cushing, J. M. (2008). Determining important parameters in the spread of malaria through the sensitivity analysis of a mathematical model. *Bulletin of Mathematical Biology*, 70(5), 1272-1296.

Cintrón-Arias, A., Castillo-Chávez, C., Bettencourt, l., Lloyd, A., & Banks, H. T. (2009). The estimation of the effective reproductive number from disease outbreak data. *Mathematical Bioscience Engineering*, 6(2), 261–282.

Corbel, M. J. (2006). *Brucellosis in humans and animals*. World Health Organization.

De Souza, V. A. F., Neto, J. S. F., Amaku, M., Dias, R. A., Telles, E. O., Grisi-Filho, J. H. H., Heinemann, M. B., & Ferreira, F. (2016). Mathematical modeling of bovine brucellosis control using the RB51 vaccine. *Semina: Ciências Agrárias*, 37(5), 3767–3775.

Dean, A. S., Crump, L., Greter, H., Schelling, E., & Zinsstag, J. (2012). Global burden of human brucellosis: a systematic review of disease frequency. *PLoS Neglected Tropical Diseases*, 6(10), 1-9.

Diekmann, O., & Heesterbeek, J. A. P. (2000). *Mathematical epidemiology of infectious diseases: model building, analysis and interpretation* (Vol. 5). John Wiley & Sons.

Diekmann, O., & Heesterbeek, J. A. P., & Metz, J. A. J. (1990). On the definition and the computation of the basic reproduction ratio R_0 in models for infectious diseases in heterogeneous populations. *Journal of Mathematical Biology*, 28(4): 365–382.

Diekmann, O., Heesterbeek, J. A. P., & Roberts, M. G. (2010). The construction of next-generation matrices for compartmental epidemic models. *Journal of the Royal Society Interface*, 7(47), 873–885.

Dobson, A., & Meagher, M. (1996). The population dynamics of brucellosis in the Yellowstone National Park. *Ecology*, 77(4), 1026–1036.

Ducrotoy, M., Bertu, W., Matope, G., Cadmus, S., Conde-Álvarez, R., Gusi, A., Welburn,S., Ocholi, R., Blasco, J., & Moriyón, I. (2017). Brucellosis in Sub-Saharan Africa: Current challenges for management, diagnosis and control. *Acta Tropica*, 165, 179–193.

El-Sayed, A., & Awad, W. (2018). Brucellosis: Evolution and expected comeback. *International Journal of Veterinary Science and Medicine*, 6(1), 31–35.

Fleming, W. H., & Rishel, R. W. (2012). *Deterministic and Stochastic Optimal Control* (Vol. 1). Springer Science & Business Media.

Franc, K., Krecek, R., Häsler, B., & Arenas-Gamboa, A. (2018). Brucellosis remains a neglected disease in the developing world. *BMC Public Health*, 18(125), 1–9.

Garner, M. G., & Beckett, S. (2005). Modelling the spread of foot-and-mouth disease in Australia. *Australian Veterinary Journal*, 83(12), 758–766.

Giraldo, J. O., & Palacio, D. H. (2008). Deterministic SIR (susceptible–infected–removed) models applied to varicella outbreaks. *Epidemiology & Infection*, 136(5), 679–687.

Godfroid, J., Cloeckaert, A., Liautard, J. P., Kohler, S., Fretin, D., Walravens, K., Garin-Bastuji, B., & Letesson, J. J. (2005). From the discovery of the malta fever's agent to the discovery of a marine mammal reservoir, brucellosis has continuously been a re-emerging zoonosis. *Veterinary Research*, 36(3), 313–326.

Grassly, N. C., & Fraser. C. (2006). Seasonal infectious disease epidemiology. *Proceedings of the Royal Society B: Biological Sciences*, 273(1600), 2541–2550.

Greenfield, R. A., Drevets, D. A., Machado, L. J., Voskuhl, G. W., Cornea, P., & Bronze, M. S. (2002). Bacterial pathogens as biological weapons and agents of bioterrorism. *The American Journal of the Medical Sciences*, 323(6), 299–315.

Hale, J. K. (1969). *Ordinary differential equations*. Brown University Providence RI Division of Applied Mathematics.

Hartwell, D., Jones, J., Baxter, L., & Shepherd, J. (2011). Peginterferon alfa and ribavirin for chronic hepatitis C in patients eligible for shortened treatment, re-treatment or in HCV/HIV co-infection: a systematic review and economic evaluation. *Health Technology Assessment (Winchester, England)*, 15(17), 1–210.

Hethcote, H. W. (1994). A thousand and one epidemic models. In *Frontiers in Mathematical Biology* (pp. 504-515). Springer, Berlin, Heidelberg.

Hou, Q., & Sun, X. D. (2016). Modeling sheep brucellosis transmission with a multi-stage model in Changling County of Jilin Province, China. *Journal of Applied Mathematics and Computing*, 51(1-2), 227–244.

Hou, Q., Sun, X., Zhang, J., Liu, Y., Wang, Y., & Zhen Jin, Z. (2013). Modeling the transmission dynamics of sheep brucellosis in Inner Mongolia Autonomous Region, China. *Mathematical Biosciences*, 242(1), 51–58.

John, K., Fitzpatrick, J., French, N., Kazwala, R., Kambarage, D., Mfinanga, G. S., MacMillan, A., & Cleaveland, S. (2010). Quantifying risk factors for human brucellosis in rural northern Tanzania. *PloS One*, 5(4), 1–6.

Kadelka, M. S. (2015). *Mathematical models of immune responses following vaccination with application to Brucella infection*. PhD thesis, Virginia Tech.

Kang, G. J., Gunaseelan, L., & Abbas, K. M. (2014). Epidemiological modeling of bovine brucellosis in india. In: *2014 IEEE International Conference on Big Data (Big Data). IEEE*, 6–10.

Keeling, M., & Danon, L. (2009). Mathematical modelling of infectious diseases. *British Medical Bulletin*, 92(1), 33–42.

Kimaro, E. G., Toribio, J. A., Gwakisa, P., & Mor, S. M. (2018). Occurrence of trypanosome infections in cattle in relation to season, livestock movement and management practices of Maasai pastoralists in Northern Tanzania. *Veterinary Parasitology: Regional Studies and Reports*, 12, 91–98.

Kitaly, J. (1984). *Bovine brucellosis in Government parastatal and Ujamaa village dairy farms in Central Zone of Tanzania: Assessment of Control measures in some farms In*. Proceedings of the 2nd Tanzania Veterinary Association Scientific Conference, 24–30.

Klok, R. M., & Postma, M. J. (2004). Four quadrants of the cost-effectiveness plane: some considerations on the south-west quadrant. *Expert Review of Pharmacoeconomics & Outcomes Research*, 4(6), 599-601.

Korobeinikov, A. (2004). Lyapunov functions and global properties for SEIR and SEIS epidemic models. *Mathematical Medicine and Biology: A Journal of the IMA*, 21(2), 75–83.

Korobeinikov, A. (2007). Global properties of infectious disease models with nonlinear incidence. *Bulletin of Mathematical Biology*, 69(6), 1871–1886.

Korobeinikov, A., & Wake, G. C. (2002). Lyapunov functions and global stability for SIR, SIRS, and SIS epidemiological models. *Applied Mathematics Letters*, 15(8), 955–960.

Lenhart, S., & Workman, J. T. (2007). *Optimal control applied to biological models*. CRC press.

Li, C., Guo, Z. G., & Zhang, Z. Y. (2017). Transmission dynamics of a brucellosis model: Basic reproduction number and global analysis. *Chaos, Solitons & Fractals*, 104, 161–172.

Li, M., Sun, G., Zhang, J., Jin, Z., Sun, X., Wang, Y., Huang, B., & Zheng, Y. (2014). Transmission dynamics and control for a brucellosis model in Hinggan League of Inner Mongolia, China. *Mathematical Bioscience and Engineering*, 11(5), 1115–1137.

Li, M. T., Sun, G. Q., Wu, Y. F., Zhang, J. & Jin, Z. (2014). Transmission dynamics of a multi-group brucellosis model with mixed cross infection in public farm. *Applied Mathematics and Computation*, 237, 582–594.

Li, M. T., Sun, G. Q., Zhang, W. Y., & Jin, Z. (2017). Model-based evaluation of strategies to control brucellosis in china. *International Journal of Environmental Research and Public Health*, 14(3), 1–15.

Lolika, P. O., Modnak, C., & Mushayabasa, S. (2018). On the dynamics of brucellosis infection in bison population with vertical transmission and culling. *Mathematical Biosciences*, 305, 42–54.

Lou, P., Zhang, L. X., Xu, J., & Wang, K. (2016). Modelling seasonal brucellosis epidemics in bayingolin mongol autonomous prefecture of Xinjiang, China, 2010-2014. *BioMed Research International*, 2016, 1–17.

Lukes, D. L. (1982). *Differential equations: classical to controlled*. Academic Press, New York.

Mantur, B. G., & Amarnath, S. K. (2008). Brucellosis in india-a review. *Journal of Biosciences*, 33(4), 539–547.

Marston, J. (1861). Report on fever (malta). *Army medical department reports*, 3, 486–521.

McCluskey, C. C. (2006). Lyapunov functions for tuberculosis models with fast and slow progression. *Mathematical Biosciences and Engineering*, 3, 1–12.

McFarlane, P. A., & Bayoumi, A. M. (2004). Acceptance and rejection: Cost-effectiveness and the working nephrologist. *Kidney International*, 66(5), 1735–1741.

Medscape. Brucellosis Pathogenicity, *https://emedicine.medscape.com/article/213430-overview*, Accessed: 2018-11-07.

Meltzer, E., Sidi, Y., Smolen, G., Banai, M., Bardenstein, S., & Schwartz, E. (2010). Sexually transmitted brucellosis in humans. *Clinical Infectious Diseases*, 51(2), e12–e15.

Mesner, O., Riesenberg, K., Biliar, N., Borstein, E., Bouhnik, L., Peled, N., & Yagupsky, P. (2007). The many faces of human-to-human transmission of brucellosis: congenital infection and outbreak of nosocomial disease related to an unrecognized clinical case. *Clinical Infectious Diseases*, 45(12), e135-e140.

Mutolo, M. J., Jenny, L. L., Buszek, A. R., Fenton, T. W., & Foran, D. R. (2016). Osteological and molecular identification of brucellosis in ancient butrint, albania. *American Journal of Physical Anthropology*, 147(2), 254–263.

N Xavier, M., A Paixao, T., B den Hartigh, A., M Tsolis, R., & L Santos, R. (2010). Pathogenesis of Brucella spp. *The Open Veterinary Science Journal*, 4(1), 109–118.

Nannyonga, B., Mwanga, G. G., & Luboobi, L. S. (2015). An optimal control problem for ovine brucellosis with culling. *Journal of Biological Dynamics*, 9(1), 198–214.

Nepomuceno, E. G., Barbosa, A. M., Silva, M. X., & Perc, M. (2018). Individual-based modelling and control of bovine brucellosis. *Royal Society Open Science*, 5(5), 180–200.

Ngeleja, R. C., Luboobi, L. S., & Nkansah-Gyekye, Y. (2017). The effect of seasonal weather variation on the dynamics of the plague disease. *International Journal of Mathematics and Mathematical Sciences*, 2017, 1–25.

Ngeleja, R. C., Luboobi, L. S., & Nkansah-Gyekye, Y. (2018). Plague disease model with weather seasonality. *Mathematical Biosciences*, 302, 80–99.

Nie, J., Sun, G. Q., Sun, X. D., Zhang, J., Wang, N., Wang, Y. M., Shen, C. J., Huang, B. X., & Jin, Z. (2014). Modeling the transmission dynamics of dairy cattle brucellosis in jilin province, China. *Journal of Biological Systems*, 22(4), 533–554.

Nyerere, N., Luboobi, L. S., Mpeshe, S. C., & Shirima, G. M. (2019). Mathematical Model for the Infectiology of Brucellosis with some Control Strategies. *New Trends in Mathematical Sciences*, 7(4), 387–405.

Nyerere, N., Matofali, A. X., Mpeshe, S. C., & Edward, S. (2017). Modeling the impact of vertical transmission in vectors on the dynamics of dengue fever. *World Journal of Modelling and Simulation*, 13(3), 219–227.

Okosun, K. O., Rachid, O., & Marcus, N. (2013). Optimal control strategies and cost-effectiveness analysis of a malaria model. *BioSystems*, 111(2), 83–101.

Okuonghae, D., & Korobeinikov, A. (2007). Dynamics of tuberculosis: the effect of direct observation therapy strategy (DOTS) in Nigeria. *Mathematical Modelling of Natural Phenomena*, 2(1), 113–128.

Padmanabhan, P., Seshaiyer, P., & Castillo-Chavez, C. (2017). Mathematical modeling, analysis and simulation of the spread of Zika with influence of sexual transmission and preventive measures. *Letters in Biomathematics*, 4(1), 148–166.

Palanduz, A., Palanduz, S., Guler, K., & Guler, N. (2000). Brucellosis in a mother and her young infant: probable transmission by breast milk. *International Journal of Infectious Diseases*, 4(1), 1–55.

Pappas, G., Papadimitriou, P., Akritidis, N., Christou, L., & Tsianos, E. V. (2006). The new global map of human brucellosis. *The Lancet Infectious Diseases*, 6(2), 91–99.

Poester, F. P., Samartino, L. E., & Santos, R. L. (2013). Pathogenesis and pathobiology of brucellosis in livestock. *Revue Scientifique et Technique* , 32(1), 105–15.

Pontryagin, L. S., Boltyanskii, V. G., Gamkrelidze, R. V., & Mishchenko, E. F. (1962). *The mathematical theory of optimal processes, translated by KN Trirogoff*. New York.

Posny, D., & Wang, J. (2014). Computing the basic reproductive numbers for epidemiological models in non-homogeneous environments. *Applied Mathematics and Computation*, 242, 473-490.

Racloz, V., Schelling, E., Chitnis, N., Roth, F., & Zinsstag, J. (2013). Persistence of brucellosis in pastoral systems. *OIE Revue Scientifique et Technique*, 32(1), 61–70.

Roth, F., Zinsstag, J., Orkhon, D., Chimed-Ochir, G., Hutton, G., Cosivi, O., Carrin, G., & Otte, J. (2003). Human health benefits from livestock vaccination for brucellosis: case study. *Bulletin of the World Health Organization*, 81, 867–876.

Schelling, E., Diguimbaye, C., Daoud, S., Nicolet, J., Boerlin, P., Tanner, M., & Zinsstag, J. (2003). Brucellosis and Q-fever seroprevalences of nomadic pastoralists and their livestock in Chad. *Preventive Veterinary Medicine*, 61(4), 279–293.

Shirima, G. M. (2005). *The epidemiology of brucellosis in animals and humans in Arusha and Manyara regions in Tanzania* . PhD thesis. University of Glasgow.

Shirima, G. M., Masola, S. N., Malangu, O. N., & Schumaker, B. A. (2014). Outbreak investigation and control case report of brucellosis: experience from livestock research centre, Mpwapwa, Tanzania. *Onderstepoort Journal of Veterinary Research*, 81(1), 1–4.

Siettos, C. I., & Russo, L. (2013). Mathematical modeling of infectious disease dynamics. *Virulence*, 4(4), 295–306.

Smith, D. L., Battle, K. E., Hay, S. I., Barker, C. M., Scott, T. W., & McKenzie, F. E. (2012). Ross, macdonald, and a theory for the dynamics and control of mosquito-transmitted pathogens. *PLoS Pathogens*, 8(4), e1002588. doi:10.1371/journal.ppat.1002588.

Swai, E. S., & Schoonman, L. (2009). Human brucellosis: seroprevalence and risk factors related to high risk occupational groups in Tanga Municipality, Tanzania. *Zoonoses and Public Health*, 56(4), 183–187.

Swai, E. S., & Schoonman, L. (2009). Human brucellosis: seroprevalence and risk factors related to high risk occupational groups in Tanga Municipality, Tanzania. *Zoonoses and Public Health*, 56(4), 183–187.

Tumwiine, J., & Robert, G. (2017). A mathematical model for treatment of bovine brucellosis in cattle population. *Journal of Mathematical Modeling*, 5(2), 137–152.

Tumwine, G., Matovu, E., Kabasa, J. D., Owiny, D. O., & Majalija, S. (2015). Human brucellosis: sero-prevalence and associated risk factors in agro-pastoral communities of Kiboga District, Central Uganda. *BMC Public Health*, 15(1), 1–8.

Tuon, F. F., Gondolfo, R. B., & Cerchiari, N. (2017). Human-to-human transmission of Brucella–a systematic review. *Tropical Medicine and International Health*, 22(5), 539–546.

Van den Driessche, P. (2017). Reproduction numbers of infectious disease models. *Infectious Disease Modelling*, 2(3), 288–303.

Van den Driessche, P., & Watmough, J. (2002). Reproduction numbers and sub-threshold endemic equilibria for compartmental models of disease transmission. *Mathematical Biosciences*, 180(1-2), 29–48.

Vassallo, D. J. (1996). The saga of brucellosis: controversy over credit for linking malta fever with goats' milk. *The Lancet*, 348(9030), 486–521.

Wang, W., & Zhao, X. Q. (2008). Threshold dynamics for compartmental epidemic models in periodic environments. *Journal of Dynamics and Differential Equations*, 20(3), 699–717.

WHO. Brucellosis in humans and animals, *http://www.who.int/resources/publications/Brucellosis.pdf*. Accessed: 2018-11-08.

Wright, A. E., & Smith, F. (1897). A note on the occurrence of malta fever in india. *British Medical Journal*, 1(1893), 911.

Wyatt, H. V. (2016). Lessons from the history of brucellosis. *Revue Scientifique et Technique Office International des Epizooties*, 32(1), 17–25.

Wyatt, H. V. (2016). Lessons from the history of brucellosis. *Journal of Maltese History*, 5(1), 75–84.

Yilma, M., Mamo, G., & Mammo, B. (2016). Review on Brucellosis Sero-prevalence and Ecology in Livestock and Human Population of Ethiopia. *Achievements in the Life Sciences*, 10(1), 80–86.

Young, E. J., Mandell, G. L., Bennett, J. E., & Dolin, R. (2009). Brucella Species Principles and Practice of Infectious Diseases. *Churchil Livingstone*, 226, 2009.

Zhang, F., Li, Z., La, X., Ma, X., Zhang, Y., Ji, P., Jiang, M., Hu, J., Zhang, Z., Lu, X., & Ding, J. (2015). Multiple-locus variable-number tandem-repeat analysis of Brucella isolates from patients in Xinjiang China. *International Journal of Clinical and Experimental Medicine*, 8(9), 15716–15723.

Zhang, J., Sun, G. Q., Sun, X. D., Hou, Q., Li, M., Huang, B., Wang, H., & Jin, Z. (2014). Prediction and control of brucellosis transmission of dairy cattle in Zhejiang Province, China. *Plos One*, 9(11), 1–13.

Zhao, X. Q. (2001). Uniform persistence in processes with application to non-autonomous competitive models. *Journal of Mathematical Analysis and Applications*, 258(1), 87-101.

Zhao, X. Q., Borwein, J., & Borwein, P. (2003). *Dynamical Systems in Population Biology*, Vol. 16. Springer.

Zhou, L., Fan, M., Hou, Q., Jin, Z., & Sun, X. (2018). Transmission dynamics and optimal control of brucellosis in Inner Mongolia of China. *Mathematical Biosciences and Engineering*, 15(2), 543–567.

Zinsstag, J., & Roth, F., Orkhon, D., Chimed-Ochir, G., Nansalmaa, M., Kolar, J., & Vounatsou, P. (2005). A model of animal–human brucellosis transmission in Mongolia. *Preventive Veterinary Medicine*, 69(1-2), 77–95.

APPENDICES

APPENDIX 1: MATLAB CODES FOR CHAPTER 3

```
%Time Series Graph for Brucellosis in Livestock and Humans
Ls*Ns+pss*x(4)-(bs*x(6)+as*x(7)+ps+ms)*x(5);
(bs*x(6)+as*x(7))*x(5)-(ms+ds)*x(6);
rc*x(3)+rs*x(6)-(e+ta)*x(7);
ph*Nh+g*x(10)-(bhc*x(3)+bhs*x(6)+bh*x(9)+ah*x(7)+mh)*x(8);
(bhc*x(3)+bhs*x(6)+bh*x(9)+ah*x(7))*x(8)-(sg+mh+dh)*x(9);
g*x(9)-(g+mh)*x(10)];
%Running File
[t,x1]=ode45(fx2,[0 15],[5000,10000,0,5000,10000,0,20,2000,0,0]);
plot(t,x1(:,1),'g',t,x1(:,2),'b',t,x1(:,3),'r',t,x1(:,4),'m',
t,x1(:,5),'c',t,x1(:,6),'y',t,x1(:,7),'k',t,x1(:,8),t,x1(:,9),
t,x1(:,10),'lineWidth',2)%Graph of infected population
grid on
grid minor
ax = gca;
ax.GridColor = [.5 .5 .5];
ax.GridLineStyle = '--';
ax.GridAlpha = 0.5;
xlabel('Time (Years)')
ylabel('Population')
legend('Vaccinated cattle','Susceptible cattle',
'Infective cattle' ,'Vaccinated small ruminants',
'Susceptible small ruminants','Infective small ruminants',
'Brucella in the environment','Susceptible human',
'Infected human','Recovered human')
% Effective reproductive number Vs effective disinfection
close all
Nc = 1500; Ns=2200;
Lc=0.1;     Ls=0.1;
pc = 0.7;    ps=0.8;
bc=0.0011;     bs=0.001;
psc = 0.4;   pss=0.5;
mc = 0.25;   ms=0.35;
rc = 10;    rs=15;
dc =.35;  ds=.4;
ac=0.00035;  as=0.00032;
e = 8;     ta=8;

ta=0:0.01:12;
R11=((bc*(e+ta)+ac*rc)*(psc+mc)*Lc*Nc)
./(mc*(mc+dc)*(e+ta)*(pc+psc+mc));
R22=((bs*(e+ta)+as*rs)*(pss+ms)*Ls*Ns)
./(ms*(ms+ds)*(e+ta)*(ps+pss+ms));
```

```
R12=((psc+mc)*ac*rs*Lc*Nc)./(mc*(ms+ds)*(e+ta)*(pc+psc+mc));
R21=((pss+ms)*as*rc*Ls*Ns)./(ms*(mc+dc)*(e+ta)*(ps+pss+ms));
Re=(R11+R22+sqrt((R22-R11).^2+4*R12.*R21))./2;
Y=[R11' R12' R21' R22' Re'];
plot(ta,Y,'lineWidth',2);
grid on
grid minor
ax = gca;
ax.GridColor = [.5 .5 .5];
ax.GridLineStyle = '--';
ax.GridAlpha = 0.5;
%title ('Reproduction number Vs Disinfection rate')
xlabel('Effective disinfection rate (per year)')
ylabel('Reproduction Number')
legend('R11','R12','R21','R22','Re')
%%
%Sensitivity Analysis
syms Nc Lc bc pc psc mc dc ac rc e ta Ns Ls bs ps pss ms ds
as rs

v=[Nc Lc bc pc psc mc dc ac rc e ta Ns Ls bs ps pss ms ds
as rs];

R11=((bc*(e+ta)+ac*rc)*(psc+mc)*Lc*Nc)./(mc*(mc+dc)*(e+ta)
*(pc+psc+mc));
R22=((bs*(e+ta)+as*rs)*(pss+ms)*Ls*Ns)./(ms*(ms+ds)*(e+ta)
*(ps+pss+ms));
R12=((psc+mc)*ac*rs*Lc*Nc)./(mc*(ms+ds)*(e+ta)*(pc+psc+mc));
R21=((pss+ms)*as*rc*Ls*Ns)./(ms*(mc+dc)*(e+ta)*(ps+pss+ms));
Re=(R11+R22+sqrt((R22-R11).^2+4*R12.*R21))./2;
P=jacobian(Re,v)
v0=[1500 0.1 0.0011 0.7 0.4 0.25 0.35 0.00035 10 8 12 2200 0.1
0.001 0.8 0.5 0.35 0.4 0.00032 15];

sensi= subs(P.*v/Re,v,v0)
double(sensi)
%hist(sensi)
```

APPENDIX 2: MATLAB CODE FOR CHAPTER 4

Function File for the Model System

```
function ydot = kims(t,yy,U,Constant)
%This function solves MU infection on livestock and humans
x=yy(1); y=yy(2); v=yy(3); z=yy(4); l=yy(5); a=yy(6); c=yy(7);
b=yy(8);
Nc=Constant(1); p1 = Constant(2); pc = Constant(3);
bc = Constant(4);psc= Constant(5); mc= Constant(6);
dc=Constant(7);ac=Constant(8);rc=Constant(9);e=Constant(10);
ta= Constant(11);Ns=Constant(12);p2= Constant(13);
ps= Constant(14);bs=Constant(15);pss=Constant(16);
ms=Constant(17); ds=Constant(18);as=Constant(19);
rs=Constant(20);gm=Constant(21); Nh=Constant(22);
ph=Constant(23);bhc=Constant(24);bhs=Constant(25);
bhh=Constant(26);mh=Constant(27);ah=Constant(28);
sg=Constant(29); dh=Constant(30);

u1 = U(1); u2=U(2);u3=U(3);u4 = U(4);
ydot1=p1*Nc-((1-u1)*(bc*y+ac*b)+mc)*x;
ydot2=(1-u1)*(bc*y+ac*b)*x-(mc+u2*dc)*y;
ydot3=p2*Ns-((1-u1)*(bs*z+as*b)+ms)*v;
ydot4=(1-u1)*(bs*y+as*b)*x-(ms+u2*ds)*z;
ydot5=ph*Nh+gm*c-((1-u4)*(bhc*y+bhs*y+bhh*a+ah*b)+mh)*l;
ydot6=(1-u4)*(bhc*y+bhs*y+bhh*a+ah*b)*l-(sg+mh+dh)*a;
ydot7=sg*a-(gm+mh)*c;
ydot8=rc*y+rs*z-(e+u3*ta)*b;
ydot  = [ydot1; ydot2; ydot3; ydot4; ydot5; ydot6; ydot7;
        ydot8];
```

Function file for costate variables

```
function ydot = kims_costate(t,y,U,X,Constant);
%This function solves a MU infection on livestock and
human type three equations
L1=y(1);L2=y(2);L3=y(3);L4=y(4);L5=y(5);L6=y(6);L7=y(7);
L8=y(8);
Nc=Constant(1);p1 = Constant(2);pc = Constant(3);
bc = Constant(4);psc = Constant(5);mc= Constant(6);
dc = Constant(7); ac = Constant(8);rc=Constant(9);
e = Constant(10);ta = Constant(11);Ns = Constant(12);
p2= Constant(13);ps= Constant(14);bs = Constant(15);
pss= Constant(16); ms= Constant(17); ds = Constant(18);
as= Constant(19);rs = Constant(20);gm=Constant(21);
Nh=Constant(22);ph=Constant(23);bhc=Constant(24);
```

```
bhs=Constant(25);bhh=Constant(26);mh=Constant(27);
ah=Constant(28);sg=Constant(29);dh=Constant(30);

% Constant weights
A1=Constant(31); A2= Constant(32); A3= Constant(33);
A4= Constant(34);B1=Constant(35);B2= Constant(36);
B3= Constant(37); B4 = Constant(38);

%list your suitable parameters
u1 = U(1); u2=U(2); u3=U(3); u4=U(4);
% variables x=S_c,y=I_c,v=S_s,z=I_s, S_h, I_h, R_h, B
x = X(1,:);y = X(2,:);v = X(3,:);z = X(4,:);l= X(5,:);
a= X(6,:); c = X(7,:);b=X(8,:);

% ODEs
ydot1=(1-u1)*(bc*y+ac*b)*(L1-L2)+mc*L1;
ydot2=-A1+(1-u1)*(L1-L2)*bc*x+L2*(mc+u2*dc)
+(1-u4)*(L5-L6)*bhc*l-L8*rc;
ydot3=(1-u1)*(bs*z+as*b)*(L3-L4)+ms*L3;
ydot4=-A2+(1-u1)*(L3-L4)*bs*v+L4*(ms+u2*ds)
+(1-u4)*(L5-L6)*bhs*l-L8*rs;
ydot5=(1-u4)*(bhc*y+bhs*z+bhh*a+ah*b)*(L5-L6)+mh*L5;
ydot6=-A4+(1-u4)*bhh*l*(L5-L6)+L6*(sg+mh+dh)-L7*sg;
ydot7=gm*(L7-L5)+(mh+dh)*L7;
ydot8=-A3+(1-u1)*(L1-L2)*ac*x+(1-u1)*(L2-L4)*as*v
+(1-u4)*(L5-L6)*ah*l+L8*(e+u3*ta);
ydot=[ydot1; ydot2; ydot3; ydot4;ydot5; ydot6;ydot7;ydot8];
```

Main or Running File

```
clc
clear all
close all
%t0 = 0; tf=10;N=4;
%t0 = 0; tf=6; N=100; %case 3
t0 = 0; tf=6; N=100; %case 3

time =linspace(t0,tf,N);
% initial condition for STATE SYSTEM
y0  = [200 10 200 5 50 10 5 100];

%---  CONSTANTS --
Constant=[500  0.3   0.7 0.0011  0.4 0.25  0.35   0.00035 10
8 12 550  0.4 0.8 0.001 0.5 0.35 0.4 0.00032 15 0.5 2500 0.04
0.00016 0.00016 0.00002 0.02 0.002 0.9 0.0002 15 20 5 10 15 10
10 10];
```

```
%Constants
Nc=Constant(1); p1 = Constant(2); pc = Constant(3);
 bc = Constant(4); psc =Constant(5); mc = Constant(6);
 dc = Constant(7); ac = Constant(8);rc=Constant(9);
 e = Constant(10); ta  = Constant(11); Ns = Constant(12);
p2= Constant(13); ps   = Constant(14); bs = Constant(15);
pss = Constant(16);ms = Constant(17); ds= Constant(18);
as= Constant(19);rs= Constant(20);gm=Constant(21);
Nh=Constant(22); ph=Constant(23);bhc=Constant(24);
bhs=Constant(25);bhh=Constant(26);mh=Constant(27);
ah=Constant(28);sg=Constant(29);dh=Constant(30);
 % weights
A1= Constant(31); A2= Constant(32); A3= Constant(33);
A4= Constant(34);B1= Constant(35); B2= Constant(36);
B3= Constant(37); B4= Constant(38);

lf  = [0 0 0 0 0 0 0 0];
init =y0;
init2 =lf;
h = (tf-t0)/N;
u = linspace(0,0,N+1);
u1=u'; u2=u'; u3=u'; u4=u';
U = [u1 u2 u3 u4];
%% IMPLIMENTATION OF THE ALGORITHM
%Test 1 stoping condition 1
delta = 0.01;
X=init;
i=0; %Initialize iteration counter
mm=size(X);
NumXX =10e10;
Xnew = rand(N+1,mm(2)).*(repmat(X,N+1,1));
DenXnew=norm(Xnew);
while  NumXX/DenXnew>delta
Xold =  Xnew;
oldu = U;
%FORWARD RUNGE KUTTA  FOR STATES
[Tx, X]=rk4foward(@kims,t0, tf,N, init,U,Constant);

% BACKWARD RUNGEKUTA FOR COSTATES
$[Tp, P]=rk4back(@kims_costate,t0,tf,N,init2,U,X,Constant)$;

%UPDATE THE CONTROLS
x = X(1,:); y = X(2,:); v = X(3,:); z = X(4,:);
    l = X(5,:); a= X(6,:); c = X(7,:); b = X(8,:);
L1 = P(1,:); L2 = P(2,:); L3 = P(3,:); L4 = P(4,:);
     L5 = P(5,:); L6 = P(6,:); L7 = P(7,:); L8 = P(8,:);
% Case0:No control,
%   u1 =zeros(1,N+1);
```

```
%   u2 =zeros(1,N+1);
%   u3 =zeros(1,N+1);
%   u4 =zeros(1,N+1);

% Case1:u1/=0, u2/=0, u3/=0,u4=0,
%      u1 =max(0,min(1,((L2-L1).*(bc.*y+ac.*b).*x
          +(L4-L3).*(bs.*z+as.*b).*v)/(B1)));
%      u2 =max(0,min(1,((y.*L2+z.*L4))./B2));
%      u3 =max(0,min(1,(L8.*b)./B3));
%      u4 =zeros(1,N+1);

% Case2:u1/=0, u2/=0, u3=0,u4/=0,
%     u1 =max(0,min(1,((L2-L1).*(bc.*y+ac.*b).*x
         +(L4-L3).*(bs.*z+as.*b.*v)/(B1)));
%     u2 =max(0,min(1,((y.*L2+z.*L4))./B2));
%     u3 =zeros(1,N+1);
%     u4 =max(0,min(1,((L6-L5).*(bhc.*y+bhs.*z
          +bhh.*a+ah.*b).*l./(B4))));

%Case3: u1/=0, u2=0, u3/=0,u4/=0,
%     u1 =max(0,min(1,((L2-L1).*(bc.*y+ac.*b).*x
         +(L4-L3).*(bs.*z+as.*b).*v)/(B1)));
%     u2 = zeros(1,N+1);
%     u3 =max(0,min(1,(L8.*b)./B3));
%     u4 =max(0,min(1,((L6-L5).*(bhc.*y+bhs.*z+bhh.*a+ah.*b)
          .*l./(B4))));

% Case4:u1=0, u2/=0, u3/=0,u4/=0,
%      u1 =zeros(1,N+1);
%      u2 =max(0,min(1,((y.*L2+z.*L4))./B2));
%      u3 =max(0,min(1,(L8.*b)./B3));
%      u4 =max(0,min(1,((L6-L5).*(bhc.*y+bhs.*z+bhh.*a
           +ah.*b).*l./(B4))));

% Case5:u1/=0, u2/=0, u3/=0, u4/=0
u1=max(0,min(1,((L2-L1).*(bc.*y+ac.*b).*x+(L4-L3)
.*(bs.*z+as.*b).*v)/(B1)));
u2 =max(0,min(1,((y.*L2+z.*L4))./B2));
u3 =max(0,min(1,(L8.*b)./B3));
u4 =max(0,min(1,((L6-L5).*(bhc.*y+bhs.*z+bhh.*a+ah.*b)
    .*l/(B4))));

Uu=[u1' u2' u3' u4'];
U = 0.5*Uu + 0.5*oldu; % Convex combination of the controls


Xnew =  X';
NumXX =abs(norm(Xnew-Xold));
```

```
DenXnew =norm(Xnew);
i=i+1 %Update iteration counter
end
%% PLOTING
X=X';
Tx =Tx';
XX=X(:,1); YY=X(:,2); VV=X(:,3); ZZ=X(:,4); LL=X(:,5);
AA=X(:,6); GG=X(:,7); BB=X(:,8);

Up = [0 0 0 0];
[T,Y] = ode45(@kims,time,y0,[],Up,Constant);

J =sum(((A1*YY(end)+A2*ZZ(end)+A3*BB(end))+A4*AA(end))
+((B1/2)*Uu(:,1).*Uu(:,1)+(B2/2)*Uu(:,2).*Uu(:,2)
+(B3/2)*Uu(:,3).*Uu(:,3)+(B4/2)*Uu(:,4).*Uu(:,4)))
%Change to the suitable objective function

S=[Tx,X];
%('C:\Users\NYERERE\Desktop\Nkuba')
save case5;
%save('case3State', 'S');
%save('case3Control', 'Uu');
%save('Cost', 'J');
figure(1)
subplot(2,2,1)
plot(Tx,X(:,2),'-b',T, Y(:,2),'--r','LineWidth',1.5);
ylim([0 100])
ylabel('I_c(t)');
xlabel('Time (years)');
legend('u_i\neq 0, i=1,2,3,4','u_i=0, i=1,2,3,4')
%
subplot(2,2,2)
plot(Tx,X(:,4),'-b',T, Y(:,4),'--r','LineWidth',1.5);
ylim([0 100])
ylabel('I_s(t)');
xlabel('Time (years)');
legend('u_i\neq 0, i=1,2,3,4','u_i=0, i=1,2,3,4')
%
subplot(2,2,3)
plot(Tx,X(:,6),'-b', T, Y(:,6),'--r','LineWidth',1.5);
%   ylim([0 10])
ylabel('I_h(t)');
xlabel('Time (years)');
legend('u_i\neq 0, i=1,2,3,4','u_i=0, i=1,2,3,4')

subplot(2,2,4)
plot(Tx,Uu(:,1),'-b',Tx,Uu(:,2),'--r',Tx,Uu(:,3),'--k',
Tx,Uu(:,4),'--g','LineWidth',1.5);
```

```
ylabel('Control Profile');
xlabel('Time (years)');
legend('u_1\neq 0','u_2\neq 0','u_3\neq 0','u_4\neq 0')

% collect all the incidence terms in the ODE
X=XX'; % solution of the optimal control
U =[0 0 0 0]; % when no control
[Tx,Y] = ode45(@kims,time,y0,[],U,Constant);
Y=(Y);
Inew=sum(Y(:,2))-sum(X(:,2))+sum(Y(:,4))-sum(X(:,4))
+sum(Y(:,6))-sum(X(:,6))+sum(Y(:,8))-sum(X(:,8)) % averted
```

APPENDIX 3: MATLAB CODE FOR CHAPTER 5

```
function dy = chap6_2(t,y)
global Beta1_0 Beta1_1 Beta2_0 Beta2_1 Beta3_0 Beta3_1
Alpha1_0 Alpha1_1 Alpha2_0 Alpha2_1 Alpha3_0 Alpha3_1
ph2_0 ph2_1 rho_0 rho_1 rho_2 rho_3 Eps_0 Eps_1 ph1_0 ph1_1
%Other parameters
pi_a=0.1; ph1_0=0.02; pa = 0.7; ps=0.4; ma = 0.25; mh=0.02;
d=0.35; ta=8;g=0.5; sg=0.8; pi_w=0.82; mw=0.07;

%Baseline parameters
Beta1_0=0.0011; Beta1_1=0.9; Beta2_0=0.0002; Beta2_1=0.9;
Beta3_0=0.005; Beta3_1=0.002; Alpha1_0=0.00035; Alpha3_0=0.03;
Alpha3_1=0.8; rho_2=0.07; rho_3=0.5; Alpha1_1=0.9; ph1_1=0.9;
Alpha2_0=0.002; Alpha2_1=0.9; rho_0=0.5; rho_1=0.9; Eps_0=12;
Eps_1=0.9; ph2_0=0.07; ph2_1=0.9;
Va=y(1);Sa=y(2);Ia=y(3);Sh=y(4);Ih=y(5);Rh=y(6);Sw=y(7);Iw=y(8);
B=y(9); tt=y(10); Na = Sa+Va+Ia; Nh=Sh+Ih+Rh; Nw = Sw+Iw;

%  System of ODEs
dVa=pa.*Sa-(ma+ps).*Va;
dSa=pi_a.*Na+ps.*Va-(G_1(tt).*Ia+Alpha1(tt).*B+ps+ma).*Sa;
dIa=(G_1(tt).*Ia+Alpha1(tt).*B).*Sa-(ma+d).*Ia;
dSh=ph_1(tt).*Nh+g.*Rh -(G_2(tt).*Ia+Alpha2(tt).*B+mh).*Sh;
dIh=(G_2(tt).*Ia+Alpha2(tt).*B).*Sh-(sg+mh).*Ih;
dRh=sg.*Ih-(g+mh).*Rh;
dSw=ph_2(tt).*Nw-(G_3(tt).*Iw+Alpha3(tt).*B).*Sw;
dIw=(G_3(tt).*Iw+Alpha3(tt).*B).*Sw-mw.*Iw;
dB=rho(tt).*Ia+rho1(tt).*Iw-(Eps(tt)+ta).*B;
ds=5;
dy=[dVa;dSa;dIa;dSh;dIh;dRh;dSw;dIw;dB;ds];

%Where functions of tt are of the form:
function r5 = rho(t)
global rho_0 rho_1
r5 = rho_0.*(1+rho_1.*sin(pi.*t./6));
```

Running File for Time series Graphs

```
global Beta1_0 Beta1_1 Beta2_0 Beta2_1 Beta3_0 Beta3_1
Alpha1_0 Alpha1_1 Alpha2_0 Alpha2_1 Alpha3_0 Alpha3_1
rho_0 rho_1 rho_2 rho_3 Eps_0 Eps_1
options = odeset('MaxStep',0.01);
% [t,y] = ode45('chap6_1',[0 10],[100,1000,10,10000,10,500,0,0]
,options); %animal population
[t,y] = ode45('chap6_2',[0 20],[1000,2000,300,5000,10,5,200 0
10,0],options); %Human population
```

```
figure(1)
plot(t,y(:,8),'lineWidth',2)
grid on
grid minor
ax = gca;
ax.GridColor = [.5 .5 .5];
ax.GridLineStyle = '--';
ax.GridAlpha = 0.5;
xlabel('Time(years))')
ylabel('Susceptible wild animals')
```

Effect of Temperature on R_e

```
% Minimum Daily Temperature for Ngorongoro;
t=1:1:365;
%Other parameters
La=0.009; p= 0.7; ps=0.4; Lw=0.0082; ma = 0.25;mw=0.07;
d=0.35;ta=8;
%Baseline parameters
Beta1_0=0.0011; Beta3_0=0.002; Alpha1_0=0.00035;
Alpha3_0=0.03;rho1=0.5; rho3=0.07; Eps_0=12;
ph2_0=0.07; ph2_1=0.9;  Na=2000;Nw=500;
% Minimum Daily Temperature 2014
L=[16.057 14.79 14.242 15.321 14.324 14.821 14.12 13.803 14.651
14.128 13.143 12.017 13.931 14.137 14.118 13.095 13.6 13.321
13.738 15.118 13.856 14.13 14.499 13.954 13.059 11.694 11.957
12.552 13.928 14.638 17.607 13.573 12.443 13.907 13.587 14.573
15.088 15.595 14.607 13.885 14.335 13.183 13.122 13.16 13.208
14.277 14.425 15.065 16.133 14.303 16.533 16.208 14.006 15.463
13.998 15.427 15.359 14.608 13.574 14.909 15.816 14.472 13.942
14.712 15.098 15.331 15.254 17.116 14.133 16.213 12.967 12 16.231
14.283 14.744 13.072 13.549 16.461 13.666 14.137 13.363 14.252
15.081 13.378 15.369 16.343 15.509 13.752 15.237 14.78 14.188
13.838 13.203 12.944 14.484 13.985 14.826 13.679 13.667 13.637
15.512 13.635 12.804 10.31 12.318 13.06 13.779 14.799 13.704
14.185 13.675 13.702 14.827 15.993 14.574 12.71 15.46 14.45
13.198 14.576 14.47 12.927 14.256 13.13 14.061 13.391 13.558
11.895 11.514 13.622 12.845 13.709 12.986 12.666 12.119 14.832
13.922 12.714 13.385 13.591 10.487 12.753 13.019 10.346 10.295
12.693 12.781 13.403 13.873 13.459 13.349 13.541 13.303 13.948
14.515 14.079 14.178 14.278 13.152 15.156 13.863 13.205 12.98
13.829 12.86 14.018 13.474 12.868 13.38 14.401 14.116 13.835
12.316 13.311 11.656 11.963 12.182 12.241 12.059 11.204 12.102
11.951 12.875 12.785 11.495 12.088 13.763 13.06 12.428 12.412
13.31 13.793 12.033 13.703 14.207 13.3 12.326 15.534 15.62 13.817
14.004 14.459 13.624 12.794 13.408 13.522 14.808 12.796 14.37
12.829 11.899 12.141]; %Minimum temperature data
```

```
%%%%%%%%%%%%%%%%%%%%%%%%%%%%%%%%%%Temperature Code
for i = 1:length(L);%i=i+1;i<=12;
if L(i)<10;
term(i) = -1;
elseif L(i)<15;
term(i)=-0.8;
elseif L(i)<20;
term(i)=-0.5;
elseif L(i)<25;
term(i)=0.5;
elseif L(i)<30;
term(i)=0.8;
elseif L(i)<40;
term(i)=1;
else
term(i) = 0;
end
i=i+1;
end
term;
%Seasonal Parameters
G_1 = Beta1_0.*(1+term.*cos(pi.*t./6));
G_3 = Beta3_0.*(1+term.*cos(pi.*t./6));
Eps= Eps_0.*(1+term.*cos(pi.*t./6));
r=rho1.*(1+term.*cos(pi.*t./6));
rw=rho3.*(1+term.*cos(pi.*t./6));
aa=Alpha1_0.*(1+term.*cos(pi.*t./6));
aw=Alpha3_0.*(1+term.*cos(pi.*t./6));
%Effective Reproduction Number
R11=((G_1.*(Eps+ta)+aa.*r).*(ps+ma).*La.*Na)
./(ma.*(ma+d).*(Eps+ta).*(p+ps+ma));
R33=((G_3.*(Eps+ta)+aw.*rw).*(ps+mw).*Lw.*Nw)
./(mw.*mw.*(Eps+ta));
R13=((ps+ma).*aa.*rw.*La.*Na)
./(ma.*mw.*(Eps+ta).*(p+ps+ma));
R31=(aw.*r.*Lw.*Nw)./(mw.*(ma+d).*(Eps+ta));
R=(R11+R33+sqrt((R33-R11).^2+4.*R13.*R31))./2;
plot(t,R,'lineWidth',1.5)
grid on
grid minor
ax = gca;
ax.GridColor = [.5 .5 .5];
ax.GridLineStyle = '--';
ax.GridAlpha = 0.5;
xlabel('Time[Days]')
ylabel('Basic Reproduction Number')
```

RESEARCH OUTPUTS

(i) **Publications**

Nyerere, **N**., Luboobi, L. S., Mpeshe, S. C., and Shirima, G. M. (2019) Mathematical Model for the Infectiology of Brucellosis with some Control Strategies, *New Trends in Mathematical Sciences*, 7(4), 387-405.

Nyerere, **N**., Luboobi, L. S., Mpeshe, S. C., and Shirima, G. M., (2020) Mathematical model for brucellosis transmission dynamics in livestock and human populations, *Communications in Mathematical Biology and Neuroscience*, vol. 2020(3), 1–29.

Nyerere, **N**., Luboobi, L. S., Mpeshe, S. C., and Shirima, G. M. (2020) Optimal Control Strategies for the Infectiology of Brucellosis, *International Journal of Mathematics and Mathematical Sciences*, 2020, 1-17.

Nyerere, **N**., Luboobi, L. S., Mpeshe, S. C., and Shirima, G. M. (2020) A Review of the Mathematical Models for Brucellosis Infectiology and Control Strategies, *Journal of Mathematics and Informatics*, 19(2020), 23-35.

Nyerere, **N**., Luboobi, L. S., Mpeshe, S. C., and Shirima, G. M. (2020) Modeling the Impact of Seasonal Weather Variations on the Infectiology of Brucellosis, *Computational and Mathematical Methods in Medicine*, 2020, 1-17.

(ii) **Poster Presentation**

114

Available online at http://scik.org
Commun. Math. Biol. Neurosci. 2020, 2020:3
https://doi.org/10.28919/cmbn/4346
ISSN: 2052-2541

MATHEMATICAL MODEL FOR BRUCELLOSIS TRANSMISSION DYNAMICS IN LIVESTOCK AND HUMAN POPULATIONS

NKUBA NYERERE[1,2], LIVINGSTONE S. LUBOOBI[3], SAUL C. MPESHE[4], GABRIEL M. SHIRIMA[5]

[1]Department of Applied Mathematics and Computational Sciences, Nelson Mandela African Institution of Science and Technology, P. O. Box 447, Arusha, Tanzania

[2]Department of Mathematics, Informatics and Computational Sciences, Sokoine University of Agriculture, P. O. Box 3038, Morogoro, Tanzania

[3]Institute of Mathematical Sciences, Strathmore University PO Box 59857-00200, Nairobi, Kenya

[4]Department of Mathematics, University of Iringa, P. O. Box 200, Iringa, Tanzania

[5]Department of Global Health and Bio-Medical Sciences, Nelson Mandela African Institution of Science and Technology, P. O. Box 447, Arusha, Tanzania

Abstract. Brucellosis is a contagious zoonotic infection caused by bacteria of genus *brucella* which affects humans and animals. The disease is of veterinary importance, public health concern and economic significance in both developed and developing countries. It is transmitted through direct or indirect contact with infected animals or their contaminated products. In this paper we formulate and analyze a deterministic mathematical model for the transmission dynamics of brucellosis. The model formulated incorporates contaminated environment to human, infected livestock to human, and human to human modes of transmission. The impacts of human treatment in controlling the spread of brucellosis in the human population is investigated. Both analytical and numerical solutions reveal that prolonged human treatment has a significant impact in reducing the spread of Brucellosis in human population only while elimination of the disease in domestic ruminants has promising results to both human and ruminants. Thus, brucellosis control strategies should always focus on elimination of the disease in domestic ruminants.

Keywords: brucellosis; mathematical model; human to human transmission.

2010 AMS Subject Classification: 92D25.

*Corresponding author

E-mail address: nyereren@nm-aist.ac.tz

Received Novemver 11, 2019

1. INTRODUCTION

Brucellosis is a contagious zoonotic infection caused by Gram-negative bacteria of genus brucella that includes; *B. abortus* primarly from cattle, *B. melitensis* from small ruminants, *B. suis* from swine, and *B. canis* from dogs [1, 2, 3, 4]. It is considered by the international organizations like Food and Agriculture Organization (FAO), the World Health Organization (WHO) and World Organization for Animal Health (Office International des Epizooties (OIE)) as one of the most widespread zoonoses in the world alongside bovine tuberculosis and rabies [5]. The disease is an ancient one that was described more than 2000 years ago by the Romans [6] and has been known by various names, including Mediterranean fever, Malta fever, gastric remittent fever, bang's disease, crimean fever, gibraltar fever, rock fever, lazybones disease and undulant fever [7].

Brucella bacteria was first isolated in 1887 from an infected individual's blood by a British military medical officer David Bruce and by that reason the disease was named brucellosis to honor his contribution [8]. Furthermore, in 1905 Zamitt carried out an experiment on goats to investigate the origin of human brucellosis, and found that, human brucellosis originates from goats [9]. To date, eight species of brucella have been identified and named primarily for the source animal or features of infection. Of these, the following four have moderate-to-significant human pathogenicity: *Brucella melitensis* (highest pathogenicity), *Brucella suis* (high pathogenicity), *Brucella abortus* (moderate pathogenicity), *Brucella canis* (moderate pathogenicity) [10, 11, 12].

Brucellosis causes devastating losses to the livestock industry especially small-scale livestock holders, thereby limiting economic growth and hindering access to international markets [13]. The economic importance of the disease is based on the fact that it causes financial losses through abortions, sterility, decreased milk production, veterinary fees and animal replacement costs. In animals, brucellosis is transmitted when a susceptible animal ingest contaminated materials by licking discharges from infected animals and suckling milk from infected dams. In humans the bacteria is transmitted through ingestion of contaminated raw blood and meat, unpasteurized milk or other dairy products. Furthermore, direct contact with aborted fetuses, vaginal discharges and occupational accidents through needle injection during mass vaccination

and during laboratory manipulation may be possible route of brucellosis transmission. In view of this, farmers, laboratory personnels, abattoir workers and veterinarians are at high risk of contracting the disease. According to Ducrotoy *et al.* [14], there are epidemiological situations in which *B. melitensis* is absent but infections of small ruminants by *B. abortus* occur in areas where they are in contact with cattle.

Infected animals exhibit clinical signs that are of economic significance to stakeholders, such as reduced fertility, late term abortion, poor weight gain, lost draught power, and a substantial decline in milk production [13, 15]. However, symptoms in human includes; continuous or intermittent fever, headache, weakness, profuse sweats, chills, joint pains, aches, weight loss as well as devastating complications that leads to miscarriage that occurs within the early trimester in pregnant women [16]. Infection may develop into chronic forms that characterised by neurological complications, endocarditis and testicular or bone abscess formation [17, 18]. The infection can also affect the liver and spleen, and may last for longer terms if not timely treated. Furthermore, the clinical signs of brucellosis in human presents diagnostic challenges because they overlap with other febrile conditions such as typhoid fever, malaria, rheumatic fever, joint diseases and relapsing fever. Since human brucellosis is debilitating disease, it requires prolonged treatment with combination of antibiotics [19].

The global burden of human brucellosis remains high and causes more than 500,000 new human cases per year worldwide. The annual number of reported cases in United States has dropped significantly to about 100 cases per year due to stringent animal vaccination programs and milk pasteurization. Most United States cases are now due to the consumption of illegally imported unpasteurized dairy products from Mexico and approximately 60% of human brucellosis cases occur in California and Texas [20].

In Africa, livestock brucellosis exists throughout sub-Saharan Africa, but the prevalence is unclear and poorly understood with varying reports from country to country, geographical regions as well as animal factors [21]. Most African countries have poor socioeconomic status, with people living with and by their livestock, while health networks, surveillance and vaccination programs are virtually non-existent [20]. Livestock brucellosis is a highly prevalent disease in many areas of Tanzania with limited data available regarding its distribution, affected

host species and impact. The first outbreak of brucellosis was reported in Arusha in 1927 [22]. Previous surveys in Tanzania have demonstrated the occurrence of the disease in cattle in various production systems, regions and zones with individual animal level seroprevalence varying from 1 to 30% while the average prevalence in humans varies from 1 to 5% [23]. A recent study by [24] shows that brucellosis incidence is moderate in northern Tanzania and suggests that the disease is endemic and an important human health problem in this area. Moreover, human cases had been reported in areas of northern, eastern, lake and western zones of Tanzania with seroprevalence varying from 0.7 to 20.5% [25, 26]. Despite the WHO, FAO, OIE efforts and interventions are available, brucellosis continues to pose great economic threat on livelihood and food security in both developed and developing countries from generation to generation. Thus, there is a need to assess the current control strategies and their effectiveness if we are to control or eradicate the disease. So far few studies [10, 27, 28, 29, 30, 31, 32], have been developed to analyze dynamics and spread of brucellosis in a homogeneous/heterogeneous populations. However, none of these studies had considered the mathematical approach to assess the impact of human to human transmission in reducing or eradicating the disease. In this paper, the dynamics and effectiveness of the control strategies for human brucellosis using mathematical models are rigorously studied.

2. MODEL FORMULATION

Human to human brucellosis transmission is possible as indicated in various studies including [16, 33, 34, 35, 36]. The possible modes of human to human brucellosis transmission are transplancental, breastfeeding, sexual, blood transfusion and organ transplantation [37]. In this section, we formulate a deterministic mathematical model for the transmission dynamics of brucellosis in domestic small ruminants, cattle and human populations. The model we formulate includes: direct transmission of brucellosis within the cattle, within small ruminants, within humans and from livestock to human, and from the environment to livestock and humans.

Furthermore, susceptible cattle and small ruminants are either vaccinated at some points (pulse vaccination) or remain susceptible. Based on the epidemiological status of individuals, the cattle population at any time t is divided into vaccinated $V_c(t)$, susceptible $S_c(t)$, and infectious $I_c(t)$ classes. Similarly, the small ruminant population at any time t is divided into

vaccinated $V_s(t)$, susceptible $S_s(t)$, and infectious $I_s(t)$ subpopulations while the total human population, $N_h(t)$ at any time t is divided into susceptible, $S_h(t)$, infected, $I_h(t)$ and recovered, $R_h(t)$ individuals. Susceptible cattle become infected through direct contact with infected cattle at the rate of β_c or through contact with the contaminated environment (indirect transmission) at the rate α_c while susceptible small ruminants become infected when they are in contact with infectious small ruminants at the rate of β_s or through contact with the contaminated environment at the rate α_s. The transmission to humans is expressed as additive contributions of transmissions from infective humans, cattle, small ruminants and contaminated environment. Appertaining to the fact that it is very difficult to determine the quantity of brucella in environment, we define the average number of brucella that is enough for a host to be infected with brucellosis as an infectious unit and let $B(t)$ to be the number of infectious units in the environment. The incubation period for brucellosis is hardly detected, but individuals at this period can infect the susceptible individuals at the same transmission rate as the infectious individual and discharge the same quantity of brucella into the environment per unit time as in [28]. It is against this background, we assume that individuals in the incubation period and post incubation period are hosted in the same population compartment called infectious class. The interaction within and between the four populations prompts that veterinary surgeons, laboratory assistants, and farmers are predominantly exposed to the brucella bacteria.

2.1. Model Assumptions. In formulation of the model we make the following assumptions:

i. The mixing of individuals in each population is homogeneous;
ii. There is no direct transmission between cattle and small ruminants;
iii. Infected animals shed brucella pathogens in the environment;
iv. Livestock seropositivity is life-long lasting;
v. Immunized individuals cannot be infected unless their resistance to infection wanes;
vi. There is constant natural mortality rate in each of the species;
vii. The birth rate for each population is greater than natural mortality rate.

The variables and parameters used in this model are respectively summarized in TABLE 1 and TABLE 2.

TABLE 1. Model Variables

Variable	Description
$S_h(t)$	Number of susceptible humans at time t
$I_h(t)$	Number of infected human at time t
$R_h(t)$	Number of recovered humans at time t
$S_c(t)$	Number of susceptible cattle at time t
$I_c(t)$	Number of infected cattle at time t
$V_c(t)$	Number of vaccinated cattle at time t
$S_s(t)$	Number of susceptible small ruminants at time t
$I_s(t)$	Number of infected small ruminants at time t
$V_s(t)$	Number of vaccinated small ruminants at time t
$B(t)$	Number of *brucella* bacteria load per unit volume in the environment at time t

2.2. Compartmental Flow Diagram for the Disease Dynamics. The interactions between the human, cattle, small ruminants populations and the brucella in the environment are illustrated in FIGURE 1.

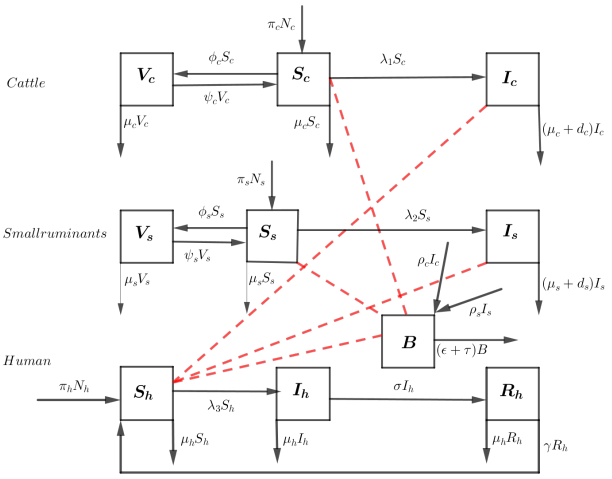

FIGURE 1. A schematic diagram for direct and indirect transmission of brucellosis in cattle, small ruminants and human populations. Solid arrows represent transfer of individuals from one subpopulation to another while dotted lines represent interactions leading to infections.

TABLE 2. Model Parameters used in the model and their description

Parameter	Description
π_c	Per capita cattle birth rate
ϕ_c	Cattle vaccination rate
π_h	Per capita human birth rate
σ	Human recovery rate
μ_h	Per capita human natural death rate
ψ_c	Cattle vaccine efficacy waning rate
β_c	Within cattle transmission rate
d_c	Culling rate of seropositive cattle
μ_c	Per capita cattle natural death rate
α_c	*Brucella* from the environment to cattle transmission rate
α_s	*Brucella* from the environment to small ruminants transmission rate
α_h	*Brucella* from the environment to human transmission rate
ρ_c	*Brucella* shedding rate by infected cattle
ρ_s	*Brucella* shedding rate by infected small ruminants
β_{ch}	Cattle to human transmission rate
β_{sh}	small ruminants to human transmission rate
ε	Decaying rate of brucella in the environment
τ	Environmental hygiene and sanitation rate
π_s	Small ruminants per capita birth rate
ϕ_s	Vaccination rate of small ruminants
ψ_s	Small ruminant vaccine efficacy waning rate
β_s	Within small ruminants transmission rate
d_s	Culling rate of seropositive small ruminants
μ_s	Per capita small ruminants natural death rate

2.3. Model Equations. Based on the assumptions and the inter-relations between the variables and the parameters shown in FIGURE 1, the transmission dynamics of Brucellosis can be described by the following ordinary differential equations:

$$
\begin{aligned}
\frac{dV_c}{dt} &= \phi_c S_c - (\psi_c + \mu_c)V_c \\
\frac{dS_c}{dt} &= \pi_c N_c + \psi_c V_c - (\lambda_1 + \phi_c + \mu_c)S_c \\
\frac{dI_c}{dt} &= \lambda_1 S_c - (\mu_c + d_c)I_c \\
\frac{dV_s}{dt} &= \phi_s S_s - (\mu_s + \psi_s)V_s \\
\frac{dS_s}{dt} &= \pi_s N_s + \psi_s V_s - (\lambda_2 + \phi_s + \mu_s)S_s \\
\frac{dI_s}{dt} &= \lambda_2 S_s - (\mu_s + d_s)I_s \\
\frac{dS_h}{dt} &= \pi_h N_h + \gamma R_h - (\lambda_3 + \mu_h)S_h \\
\frac{dI_h}{dt} &= \lambda_3 S_h - (\sigma + \mu_h + d_h)I_h \\
\frac{dR_h}{dt} &= \sigma I_h - (\gamma + \mu_h)R_h \\
\frac{dB}{dt} &= \rho_c I_c + \rho_s I_s - (\varepsilon + \tau)B
\end{aligned} \tag{1}
$$

where,

$$\lambda_1 = \beta_c I_c + \alpha_c B. \tag{2}$$

$$\lambda_2 = \beta_s I_s + \alpha_s B. \tag{3}$$

$$\lambda_3 = \beta_{hc} I_c + \beta_{hh} I_h + \beta_{hs} I_s + \alpha_h B. \tag{4}$$

3. Model Properties

3.1. Invariant Region. In this subsection we assess the well-posedness of the model by investigating the existence and feasibility of its solution. In other words, we investigate whether the solutions are epidemiologically (variables have biological interpretation) and mathematically (a unique bounded solution exists for all the time) well-posed. That is solutions of model system

(1) with nonnegative initial data remain nonnegative for all time $t \geq 0$. The model system (1) can be expressed in the compact form as:

$$\frac{dX}{dt} = AX + F$$

where,

$$A = \begin{bmatrix}
-(\mu_c+\psi_c) & \phi_c & 0 & 0 & 0 & 0 & 0 & 0 & 0 & 0 \\
\psi_c & -d_0 & 0 & 0 & 0 & 0 & 0 & 0 & 0 & 0 \\
0 & \lambda_1 & -(\mu_c+d_c) & 0 & 0 & 0 & 0 & 0 & 0 & 0 \\
0 & 0 & 0 & -(\mu_s+\psi_s) & \phi_s & 0 & 0 & 0 & 0 & 0 \\
0 & 0 & 0 & \psi_s & -d_1 & 0 & 0 & 0 & 0 & 0 \\
0 & 0 & 0 & 0 & \lambda_2 & -(\mu_s+d_s) & 0 & 0 & 0 & 0 \\
0 & 0 & 0 & 0 & 0 & 0 & -d_2 & 0 & \gamma & 0 \\
0 & 0 & 0 & 0 & 0 & 0 & \lambda_3 & -d_3 & 0 & 0 \\
0 & 0 & \rho_c & 0 & 0 & 0 & 0 & \sigma & -(\gamma+\mu_h) & 0 \\
0 & 0 & \rho_c & 0 & 0 & \rho_s & 0 & 0 & 0 & -(\varepsilon+\tau)
\end{bmatrix}$$

with,

$$d_0 = (\lambda_1 + \phi_c + \mu_c),\ d_1 = (\lambda_2 + \phi_s + \mu_s),$$

$$d_2 = (\lambda_3 + \mu_h),\ d_3 = (\sigma + \mu_h + d_h),$$

$$X = (V_c, S_c, I_c, V_s, S_s, I_s, S_h, I_h, R_h, B),$$

and F is a column vector given by

$$F = (0, \pi_c N_c^0, 0, 0, \pi_s N_s^0, 0, \pi_h N_h^0, 0, 0, 0)^T.$$

It can be noticed that AX is Meltzer matrix since all of its off diagonal entries are non negative, for all $X \in \mathbb{R}_+^{10}$. Therefore, using the fact that $F > 0$, the model system (1) is positively invariant in $\mathbb{R}_+^{10}$, which means that an arbitrary trajectory of the system starting in $\mathbb{R}_+^{10}$ remains in $\mathbb{R}_+^{10}$ forever. In addition, the right hand F is Lipschitz continuous. Thus, a unique maximal solution exists and so:

$$\Omega = \{(V_c, S_c, I_c, V_s, S_s, I_s, S_h, I_h, R_h, B) \geq 0\} \in \mathbb{R}_+^{10}.$$

is the feasible region for the model (1). Thus, the model (1) is epidemiologically and mathematically well-posed in the region Ω.

4. Model Analysis

4.1. Disease Free Equilibrium. The Brucellosis free equilibrium point is obtained by setting the right hand side of equations in model system (1) to zero, that is:

$$\frac{dV_c}{dt} = \frac{dS_c}{dt} = \frac{dI_c}{dt} = \frac{dV_s}{dt} = \frac{dS_s}{dt} = \frac{dI_s}{dt} = \frac{dS_h}{dt} = \frac{dI_h}{dt} = \frac{dR_h}{dt} = \frac{dB}{dt} = 0.$$

Let the disease free equilibrium point of Brucellosis model be E^0. In case there is no disease $I_c = I_s = I_h = B = 0$ that is, the sum of susceptible and vaccinated populations is equal to total population. There exists a disease free equilibrium $E^0 = (V_c^0, S_c^0, 0, V_s^0, S_s^0, 0, S_h^0, 0, 0, 0)$ for model system (1) where:

$$V_c^0 = \frac{\phi_c \pi_c N_c^0}{\mu_c(\phi_c + \psi_c + \mu_c)}, S_c^0 = \frac{(\mu_c + \psi_c)\pi_c N_c^0}{\mu_c(\phi_c + \psi_c + \mu_c)}, V_s^0 = \frac{\phi_s \pi_s N_s^0}{\mu_s(\phi_s + \psi_s + \mu_s)}, \; S_s^0 = \frac{(\mu_s + \psi_s)\pi_s N_s^0}{\mu_s(\phi_s + \psi_s + \mu_s)},$$

and

$$S_h^0 = \frac{\pi_h N_h^0}{\mu_h}.$$

4.2. The Effective Reproduction Number. In this subsection, we compute the effective reproduction number for model system (1) using the standard method of the next generation matrix developed in [38, 39]. The effective reproduction number, R_e is defined as the measure of average number of infections caused by a single infectious individual introduced in a community in which intervention strategies are administered [40]. The magnitude of the effective reproduction number is used to indicate both the risk of an epidemic and effort required to control an infection. When there are no interventions or controls, the number of secondary infections caused by typical infected individual during his entire period of infectiousness is called basic reproduction number, R_0. Moreover, due to the natural history of some infections, transmissibility is better quantified by the effective reproduction number rather than the basic

reproduction number [42]. Considering the system for the infective variables:

$$\begin{aligned}
\frac{dI_c}{dt} &= (\beta_c I_c + \alpha_c B)S_c - (\mu_c + d_c)I_c \\
\frac{dI_s}{dt} &= (\beta_s I_s + \alpha_s B)S_s - (\mu_s + d_s)I_s \\
\frac{dI_h}{dt} &= (\beta_{hc} I_c + \beta_{hs} I_s + \beta_{hh} I_h + \alpha_h B)S_h - (\mu_h + d_h)I_h \\
\frac{dB}{dt} &= \rho_c I_c + \rho_s I_s - (\varepsilon + \tau)B
\end{aligned} \tag{5}$$

The effective reproduction number is obtained by taking the spectral radius of the next generation matrix:

$$FV^{-1} = \left[\frac{\partial \mathscr{F}_i(E^0)}{\partial t}\right]\left[\frac{\partial \mathscr{V}_i(E^0)}{\partial t}\right]^{-1}$$

where E^0 is the brucellosis-free equilibrium point while $\mathscr{F}_i$ and $\mathscr{V}_i$ are vectors representing respectively, the rate of appearance of new infection in compartment i and the transfer of infections from compartment i to another, such that:

$$\mathscr{F}_i = \begin{bmatrix} (\beta_c I_c + \alpha_c B)S_c \\ (\beta_s I_s + \alpha_s B)S_s \\ (\beta_{hc} I_c + \beta_{hs} I_s + \beta_{hh} I_h + \alpha_h B)S_h \\ 0 \end{bmatrix}$$

$$\mathscr{V}_i = \begin{bmatrix} (\mu_c + d_c)I_c \\ (\mu_s + d_s)I_s \\ (\sigma + \mu_h + d_h)I_h \\ -\rho_c I_c - \rho_s I_s + (\varepsilon + \tau)B \end{bmatrix}$$

It is important to note that $\mathscr{V}_i$ is a resultant vector of the two vectors: $\mathscr{V}_i^+$, defined as the rate of transfer of individuals into compartment i by all other means(e.g births and immigration); and $\mathscr{V}_i^-$, which is the rate of transfer of individuals out of compartment i (e.g deaths, recovery and emigration). In particular:

$$\mathscr{V}_i = \mathscr{V}_i^- - \mathscr{V}_i^+, i = \{1,2,3,4\}$$

The Jacobian matrices F of $\mathscr{F}_i$ and V of $\mathscr{V}_i$ evaluated at E^0 are respectively:

$$F = \begin{bmatrix} \beta_c S_c^0 & 0 & 0 & \alpha_c S_c^0 \\ 0 & \beta_s S_s^0 & 0 & \alpha_s S_s^0 \\ \beta_{hc} S_h & \beta_{hs} S_h & \beta_{hh} S_h & \alpha_h B \\ 0 & 0 & 0 & 0 \end{bmatrix}$$

and

$$V = \begin{bmatrix} \mu_c + d_c & 0 & 0 & 0 \\ 0 & \mu_s + d_s & 0 & 0 \\ 0 & 0 & \sigma + \mu_h + d_h & 0 \\ -\rho_c & -\rho_s & 0 & (\varepsilon + \tau) \end{bmatrix}$$

Referring to the infected states with indices i and j, for $i, j \in [1,2,3,4]$, the entry F_{ij} is the rate at which individuals in infected state j give rise or produce new infections to individuals in infected state i, in the linearized system. Thus, when there is no new cases produced in infected state i by an individual in infected state j immediately after infection, we have $F_{ij} = 0$. The inverse of V is found to be:

$$V^{-1} = \begin{bmatrix} \frac{1}{\mu_c + d_c} & 0 & 0 & 0 \\ 0 & \frac{1}{\mu_s + d_s} & 0 & 0 \\ 0 & 0 & \frac{1}{\sigma + \mu_h + d_h} & 0 \\ \frac{\rho_c}{(\mu_c + d_c)(\varepsilon + \tau)} & \frac{\rho_s}{(\mu_s + d_s)(\varepsilon + \tau)} & 0 & \frac{1}{\varepsilon + \tau} \end{bmatrix}$$

The entry $\left(V^{-1}\right)_{ij}$ is the average length of time an infected individual spends in compartment j during its lifetime when introduced into the compartment i of disease free equilibrium, assuming that the population remains near the disease free equilibrium and barring reinfection. In particular, $\frac{1}{\mu_c + d_c}$, $\frac{1}{\mu_s + d_s}$, $\frac{1}{\sigma + \mu_h + d_h}$ are respectively the average times an infectious cattle, small ruminant, human spend in the state of being infective, and $\frac{1}{\varepsilon + \tau}$ is the average time *brucella* bacteria spend in the environment. Furthermore, *brucella* from cattle will spend $\frac{\rho_c}{\mu_c + d_c} \times \frac{1}{\varepsilon + \tau}$ time in the environment where, $\frac{\rho_c}{\mu_c + d_c}$ is the probability that an infective cattle will shed *brucella* into the environment. On the other hand, *brucella* shed by small ruminants will spend $\frac{\rho_s}{\mu_s + d_s} \times \frac{1}{\varepsilon + \tau}$ time in the environment where $\frac{\rho_s}{\mu_s + d_s}$ is the probability that an infected small ruminant will shed *brucella* into the environment. Moreover, the Next Generation

Matrix is calculated to be:

$$FV^{-1} = \begin{bmatrix} R_{11} & R_{12} & 0 & \frac{\alpha_c S_c^0}{\varepsilon+\tau} \\ R_{21} & R_{22} & 0 & \frac{\alpha_s S_s^0}{\varepsilon+\tau} \\ R_{31} & R_{32} & R_{33} & \frac{\alpha_h S_h^0}{\varepsilon+\tau} \\ 0 & 0 & 0 & 0 \end{bmatrix} \tag{6}$$

where,

$$\begin{aligned}
R_{11} &= \frac{\beta_c S_c^0}{\mu_c + d_c} + \frac{\alpha_c \rho_c S_c^0}{(\mu_c + d_c)(\varepsilon+\tau)}, \\
R_{12} &= \frac{\alpha_c \rho_s S_c^0}{(\mu_s + d_s)(\varepsilon+\tau)}, \\
R_{21} &= \frac{\alpha_s \rho_c S_s^0}{(\mu_c + d_c)(\varepsilon+\tau)}, \\
R_{22} &= \frac{\beta_s S_s^0}{\mu_s + d_s} + \frac{\alpha_s \rho_s S_s^0}{(\mu_s + d_s)(\varepsilon+\tau)}, \\
R_{31} &= \frac{\beta_{hc} S_h^0}{\mu_c + d_c} + \frac{\alpha_h \rho_c S_h^0}{(\mu_c + d_c)(\varepsilon+\tau)}, \\
R_{32} &= \frac{\beta_{hs} S_h^0}{\mu_s + d_s} + \frac{\alpha_h \rho_s S_h^0}{(\mu_c + d_c)(\varepsilon+\tau)}, \\
R_{33} &= \frac{\beta_{hh} S_h^0}{(\sigma + \mu_h + d_h)}.
\end{aligned}$$

The matrix FV^{-1} can be written as: The (i,k) entry of the Next Generation Matrix FV^{-1} is the expected number of secondary infections in compartment i produced by individuals initially in compartment k assuming that the environment of an infective individual remains homogeneous for the duration of its infection [41, 42, 43]. In particular; R_{11} is the expected number of infected cattle produced by one infectious cattle, R_{12} is the expected number of infected cattle produced by one infectious small ruminant via consumption of brucella from the environment, R_{21} is the expected number of infected small ruminant as a result of one infected cattle, R_{22} is the expected number of infected small ruminant as a result of effective contact with one infected small ruminant, R_{31} is the expected number of infected people caused by one infectious cattle,R_{32} is the expected number of infected people caused as a result of contact with brucella from small ruminants, R_{33} is the expected number of infected people caused by one infectious

person, and R_{34} is the expected number of infected people as a result of contact of brucella from the environment. It can further be noticed that, matrix FV^{-1} is non-negative and therefore, has a nonnegative eigenvalue. The non-negative eigenvalue is associated with a non-negative eigenvector which represents the distribution of infected individuals that produces the greatest number R_e of secondary infections per generation [44]. Thus, the spectral radius for our Next Generation Matrix is:

$$\rho(FV^{-1}) = R_e = max\left\{\frac{R_{11}+R_{22}+\sqrt{(R_{22}-R_{11})^2+4R_{12}R_{21}}}{2}, \frac{\beta_{hh}\pi_h N_h^0}{\mu_h(\sigma+\mu_h+d_h)}\right\} \tag{7}$$

where,

$$\begin{aligned}
R_{11} =& \frac{(\beta_c(\varepsilon+\tau)+\alpha_c\rho_c)(\psi_c+\mu_c)\pi_c N_c^0}{\mu_c(\mu_c+d_c)(\varepsilon+\tau)(\phi_c+\psi_c+\mu_c)},\\
R_{12} =& \frac{(\psi_c+\mu_c)\alpha_c\rho_s\pi_c N_c^0}{\mu_c(\mu_s+d_s)(\varepsilon+\tau)(\phi_c+\psi_c+\mu_c)},\\
R_{22} =& \frac{(\beta_s(\varepsilon+\tau)+\alpha_s\rho_s)(\psi_s+\mu_s)\pi_s N_s^0}{\mu_s(\mu_s+d_s)(\varepsilon+\tau)(\phi_s+\psi_s+\mu_s)},\\
R_{21} =& \frac{(\psi_s+\mu_s)\alpha_s\rho_c\pi_s N_s^0}{\mu_s(\mu_c+d_c)(\varepsilon+\tau)(\phi_s+\psi_s+\mu_s)}.
\end{aligned}$$

The first and the second expressions of equation (7) represents respectively the effective reproduction numbers in the livestock and human populations. It can further be noticed that, the first expression which is independent of the human population represents the threshold transmission dynamics of brucellosis in the cattle and small ruminants populations that was analyzed and discussed in [45]. The fact that human brucellosis significantly reduces work performance of individuals calls for a special interest of investigating the transmission dynamics and controls of human brucellosis. Thus, we focus on brucellosis transmission dynamics within the human population. The effective reproduction number within the human population is found to be:

$$R_{eh} = \frac{\beta_{hh}\pi_h N_h^0}{\mu_h(\sigma+\mu_h+d_h)}.$$

When there is no treatment, $\sigma = 0$, we have the within human basic reproduction number which is given by:

$$R_{0h} = \frac{\beta_{hh}\pi_h N_h^0}{\mu_h(\mu_h+d_h)}.$$

Besides, brucellosis is a zoonosis; it is transmitted to human from animals, referring to our particular case in the next generation matrix (6) the cattle to human effective reproduction number is intuitively given by:

$$R_{hc} = R_{31} = \frac{(\beta_{hc}(\varepsilon+\tau)+\alpha_h\rho_c)\pi_h N_h^0}{(\mu_c+d_c)(\varepsilon+\tau)}.$$

On the other hand, the small ruminants to human effective reproduction number is given by:

$$R_{hs} = R_{32} = \frac{(\beta_{hs}(\varepsilon+\tau)+\alpha_h\rho_s)\pi_h N_h^0}{(\mu_s+d_s)(\varepsilon+\tau)}.$$

Moreover, equation (4) indicates that, the transmission of brucellosis in the human population results from human to human transmission, small ruminants to human transmission, cattle to human transmission and environment to human transmission. Thus, if it happens one infected cattle, one infected small ruminant and one infected human are simultaneously introduced in the human population, then the effective human reproduction number is intuitively given by:

$$R_h = \frac{\beta_{hh}\pi_h N_h^0}{\mu_h(\sigma+\mu_h+d_h)} + \frac{(\beta_{hc}(\varepsilon+\tau)+\alpha_h\rho_c)\pi_h N_h^0}{(\mu_c+d_c)(\varepsilon+\tau)} + \frac{(\beta_{hs}(\varepsilon+\tau)+\alpha_h\rho_s)\pi_h N_h^0}{(\mu_s+d_s)(\varepsilon+\tau)}. \tag{8}$$

4.3. Local Stability of the Disease Free Equilibrium. In this subsection we use the trace-determinant method to investigate the local stability of the brucellosis free equilibrium point.

Theorem 4.1. *The disease free equilibrium for the brucellosis model system(1) is locally asymptotically stable if* $R_0 < 1$ *and unstable if* $R_0 > 1$.

Proof. We show that, variational matrix $J(E_0)$ of the brucellosis model at DFE has a negative trace and positive determinant. The Jacobian matrix for system (1) is given by:

$$J(E_0) = \begin{bmatrix} -a_1 & \phi_c & 0 & 0 & 0 & 0 & 0 & 0 & 0 & 0 \\ \psi_c & -a_2 & a_3 & 0 & 0 & 0 & 0 & 0 & 0 & -\alpha_c S_c^0 \\ 0 & 0 & a & 0 & 0 & 0 & 0 & 0 & 0 & \alpha_c S_c^0 \\ 0 & 0 & 0 & -b_1 & \phi_s & 0 & 0 & 0 & 0 & 0 \\ 0 & 0 & 0 & \psi_s & b_2 & b_3 & 0 & 0 & 0 & -\alpha_s S_s^0 \\ 0 & 0 & 0 & 0 & 0 & b & 0 & 0 & 0 & \alpha_s S_s^0 \\ 0 & 0 & -\beta_{hc} S_h & 0 & 0 & -\beta_{hs} S_h & -\mu_h & -c_1 & \gamma & -\alpha_h S_h^0 \\ 0 & 0 & \beta_{hc} S_h & 0 & 0 & \beta_{hs} S_h & 0 & c & 0 & \alpha_h S_h^0 \\ 0 & 0 & 0 & 0 & 0 & 0 & 0 & \sigma & -(\gamma+\mu_h) & 0 \\ 0 & 0 & \rho_c & 0 & 0 & \rho_s & 0 & 0 & 0 & -(\varepsilon+\tau) \end{bmatrix}$$

where,

$$a_1 = \mu_c + \psi_c,\ a_2 = (\phi_c + \mu_c)\ , a_3 = -\beta_c S_c^0,$$

$$b_1 = \mu_s + \psi_s,\ b_2 = -(\phi_s + \mu_s)\ , b_3 = -\beta_s S_s^0,$$

$$c_1 = \beta_{hh} S_h^0,\ , c = \beta_{hh} S_h^0 - (\sigma + \mu_h + d_h),$$

$$a = \beta_c S_c^0 - (\mu_c + d_c),$$

and

$$b = \beta_s S_s^0 - (\mu_s + d_s).$$

The trace of the Jacobian matrix $J(E_0)$is given by:

$$\begin{aligned} Tr(J(E_0)) = &-(\mu_c + d_c)\left(1 - \frac{\beta_c S_c^0}{\mu_c + d_c}\right) - (\mu_s + d_s)\left(1 - \frac{\beta_s S_s^0}{\mu_s + d_s}\right) \\ &-(\sigma + \mu_h + d_h)\left(1 - \frac{\beta_{hh} S_h^0}{\sigma + \mu_h + d_h}\right) - (\phi_c + \psi_c + 2\mu_c) \\ &-(\phi_s + \psi_s + 2\mu_s) - (\gamma + 2\mu_h) - (\varepsilon + \tau) \end{aligned}$$

Thus, the trace of the Jocobian matrix is the less than zero, that is $Tr(J(E_0)) < 0$ if:

$$\frac{\beta_c S_c^0}{\mu_c + d_c} < 1,\ \frac{\beta_s S_s^0}{\mu_c + d_s} < 1 \text{ and } \frac{\beta_{hh} S_h^0}{\sigma + \mu_h + d_h} < 1.$$

Furthermore, the determinant of matrix $J(E_0)$ is computed using Maple 16 Software and is found to be:

$$Det(J(E_0)) = a_0(1-R_h)\left((1-R_c)(1-R_{ec}) - \frac{\rho_c\alpha_c S_c^0}{(\mu_c+d_c)(\varepsilon+\tau)}(1-R_s)\right).$$

where,

$$R_h = \frac{\beta_{hh}S_h^0}{\sigma+\mu_h+d_h},\ R_s = \frac{\beta_s S_s^0}{\mu_s+d_s},\ R_c = \frac{\beta_c S_c^0}{\mu_c+d_c},\ R_{es} = \frac{(\varepsilon+\tau)\beta_s S_s^0}{(\varepsilon+\tau)(\mu_s+d_s)},$$

and

$$a_0 = (\phi_c+\psi_c+\mu_c)(\phi_s+\psi_s+\mu_s)(\gamma+\mu_h)(\sigma+\mu_h+d_h)(\mu_c+d_c)(\mu_s+d_s)(\varepsilon+\tau)\mu_c\mu_s\mu_h.$$

The determinant of the Jacobian matrix is positive (i.e. $J(E_0) > 0$) if:

$$R_c < 1,\ R_s < 1,\ R_{es} < 1, \text{ and } (1-R_c)(1-R_{ec}) > \frac{\rho_c\alpha_c S_c^0}{(\mu_c+d_c)(\varepsilon+\tau)}(1-R_s).$$

Furthermore, R_h, R_s, R_c, and R_{es} are respectively the average number of secondary human infections as a result of direct contact between susceptible and infected humans, susceptible and infected small ruminants, susceptible and infected cattle, and the average number of secondary infections caused directly or indirectly by one infected small ruminant in the susceptible ruminant population. Thus, the brucellosis free equilibrium for each population is locally asymptotically stable if $R_e < 1$. A similar result is found on Theorem 2 of [41] and Theorem 6.13 of [46]. □

4.4. Global Stability of the Disease-Free Equilibrium. In this section, we analyze the global stability of the disease-free equilibrium point by applying the [47] approach. We write model system (1) in the form:

$$\begin{cases} \dfrac{dX_s}{dt} = A(X_s - X_{DFE,S}) + A_1 X_i \\ \dfrac{dX_i}{dt} = A_2 X_i \end{cases} \tag{9}$$

where X_s is the vector representing the non-transmitting compartments and X_i is the vector representing the transmitting components. The DFE is globally asymptotically stable if A has

real negative eigenvalues and A_2 is a Metzler matrix (i.e. the off-diagonal elements of A_2 are non-negative). From model system (1) we have:

$$X_i = (I_c, I_s, I_h, B)^T, X_s = (V_c, S_c, V_s, S_s, S_h, R_h)^T,$$

$$X_s - X_{DFE,s} = \begin{bmatrix} V_c - \dfrac{\phi_c \pi_c N_c^0}{\mu_c(\psi_c + \phi_c + \mu_c)} \\ S_c - \dfrac{(\phi_c + \mu_c)\pi_c N_c^0}{\mu_c(\psi_c + \phi_c + \mu_c)} \\ V_s - \dfrac{\phi_s \pi_s N_s^0}{\mu_s(\psi_s + \phi_s + \mu_s)} \\ S_s - \dfrac{(\phi_s + \mu_s)\pi_s N_s^0}{\mu_s(\psi_s + \phi_s + \mu_s)} \\ S_h - \dfrac{\pi_h N_h^0}{\mu_h} \\ R_h \end{bmatrix}$$

and

$$A_1 = \begin{bmatrix} 0 & 0 & 0 & 0 \\ -\beta_c S_c & 0 & 0 & -\alpha_c S_c \\ 0 & 0 & 0 & 0 \\ 0 & -\beta_s S_s & 0 & -\alpha_s S_s \\ -\beta_{hc} S_h & -\beta_{hs} S_h & -\beta_{hc} S_h & -\alpha_h S_h \\ 0 & 0 & \sigma & 0 \end{bmatrix}$$

We need to check whether a matrix A for the non-transmitting compartments has real negative eigenvalues and that A_2 is a Metzler matrix. From the equation for non-transmitting compartments in (1) we have:

$$A = \begin{bmatrix} -(\psi_c+\mu_c) & \phi_c & 0 & 0 & 0 & 0 \\ \psi_c & -(\phi_c+\mu_c) & 0 & 0 & 0 & 0 \\ 0 & 0 & -(\psi_s+\mu_s) & \phi_s & 0 & 0 \\ 0 & 0 & \psi_s & -(\phi_s+\mu_s) & 0 & 0 \\ 0 & 0 & 0 & 0 & -\mu_h & \gamma \\ 0 & 0 & 0 & 0 & 0 & -(\gamma+\mu_h) \end{bmatrix}$$

with eigenvalues $\lambda_1 = -\mu_s, \lambda_2 = -(\psi_s+\phi_s+\mu_s), \lambda_3 = -\mu_c, \lambda_4 = -(\psi_c+\phi_c+\mu_c)$; and

$$A_2 = \begin{bmatrix} \beta_c S_c^0 - (\mu_c+d_c) & 0 & 0 & \alpha_c S_c^0 \\ 0 & \beta_s S_s^0 - (\mu_s+d_s) & 0 & \alpha_s S_s^0 \\ \beta_{hc} S_h & \beta_{hs} S_h^0 & \beta_{hh} S_h - (\mu_h+d_h) & \alpha_h S_h^0 \\ \rho_c & \rho_s & 0 & -(\varepsilon+\tau) \end{bmatrix}$$

Appertaining the fact that all model parameters and variables are non-negative, it is evident that A_2 is a Metzler matrix and A, have real negative eigenvalues. This implies that the disease free equilibrium for the model system (1) is globally asymptotically stable.

4.5. Global Stability of Endemic Equilibrium. The local stability of the disease free equilibrium suggests local stability of the endemic equilibrium for the reverse condition. In this subsection we study the global behaviour of the endemic equilibrium, E^* for the model system (1).

Theorem 4.2. *The endemic equilibrium point for the brucellosis model system (1) is globally asymptotically stable on* Ω *if* $R_0 > 1$.

Proof. We construction an explicit Lyapunov function for model system (1) using [48, 49, 50, 51, 52] approach as it is useful to most of the sophisticated compartmental epidemiological models. In this approach, we construct Lyapunov functions of the form:

$$V = \sum a_i (x_i - x_i^* \ln x)$$

where a_i is a properly selected positive constant, x_i is the population of the i^{th} compartment and x_i^* is the equilibrium level. We define the Lyapunov function candidate V for model system (1) as:

$$\begin{aligned} L =&(S_c - S_c^* \ln S_c) + A_1(V_c - V_c^* \ln V_c) + A_2(I_c - I_c^* \ln I_c) + (S_s - S_s^* \ln S_s) \\ &+ A_3(V_s - V_s^* \ln V_s) + A_4(I_s - I_s^* \ln I_s) + (S_h - S_h^* \ln S_h) + A_5(I_h - I_h^* \ln I_h) \\ &+ A_6(R_h - R_h^* + A_7(B - B^* \ln B)). \end{aligned} \tag{10}$$

where $A_1, A_2, A_3, A_4, A_5, A_6$ and A_7 are positive constants. The time derivative of the Lyapunov function L is given by:

$$\begin{aligned} \frac{dL}{dt} =& \left(1 - \frac{S_c^*}{S_c}\right)\frac{dS_c}{dt} + A_1\left(1 - \frac{V_c^*}{V_c}\right)\frac{dV_c}{dt} + A_2\left(1 - \frac{I_c^*}{I_c}\right)\frac{dI_c}{dt} + \left(1 - \frac{S_s^*}{S_s}\right)\frac{dS_s}{dt} \\ &+ A_3\left(1 - \frac{V_s^*}{V_s}\right)\frac{dV_s}{dt} + A_4\left(1 - \frac{I_s^*}{I_s}\right)\frac{dI_s}{dt} + \left(1 - \frac{S_h^*}{S_h}\right)\frac{dS_h}{dt} + A_5\left(1 - \frac{I_h^*}{I_h}\right)\frac{dI_h}{dt} \\ &A_6\left(1 - \frac{R_h^*}{R_h}\right)\frac{dR_h}{dt} + A_7\left(1 - \frac{B^*}{B}\right)\frac{dB}{dt}. \end{aligned} \tag{11}$$

Considering (1) at the endemic equilibrium solution E^* we have:

$$\pi_h N_h = -\gamma R_h^* + (\beta_{hc} I_c^* + \beta_{hs} I_s^* + \beta_{hh} I_h^* + \alpha_h B^*) S_h^*,$$

$$\sigma + \mu_h + d_h = (\beta_{hc} I_c^* + \beta_{hs} I_s^* + \beta_{hh} I_h^* + \alpha_h B^*)\frac{S_h^*}{I_h^*},$$

$$\pi_s N_s = (\beta_s I_s^* + \alpha_s B^* + \phi_s + \mu_s) S_s^* - \psi_s V_s^*,$$

$$\pi_c N_c = (\beta_c I_c^* + \alpha_c B^* + \phi_c + \mu_c) S_c^* - \psi_c V_c^*,$$

$$\mu_c + d_c = \frac{(\beta_c I_c^* + \alpha_c B^*) S_c^*}{I_c^*},$$

$$\mu_s + d_s = \frac{(\beta_s I_s^* + \alpha_s B^*) S_s^*}{I_s^*},$$

$$(\varepsilon + \tau) = \frac{\rho_c I_c^* + \rho_s I_s^*}{B^*},$$

$$\phi_c = \frac{(\psi_c + \mu_c) V_c^*}{S_c^*},$$

$$\phi_s = \frac{(\psi_s + \mu_s) V_s^*}{S_s^*},$$

$$\sigma = \frac{(\gamma + \mu_h) R_h^*}{I_h^*}.$$

Then, equation (11) may be re-written as:

$$\begin{aligned}
\frac{dL}{dt} =& -(\phi_c+\mu_c)S_c\left(1-\frac{S_c^*}{S_c}\right)^2-(\phi_s+\mu_s)S_s\left(1-\frac{S_s^*}{S_s}\right)^2-\mu_h S_h\left(1-\frac{S_h^*}{S_h}\right)^2\\
&-\left(1-\frac{S_c^*}{S_c}\right)\left(\beta_c I_c S_c\left(1-\frac{I_c^*S_c^*}{I_cS_c}\right)+\alpha_c BS_c\left(1-\frac{B^*S_c^*}{BS_c}\right)+\psi_c V_c\left(\frac{V_c^*}{V_c}-1\right)\right)\\
&-\left(1-\frac{S_s^*}{S_s}\right)\left(\beta_s I_s S_s\left(1-\frac{I_s^*S_s^*}{I_sS_s}\right)+\alpha_s BS_s\left(1-\frac{B^*S_s^*}{BS_s}\right)+\psi_s V_s\left(\frac{V_s^*}{V_s}-1\right)\right)\\
&-a_1\left(1-\frac{V_c^*}{V_c}\right)\left(1-\frac{V_c^*S_c}{V_cS_c^*}\right)-(\psi_s+\mu_s)BV_sA_3\left(1-\frac{V_s^*}{V_s}\right)\left(1-\frac{V_s^*S_s}{V_sS_s^*}\right)\\
&+A_2\left(1-\frac{I_c^*}{I_c}\right)\left(\beta_c I_c S_c\left(1-\frac{S_c^*}{S_c}\right)+\alpha_c BS_c\left(1-\frac{B^*S_c^*I_c}{BS_cI_c^*}\right)\right)\\
&+A_4\left(1-\frac{I_s^*}{I_s}\right)\left(\beta_s I_s S_s\left(1-\frac{S_s^*}{S_s}\right)+\alpha_s BS_s\left(1-\frac{B^*S_s^*I_s}{BS_sI_s^*}\right)\right)\\
&-A_5\left(1-\frac{S_h^*}{S_h}\right)\left(a_2\left(\frac{R_h^*}{R_h}-1\right)+a\left(1-\frac{I_c^*S_h^*}{I_cS_h}\right)+b\left(1-\frac{I_s^*S_h^*}{I_sS_h}\right)+c\left(1-\frac{B^*S_h^*}{BS_h}\right)\right)\\
&+A_6\left(1-\frac{I_h^*}{I_h}\right)\left(\beta_{hc}I_cS_h\left(1-\frac{I_c^*S_h^*I_h}{I_cS_hI_h^*}\right)+\beta_{hs}I_sS_h\left(1-\frac{I_s^*S_h^*I_h}{I_sS_hI_h^*}\right)\right)\\
&+A_6\left(1-\frac{I_h^*}{I_h}\right)\left(\beta_{hh}I_hS_h\left(1-\frac{I_h^*S_h^*I_h}{I_hS_hI_h^*}\right)+\alpha_h BS_h\left(1-\frac{B^*S_h^*I_h}{BS_hI_h^*}\right)\right)\\
&-A_7(\gamma+\mu_h)R_h\left(1-\frac{R_h^*}{R_h}\right)\left(1-\frac{I_hR_h^*}{I_h^*R_h}\right)\\
&+A_8\left(1-\frac{B^*}{B}\right)\left(\rho_cI_c\left(1-\frac{BI_c^*}{B^*I_c}\right)+\rho_sI_s\left(1-\frac{BI_s^*}{B^*I_s}\right)\right). \qquad (12)
\end{aligned}$$

where,

$$a_1=(\psi_c+\mu_c)BV_cA_1,\ a_2=\gamma R_h,$$

$$a=\beta_{hc}I_cS_h,\ b=\beta_{hs}I_sS_h,\ c=\alpha_hBS_h.$$

Equation (12) can be written as:

$$\begin{aligned}
\frac{dL}{dt} =& -\left((\phi_c+\mu_c)S_c\left(1-\frac{S_c^*}{S_c}\right)^2+(\phi_s+\mu_s)S_s\left(1-\frac{S_s^*}{S_s}\right)^2+\mu_hS_h\left(1-\frac{S_h^*}{S_h}\right)^2\right)\\
&+F(S_c,V_c,I_c,S_s,V_s,I_s,B).
\end{aligned}$$

where, F is the balance of the right hand terms of equation (12). Following the approach of [29, 48, 49, 51, 50, 52], F is a non-positive function for $S_c,V_c,I_c,S_s,V_s,I_s,S_h,I_h,R_h,B\geq 0$. Thus, $\frac{dL}{dt}<0$ for $S_c,V_c,I_c,S_s,V_s,I_s,S_h,I_h,R_h,B\geq 0$ and is zero if $S_c=S_c^*,V_c=V_c^*,I_c=I_c^*,S_s=$

$S_s^*, V_s = V_s^*, I_s = I_s^*, S_h = S_h^*, I_h = I^*, R_h = R_h^*$, and $B = B^*$. Therefore, if $R_e > 1$, model system (1) has a unique endemic equilibrium point E^* which is globally asymptotically stable. □

5. NUMERICAL SIMULATIONS

This section presents numerical simulations of model system (1) for the purpose of verifying some of the analytical results. The parameter values used in our computations are mainly from [3], a literature similar to this work. The parameter values are in TABLE 3 and FIGURE 2 illustrates the variations in livestock, human and brucella subpopulations as time increases.

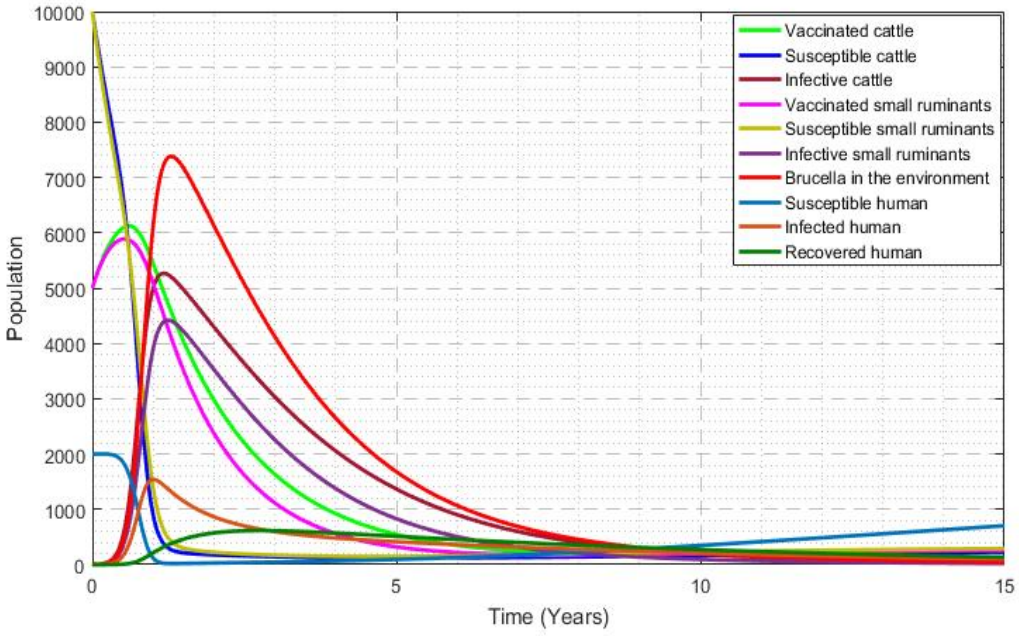

FIGURE 2. Time Series graph for Brucellosis

Furthermore, FIGURE 2 shows that susceptible human subpopulation decreases rapidly as time increases due to brucellosis infections and natural mortality rate. On the other hand, the number of infective humans initially increases with time due to large number of susceptible individuals that gets infected while its decrease is associated with the increase and decrease in effective treatment and susceptibility of individuals respectively. The recovered population increases as a result of increase in the effective treatment of infected humans.

Similarly, from FIGURE 3a we see that effective environmental hygiene and sanitation controls the transmission route of brucellosis from contaminated environment to human population.

TABLE 3. Model Parameter Values

Parameter	Value	Unit
π_c	0.3	$year^{-1}$
β_c	0.0011	$year^{-1}$
ϕ_c	0.7	$year^{-1}$
ψ_c	0.4	$year^{-1}$
μ_c	0.25	$year^{-1}$
d_c	0.35	$year^{-1}$
α_c	0.00035	$year^{-1}$
ρ_c	10	$year^{-1}$
ϕ_h	0.03	$year^{-1}$
β_h	0.0002	$year^{-1}$
σ_h	0.9	$year^{-1}$
μ_h	0.00005	$year^{-1}$
d_h	0.000002	$year^{-1}$
α_h	0.002	$year^{-1}$
β_{hc}	0.000158	$year^{-1}$
β_{hs}	0.000158	$year^{-1}$
γ	0.5	$year^{-1}$
ε	8	$year^{-1}$
τ	12	$year^{-1}$
π_s	0.4	$year^{-1}$
β_s	0.001	$year^{-1}$
ϕ_s	0.8	$year^{-1}$
ψ_s	0.5	$year^{-1}$
μ_s	0.35	$year^{-1}$
d_s	0.4	$year^{-1}$
α_s	0.00032	$year^{-1}$
ρ_s	15	$year^{-1}$

However, the ruminants to human effective reproduction number does not reduce to less than unit due to the fact that direct contact between infective cattle or small ruminants is not effectively controlled. In addition FIGURE 3b illustrates that, human treatment has a significant

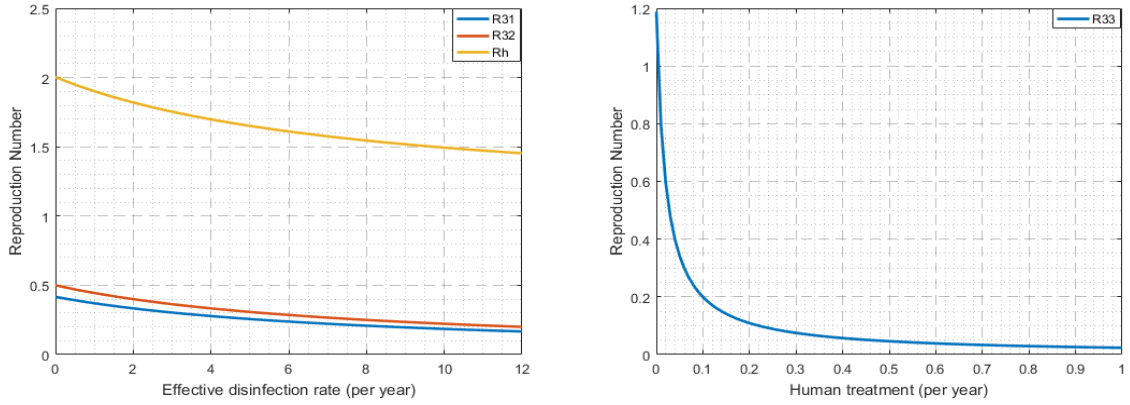

(A) (B)

FIGURE 3. Variations in the effective reproduction number with respect to changes in environmental hygiene and human treatment

contribution in reduction or elimination of human to human brucellosis transmission. This is based on the fact that human treatment reduces the number of infective humans.

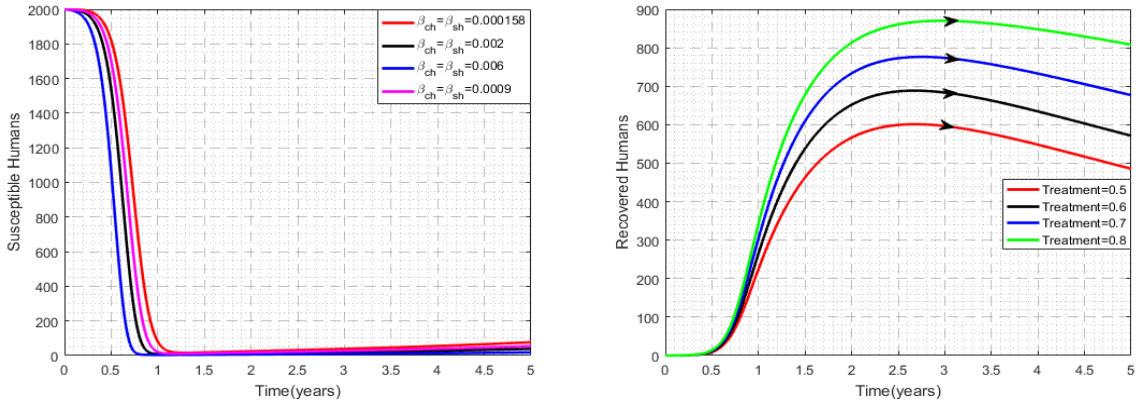

(A) (B)

FIGURE 4. The impact of transmission rates on susceptible humans and treatment rate on recovered human populations with respect to time.

Moreover, FIGURE 4a shows that both cattle to human and small ruminants to human transmission reduces the number of susceptible humans to almost zero in one year period of time. On the other hand, FIGURE 4b illustrates that, recovered humans increases with the increase in treatment rate. This implies that, in order to minimize or eliminate the prevalence of brucellosis

in the human population, measures should be taken to control the disease in animals as well as eliminating the disease in humans through treatment.

6. CONCLUSION

This paper aimed at formulating and analyzing a mathematical model to investigate the impacts of different control parameters to the transmission dynamics of brucellosis in the human and animal populations. We focused on livestock vaccination, gradual culling of ruminants through slaughter, environmental hygiene and sanitation, and human treatment. Analytical solutions as well as numerical simulations reveals that human brucellosis can be prevented or controlled only if the prevalence in both ruminants and humans can be controlled. Moreover, prevention of human brucellosis largely depends on prevention of the disease in domestic animals. In view of that, the effective control of brucellosis needs cooperation between public health and animal health sectors.

CONFLICT OF INTERESTS

The author(s) declare that there is no conflict of interests.

REFERENCES

[1] WHO. Brucellosis in humans and animals, http://www.who.int/csr/resources/publications/Brucellosis.pdf. Accessed: 2018-11-08.

[2] F. P. Poester, L. E. Samartino, R. L. Santos. Pathogenesis and pathobiology of brucellosis in livestock, Rev. Sci. Tech. 32 (1) (2013), 105–115.

[3] M. Li, G. Sun, Y. Wu, J. Zhang, and Z. Jin. Transmission dynamics of a multi-group brucellosis model with mixed cross infection in public farm, Appl. Math. Comput. 237 (2014), 582–594.

[4] CFSPH. Brucellosis Brucella abortus, http://cfsph.iastate.edu/Factsheets/pdfs/brucellosis-abortus.pdf. Accessed 2018-11-07.

[5] E. Schelling, C. Diguimbaye, S. Daoud, J. Nicolet, P. Boerlin, M. Tanner, and J. Zinsstag. Brucellosis and Q-fever seroprevalences of nomadic pastoralists and their livestock in Chad, Prev. Vet. Med. 61 (4) (2003), 279–293.

[6] R. A. Greenfield, D. A. Drevets, L. J. Machado, G. W. Voskuhl, P. Cornea, and M. S. Bronze. Bacterial pathogens as biological weapons and agents of bioterrorism, Amer. J. Med. Sci. 323 (6) (2002), 299–315.

[7] J. Zhang, G. Sun, X. Sun, Q. Hou, M. Li, B. Huang, H. Wang, and Z. Jin. Prediction and control of brucellosis transmission of dairy cattle in Zhejiang Province, China, Plos one, 9 (11) (2014), e108592.

[8] F. Zhang, Z. Li, X. La, X. Ma, Y. Zhang, P. Ji, M. Jiang, J. Hu, Z. Zhang, X. Lu, and J. Ding. Multiple-locus variable-number tandem-repeat analysis of Brucella isolates from patients in Xinjiang China, Int. J. Clinic. Exp. Med. 8 (9) (2015), 15716–15723.

[9] B. Ainseba, C. Benosman, and P. Magal. A model for ovine brucellosis incorporating direct and indirect transmission, J. Biol. Dyn. 4 (1) (2010), 2–11.

[10] J. Zinsstag, and F. Roth, D. Orkhon, G. Chimed-Ochir, M. Nansalmaa, J. Kolar, and P. Vounatsou. A model of animal–human brucellosis transmission in Mongolia, Prev. Vet. Med. 69 (1–2) (2005), 77–95.

[11] M. N Xavier, T. A. Paixao, A. B. den Hartigh, R. M. Tsolis, and R. L. Santos. Pathogenesis of Brucella spp., Open Vet. Sci. J. 4 (1) (2010), 109–118.

[12] Medscape. Brucellosis Pathogenicity, https://emedicine.medscape.com/article/213430-overview, Accessed: 2018-11-07.

[13] K. A. Franc, R. C. Krecek, B. N. Häsler, and A. M. Arenas-Gamboa. Brucellosis remains a neglected disease in the developing world, BMC Public Health, 18 (1) (2018), 18-125.

[14] M. Ducrotoy, W. J. Bertu, G. Matope, S. Cadmus, R. Conde-Álvarez, A. M. Gusi, S. Welburn, R. Ocholi, J. M. Blasco, and I. Moriyón. Brucellosis in Sub-Saharan Africa: current challenges for management, diagnosis and control, Acta Tropica, 165 (2017), 179–193.

[15] M. Yilma, and G. Mamo, and B. Mammo. Review on Brucellosis Sero-prevalence and Ecology in Livestock and Human Population of Ethiopia, Ach. Life Sci. 10 (1) (2016), 80–86.

[16] M. J. Michael. Brucellosis in humans and animals, World Health Organization, 2006.

[17] A. S. Dean, L. Crump, H. Greter, E. Schelling, and J. Zinsstag. Global burden of human brucellosis: a systematic review of disease frequency, PLoS Negl. Trop. Dis. 6 (10) (2012), e1865.

[18] CDC. Brucellosis Signs and Symptoms, https://www.cdc.gov/brucellosis/symptoms/index.html. Accessed 2018-11-07.

[19] K. John, J. Fitzpatrick, N. French, R. Kazwala, D. Kambarage, G. S. Mfinanga, A. MacMillan, and S. Cleaveland. Quantifying risk factors for human brucellosis in rural northern Tanzania, PloS one, 5 (4) (2010), e9968.

[20] G. Pappas, P. Papadimitriou, N. Akritidis, L. Christou, and E. V. Tsianos. The new global map of human brucellosis, Lancet Infect. Dis. 6 (2) (2006), 91–99.

[21] G. Tumwine, E. Matovu, J. D. Kabasa, D. O. Owiny, and S. Majalija. Human brucellosis: sero-prevalence and associated risk factors in agro-pastoral communities of Kiboga District, Central Uganda, BMC Public Health, 15 (2015), 900.

[22] J. Kitaly. Bovine brucellosis in Government parastatal and Ujamaa village dairy farms in Central Zone of Tanzania: Assessment of Control measures in some farms In. In Proceedings of the 2 nd Tanzania Veterinary Association Scientific Conference (pp. 24-30), 1984.

[23] E. S. Swai, and L. Schoonman. Human brucellosis: seroprevalence and risk factors related to high risk occupational groups in Tanga Municipality, Tanzania, Zoonoses Public Health, 56 (4) (2009), 183–187.

[24] M. Carugati, H. M. Biggs, M. J. Maze, R. A. Stoddard, S. Cash-Goldwasser, J. T. Hertz, J. E. B. Halliday, W. Saganda, B. F. Lwezaula, R. R. Kazwala, S. Cleaveland, V. P. Maro, M. P. Rubach, and J. A. Crump. Incidence of human brucellosis in the Kilimanjaro Region of Tanzania in the periods 2007–2008 and 2012–2014, Trans. R. Soc. Trop. Med. Hyg. 112 (3) (2018), 136–143.

[25] G. M. Shirima. The epidemiology of brucellosis in animals and humans in Arusha and Manyara regions in Tanzania, PhD thesis. University of Glasgow, 2005.

[26] E. S. Swai, and L. Schoonman. A survey of zoonotic diseases in trade cattle slaughtered at Tanga city abattoir: a cause of public health concern, Asian Pac. J. Trop. Biomed. 2 (1) (2012), 55–60.

[27] A. G. Alhamada, I. Habib, A. Barnes, and I. Robertson. Risk factors associated with brucella seropositivity in sheep and goats in Duhok Province, Iraq, Vet Sci. 4 (4) (2017), 65.

[28] Q. Hou, X. Sun, J. Zhang, Y. Liu, Y. Wang, and Z. Jin. Modeling the transmission dynamics of sheep brucellosis in Inner Mongolia Autonomous Region, China, Math. Biosci. 242 (1) (2013), 51–58.

[29] C. Li, Z. Guo, and Z. Zhang. Transmission dynamics of a brucellosis model: Basic reproduction number and global analysis, Chaos Solitons Fractals, 104 (2017), 161–172.

[30] B. Nannyonga, G. G. Mwanga, and L.S. Luboobi. An optimal control problem for ovine brucellosis with culling, J. Biol. Dyn. 9 (1) (2015), 198–214.

[31] P. O. Lolika, C. Modnak, and S. Mushayabasa. On the dynamics of brucellosis infection in bison population with vertical transmission and culling, Math. Biosci. 305 (2018), 42–54.

[32] F. Roth, J. Zinsstag, D. Orkhon, G. Chimed-Ochir, G. Hutton, O. Cosivi, G. Carrin, and J. Otte. Human health benefits from livestock vaccination for brucellosis: case study, Bull. World Health Organ. 81 (2003), 867–876.

[33] A. Palanduz, S. Palanduz, K. Guler and N. Guler. Brucellosis in a mother and her young infant: probable transmission by breast milk, Int. J. Infect. Dis. 4 (1) (2000), 55–56.

[34] O. Mesner, K. Riesenberg, N. Biliar, E. Borstein, L. Bouhnik, N. Peled, and P. Yagupsky. The many faces of human-to-human transmission of brucellosis: congenital infection and outbreak of nosocomial disease related to an unrecognized clinical case, Clin. Infect. Dis. 45 (12) (2007), e135-e140, .

[35] E. Meltzer, Y. Sidi, G. Smolen, M. Banai, S. Bardenstein, and E. Schwartz. Sexually transmitted brucellosis in humans, Clin. Infect. Dis. 51 (2) (2010), e12–e15.

[36] A. El-Sayed and W. Awad. Brucellosis: Evolution and expected comeback, Int. J. Vet. Sci. Med. 6 (sup 1) (2018), S31-S35..

[37] F. F. Tuon, R. B. Gondolfo, and N. Cerchiari. Human-to-human transmission of Brucella–a systematic review, Trop. Med. Int. Health, 22 (5) (2017), 539–546.

[38] O. Diekmann, J. A. P. Heesterbeek, and J. A.J. Metz. On the definition and the computation of the basic reproduction ratio R_0 in models for infectious diseases in heterogeneous populations,J. Math. Biol. 28 (4) (1990), 365–382.

[39] O. Diekmann, J.A.P. Heesterbeek, and M.G. Roberts. The construction of next-generation matrices for compartmental epidemic models, J. R. Soc. Interface, 7 (47) (2010), 873–885.

[40] D. Okuonghae, and A. Korobeinikov. Dynamics of tuberculosis: the effect of direct observation therapy strategy (DOTS) in Nigeria, Math Model Nat Phenom. 2 (1) (2007), 113–128.

[41] P. van den Driessche, and J. Watmough. Reproduction numbers and sub-threshold endemic equilibria for compartmental models of disease transmission, Math. Biosci. 180 (1-2) (2002), 29–48.

[42] A. Cintrón-Arias, C. Castillo-Chávez, Luıs M.A. Bettencourt, A. L. Lloyd, and H.T. Banks. The estimation of the effective reproductive number from disease outbreak data, Math. Biosci. Eng. 6 (2) (2009), 261–282.

[43] P. van den Driessche. Reproduction numbers of infectious disease models, Infect. Dis. Model. 2 (3) (2017), 288–303.

[44] P. Padmanabhan, P. Seshaiyer, and C. C. Chavez. Mathematical modeling, analysis and simulation of the spread of Zika with influence of sexual transmission and preventive measures, Lett. Biomath. 4 (1) (2017), 148–166.

[45] N. Nyerere, L. S. Luboobi, S. C. Mpeshe, and G. M. Shirima. Mathematical Model for the Infectiology of Brucellosis with some Control Strategies, New Trends Math. Sci. 7 (4) (2019), 387–405.

[46] O. Diekmann and J.A.P. Heesterbeek. Mathematical epidemiology of infectious diseases: model building, analysis and interpretation; John Wiley & Sons, Vol. 5, 2000.

[47] C.C. Chavez, S. Blower, P. van den Driessche, D. Kirschner, and A. Yakubu. Mathematical approaches for emerging and reemerging infectious diseases: an introduction, Vol. 1. Springer Science & Business Media, 2002.

[48] A. Korobeinikov, and G. C. Wake. Lyapunov functions and global stability for SIR, SIRS, and SIS epidemiological models, Appl. Math. Lett. 15 (8) (2002), 955–960.

[49] A. Korobeinikov. Lyapunov functions and global properties for SEIR and SEIS epidemic models, Math. Med. Biol. 21 (2) (2004), 75–83.

[50] A. Korobeinikov. Global properties of infectious disease models with nonlinear incidence, Bull. Math. Biol. 69 (6) (2007), 1871–1886.

[51] C. C. McCluskey. Lyapunov functions for tuberculosis models with fast and slow progression, Math. Biosci. Eng. 3 (2006), 603614.

[52] S. Bowong, J. J. Tewa, and J. C. Kamgang. Stability analysis of the transmission dynamics of tuberculosis models, World J. Model. Simul. 7 (2) (2011), 83–100.

New Trends in Mathematical Sciences
http://dx.doi.org/10.20852/ntmsci.2019.380

Mathematical model for the infectiology of brucellosis with some control strategies

Nkuba Nyerere[1,5], *Livingstone S. Luboobi*[2], *Saul C. Mpeshe*[3] *and Gabriel M. Shirima*[4]

[1]Department of Applied Mathematics and Comp. Sciences, Nelson Mandela African Ins. of Science and Tech., Arusha, Tanzania
[2]Institute of Mathematical Sciences, Strathmore University, Nairobi, Kenya
[3] Department of Mathematics, University of Iringa, P.O. Box 200, Iringa, Tanzania
[4] Department of Global Health and Bio-Medical Sciences, Nelson Mandela African Ins. of Science and Tech., Arusha, Tanzania
[5] Department of Mathematics, Informatics and Computational Sciences, Sokoine University of Agriculture, Tanzania

Received: 21 June 2019, Accepted: 8 October 2019
Published online: 25 December 2019.

Abstract: Brucellosis is a neglected zoonotic infection caused by gram-negative bacteria of genus brucella. In this paper, a deterministic mathematical model for the infectiology of brucellosis with vaccination of ruminants, culling of seropositive animals through slaughter, and proper environmental hygiene and sanitation is formulated and analyzed. A positive invariant region of the formulated model is established using the Box Invariance method, the effective reproduction number, R_e of the model is computed using the standard next generation approach. We prove that the brucellosis free equilibrium exists, locally and globally asymptotically stable if $R_e < 1$ while the endemic equilibrium point exists, locally and globally asymptotically stable if $R_e > 1$. Sensitivity analysis of the effective reproductive number shows that, natural mortality rate of ruminants, recruitment rate, ruminant to ruminant transmission rate, vaccination rate, and disease induced culling rate are the most sensitive parameters and should be targeted in designing of the control strategies for the disease. Numerical simulation is done to show the variations of each subpopulation with respect to the control parameters.

Keywords: Brucellosis, mathematical model, infectiology, environmental hygiene.

1 Introduction

Brucellosis is a zoonotic infection caused by gram-negative bacteria of genus brucella (*B. abortus* primarily from cattle, *B. melitensis* from small ruminants, *B. suis* from swine, and *B. canis* from dogs) [14,34,52,57]. It is considered by the Food and Agriculture Organisation (FAO), the World Health Organisation (WHO) and World Organization for Animal Health (Office International des Epizooties (OIE)) as one of the most widespread zoonoses in the world alongside bovine tuberculosis and rabies [45]. The disease is an ancient one that was described more than 2000 years ago by the Romans [24] and has been known by various names, including Mediterranean fever, Malta fever, gastric remittent fever, bang's disease, crimean fever, gibraltar fever, rock fever, lazybones disease and undulant fever [55]. A British military medical officer David Bruce isolated brucella bacteria from an infected individual's blood for the first time in 1887 and hence the disease was named brucellosis to honor his contribution [54]. Furthermore, in 1905 Zamitt carried out an experiment on goats to investigate the origin of human brucellosis, and found that, human brucellosis originates from goats [2]. To date, eight species have been identified and named primarily for the source animal or features of infection. Of these, the following four have moderate-to-significant human pathogenicity: *Brucella melitensis* (highest pathogenicity), *Brucella suis* (high pathogenicity) named after the source animal (swine), *Brucella abortus* (moderate pathogenicity) named after the feature of infection, *Brucella canis* named after the source animal (moderate pathogenicity) [37,38,56].

* Corresponding author e-mail: nyereren@nm-aist.ac.tz

In animals, brucellosis is transmitted when susceptible animals ingest contaminated materials like tissues or discharges from infected animals while in humans the bacteria is transmitted by ingestion of contaminated unpasteurized milk or other dairy products. Furthermore, direct contact with aborted fetuses, discharges and occupational accidents through needle injection during mass vaccination and during laboratory manipulation is another route of brucellosis transmission in the human population. In this view, farmers, laboratory personnels, abattoir workers and veterinarians are more susceptible to the disease. Infected animals exhibit clinical signs that are of economic significance to stakeholders and include reduced fertility, abortion, poor weight gain, lost draught power, and a substantial decline in milk production [21, 53]. Symptoms in humans include: continuous or intermittent fever, headache, weakness, profuse sweats, chills, joint pains, aches, weight loss as well as devastating complications in pregnant women. Neurological complications, endocarditis and testicular or bone abscess formation can also occur [13, 16]. The infection can also affect the liver and spleen, it may last for days or months, and sometimes for a year or more if not treated. The clinical signs in human present diagnostic difficulties because the disease can be confused with typhoid fever, malaria, rheumatic fever, joint diseases and relapsing fever. Human brucellosis is debilitating and requires prolonged treatment with combination of antibiotics [27].

The global burden of human brucellosis remains enormous: The infection causes more than 500,000 cases per year worldwide. The annual number of reported cases in United States (now about 100) has dropped significantly because of aggressive animal vaccination programs and milk pasteurization. Most US cases are now due to the consumption of illegally imported unpasteurized dairy products from Mexico. Approximately 60% of human brucellosis cases in the United States now occur in California and Texas [43].

In Africa Brucellosis exists throughout sub-Saharan Africa, but the prevalence is unclear and poorly understood with varying reports from country to country, geographical regions as well as animal factors [50]. Most African countries are of poor socioeconomic status, with people living with and by their livestock, while health networks, surveillance and vaccination programs are virtually non-existent. In Tanzania, the first outbreak of brucellosis was reported in Arusha in 1927 [48]. Previous surveys in Tanzania have demonstrated the occurrence of the disease in cattle in various production systems, regions and zones with individual animal level seroprevalence varying from 1 to 30%. There has been isolation of *Brucella* for more than 50 years ago and at that time *B. abortus* and *B. melitensis* were isolated from cattle and small ruminants respectively. In humans, the average prevalence varies from 1 to 5% [49], a recent study by [8]shows that brucellosis incidence is moderate in northern Tanzania and suggests that the disease is endemic and an important human health problem in this area. Moreover, special cases had been reported in areas of northern, eastern, lake and western zones with seroprevalence varying from 0.7 to 20.5%. [46].

Despite the WHO, FAO, OIE efforts and interventions are available, brucellosis continues to pose great economic threat by affecting livelihood and food security in both developed and developing countries; it is endemic in most of the developing world and causes devastating losses to the livestock industry especially small-scale livestock holders, thereby limiting economic growth and hindering access to international markets [21] from generation to generation. Thus, there is a need to assess the current control strategies and their cost-effectiveness if we are to control or eradicate the disease. So far few studies [3, 25, 33, 39, 40, 44, 56], have been developed to analyze dynamics of and spread of brucellosis in a homogeneous/heterogeneous populations. However, none of these studies have considered the mathematical approach for the impact of vaccination of ruminants, culling of seropositive animals through slaughter, and proper environmental hygiene and sanitation in reducing or eradicating the disease in cattle, small ruminants and human populations using mathematical models. This paper is at hand to fill the gap.

2 Model formulation

2.1 Dynamics of brucellosis

In this section, we formulate a deterministic mathematical model for the transmission dynamics of Brucellosis in domestic small ruminants, cattle and human populations. The model includes: direct transmission of brucellosis within the cattle population, within small ruminants (sheep and goats) and from both species to human and indirect transmission from the environment to livestock and humans. Cattle and small ruminants newborns are either vaccinated or remain susceptible. Based on the epidemiological status, the cattle population at any time t is divided into vaccinated $V_c(t)$, susceptible $S_c(t)$, and infective $I_c(t)$ classes. Similarly, the small ruminant population at any time t is divided into vaccinated $V_s(t)$, susceptible $S_s(t)$, and infectious $I_s(t)$ subpopulations while the total human population, $N_h(t)$ at any time t is divided into susceptible, $S_h(t)$, infected, $I_h(t)$ and recovered, $R_h(t)$ individuals. Susceptible cattle become infected when they are in contact with infected cattle (direct transmission) at the rate of β_c or through contact with infected raw blood, meat, placentas, aborted fetus, unpasteurized milk or other dairy products (indirect transmission) at the rate α_c, and susceptible small ruminants become infected when they are in contact with infectious small ruminants at the rate of β_s or through contact with their products at the rate α_s while the transmission to humans is expressed as additive contributions of transmission from infective cattle, small ruminants and their products. Appertaining to the fact that it is very difficult to determine the quantity of brucella in environment, we define the average number of brucella that is enough for a host to be infected with brucellosis as an infectious unit and let $B(t)$ to be the number of infectious units in the environment. During the incubation period, Brucellosis is hardly detected, but individuals at this period can infect the susceptible individuals at the same transmission rate as the infectious individual and discharge the same quantity of brucella into the environment per unit time. It is against this background, we assume that individuals in the incubation period and post incubation period are hosted in the same population compartment called infectious. The interaction within and between the four populations shows that, veterinary surgeons, laboratory assistants, and farmers are predominantly exposed to the pathogen (See Figure 1).

2.2 Model assumptions

In formulation of the model, the following assumptions are taken into consideration:

(i) There is no direct transmission between cattle and small ruminants.
(ii) Infected animals shed the brucellosis pathogen in the environment.
(iii) Livestock seropositivity is a life-long lasting.
(iv) Immunized individuals cannot be infected unless their vaccine efficacy wanes.
(v) There is constant natural mortality rate in each of the species.
(vi) The mixing in each population is homogeneous.
(vii) The birth rate for each population is greater than natural mortality rate.

The variables and parameters used in this model are respectively summarized in Table 1 and Table 2.

2.3 Compartmental Flow Diagram for the Disease Dynamics

The interactions between the human, cattle, small ruminants populations and the brucella in the environment are illustrated in Figure 1.

Table 1: Model Variables

Variable	Description
$S_h(t)$	Number of susceptible humans at time t
$I_h(t)$	Number of infected human at time t
$R_h(t)$	Number of recovered humans at time t
$S_c(t)$	Number of susceptible cattle at time t
$I_c(t)$	Number of infected cattle at time t
$V_c(t)$	Number of vaccinated cattle at time t
$S_s(t)$	Number of susceptible small ruminants at time t
$I_s(t)$	Number of infected small ruminants at time t
$V_s(t)$	Number of vaccinated small ruminants at time t
$B(t)$	Number of brucella bacteria load per unit volume in the environment at time t

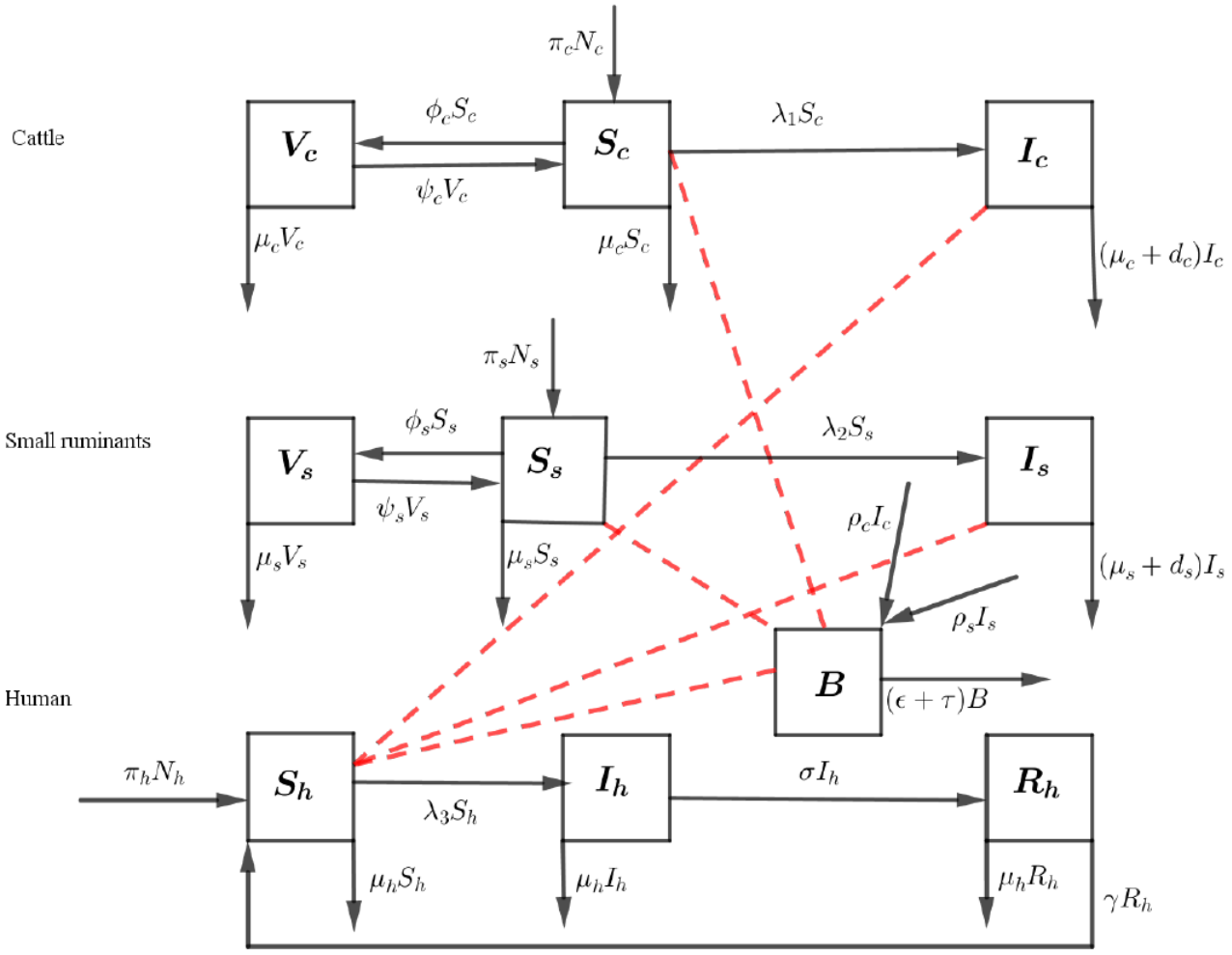

Fig. 1: A schematic diagram for direct and indirect transmission of brucellosis in cattle, small ruminants and human populations. Solid arrows represent transfer of individuals from one subpopulation to another while dotted lines represent interactions leading to infections.

Table 2: Model Parameters used in the model and their description

Parameter	Description
π_c	Per capita cattle birth rate
ϕ_c	Cattle vaccination rate
π_h	Per capita human birth rate
σ	Human recovery rate
μ_h	Per capita human natural death rate
ψ_c	Cattle vaccine efficacy waning rate
β_c	Within cattle transmission rate
d_c	Culling rate of seropositive cattle
μ_c	Per capita cattle natural death rate
α_c	Brucella from the environment to cattle transmission rate
α_s	Brucella from the environment to small ruminants transmission rate
α_h	Brucella from the environment to human transmission rate
ρ_c	Brucella shedding rate by infected cattle
ρ_s	Brucella shedding rate by infected small ruminants
β_{ch}	Cattle to human transmission rate
β_{sh}	Small ruminants to human transmission rate
γ	The rate at which recovered human become susceptible
ε	Decaying rate of brucella in the environment
τ	Environmental hygiene and sanitation rate
π_s	Small ruminants per capita birth rate
ϕ_s	Vaccination rate of small ruminants
ψ_s	Small ruminant vaccine efficacy
β_s	Within small ruminants transmission rate
d_s	Culling rate of seropositive small ruminants
μ_s	Per capita small ruminants natural mortality rate

2.4 Model equations

Based on the assumptions and the inter-relations between the variables and the parameters as shown in Figure 1, the transmission dynamics of Brucellosis can be described by the following ordinary differential equations:

$$
\begin{aligned}
\frac{dV_c}{dt} &= \phi_c S_c - (\mu_c + \psi_c)V_c, \\
\frac{dS_c}{dt} &= \pi_c N_c + \psi_c V_c - (\lambda_1 + \phi_c + \mu_c)S_c, \\
\frac{dI_c}{dt} &= \lambda_1 S_c - (\mu_c + d_c)I_c, \\
\frac{dV_s}{dt} &= \phi_s S_s - (\mu_s + \psi_s)V_s, \\
\frac{dS_s}{dt} &= \pi_s N_s + \psi_s V_s - (\lambda_2 + \phi_s + \mu_s)S_s, \\
\frac{dI_s}{dt} &= \lambda_2 S_s - (\mu_s + d_s)I_s, \\
\frac{dB}{dt} &= \rho_c I_c + \rho_s I_s - (\varepsilon + \tau)B, \\
\frac{dS_h}{dt} &= \pi_h N_h + \gamma R_h - (\lambda_3 + \mu_h)S_h, \\
\frac{dI_h}{dt} &= \lambda_3 S_h - (\sigma + \mu_h)I_h, \\
\frac{dR_h}{dt} &= \sigma I_h - (\gamma + \mu_h)R_h,
\end{aligned}
\tag{1}
$$

where, $\lambda_1 = \beta_c I_c + \alpha_c B, \lambda_2 = \beta_s I_s + \alpha_s B$ and $\lambda_3 = \beta_{hc} I_c + \beta_{hs} I_s + \alpha_h B$.

3 Model properties

Basing on the fact that the first seven equations of system (1) are independent of the last three equations, let us first consider the following model for cattle and the ruminants:

$$\begin{aligned}
\frac{dV_c}{dt} &= \phi_c S_c - (\mu_c + \psi_c) V_c, \\
\frac{dS_c}{dt} &= \pi_c N_c + \psi_c V_c - (\lambda_1 + \phi_c + \mu_c) S_c, \\
\frac{dI_c}{dt} &= \lambda_1 S_c - (\mu_c + d_c) I_c, \\
\frac{dV_s}{dt} &= \phi_s S_s - (\mu_s + \psi_s) V_s, \\
\frac{dS_s}{dt} &= \pi_s N_s + \psi_s V_s - (\lambda_2 + \phi_s + \mu_s) S_s, \\
\frac{dI_s}{dt} &= \lambda_2 S_s - (\mu_s + d_s) I_s, \\
\frac{dB}{dt} &= \rho_c I_c + \rho_s I_s - (\varepsilon + \tau) B.
\end{aligned} \tag{2}$$

3.1 Invariant region

In this subsection we use Box Invariance method proposed by [1] to assess the well-posedness of the model by investigating the existence and feasibility of its solution. In other words, we investigate whether the solutions are epidemiologically (variables have biological interpretation) and mathematically well-posed (a unique bounded solution exists for all the time). That is solutions of model system (2) with nonnegative initial data remain nonnegative for all time $t \geq 0$. The model system (2) can be expressed in the compact form as:

$$\frac{dX}{dt} = A(X) + F.$$

where, $X = (V_c, S_c, I_c, V_s, S_s, I_s, B)$, F is a column vector given by $F = (0, \pi_c N_c, 0, 0, \pi_s N_s, 0, 0, 0)^T$ and

$$A = \begin{bmatrix}
-(\mu_c + \psi_c) & \phi_c & 0 & 0 & 0 & 0 & 0 \\
\psi_c & -(\lambda_1 + \phi_c + \mu_c) & 0 & 0 & 0 & 0 & 0 \\
0 & \lambda_1 & -(\mu_c + d_c) & 0 & 0 & 0 & 0 \\
0 & 0 & 0 & -(\mu_s + \psi_s) & \phi_c & 0 & 0 \\
0 & 0 & 0 & \psi_s & -(\lambda_2 + \phi_s + \mu_s) & 0 & 0 \\
0 & 0 & 0 & 0 & \lambda_2 & -(\mu_s + d_s) & 0 \\
0 & 0 & \rho_c & 0 & 0 & \rho_s & -(\varepsilon + \tau)
\end{bmatrix}.$$

It can be noticed that $A(X)$ is Meltzer matrix since all of its off diagonal entries are non negative, for all $X \in \mathbb{R}^7_+$. Therefore, using the fact that $F \geq 0$, the model system (2) is positively invariant in $\mathbb{R}^7_+$ which means that an arbitrary trajectory of the system starting in $\mathbb{R}^7_+$ remains in $\mathbb{R}^7_+$ forever. In addition, the right hand F is Lipschitz continuous. Thus, a unique maximal solution exists and so

$$\Omega = \{(V_c, S_c, I_c, V_s, S_s, I_s, B) \geq 0\} \in \mathbb{R}^7_+,$$

is the feasible region for the model (2). Thus, the model (2) is epidemiologically and mathematically well-posed in the region Ω.

4 Model analysis

4.1 Disease free equilibrium

The Brucellosis free equilibrium point is obtained by setting the right hand side of equations in model system (2) to zero, that is:

$$\frac{dV_c}{dt} = \frac{dS_c}{dt} = \frac{dI_c}{dt} = \frac{dV_s}{dt} = \frac{dS_s}{dt} = \frac{dI_s}{dt} = \frac{dB}{dt} = 0.$$

Let the disease free equilibrium point of Brucellosis model be E^0. In case there is no disease $I_c = I_s = B = 0$ that is, the sum of susceptible and vaccinated populations is equal to total population. There exists a disease free equilibrium $E^0 = (V_c^0, S_c^0, 0, V_s^0, S_s^0, 0, 0)$ for model system (2) where:

$$S_c^0 = \frac{(\mu_c + \psi_c)\pi_c N_c^0}{\mu_c(\phi_c + \psi_c + \mu_c)}, \qquad S_s^0 = \frac{(\mu_s + \psi_s)\pi_s N_s^0}{\mu_s(\phi_s + \psi_s + \mu_s)}, \qquad V_c^0 = \frac{\phi_c \pi_c N_c^0}{\mu_c(\phi_c + \psi_c + \mu_c)},$$

$$V_s^0 = \frac{\phi_s \pi_s N_s^0}{\mu_s(\phi_s + \psi_s + \mu_s)}.$$

4.2 The effective reproduction number

In this subsection, we compute the effective reproduction number for model system (2) using the standard method of the next generation matrix developed in [17,18]. The effective reproduction number, R_e is defined as the measure of average number of infections caused by a single infectious individual introduced in a community in which intervention strategies are administered [41]. Its magnitude is a useful indicator of both the risk of an epidemic and the effort required to control an infection [58]. When there are no interventions or controls, the number of secondary infections caused by typical infected individual in a completely susceptible population during its entire period of infectiousness is called basic reproduction number, R_0. It is the threshold parameter to determine whether or not the disease can invade the susceptible population successfully. Due to the natural history of some infections, transmissibility is better quantified by the effective reproduction number rather than the basic reproduction number [15]. Considering the system for the infective variables:

$$\begin{aligned}
\frac{dI_c}{dt} &= (\beta_c I_c + \alpha_c B)S_c - (\mu_c + d_c)I_c, \\
\frac{dI_s}{dt} &= (\beta_s I_s + \alpha_s B)S_s - (\mu_s + d_s)I_s, \\
\frac{dB}{dt} &= \rho_c I_c + \rho_s I_s - (\varepsilon + \tau)B.
\end{aligned} \tag{3}$$

The effective reproduction number is obtained by taking the spectral radius of the next generation matrix

$$FV^{-1} = \left[\frac{\partial \mathscr{F}_i(E^0)}{\partial t}\right]\left[\frac{\partial \mathscr{V}_i(E^0)}{\partial t}\right]^{-1},$$

where E^0 is the brucellosis-free equilibrium point while $\mathscr{F}_i$ and $\mathscr{V}_i$ are vectors representing respectively, the rate of appearance of new infection in compartment i and the transfer of infections from one compartment i to another, such that:

$$\mathscr{F}_i = \begin{bmatrix} (\beta_c I_c + \alpha_c B)S_c \\ (\beta_s I_s + \alpha_s B)S_s \\ 0 \end{bmatrix},$$

$$\mathscr{V}_i = \begin{bmatrix} (\mu_c + d_c)I_c \\ (\mu_s + d_s)I_s \\ -\rho_c I_c - \rho_s I_s + (\varepsilon + \tau)B \end{bmatrix}.$$

It is important to note that $\mathscr{V}_i$ is a resultant vector of the two vectors $\mathscr{V}_i^+$ defined as the rate of transfer of individuals into compartment i by all other means, and $\mathscr{V}_i^-$ which is the rate of transfer of individuals out of compartment i. That is:

$$\mathscr{V}_i = \mathscr{V}_i^- - \mathscr{V}_i^+, i = \{1,2,3\}.$$

The Jacobian matrices F of $\mathscr{F}_i$ and V of $\mathscr{V}_i$ evaluated at E^0 are respectively:

$$F = \begin{bmatrix} \beta_c S_c^0 & 0 & \alpha_c S_c^0 \\ 0 & \beta_s S_s^0 & \alpha_s S_s^0 \\ 0 & 0 & 0 \end{bmatrix},$$

and

$$V = \begin{bmatrix} \mu_c + d_c & 0 & 0 \\ 0 & \mu_s + d_s & 0 \\ -\rho_c & -\rho_s & (\varepsilon + \tau) \end{bmatrix}.$$

Referring to the infected states with indices i and j, for $i, j \in [1,2,3]$, the entry F_{ij} is the rate at which individuals in infected state j give rise or produce new infections to individuals in infected state i, in the linearized system. Thus, when there is no new cases produced in infected state i by an individual in infected state j immediately after infection, we have $F_{ij} = 0$. The inverse of V is found to be

$$V^{-1} = \begin{bmatrix} \frac{1}{\mu_c + d_c} & 0 & 0 \\ 0 & \frac{1}{\mu_s + d_s} & 0 \\ \frac{\rho_c}{(\mu_c + d_c)(\varepsilon + \tau)} & \frac{\rho_s}{(\mu_s + d_s)(\varepsilon + \tau)} & \frac{1}{\varepsilon + \tau} \end{bmatrix}.$$

The entry $\left(V^{-1}\right)_{ij}$ is the average length of time an infected individual spends in compartment j during its lifetime when introduced into the compartment i of disease free equilibrium, assuming that the population remains near the disease free equilibrium and barring reinfection. In particular, $\frac{1}{\mu_c + d_c}$ is an average time an infectious cattle spends in the state of being infective, $\frac{1}{\mu_s + d_s}$ is the average time spent by an infective small ruminant in the infectious state and $\frac{1}{\varepsilon + \tau}$ is the average time *brucella* spend in the environment. Furthermore, $\frac{\rho_c}{(\mu_c + d_c)}$ is the probability that an infective cattle will shed *brucella* into the environment while $\frac{\rho_s}{(\mu_s + d_s)}$ is the probability that an infected small ruminant will shed *brucella* into the environment. Moreover, the Next Generation Matrix is calculated to be:

$$FV^{-1} = \begin{bmatrix} \frac{\beta_c S_c^0}{\mu_c + d_c} + \frac{\alpha_c \rho_c S_c^0}{(\mu_c + d_c)(\varepsilon + \tau)} & \frac{\alpha_c \rho_s S_c^0}{(\mu_s + d_s)(\varepsilon + \tau)} & \frac{\alpha_c S_c^0}{\varepsilon + \tau} \\ \frac{\alpha_s \rho_c S_s^0}{(\mu_c + d_c)(\varepsilon + \tau)} & \frac{\beta_s S_s^0}{\mu_s + d_s} + \frac{\alpha_s \rho_s S_s^0}{(\mu_s + d_s)(\varepsilon + \tau)} & \frac{\alpha_s S_s^0}{\varepsilon + \tau} \\ 0 & 0 & 0 \end{bmatrix}.$$

The matrix FV^{-1} can be written as:

$$FV^{-1} = \begin{bmatrix} R_{11} & R_{12} & R_{13} \\ R_{21} & R_{22} & R_{23} \\ 0 & 0 & 0 \end{bmatrix}.$$

The (i,k) entry of the Next Generation Matrix FV^{-1} is the expected number of secondary infections in compartment i produced by individuals initially in compartment k assuming that the environment seen by the individual remains homogeneous for the duration of its infection [51]. In particular; R_{11} is the expected number of infected cattle produced by one infectious cattle, R_{12} is the expected number of infected cattle produced by one infectious small ruminant via consumption of brucella from the environment, R_{21} is the expected number of infected small ruminant as a result of one infected cattle, and R_{22} is the expected number of infected small ruminant as a result of one infected small ruminant. It can further be noticed that, matrix FV^{-1} is non-negative and therefore, has a nonnegative eigenvalue. The non-negative eigenvalue is associated with a non-negative eigenvector which represents the distribution of infected individuals that produces the greatest number R_e of secondary infections per generation [42]. Thus, the spectral radius for our Next Generation Matrix is

$$\rho(FV^{-1}) = R_e = \frac{R_{11} + R_{22} + \sqrt{(R_{22} - R_{11})^2 + 4R_{12}R_{21}}}{2} \tag{4}$$

where,

$$R_{11} = \frac{(\beta_c(\varepsilon+\tau) + \alpha_c\rho_c)(\psi_c+\mu_c)\pi_c N_c^0}{\mu_c(\mu_c+d_c)(\varepsilon+\tau)(\phi_c+\psi_c+\mu_c)}, \quad R_{22} = \frac{(\beta_s(\varepsilon+\tau) + \alpha_s\rho_s)(\psi_s+\mu_s)\pi_s N_s^0}{\mu_s(\mu_s+d_s)(\varepsilon+\tau)(\phi_s+\psi_s+\mu_s)},$$

$$R_{12} = \frac{(\psi_c+\mu_c)\alpha_c\rho_s\pi_c N_c^0}{\mu_c(\mu_s+d_s)(\varepsilon+\tau)(\phi_c+\psi_c+\mu_c)}, \quad R_{21} = \frac{(\psi_s+\mu_s)\alpha_s\rho_c\pi_s N_s^0}{\mu_s(\mu_c+d_c)(\varepsilon+\tau)(\phi_s+\psi_s+\mu_s)},$$

When there is no livestock vaccination: $\psi_c = \psi_s = \phi_c = \phi_s = 0$ and

$$R_{11} = \frac{(\beta_c(\varepsilon+\tau) + \alpha_c\rho_c)\pi_c N_c^0}{\mu_c(\mu_c+d_c)(\varepsilon+\tau)}, \quad R_{22} = \frac{(\beta_s(\varepsilon+\tau) + \alpha_s\rho_s)\pi_s N_s^0}{\mu_s(\mu_s+d_s)(\varepsilon+\tau)},$$

,

$$R_{12} = \frac{\alpha_c\rho_s\pi_c N_c^0}{\mu_c(\mu_s+d_s)(\varepsilon+\tau)}, \quad R_{21} = \frac{\alpha_s\rho_c\pi_s N_s^0}{\mu_s(\mu_c+d_c)(\varepsilon+\tau)},$$

When there is no intervention: $\psi_c = \psi_s = \phi_c = \phi_s = \tau = 0$, the effective reproduction number becomes the basic reproduction number:

$$R_0 = \frac{R_{11}^0 + R_{22}^0 + \sqrt{(R_{22}^0 - R_{11}^0)^2 + 4R_{12}^0 R_{21}^0}}{2}, \tag{5}$$

where,

$$R_{11}^0 = \frac{(\beta_c\varepsilon + \alpha_c\rho_c)\pi_c N_c^0}{\mu_c(\mu_c+d_c)\varepsilon}, R_{22}^0 = \frac{(\beta_s\varepsilon + \alpha_s\rho_s)\pi_s N_s^0}{\mu_s(\mu_s+d_s)\varepsilon}, R_{12}^0 = \frac{\alpha_c\rho_s\pi_c N_c^0}{\mu_c(\mu_s+d_s)\varepsilon},$$

and

$$R_{21}^0 = \frac{\alpha_s\rho_c\pi_s N_s^0}{\mu_s(\mu_c+d_c)\varepsilon}.$$

In view of the fact that, the first seven equations of model system (1) are independent of the last three equations, system (1) and system (2) have the same effective reproduction and the same basic reproduction number. Thus, the effective reproduction and basic reproduction number for system (1) are R_e and R_0, respectively.

4.3 Local stability of the disease free equilibrium

In this subsection we use the trace-determinant method to investigate the local stability of the brucellosis free equilibrium point.

Theorem 1. *The disease free equilibrium for the brucellosis model system(2) is locally asymptotically stable if* $R_0 < 1$ *and unstable if* $R_0 > 1$.

Proof. We show that, variational matrix $J(E_0)$ of the brucellosis model at DFE has a negative trace and positive determinant.
The Jacobian matrix for system 3.2 is given by:

$$J(E_0) = \begin{bmatrix} -(\mu_c+\psi_c) & \phi_c & 0 & 0 & 0 & 0 & 0 \\ \psi_c & -(\phi_c+\mu_c) & -\beta_c S_c^0 & 0 & 0 & 0 & -\alpha_c S_c^0 \\ 0 & 0 & a_0 & 0 & 0 & 0 & \alpha_c S_c^0 \\ 0 & 0 & 0 & -(\mu_s+\psi_s) & \phi_s & 0 & 0 \\ 0 & 0 & 0 & \psi_s & -(\phi_s+\mu_s) & -\beta_s S_s^0 & -\alpha_s S_s^0 \\ 0 & 0 & 0 & 0 & 0 & a_1 & \alpha_s S_s^0 \\ 0 & 0 & \rho_c & 0 & 0 & \rho_s & -(\varepsilon+\tau) \end{bmatrix}$$

where,

$$a_0 = \beta_c S_c^0 - (\mu_c + d_c),$$

$$a_1 = \beta_s S_s^0 - (\mu_s + d_s).$$

The trace of the Jacobian matrix $J(E_0)$ is given by:

$$\begin{aligned} Tr(J(E_0)) =& -(\phi_c+\psi_c+2\mu_c+\varepsilon+\tau+\phi_s+\psi_s+2\mu_s)+\beta_c S_c^0-(\mu_c+d_c)+\beta_s S_s^0-(\mu_s+d_s), \\ =& -(\phi_c+\psi_c+2\mu_c+\varepsilon+\tau+\phi_s+\psi_s+2\mu_s), \\ & -(\mu_c+d_s)\left(1-\frac{\beta_c S_c^0}{\mu_c+d_c}\right)-(\mu_s+d_s)\left(1-\frac{\beta_s S_s^0}{\mu_s+d_s}\right). \end{aligned}$$

Thus, the trace of the Jocobian matrix is the less than zero, that is $Tr(J(E_0)) < 0$, if:

$$\frac{\beta_c S_c^0}{\mu_c+d_c} < 1 \text{ and } \frac{\beta_s S_s^0}{\mu_c+d_s} < 1.$$

On the hand, the determinant of matrix $J(E_0)$ is:

$$\begin{aligned} Det(J(E_0)) =& \mu_c\mu_s(\phi_c+\psi_c+\mu_c)(\phi_s+\psi_s+\mu_s)[(\mu_s+d_s)(\varepsilon+\tau)\beta_c S_c^0\left(1-\frac{\beta_s S_s^0}{\mu_s+d_s}\right) \\ & +(\mu_c+d_c)\rho_s\alpha_s S_s^0\left(1-\frac{\beta_c S_c^0}{\mu_c+d_c}\right)+(\mu_s+d_s)\rho_c\alpha_c S_c^0\left(1-\frac{\beta_s S_s^0}{\mu_s+d_s}\right) \\ & -(\mu_c+d_c)(\mu_s+d_s)(\varepsilon+\tau)\left(1-\frac{\beta_s S_s^0}{\mu_s+d_s}\right)], \\ =& \mu_c\mu_s(\phi_c+\psi_c+\mu_c)(\phi_s+\psi_s+\mu_s)(\mu_c+d_c)(\mu_s+d_s)(\varepsilon+\tau) \\ & \left(\frac{\alpha_c\rho_c S_c^0\left(1-\frac{\beta_s S_s^0}{\mu_s+d_s}\right)}{(\varepsilon+\tau)(\mu_s+d_s)}-\left(1-\frac{\beta_c S_c^0}{\mu_c+d_c}\right)\left(1-\frac{(\beta_s(\varepsilon+\tau)+\alpha_s\rho_s)S_s^0}{(\varepsilon+\tau)(\mu_s+d_s)}\right)\right). \end{aligned}$$

The determinant of the Jacobian matrix is positive (i.e. $J(E_0) > 0$) iff:

$$\left(\frac{\alpha_c \rho_c S_c^0 \left(1 - \frac{\beta_s S_s^0}{\mu_s + d_s}\right)}{(\varepsilon + \tau)(\mu_s + d_s)} > \left(1 - \frac{\beta_c S_c^0}{\mu_c + d_c}\right)\left(1 - \frac{(\beta_s(\varepsilon + \tau) + \alpha_s \rho_s) S_s^0}{(\varepsilon + \tau)(\mu_s + d_s)}\right) \right),$$

$$\frac{\beta_c S_c^0}{\mu_c + d_c} < 1, \qquad \frac{\beta_s S_s^0}{\mu_c + d_s} < 1,$$

and

$$\frac{((\varepsilon + \tau)\beta_c + \rho_c \alpha_c) S_c^0}{(\varepsilon + \tau)(\mu_c + d_c)} < 1.$$

Furthermore, $\frac{\beta_c S_c^0}{\mu_c + d_c}$ and $\frac{\beta_s S_s^0}{\mu_c + d_s}$ are respectively the average number of cattle infections as a result of direct contact between susceptible and infected cattle and the average number of small ruminant infections as a result of direct contact between susceptible and infected small ruminant, and $\frac{((\varepsilon + \tau)\beta_c + \rho_c \alpha_c) S_c^0}{(\varepsilon + \tau)(\mu_c + d_c)}$ is the expected number of infected cattle caused directly or indirectly by one infectious cattle. Thus, the brucellosis free equilibrium for each population is locally asymptotically stable if and only if the number of secondary infections, (R_e) is less than unit, that is $R_0 < 1$. This completes the proof.

4.4 Global stability of the disease-free equilibrium

In this section, we analyze the global stability of the disease-free equilibrium point by applying the [11] approach. We write model system (2) in the form:

$$\begin{cases} \frac{dX_s}{dt} = A(X_s - X_{DFE,S}) + A_1 X_i, \\ \frac{dX_i}{dt} = A_2 X_i, \end{cases} \tag{6}$$

where X_s is the vector representing the non-transmitting compartments and X_i is the vector representing the transmitting components. The DFE is globally asymptotically stable if A has real negative eigenvalues and A_2 is a Metzler matrix (i.e. the off-diagonal elements of A_2 are non-negative). From model system (2) we have:

$$X_i = (I_c, I_s, B)^T, X_s = (V_c, S_c, V_s, S_s)^T, X_s - X_{DFE,s} = \begin{bmatrix} V_c - \frac{\phi_c \pi_c N_c^0}{\mu_c(\phi_c + \mu_c + \psi_c) + \psi_c} \\ S_c - \frac{(\phi_c + \mu_c)\pi_c N_c^0}{\mu_c(\phi_c + \mu_c + \psi_c) + \psi_c} \\ V_s - \frac{\phi_s \pi_s N_s^0}{\mu_s(\phi_s + \mu_s + \psi_s) + \psi_s} \\ S_s - \frac{(\phi_s + \mu_s)\pi_s N_s^0}{\mu_s(\phi_s + \mu_s + \psi_s) + \psi_s} \end{bmatrix},$$

and

$$A_1 = \begin{bmatrix} 0 & 0 & 0 \\ -\beta_c S_c & 0 & -\alpha_c \\ 0 & 0 & 0 \\ 0 & -\beta_s S_s & -\alpha_s \end{bmatrix}.$$

We need to check whether a matrix A for the non-transmitting compartments has real negative eigenvalues and that A_2 is a Metzler matrix. From the equation for non-transmitting compartments in (2) we have:

$$A = \begin{bmatrix} -(\psi_c+\mu_c) & \phi_c & 0 & 0 \\ \psi_c & -(\phi_c+\mu_c) & 0 & 0 \\ 0 & 0 & -(\psi_s+\mu_s) & \phi_s \\ 0 & 0 & \psi_s & -(\phi_s+\mu_s) \end{bmatrix},$$

with eigenvalues $\lambda_1 = -\mu_s, \lambda_2 = -(\psi_s+\phi_s+\mu_s), \lambda_3 = -\mu_c, \lambda_4 = -(\psi_c+\phi_c+\mu_c)$ and

$$A_2 = \begin{bmatrix} \beta_c S_c^0 - (\mu_c+d_c) & 0 & \alpha_c S_c^0 \\ 0 & \beta_s S_s^0 - (\mu_s+d_s) & \alpha_s S_s^0 \\ \rho_c & \rho_s & -(\varepsilon+\tau) \end{bmatrix}.$$

It can be seen that, A_2 which is a Metzler matrix, and A, have real negative eigenvalues. This implies that the disease free equilibrium for the model system (2) is globally asymptotically stable.

4.5 Global stability of endemic equilibrium

The local stability of the disease free equilibrium suggests local stability of the endemic equilibrium for the reverse condition [9,10,51]. In this subsection we study the global behaviour of the endemic equilibrium, E^* for the model system (2).

Theorem 2. *The endemic equilibrium point for the brucellosis model system (2) is globally asymptotically stable on Ω if $R_0 > 1$.*

Proof. We construction an explicit Lyapunov function for model system (2) using [7,30,31,32,36] approach as it is useful to most of the sophisticated compartmental epidemiological models. In this approach, we construct Lyapunov function of the form:

$$V = \sum a_i (x_i - x_i^* \ln x),$$

where a_i is a properly selected positive constant, x_i is the population of the i^{th} compartment and x_i^* is the equilibrium level. We define the Lyapunov function candidate V for model system (2) as:

$$\begin{aligned} L =& (S_c - S_c^* \ln S_c) + A_1 (V_c - V_c^* \ln V_c) + A_2 (I_c - I_c^* \ln I_c) + (S_s - S_s^* \ln S_s) \\ &+ A_3 (V_s - V_s^* \ln V_s) + A_4 (I_s - I_s^* \ln I_s) + A_5 (B - B^* \ln B), \end{aligned} \tag{7}$$

where A_1, A_2, A_3, A_4 and A_5 are positive constants. The time derivative of the Lyapunov function L is given by:

$$\begin{aligned} \frac{dL}{dt} =& \left(1 - \frac{S_c^*}{S_c}\right)\frac{dS_c}{dt} + A_1\left(1 - \frac{V_c^*}{V_c}\right)\frac{dV_c}{dt} + A_2\left(1 - \frac{I_c^*}{I_c}\right)\frac{dI_c}{dt} + \left(1 - \frac{S_s^*}{S_s}\right)\frac{dS_s}{dt} \\ &+ A_3\left(1 - \frac{V_s^*}{V_s}\right)\frac{dV_s}{dt} + A_4\left(1 - \frac{I_s^*}{I_s}\right)\frac{dI_s}{dt} + A_5\left(1 - \frac{B^*}{B}\right)\frac{dB}{dt}. \end{aligned} \tag{8}$$

Considering (2) at E^* we have:

$$\phi = \frac{(\psi_c + \mu_c)V_c^*}{S_c^*},$$

$$\pi_c N_c^* = (\beta_c I_c^* + \alpha_c B^* + \phi_c + \mu_c)S^* - \psi_c V_c^*,$$

$$\mu_c + d_c = \frac{(\beta_c I_c^* + \alpha_c B^*)S^*}{I_c^*},$$

$$(\varepsilon + \tau) = \frac{\rho_c I_c^* + \rho_s I_s^*}{I_c^*}.$$

Then, equation (8) may be re-written as:

$$\begin{aligned}
\frac{dL}{dt} =& -(\phi_c + \mu_c)S_c\left(1 - \frac{S_c^*}{S_c}\right)^2 - (\phi_s + \mu_s)S_s\left(1 - \frac{S_s^*}{S_s}\right)^2 \\
&- \left(1 - \frac{S_c^*}{S_c}\right)\left(\beta_c I_c S_c\left(1 - \frac{I_c^* S_c^*}{I_c S_c}\right) + \alpha_c B S_c\left(1 - \frac{B^* S_c^*}{B S_c}\right) + \psi_c V_c\left(\frac{V_c^*}{V_c} - 1\right)\right) \\
&- \left(1 - \frac{S_s^*}{S_s}\right)\left(\beta_s I_s S_s\left(1 - \frac{I_s^* S_s^*}{I_s S_s}\right) + \alpha_s B S_s\left(1 - \frac{B^* S_s^*}{B S_s}\right) + \psi_s V_s\left(\frac{V_s^*}{V_s} - 1\right)\right) \\
&- (\psi_c + \mu_c)BV_c A_1\left(1 - \frac{V_c^*}{V_c}\right)\left(1 - \frac{V_c^*}{V_c S_c^*}\right) - (\psi_s + \mu_s)BV_s A_3\left(1 - \frac{V_s^*}{V_s}\right)\left(1 - \frac{V_s^*}{V_s S_s^*}\right) \\
&+ A_2\left(1 - \frac{I_c^*}{I_c}\right)\left(\beta_c I_c S_c\left(1 - \frac{S_c^*}{S_c}\right) + \alpha_c B S_c\left(1 - \frac{B^* S_c^* I_c}{B S_c I_c^*}\right)\right) \\
&+ A_4\left(1 - \frac{I_s^*}{I_s}\right)\left(\beta_s I_s S_s\left(1 - \frac{S_s^*}{S_s}\right) + \alpha_s B S_s\left(1 - \frac{B^* S_s^* I_s}{B S_s I_s^*}\right)\right) \\
&+ A_5\left(1 - \frac{B^*}{B}\right)\left(\rho_c I_c\left(1 - \frac{B I_c^*}{B^* I_c}\right) + \rho_s I_s\left(1 - \frac{B I_s^*}{B^* I_s}\right)\right).
\end{aligned} \tag{9}$$

Equation (9) can be written as:

$$\frac{dL}{dt} = -\left((\phi_c + \mu_c)S_c\left(1 - \frac{S_c^*}{S_c}\right)^2 + (\phi_s + \mu_s)S_s\left(1 - \frac{S_s^*}{S_s}\right)^2\right) + F(S_c, V_c, I_c, S_s, V_s, I_s, B),$$

where F is the balance of the right hand terms of equation (9). Following the approach of [7,30,31,32,33,36], F is a non-positive function for $S_c, V_c, I_c, S_s, V_s, I_s, B > 0$. Thus, $\frac{dL}{dt} < 0$ for $S_c, V_c, I_c, S_s, V_s, I_s, B > 0$ and is zero if $S_c = S_c^*, V_c = V_c^*, I_c = I_c^*, S_s = S_s^*, V_s = V_s^*, I_s = I_s^*$, and $B = B^*$. Therefore, if $R_e > 1$, model system (2) has a an endemic equilibrium point E^* which is locally and globally asymptotically stable.

5 Sensitivity analysis

In this section, we investigate the relative importance of the parameters featuring in the effective reproduction number. Brucellosis incidences and prevalences can best be reduced or eradicated if the parameters with significant impact in the transmission dynamics of the disease are taken into consideration when planning for and implementing intervention strategies. Sensitivity analysis is commonly used to determine the robustness of model predictions to parameter values, since there are usually errors in data collection and presumed parameter values [12]. Sensitivity indices provide information on how vital each parameter is to disease transmission and prevalence, and permits measurement of relative changes in a state variable when a parameter changes. Thus, we use sensitivity analysis to discover parameters that have

high impact on the reproduction number, R_e and that should be targeted by intervention strategies. We know that initial disease transmission is directly related to R_e, therefore we compute the sensitivity indices of R_e for the parameters in model 2. The explicit expression of R_e is given by equation 4. Since R_e depends only on twenty parameters, we derive an analytical expression for its sensitivity to each parameter using the normalized forward sensitivity index [35] as follows:

$$\Upsilon_{\mu_c}^{R_e} = \frac{\partial R_e}{\partial \mu_c} \times \frac{\mu_c}{R_e} = -0.84,$$

$$\Upsilon_{\pi_c}^{R_e} = \frac{\partial R_e}{\partial \pi_c} \times \frac{\pi_c}{R_e} = +0.69.$$

In a similar fashion, we compute the sensitivity indices for all parameters used in equation 4 and present the results in Table 3. Table 3 shows that the most sensitive parameters of the effective reproductive number in each population are natural

Table 3: Sensitivity indices for R_e parameters

Parameter	Value	Unit	Sensitivity Index
π_c	0.3	$year^{-1}$	0.69
β_c	0.0011	$year^{-1}$	0.54
ϕ_c	0.7	$year^{-1}$	-0.36
ψ_c	0.4	$year^{-1}$	0.22
μ_c	0.25	$year^{-1}$	-0.84
d_c	0.35	$year^{-1}$	-0.40
α_c	0.00035	$year^{-1}$	0.15
ρ_c	10	$year^{-1}$	0.15
ε	8	$year^{-1}$	-0.10
τ	12	$year^{-1}$	-0.16
π_s	0.4	$year^{-1}$	0.31
β_s	0.001	$year^{-1}$	0.20
ϕ_s	0.8	$year^{-1}$	-0.15
ψ_s	0.5	$year^{-1}$	0.09
μ_s	0.35	$year^{-1}$	-0.39
d_s	0.4	$year^{-1}$	-0.16
α_s	0.00032	$year^{-1}$	0.11
ρ_s	15	$year^{-1}$	0.11

death rate, birth rate, transmission rate, gradual culling rate of sero-positive ruminants through slaughter and vaccination rate. The positive sign in the sensitivity index means that an increase in that parameter leads to an increase in R_e and vise-versa. For instance, an increase or decrease of cattle birth rate by 10% leads to an increase or decrease of R_e by 6.9%. On the other hand, the negative sign in the sensitivity index of a parameter indicates that an increase or decrease in a parameter value leads to a decrease or increase in R_e respectively. For instance, a 10% increase in cattle natural mortality rate leads to a 8.4% decrease in the effective reproductive number. This implies that culling in large livestock flocks is inevitable if we want to control brucellosis transmissions.

6 Numerical Simulations

This section presents numerical simulations for model system 1 for the purpose of verifying some of the analytical results. The parameter values used in our computations are mainly from [34], a literature similar to this work. The parameter values are in Table 3. Figure 2 illustrates the variations in livestock and brucella subpopulations as time increases. Figure 2 shows that susceptible ruminants decrease rapidly due to brucellosis epidemic and vaccination of susceptible ruminants, while the infective subpopulations initially increase with time. However, after a two-year period these subpopulations start decreasing. The increase in the infective classes is due to high brucellosis transmission rate

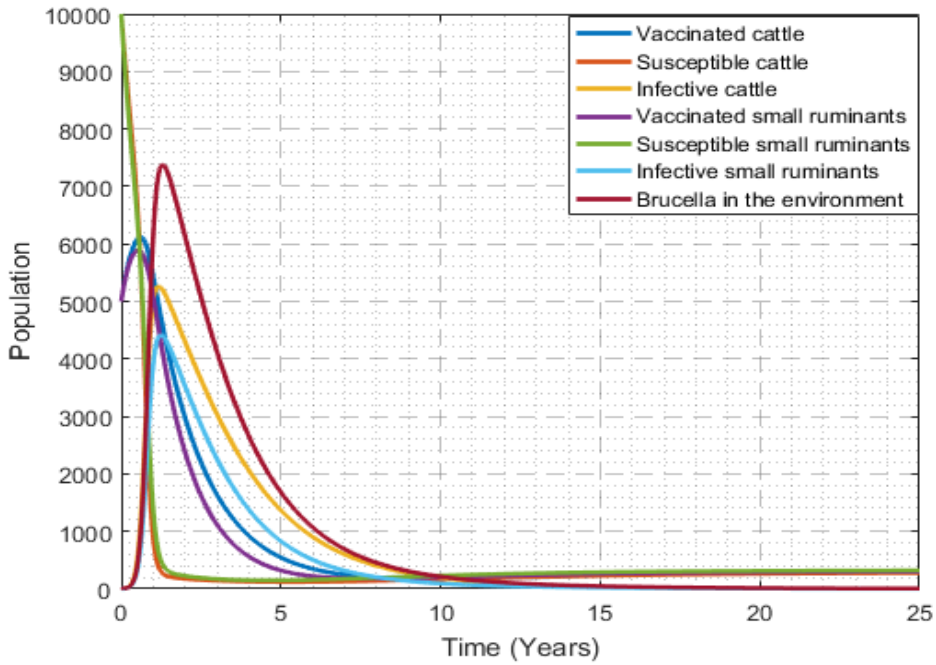

Fig. 2: Ruminants subpopulations variation

and the decrease is due to different interventions like gradual culling of infective ruminants, environmental hygiene and sanitation, and immunization of susceptible ruminants. The graph for vaccinated classes initially increase because large number of susceptible livestock are vaccinated at the beginning of any vaccination program and decrease due to reduction in the number of susceptible livestock. Furthermore, the number of all infective classes goes to zero after 10 years. From Figure 3 we see that the combination of timely environmental hygiene and sanitation and ruminants vaccination significantly controls the indirect transmission of brucella from cattle to small ruminants and vice versa. In addition, the disease can be eliminated from the population if gradual culling of seropositive ruminants through slaughter eliminates at least 35% and 40% of the infective cattle and small ruminants respectively.

Furthermore, Figure 4a shows that an increase in cattle vaccination rate leads to a decrease in the effective reproduction number. For instance, the cattle population attains its disease free equilibrium at 10% vaccination rate provided that other controls are kept constant. This implies that cattle vaccination at some points plays a significant contribution in reducing the transmission dynamics of brucellosis. A similar trend is observed from Figure 4b that vaccination of small ruminants significantly reduces their secondary brucellosis infections and the small ruminants brucellosis free state is achieved at 9% vaccination rate. Moreover, if other control parameters are kept constant and disease-induced rate is varied, we obtain the brucellosis free equilibrium ($R_e < 1$) at 12.5% and 10% diseased induced elimination rates for cattle and small ruminants respectively (see Figure 5a and Figure 5b).

Generally, the combination of ruminants vaccination, test-and-slaughter and disinfection of the environment minimizes or eliminates the disease from the populations. In line with this [47] pointed out that, gradual culling of seropositive animals through slaughter, isolation and confinement of pregnant cows close to calving; proper disposal of placentas and aborted foetuses, the use of the S19 vaccine, and restricted introduction of new animals leads to brucellosis elimination in animal herds.

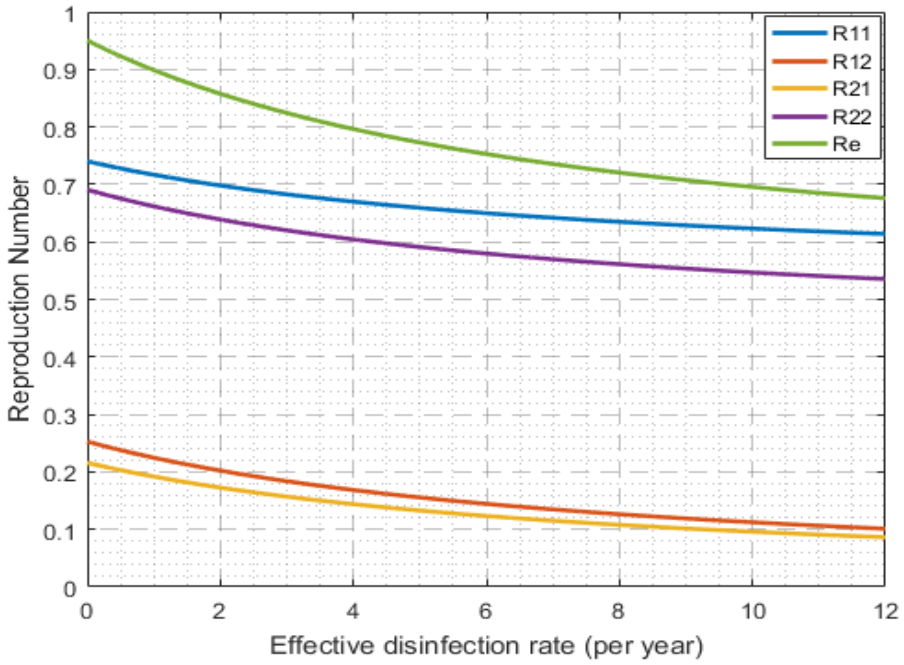

Fig. 3: The impact of environmental hygiene and sanitation on brucelosis transmission

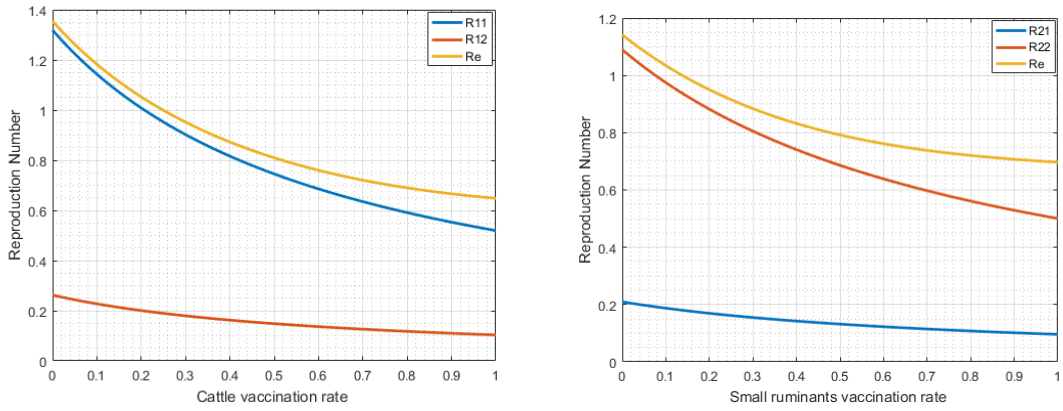

(a) **(b)**

Fig. 4: The impact of ruminants vaccination on brucelosis transmission.

Conflict of Interest

The authors declares no conflict of interest regarding the publication of this manuscript.

Authors' contributions

All authors have contributed to all parts of the article. All authors read and approved the final manuscript.

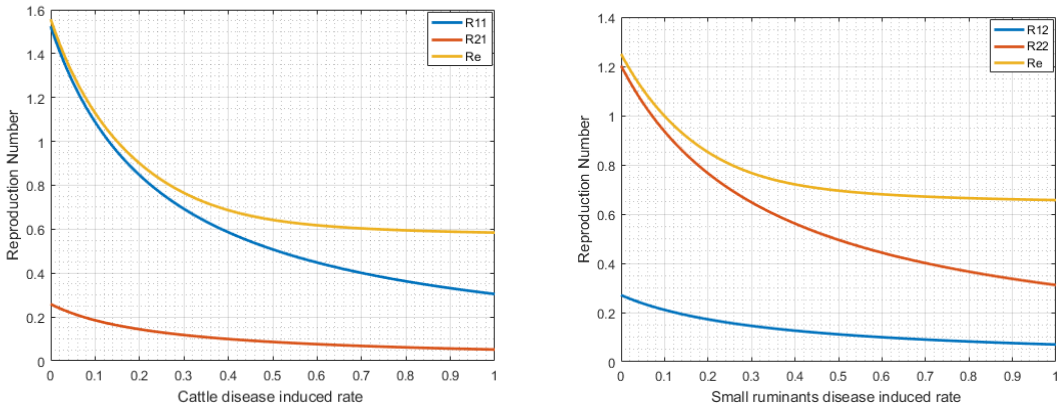

(a) **(b)**

Fig. 5: The impact of seropositive ruminants culling on the transmission of brucellosis.

References

[1] Alessandro Abate, Ashish Tiwari, and Shankar Sastry. Box invariance in biologically-inspired dynamical systems, *Automatica*; 45(9): 1601–1610, 2009.

[2] Bedr'Eddine Ainseba, Chahrazed Benosman, and Pierre Magal. A model for ovine brucellosis incorporating direct and indirect transmission, *Journal of biological dynamics*; 4(1): 2–11, 2010.

[3] Ali G Alhamada, Ihab Habib, Anne Barnes, and Ian Robertson. Risk factors associated with brucella seropositivity in sheep and goats in Duhok Province, Iraq, *Veterinary sciences*,4(65): 1–9, 2017.

[4] M Amaku, RA Dias, JS Ferreira Neto, and F Ferreira. Mathematical modeling of bovine brucellosis control by vaccination, *Arquivo Brasileiro de Medicina Veterinária e Zootecnia*, 61:135–141, 2009.

[5] J Awah-Ndukum, MMM Mouiche, HN Bayang, V Ngu Ngwa, E Assana, KJM Feussom, TK Manchang, and PA Zoli. Seroprevalence and Associated Risk Factors of Brucellosis among Indigenous Cattle in the Adamawa and North Regions of Cameroon, *Veterinary medicine international*, 2018. URL:*https://doi.org/10.1155/2018/3468596*.

[6] Andrew J Bouley, Holly M Biggs, Robyn A Stoddard, Anne B Morrissey, John A Bartlett, Isaac A Afwamba, Venance P Maro, Grace D Kinabo, Wilbrod Saganda, Sarah Cleaveland, and John A Crump. Brucellosis Among Hospitalized Febrile Patients in Northern Tanzania, *The American journal of tropical medicine and hygiene*, 87(6):1105–1111, 2012.

[7] Samuel Bowong, Jean Jules Tewa, and Jean Claude Kamgang. Stability analysis of the transmission dynamics of tuberculosis models, *World Journal of Modelling and Simulation*; 7(2): 83–100, 2011.

[8] Manuela Carugati, Holly M Biggs, Michael J Maze, Robyn A Stoddard, Shama Cash-Goldwasser, Julian T Hertz, Jo EB Halliday, Wilbrod Saganda, Bingileki F Lwezaula, Rudovick R Kazwala, Sarah Cleaveland, Venance P Maro, Mathew P Rubach, and John A Crump. Incidence of human brucellosis in the Kilimanjaro Region of Tanzania in the periods 2007–2008 and 2012–2014, *Transactions of The Royal Society of Tropical Medicine and Hygiene*; 112(3): 136–143, 2018.

[9] Saul C Mpeshe, Livingstone S Luboobi, and Yaw Nkansah-Gyekye. Stability analysis of the Rift Valley fever dynamical model,*Journal of Mathematical and Computational Science*, 4(4): 740–762, 2014.

[10] N Nyerere, LS Luboobi, and Y Nkansah-Gyekye. Bifurcation and Stability analysis of the dynamics of Tuberculosis model incorporating, vaccination, Screening and treatment,*Communications in Mathematical biology and Neuroscience*, 1:Article–ID, 2014.

[11] Carlos Castillo-Chavez, Sally Blower, Pauline van den Driessche, Denise Kirschner, and Abdul-AzizYakubu. *Mathematical approaches for emerging and reemerging infectious diseases: an introduction*, 1: 2002.

[12] Nakul Chitnis, James M Hyman, and Jim M Cushing. Determining important parameters in the spread of malaria through the sensitivity analysis of a mathematical model, *Bulletin of mathematical biology*, 70(5): 1272, 2008.

[13] CDC. Brucellosis Signs and Symptoms, *https://www.cdc.gov/brucellosis/symptoms/index.html*. Accessed 2018-11-07.

[14] CFSPH. Brucellosis Brucella abortus, *http://cfsph.iastate.edu/Factsheets/pdfs/brucellosis_abortus.pdf*. Accessed 2018-11-07.

[15] Ariel Cintrón-Arias, Carlos Castillo-Chávez, Luıs MA Bettencourt, Alun L Lloyd, and HT Banks. The estimation of the effective reproductive number from disease outbreak data, *Math Biosci Eng*, 6(2): 261–282, 2009.

[16] Anna S Dean, Lisa Crump, Helena Greter, Esther Schelling, and Jakob Zinsstag. Global burden of human brucellosis: a systematic review of disease frequency, *PLoS neglected tropical diseases*, 6(10): 1-9, 2012.

[17] Odo Diekmann, Johan Andre Peter Heesterbeek, and Johan AJ Metz. On the definition and the computation of the basic reproduction ratio R_0 in models for infectious diseases in heterogeneous populations,*Journal of mathematical biology*, 28(4): 365–382, 1990.

[18] O Diekmann, JAP Heesterbeek, and MG Roberts. The construction of next-generation matrices for compartmental epidemic models, *Journal of the Royal Society Interface*, 7(47): 873–885, 2010.

[19] Andrew Dobson, and Mary Meagher. The population dynamics of brucellosis in the Yellowstone National Park, *Ecology*, 77(4): 1026–1036, 1996.

[20] M Ducrotoy, WJ Bertu, G Matope, S Cadmus, R Conde-Álvarez, AM Gusi, S Welburn, R Ocholi, JM Blasco, and I Moriyón. Brucellosis in Sub-Saharan Africa: current challenges for management, diagnosis and control, *Acta tropica*, 165: 179–193, 2017.

[21] KA Franc, RC Krecek, BN Häsler, and AM Arenas-Gamboa. Brucellosis remains a neglected disease in the developing world, *BMC public health*, 18(125): 2018.

[22] M Graeme Garner, and SD Beckett . Modelling the spread of foot-and-mouth disease in Australia, *Australian Veterinary Journal*, 83(12): 758–766, 2005.

[23] Giraldo J Ospina and Palacio D Hincapié. Deterministic SIR (Susceptible–Infected–Removed) models applied to varicella outbreaks, *Epidemiology & Infection*, 136(5): 679–687, 2008.

[24] Ronald A Greenfield, Douglas A Drevets, Linda J Machado, Gene W Voskuhl, Paul Cornea, and Michael S Bronze. Bacterial pathogens as biological weapons and agents of bioterrorism, *The American journal of the medical sciences*, 323(6): 299–315, 2002.

[25] Qiang Hou, Xiangdong Sun, Juan Zhang, Yongjun Liu, Youming Wang, and Zhen Jin. Modeling the transmission dynamics of sheep brucellosis in Inner Mongolia Autonomous Region, China, *Mathematical biosciences*, 242(1): 51–58, 2013.

[26] Qiang Hou, and Xiang-Dong Sun. Modeling sheep brucellosis transmission with a multi-stage model in Changling County of Jilin Province, China, *Journal of Applied Mathematics and Computing*, 51(1-2): 227–244, 2016.

[27] Kunda John, Julie Fitzpatrick, Nigel French, Rudovick Kazwala, Dominic Kambarage, Godfrey S Mfinanga, Alastair MacMillan, and Sarah Cleaveland. Quantifying risk factors for human brucellosis in rural northern Tanzania, *PloS one*, 5(4): 1–6, 2010.

[28] Mirjam Sarah Kadelka. *Mathematical models of immune responses following vaccination with application to Brucella infection* , Virginia Tech, 242(1): 2015.

[29] MJ Keeling, and L Danon. Mathematical modelling of infectious diseases, *British Medical Bulletin*, 92(1): 33–42, 2009.

[30] Andrei Korobeinikov, and Graeme C Wake. Lyapunov functions and global stability for SIR, SIRS, and SIS epidemiological models, *Applied Mathematics Letters*, 15(8): 955–960, 2002.

[31] Andrei Korobeinikov. Lyapunov functions and global properties for SEIR and SEIS epidemic models, *Mathematical medicine and biology: a journal of the IMA*, 21(2): 75–83, 2004.

[32] Andrei Korobeinikov. Global properties of infectious disease models with nonlinear incidence, *Bulletin of Mathematical Biology*, 69(6): 1871–1886, 2007.

[33] Can Li, Zun-Guang Guo, and Zhi-Yu Zhang. Transmission dynamics of a brucellosis model: Basic reproduction number and global analysis, *Chaos, Solitons & Fractals*, 104: 161–172, 2017.

[34] Ming-Tao Li, Gui-Quan and Sun, Yan-Fang Wu, Juan Zhang, and Zhen Jin. Transmission dynamics of a multi-group brucellosis model with mixed cross infection in public farm, *Applied Mathematics and Computation*, 237: 582–594, 2014.

[35] Pauline van den Driessche. Reproduction numbers of infectious disease models, *Infectious Disease Modelling*, 2(3): 288–303, 2017.

[36] C Connell McCluskey. Lyapunov functions for tuberculosis models with fast and slow progression, *Mathematical Biosciences and Engineering*, 3 : 1–12, 2006.

[37] Medscape. Brucellosis Pathogenicity, *https://emedicine.medscape.com/article/213430-overview*, Accessed: 2018-11-07.

[38] Mariana N Xavier, Tatiane A Paixao, Andreas B den Hartigh, Renee M Tsolis, and Renato L Santos. Pathogenesis of Brucella spp., *The open veterinary science journal*, 4(1): 109–118, 2010.

[39] B Nannyonga, GG Mwanga, and LS Luboobi. An optimal control problem for ovine brucellosis with culling, *Journal of biological dynamics*, 9(1):198–214, 2015.

[40] Paride O Lolika, Chairat Modnak, and Steady Mushayabasa. On the dynamics of brucellosis infection in bison population with vertical transmission and culling, *Mathematical biosciences*,305: 42–54, 2018.

[41] Daniel Okuonghae, and Andrei Korobeinikov. Dynamics of tuberculosis: the effect of direct observation therapy strategy (DOTS) in Nigeria, *Mathematical modelling of natural phenomena*, 2(1): 113–128, 2007.

[42] P Padmanabhan, P Seshaiyer, and C Castillo-Chavez. Mathematical modeling, analysis and simulation of the spread of Zika with influence of sexual transmission and preventive measures, *Letters in Biomathematics*, 4(1): 148–166, 2017.

[43] Georgios Pappas, Photini Papadimitriou, Nikolaos Akritidis, Leonidas Christou, and Epameinondas V Tsianos. The new global map of human brucellosis, *The Lancet infectious diseases*, 6(2): 91–99, 2006.

[44] Felix Roth, Jakob Zinsstag, Dontor Orkhon, G Chimed-Ochir, Guy Hutton, Ottorino Cosivi, Guy Carrin, and Joachim Otte. Human health benefits from livestock vaccination for brucellosis: case study, *Bulletin of the World health Organization*, 81:867–876, 2003.

[45] E Schelling, C Diguimbaye, S Daoud, J Nicolet, P Boerlin, M Tanner, and J Zinsstag. Brucellosis and Q-fever seroprevalences of nomadic pastoralists and their livestock in Chad, *Preventive veterinary medicine*, 61(4): 279–293, 2003.

[46] Gabriel Mkilema Shirima. *The epidemiology of brucellosis in animals and humans in Arusha and Manyara regions in Tanzania* , PhD thesis. University of Glasgow, 2005.

[47] Gabriel M Shirima, Seleman N Masola, Obeid N Malangu, and Brant A Schumaker. Outbreak investigation and control case report of brucellosis: experience from livestock research centre, Mpwapwa, Tanzania, *Onderstepoort Journal of Veterinary Research*, 81(1):1–4, 2014.

[48] J Kitaly. *Bovine brucellosis in Government parastatal and Ujamaa village dairy farms in Central Zone of Tanzania: Assessment of Control measures in some farms In*, Proceedings of the 2 nd Tanzania Veterinary Association Scientific Conference, 24–30, 1984.

[49] Emmanuel S Swai, and Luuk Schoonman. Human brucellosis: seroprevalence and risk factors related to high risk occupational groups in Tanga Municipality, Tanzania, *Zoonoses and Public Health*, 56(4):183–187, 2009.

[50] Gabriel Tumwine, Enock Matovu, John David Kabasa, David Okello Owiny, and Samuel Majalija. Human brucellosis: sero-prevalence and associated risk factors in agro-pastoral communities of Kiboga District, Central Uganda, *BMC public health*, 15(1): 1–8, 2015.

[51] Pauline Van den Driessche, and James Watmough. Reproduction numbers and sub-threshold endemic equilibria for compartmental models of disease transmission, *Mathematical biosciences*, 180(1-2): 29–48, 2002.

[52] WHO. Brucellosis in humans and animals, *http://http://www.who.int/csr/resources/publications/Brucellosis.pdf*. Accessed: 2018-11-08.

[53] Melese Yilma, and Gezahegne Mamo, and Bedaso Mammo. Review on Brucellosis Sero-prevalence and Ecology in Livestock and Human Population of Ethiopia, *Achievements in the Life Sciences*, 10(1): 80–86, 2016.

[54] Fengbo Zhang, Zhiwei Li, Xiaolin La, Xiumin Ma, Yaoxin Zhang, Ping Ji, Min Jiang, Jinwei Hu, Zhaoxia Zhang, Xiaobo Lu, and Jianbing Ding. Multiple-locus variable-number tandem-repeat analysis of Brucella isolates from patients in Xinjiang China, *International journal of clinical and experimental medicine*, 8(9): 15716–15723, 2015.

[55] Juan Zhang, Gui-Quan Sun, Xiang-Dong Sun, Qiang Hou, Mingtao Li, Baoxu Huang, Haiyan Wang, and Zhen Jin. Prediction and control of brucellosis transmission of dairy cattle in Zhejiang Province, China, *Plos one*, 9(11): 1–13, 2014.

[56] J Zinsstag, and F Roth, D Orkhon, G Chimed-Ochir, M Nansalmaa, J Kolar, and P Vounatsou. A model of animal–human brucellosis transmission in Mongolia, *Preventive veterinary medicine*, 69(1-2): 77–95, 2005.

[57] FP Poester, LE Samartino, RL Santos. Pathogenesis and pathobiology of brucellosis in livestock, *Rev Sci Tech*, 32(1): 105–15, 2013.

[58] Wendi Wang, and Xiao-Qiang Zhao. Threshold dynamics for compartmental epidemic models in periodic environments, *Journal of Dynamics and Differential Equations*, 20(3): 699–717, 2008.

Hindawi
International Journal of Mathematics and Mathematical Sciences
Volume 2020, Article ID 1214391, 17 pages
https://doi.org/10.1155/2020/1214391

Research Article

Optimal Control Strategies for the Infectiology of Brucellosis

Nkuba Nyerere,[1,2] **Livingstone S. Luboobi**,[3] **Saul C. Mpeshe**,[4] **and Gabriel M. Shirima**[5]

[1]*Department of Applied Mathematics and Computational Sciences, Nelson Mandela African Institution of Science and Technology, P. O. Box 447, Arusha, Tanzania*
[2]*Department of Mathematics, Informatics and Computational Sciences, Sokoine University of Agriculture, P. O. Box 3038, Morogoro, Tanzania*
[3]*Institute of Mathematical Sciences, Strathmore University, P. O. Box 59857-00200, Nairobi, Kenya*
[4]*Department of Mathematics, University of Iringa, P. O. Box 200, Iringa, Tanzania*
[5]*Department of Global Health and Bio-Medical Sciences, Nelson Mandela African Institution of Science and Technology, P. O. Box 447, Arusha, Tanzania*

Correspondence should be addressed to Nkuba Nyerere; emmankuba@sua.ac.tz

Received 28 February 2020; Accepted 22 April 2020; Published 11 May 2020

Academic Editor: Vladimir V. Mityushev

Brucellosis is a zoonotic infection caused by Gram-negative bacteria of genus *Brucella*. The disease is of public health, veterinary, and economic significance in most of the developed and developing countries. Direct contact between susceptible and infective animals or their contaminated products are the two major routes of the disease transmission. In this paper, we investigate the impacts of controls of livestock vaccination, gradual culling through slaughter of seropositive cattle and small ruminants, environmental hygiene and sanitation, and personal protection in humans on the transmission dynamics of Brucellosis. The necessary conditions for an optimal control problem are rigorously analyzed using Pontryagin's maximum principle. The main ambition is to minimize the spread of brucellosis disease in the community as well as the costs of control strategies. Findings showed that the effective use of livestock vaccination, gradual culling through slaughter of seropositive cattle and small ruminants, environmental hygiene and sanitation, and personal protection in humans have a significant impact in minimizing the disease spread in livestock and human populations. Moreover, cost-effectiveness analysis of the controls showed that the combination of livestock vaccination, gradual culling through slaughter, environmental sanitation, and personal protection in humans has high impact and lower cost of prevention.

1. Introduction

Brucellosis is a zoonotic infection caused by Gram-negative bacteria of genus *Brucella* which includes; *B. abortus* primarly from cattle, *B. melitensis* from small ruminants, *B. suis* from swine, and *B. canis* from dogs [1–4]. It is considered by the Food and Agriculture Organisation (FAO), the World Health Organisation (WHO), and World Organization for Animal Health (Office International des Epizooties (OIE)) as one of the most widespread zoonoses in the world alongside bovine tuberculosis and rabies [5]. The disease is an ancient one that was described more than 2000 years ago by the Romans [6] and has been known by various names, including Mediterranean fever, Malta fever, gastric remittent fever, Bang's disease, Crimean fever, Gibraltar fever, rock fever, lazybones disease, and undulant fever [7].

Brucella bacteria was first isolated in 1887 from an infected individual's blood by a British military medical officer David Bruce and by that reason the disease was named brucellosis to honor his contribution [8]. Furthermore, in 1905, Zamitt carried out an experiment on goats to investigate the origin of human brucellosis and found that human brucellosis originates from goats [9]. To date, ten brucella species have been identified and primarily named after the features of infection or the animal source. Of these, the following four have moderate-to-significant human pathogenicity: *Brucella melitensis* (highest pathogenicity), *Brucella suis* (high pathogenicity), *Brucella*

abortus (moderate pathogenicity), and *Brucella canis* (moderate pathogenicity) [10–12].

Brucellosis is endemic in most of the developing world. It causes devastating losses to the livestock industry especially small-scale livestock holders, thereby limiting economic growth and hindering access to international markets [13]. The economic importance of the disease is based on the fact that it causes financial losses from abortions, sterility, decreased milk production, veterinary fees, and costs of replacement of animals. In animals, brucellosis is transmitted when a susceptible animal ingests contaminated materials such as tissues or discharges from infected animals, while in humans the bacteria is transmitted by ingestion of contaminated unpasteurized milk or other dairy products and direct contact through occupational activities such as farmers, laboratory personnel, abattoir workers, and veterinarians. According to Ducrotoy et al. [14], there are epidemiological situations in which infections of small ruminants by *B. abortus* occur in areas where they are in contact with cattle and *B. melitensis* is absent. Ducrotoy et al. [14] suggests that coinfections by two different brucellae are rather unlikely because of the development of immunity in an ongoing infection and, in fact, they have never been convincingly proven.

Infected animals exhibit clinical signs that are of economic significance to stakeholders. These signs include reduced fertility, abortion, poor weight gain, lost draught power, and a substantial decline in milk production [13, 15]. Symptoms in human includes continuous or intermittent fever, headache, weakness, profuse sweats, chills, joint pains, aches, and weight loss, as well as devastating complications that leads to miscarriage in pregnant women. Neurological complications, endocarditis, and testicular or bone abscess formation can also occur [16, 17]. The infection can also affect the liver and spleen and may last for longer terms if not treated. Furthermore, the clinical signs of brucellosis in humans present diagnostic difficulties because they overlap with those of typhoid fever, malaria, rheumatic fever, joint diseases, and relapsing fever. Human brucellosis is debilitating and requires prolonged treatment with combination of antibiotics [18].

The global burden of human brucellosis remains enormous: The infection causes more than 500,000 new cases per year worldwide. The annual number of reported cases in the United States has dropped significantly to about 100 cases per year due to aggressive animal vaccination programs and milk pasteurization. Most United States cases are now due to the consumption of illegally imported unpasteurized dairy products from Mexico, and approximately 60% of human brucellosis cases occur in California and Texas [19]. In Africa, brucellosis exists throughout sub-Saharan Africa, but the prevalence is unclear and poorly understood with varying reports from country to country and geographical regions, as well as animal factors [20]. Most African countries have poor socioeconomic status, with people living with and by their livestock, while health networks, surveillance, and vaccination programs are virtually nonexistent. In Tanzania, the first outbreak of brucellosis was reported in Arusha in 1927 [21]. Previous surveys in Tanzania have demonstrated the occurrence of the disease in cattle in various production systems, regions, and zones with individual animal level seroprevalence varying from 1 to 30%. In humans, the average prevalence varies from 1 to 5% [22]; a recent study by [23] shows that brucellosis incidence is moderate in northern Tanzania and suggests that the disease is endemic and an important human health problem in this area. Moreover, human cases had been reported in areas of northern, eastern, lake, and western zones with seroprevalence varying from 0.7 to 20.5% [24, 25]. Despite the WHO, FAO, and OIE efforts and interventions being available, brucellosis continues to pose great economic threat by affecting livelihood and food security in both developed and developing countries from generation to generation. Thus, there is a need to assess the current control strategies and their cost effectiveness if we are to control or eradicate the disease. So far, few studies [10, 26–33] have been developed to analyze dynamics and spread of brucellosis in homogeneous/heterogeneous populations. However, none of these studies had considered the mathematical approach for optimal control and cost effectiveness in reducing or eradicating the disease in cattle, small ruminants, and human populations. In this paper, the dynamics and cost effectiveness of the control strategies for brucellosis using mathematical models are rigorously studied.

2. Model Formulation

A mathematical model for the transmission dynamics of brucellosis incorporating the time-dependent controls to some parameters is formulated in this section. Some assumptions used in this section are similar to those in [27, 28], but the time-dependent parameters $u_1(t), u_2(t), u_3(t)$, and $u_4(t)$ make the difference between our previous brucellosis works and the current work. The most important reason for taking preventive and control measures on brucellosis is to minimize the prevalence of the disease, and if possible eradicate it from the population. Particularly, the level of susceptibility of healthy individuals against the infection is minimized by protective measures, whereas the number of infective individuals in the community is reduced by control measures. In this paper, a time-dependent variable $u_1(t)$ is introduced as a control that aims at reducing the number of susceptible animals in the herds and consequently to reduce the disease transmission to the vaccination coverage failure rate $(1-u_1(t))\lambda_1$. In other words, $u_1(t)$ is the measure of the effectiveness of S19 and Rev1 vaccine for cattle and small ruminants, and $(1-u_1(t))\lambda_1$ is the failure rate of vaccination for ruminants. That is, if vaccination of ruminant coverage is 100% effective, zero brucellosis incidence may be recorded in that particular region. Thus, $u_1(t)$ aims at reducing the susceptibility level of healthy animals on the disease as well as the disease transmission rate. Based on the fact that there is neither disease-induced deaths nor treatment for infected ruminants, we introduce $u_2(t)$, a control variable that measures the efficiency of gradual culling of seropositive animal parameters d_c and d_s for the infected cattle and small ruminants, respectively. Furthermore,

gradual culling of seropositive animals targets at curtailing the number of infectious ruminants in the community and consequently reduces the disease transmission rate to $u_2(t)d_c$ and $u_2(t)d_s$ in cattle and small ruminants, respectively. To reduce or eliminate the number of *Brucella* in the environment, the control variable $u_3(t)$ is introduced as the measure of effectiveness of environmental hygiene and sanitation parameter τ. In particular, environmental hygiene and sanitation refers to proper disposal of placentas and aborted foetuses. A time-dependent control variable $u_4(t)$ is introduced in the model as the measure of the effectiveness of personal protection in humans so that $(1-u_4(t))\lambda_1$ is the failure rate of the control strategy. In this context, personal protection refers to personal hygiene, protection of the environment, food hygiene (adequate boiling of fresh milk intended for drinking or making other milk products), and adoption to safe working practices including use of personal protection equipments such as gloves, masks, eye wear, and closed footwear when handling potentially infected materials such as aborted foetus, placenta, and gravid uterus practices. Based on the fact that treatment of human brucellosis reduces the risk of disease and that has a very low or negligible transmission blocking effect, the time-dependent control for this parameter is not of much concern. To determine the necessary conditions for optimal impact of incorporated parameters, we use Pontryagin's Maximum Principle as the method for obtaining the optimal combination of incorporated controls. The aim is to limit and prevent the spread of brucellosis disease and at the same time the cost of administering these controls is minimized.

2.1. Model Assumptions. Formulation of the optimal control model is guided by the following assumptions:

(i) The mixing of individuals in each population is homogeneous

(ii) There is no direct transmission between cattle and small ruminants

(iii) Infected animals shed *Brucella* pathogens in the environment

(iv) Livestock seropositivity is life-long lasting

(v) Immunized individuals cannot be infected unless they are resistant to infection wanes

(vi) There is a constant natural mortality rate in each of the species

(vii) The birth rate for each population is greater than the natural mortality rate

The compartmental diagram with the time-dependent control strategies is shown in Figure 1, whereas the variables and parameters used in this model are, respectively, summarized in Tables 1 and 2.

2.2. Compartmental Flow Diagram for the Disease Dynamics. The interactions between human, cattle, small ruminant populations, and *Brucella* in the environment are illustrated in Figure 1.

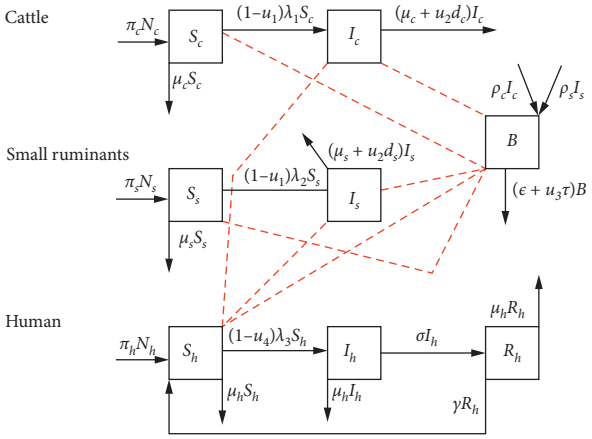

FIGURE 1: A schematic diagram for direct and indirect transmission of brucellosis in cattle, small ruminant, and human populations. Solid arrows represent transfer of individuals from one subpopulation to another while dotted lines represent interactions that lead to infection.

The resulting model is shown as a system of differential equations:

$$
\begin{aligned}
\frac{dS_c}{dt} &= \pi_c N_c - \left((1-u_1(t))\left(\beta_c I_c + \alpha_c B\right) + \mu_c\right) S_c,\\
\frac{dI_c}{dt} &= \left(1-u_1(t)\right)\left(\beta_c I_c + \alpha_c B\right) S_c - \left(\mu_c + u_2(t) d_c\right) I_c,\\
\frac{dS_s}{dt} &= \pi_s N_s - \left((1-u_1(t))\left(\beta_s I_s + \alpha_s B\right) + \mu_s\right) S_s,\\
\frac{dI_s}{dt} &= \left(1-u_1(t)\right)\left(\beta_s I_s + \alpha_s B\right) S_s - \left(\mu_s + u_2(t) d_s\right) I_s,\\
\frac{dS_h}{dt} &= \pi_h N_h + \gamma R_h - \left((1-u_4(t))\left(\beta_{hc}(t) I_c + \beta_{hs} I_s\right.\right.\\
&\quad \left.\left. + \beta_{hh}(t) I_h + \alpha_h B\right) + \mu_h\right) S_h,\\
\frac{dI_h}{dt} &= \left(1-u_4(t)\right)\left(\beta_{hc} I_c + \beta_{hs} I_s + \beta_{hh} I_h + \alpha_h B\right) S_h\\
&\quad - \left(\sigma + \mu_h + d_h\right) I_h,\\
\frac{dR_h}{dt} &= \sigma I_h - \left(\gamma + \mu_h\right) R_h,\\
\frac{dB}{dt} &= \rho_c I_c + \rho_s I_s - \left(\epsilon + u_3(t)\tau\right) B.
\end{aligned}
\tag{1}
$$

3. Model Properties

3.1. Invariant Region. In this section, we investigate whether model variables have biological interpretation and have a unique bounded solution that exists for all the time. That is solutions of model system (1) with nonnegative initial data remain nonnegative for all time $t \geq 0$. We apply the approach

Table 1: Model variables.

Variable	Description
$S_h(t)$	Number of susceptible humans at time t
$I_h(t)$	Number of infected human at time t
$R_h(t)$	Number of recovered humans at time t
$S_c(t)$	Number of susceptible cattle at time t
$I_c(t)$	Number of infected cattle at time t
$S_s(t)$	Number of susceptible small ruminants at time t
$I_s(t)$	Number of infected small ruminants at time t
$B(t)$	Number of *Brucella* bacteria load per unit volume in the environment at time t

Table 2: Model parameters used in the model and their description.

Parameter	Description
π_c	Per capita cattle birth rate
π_h	Per capita human birth rate
σ	Human recovery rate
μ_h	Per capita human natural death rate
β_c	Within cattle transmission rate
α_c	*Brucella* from the environment to cattle transmission rate
α_s	*Brucella* from the environment to small ruminant transmission rate
α_h	*Brucella* from the environment to human transmission rate
β_{ch}	Cattle to human transmission rate
β_{sh}	Small ruminants to human transmission rate
π_s	Small ruminants per capita birth rate
β_s	Within small ruminant transmission rate
μ_s	Per capita small ruminant natural death rate
τ	Environmental hygiene and sanitation rate
ε	Decaying rate of *Brucella* in the environment
d_c	Culling rate of seropositive cattle
d_s	Culling rate of seropositive small ruminants

in [27, 28] to the optimal control model (1). Model system (1) can be expressed in the compact form as follows:

$$\frac{dX}{dt} = MX + F, \tag{2}$$

where

$$M = \begin{bmatrix} -d_0 & 0 & 0 & 0 & 0 & 0 & 0 & 0 \\ (1-u_1)\lambda_1 & -d_3 & 0 & 0 & 0 & 0 & 0 & 0 \\ 0 & 0 & -d_1 & 0 & 0 & 0 & 0 & 0 \\ 0 & 0 & (1-u_1)\lambda_2 & -d_4 & 0 & 0 & 0 & 0 \\ 0 & 0 & 0 & 0 & -d_2 & -(\mu_s + u_2 d_s) & 0 & 0 \\ 0 & 0 & 0 & 0 & (1-u_4)\lambda_3 & -(\sigma + \mu_h + d_h) & 0 & 0 \\ 0 & 0 & 0 & 0 & 0 & \sigma & -(\gamma + \mu_h) & 0 \\ 0 & \rho_c & 0 & \rho_s & 0 & 0 & 0 & -(\varepsilon + u_3\tau) \end{bmatrix}, \tag{3}$$

with

$$\begin{aligned} d_0 &= ((1-u_1)\lambda_1 + \mu_c),\\ d_1 &= ((1-u_1)\lambda_1 + \mu_s),\\ d_2 &= ((1-u_4)\lambda_3 + \mu_h),\\ d_3 &= (\mu_c + u_2 d_c),\\ d_4 &= (\mu_s + u_2 d_s),\\ X &= (S_c, I_c, S_s, I_s, S_h, I_h, R_h, B), \end{aligned} \tag{4}$$

and F is a column vector given by

$$F = \left(\pi_c N_c^0, 0, \pi_s N_s^0, 0, \pi_h N_h^0, 0, 0, 0\right)^T. \tag{5}$$

It can be noticed that MX is Meltzer matrix since all of its off-diagonal entries are nonnegative, for all $X \in \mathbb{R}_+^8$. Therefore, using the fact that $F > 0$, the model system (1) is positively invariant in $\mathbb{R}_+^8$, which means that an arbitrary trajectory of the system starting in $\mathbb{R}_+^8$ remains in $\mathbb{R}_+^8$ forever. In addition, the right hand F is Lipschitz continuous. Thus, a unique maximal solution exists and so

$$\Omega = \{(S_c, I_c, S_s, I_s, S_h, I_h, R_h, B) \geq 0\} \in \mathbb{R}_+^8, \tag{6}$$

is the feasible region for model (1). Thus, model (1) is epidemiologically and mathematically well posed in the region Ω.

4. Model Analysis

4.1. Disease Free Equilibrium. The Brucellosis free equilibrium point E^0 for the constant controls case was computed by setting the right-hand side of equations in model system (1) to zero, and it was found to be

$$E^0 = \left(S_c^0, 0, S_s^0, 0, S_h^0, 0, 0, 0\right), \tag{7}$$

where

$$\begin{aligned} S_c^0 &= \frac{\pi_c N_c^0}{\mu_c},\\ S_s^0 &= \frac{\pi_s N_s^0}{\mu_s},\\ S_h^0 &= \frac{\pi_h N_h^0}{\mu_h}. \end{aligned} \tag{8}$$

4.2. The Effective Reproduction Number. Computation of the effective reproduction number R_e for model system (1) using the standard method of the next generation matrix developed by Diekmann et al. [34, 35] is carried out in this section. R_e is defined as the measure of average number of infections caused by a single infectious individual introduced in a community in which intervention strategies are administered [36]. When there are no interventions or controls, the number of secondary infections caused by typical infected individual during his entire period of infectiousness is called basic reproduction number, R_0. Upon computation, the effective reproduction number was found to be

$$R_e = \max\left\{\frac{R_{11} + R_{22} + \sqrt{(R_{22} - R_{11})^2 + 4R_{12}R_{21}}}{2}, \frac{(1-u_4)\beta_{hh}\pi_h N_h^0}{\mu_h(\sigma + \mu_h + d_h)}\right\}, \tag{9}$$

where

$$\begin{aligned} R_{11} &= \frac{((1-u_1)(\varepsilon + u_3\tau)\beta_c + \alpha_c\rho_c)\pi_c N_c^0}{\mu_c(\mu_c + u_2 d_c)(\varepsilon + u_3\tau)},\\ R_{12} &= \frac{\alpha_c\rho_s\pi_c N_c^0}{\mu_c(\mu_s + u_2 d_s)(\varepsilon + u_3\tau)},\\ R_{22} &= \frac{((1-u_1)(\varepsilon + u_2\tau)\beta_s + \alpha_s\rho_s)\pi_s N_s^0}{\mu_s(\mu_s + u_2 d_s)(\varepsilon + u_3\tau)},\\ R_{21} &= \frac{\alpha_s\rho_c\pi_s N_s^0}{\mu_s(\mu_c + u_2 d_c)(\varepsilon + u_3\tau)}. \end{aligned} \tag{10}$$

The first and the second expressions of equation (9) represent, respectively, the effective reproduction numbers in the livestock and human populations. When there are no controls ($u_1 = u_2 = u_3 = 0$) for the disease in both human population and livestock, the effective reproduction is reduced to the basic reproduction number given by

$$R_0 = \max\left\{\frac{R_{11}^0 + R_{22}^0 + \sqrt{(R_{22}^0 - R_{11}^0)^2 + 4R_{12}^0R_{21}^0}}{2}, \frac{\beta_{hh}\pi_h N_h^0}{\mu_h(\mu_h + d_h)}\right\}, \tag{11}$$

where

$$\begin{aligned} R_{11}^0 &= \frac{(\varepsilon\beta_c + \alpha_c\rho_c)\pi_c N_c^0}{\mu_c^2\varepsilon},\\ R_{12}^0 &= \frac{\alpha_c\rho_s\pi_c N_c^0}{\mu_c\mu_s\varepsilon},\\ R_{22}^0 &= \frac{(\varepsilon\beta_s + \alpha_s\rho_s)\pi_s N_s^0}{\mu_s^2\varepsilon},\\ R_{21}^0 &= \frac{\alpha_s\rho_c\pi_s N_s^0}{\mu_s\mu_c\varepsilon}, \end{aligned} \tag{12}$$

as in [27, 28]. Based on the fact that human-to-human transmission is less than within livestock transmission [37–42] and that environmental contamination by humans is negligible, the effective reproduction number and basic reproductive number are, respectively, given by

$$R_e = \frac{R_{11} + R_{22} + \sqrt{(R_{22} - R_{11})^2 + 4R_{12}R_{21}}}{2}, \tag{13}$$

and

$$R_0 = \frac{R_{11}^0 + R_{22}^0 + \sqrt{\left(R_{22}^0 - R_{11}^0\right)^2 + 4R_{12}^0 R_{21}^0}}{2}. \quad (14)$$

The numerical simulations for the comparison between effective or control reproductive number and basic reproductive number with respect to variations in some parameters are illustrated in Figures 2 and 3. Parameter values used for the simulations are presented in Table 3.

Figure 2 shows that both R_0 and R_e increases with the increase in effective contact rate between livestock (direct transmission). For instance, when within cattle effective contact rate β_c is 0.3, the control reproduction number and basic reproduction are, respectively, 0.3 and 1.4. On the contrary, if the within small ruminants effective contact rate β_s is 0.3, R_0 and R_e are 1.2 and 0.25, respectively.

Similarly, Figure 3 shows that both R_0 and R_e increases with the increase in consumption rate of *Brucella* from the contaminated environment by livestock (indirect transmission). In particular, when *Brucella* consumption rate by cattle α_c is 0.3, R_0 and R_e are, respectively, 0.1 and 1.1. On the contrary, if the small ruminants consumption rate of *Brucella* from the environment α_s is 0.3, R_0 and R_e are 2 and 1.1, respectively. More importantly, Figure 3(b) reveals that $\alpha_s > 0.3$ leads to $R_e > 1$ (disease persistence) and that small ruminants are more susceptible to the contaminated environment than cattle. The possible reasons include small ruminant density and herd turnover due to births and introduction of new animals, as pointed in [43].

Generally, the controls u_1, u_2, and u_3 have high impact on R_e by keeping it always less than R_0.

4.3. Local Stability of the Equilibria. In this section, the trace-determinant method is employed to investigate the local stability of the Brucellosis free equilibrium point for the model system (1).

Theorem 1. *The disease-free equilibrium for the Brucellosis model system (1) is locally asymptotically stable if* $R_0 < 1$ *and unstable if* $R_0 > 1$.

Proof. We show that the variational matrix $J(E_0)$ of the brucellosis free model system has a negative trace and positive determinant. The Jacobian matrix for system (1) is given by

$$J(E_0) = \begin{bmatrix} -(1-u_1)\mu_c & -(1-u_1)\beta_c S_c^0 & 0 & 0 & 0 & 0 & 0 & -a \\ 0 & -a_1 & 0 & 0 & 0 & 0 & 0 & a \\ 0 & 0 & -a_2 & -a_3 & 0 & 0 & 0 & -b \\ 0 & 0 & 0 & b_1 & 0 & 0 & 0 & b \\ 0 & -(1-u_4)\beta_{hc} S_h^0 & 0 & -b_2 & -b_3 & -b_4 & \gamma & -c \\ 0 & (1-u_4)\beta_{hc} S_h^0 & 0 & b_2 & 0 & c_1 & 0 & c \\ 0 & 0 & 0 & 0 & 0 & \sigma & -(\gamma+\mu_h) & 0 \\ 0 & \rho_c & 0 & \rho_s & 0 & 0 & 0 & -r \end{bmatrix}, \quad (15)$$

where

$$\begin{aligned} a &= (1-u_1)\alpha_c S_c^0, \\ a_1 &= (1-u_1)\beta_c S_c^0 - (\mu_c + u_2 d_c), \\ a_2 &= (1-u_1)\mu_s, \\ a_3 &= (1-u_1)\beta_s S_s^0, \\ b &= (1-u_1)\alpha_s S_s^0, \\ b_1 &= (1-u_1)\beta_s S_s^0 - (\mu_s + u_2 d_s), \\ b_2 &= (1-u_4)\beta_{hs} S_h^0, \\ b_3 &= (1-u_4)\mu_h, \\ b_4 &= (1-u_4)\beta_{hh} S_h^0, \\ c_1 &= \beta_{hh} S_h^0 - (\sigma + \mu_h + d_h), \\ r &= (\varepsilon + u_3\tau). \end{aligned} \quad (16)$$

Direct computation of the Jacobian matrix $J(E_0)$ gives

$$\begin{aligned} Tr(J(E_0)) = &-(\mu_c + u_2 d_c)\left(1 - \frac{(1-u_1)\beta_c S_c^0}{\mu_c + u_2 d_c}\right) \\ &- (\mu_s + u_2 d_s)\left(1 - \frac{(1-u_1)\beta_s S_s^0}{\mu_s + u_2 d_s}\right) \\ &- (\sigma + \mu_h + d_h)\left(1 - \frac{(1-u_4)\beta_{hh} S_h^0}{\sigma + \mu_h + d_h}\right) \\ &- \left((1-u_1)(\mu_c + \mu_s) + (1-u_4)\mu_h\right) \\ &- (\gamma + \mu_h + \varepsilon + u_3\tau). \end{aligned} \quad (17)$$

Thus, the trace of the Jacobian matrix is less than zero, that is, $Tr(J(E_0)) < 0$ if

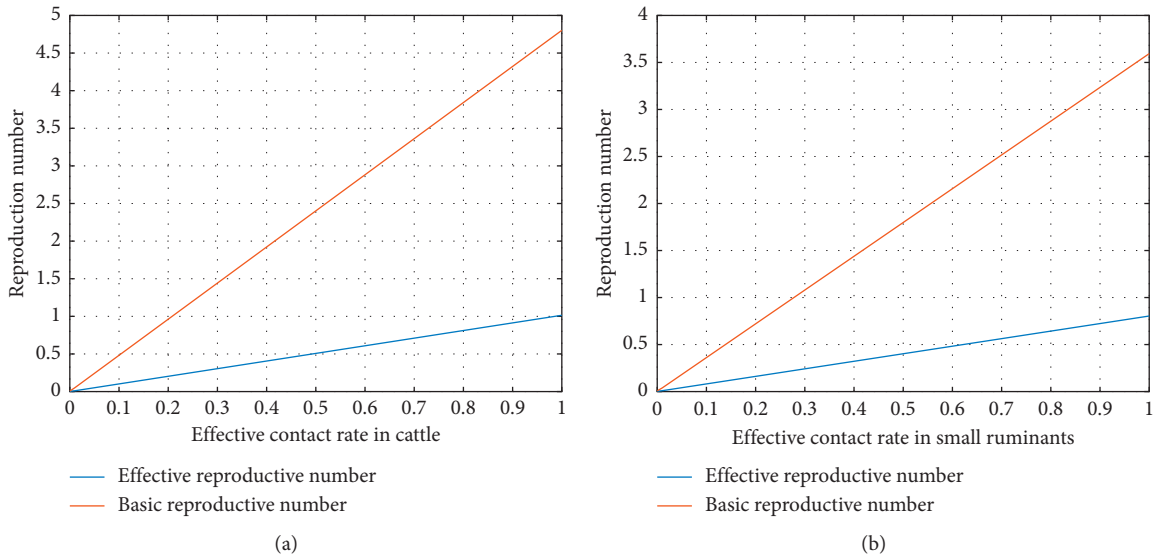

Figure 2: Variations in the reproduction number with respect to changes in effective contact rate in livestock.

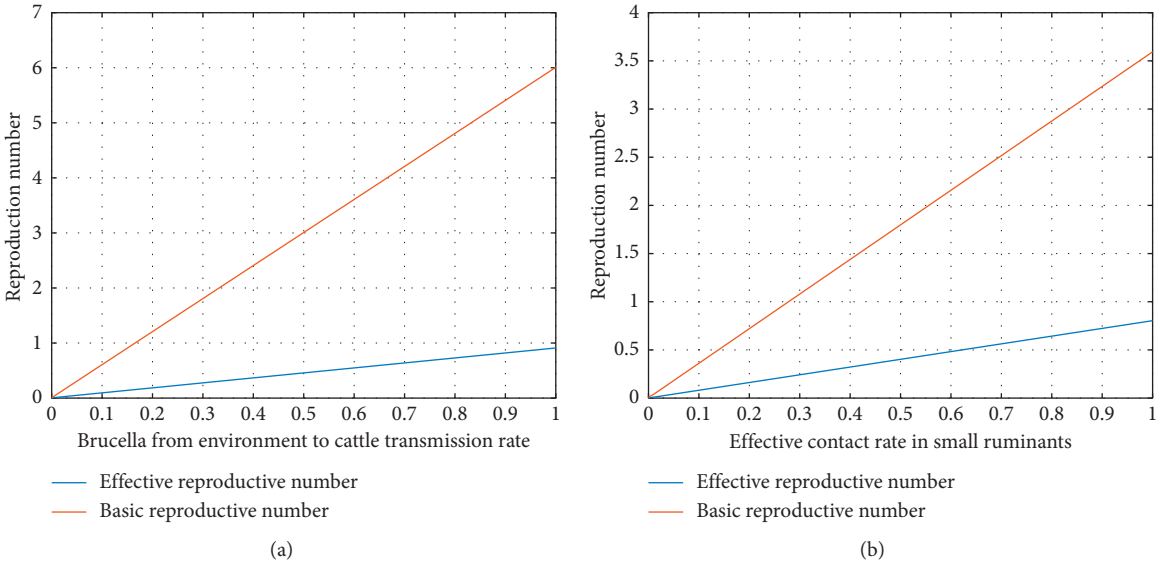

Figure 3: Variations in the reproduction number with respect to changes of the consumption rate of *Brucella* from the environment by livestock.

$$\frac{(1-u_1)\beta_c S_c^0}{\mu_c + u_2 d_c} < 1,$$
$$\frac{(1-u_1)\beta_s S_s^0}{\mu_c + u_2 d_s} < 1, \tag{18}$$
$$\frac{(1-u_4)\beta_{hh} S_h^0}{\sigma + \mu_h + d_h} < 1.$$

On the contrary, the determinant of matrix $J(E_0)$ is computed using Maple 16 Software and was found to be

$$\begin{aligned}\mathrm{Det}\left(J(E_0)\right) = {} & Q_0(1-R_h)\left(Q_1(1-R_c) + (\mu_s + u_2 d_s)\right. \\ & \left. \cdot (1-R_s)(Q_2 + Q_3(1-R_c))\right),\end{aligned} \tag{19}$$

where

Table 3: Model parameter values.

Parameter	Value	Unit
π_c	0.3	year^{-1}
β_c	0.0011	year^{-1}
μ_c	0.25	year^{-1}
d_c	0.35	year^{-1}
α_c	0.00035	year^{-1}
ρ_c	10	year^{-1}
ϵ	8	year^{-1}
τ	12	year^{-1}
π_s	0.4	year^{-1}
β_s	0.001	year^{-1}
μ_s	0.35	year^{-1}
d_s	0.4	year^{-1}
α_s	0.00032	year^{-1}
ρ_s	15	year^{-1}

$$R_h = \frac{(1-u_4)\beta_{hh}S_h^0}{\sigma+\mu_h+d_h},$$

$$R_s = \frac{(1-u_1)\beta_s S_s^0}{\mu_s+u_2 d_s},$$

$$R_c = \frac{(1-u_1)\beta_c S_c^0}{\mu_c+u_2 d_c},$$

$$Q_0 = (1-u_1)^2(1-u_4)(\gamma+\mu_h)(\sigma+\mu_h+d_h)\mu_c\mu_s\mu_h,$$

$$Q_1 = (1-u_1)(\mu_c+u_2 d_c)\alpha_s\rho_s S_s^0,$$

$$Q_2 = (1-u_1)\alpha_c\rho_c S_c^0,$$

$$Q_3 = (\varepsilon+u_3\tau)(\mu_c+u_2 d_c). \tag{20}$$

It follows that $\mathrm{Det}(J(E_0)) > 0$ if $R_h < 1$, $R_c < 1$, and $R_s < 1$. Thus, the Brucellosis free equilibrium for model system (1) is locally asymptotically stable if $R_h < 1$, $R_c < 1$, and $R_s < 1$. Local stability of the Brucellosis free equilibrium suggests local stability of the endemic equilibrium for the reverse condition [28]. □

5. Optimal Control

To investigate the optimal level of efforts that would be required to control brucellosis infections, we first formulate the objective function J to be minimized subject to the number of ruminants and human infections and cost of applying the controls:

$$J = \int_0^{t_f}\left(A_1 I_c + A_2 I_s + A_3 B + A_4 I_h + \frac{B_1 u_1^2}{2} + \frac{B_2 u_2^2}{2} + \frac{B_3 u_3^2}{2} + \frac{B_4 u_4^2}{2}\right)\mathrm{d}t, \tag{21}$$

where A_1, A_2, A_3, and A_4 are positive weight constants of infected cattle, infected small ruminants, *Brucella* in the environment, and infected human classes, respectively. Furthermore, the constants B_1, B_2, B_3, and B_4 are positive weights which balance the cost factors associated with control strategies u_1, u_2, u_3, and u_4, respectively. More importantly, the cost of each control strategy is assumed to be nonlinear and takes the quadratic form that is $B_1 u_1^2/2$ is the cost of control strategy associated with vaccination of ruminants, $B_2 u_2^2/2$ is the cost associated with gradual culling of seropositive animals strategy, $B_3 u_3^2/2$ is the cost associated with environmental hygiene and sanitation, and $B_4 u_4^2/2$ is the cost associated with personal protections in humans.

With the objective function $J(u_1, u_2, u_3, u_4)$, our goal is to minimize the number of infected ruminants and humans, while minimizing the cost of controls, $u_1(t), u_2(t), u_3(t)$, and $u_4(t)$. We seek an optimal control $u_1^*(t), u_2^*(t), u_3^*(t)$, and $u_4^*(t)$ such that

$$J(u_1^*, u_2^*, u_3^*, u_4^*) = \min\left\{J(u_1, u_2, u_3, u_4) \,\middle|\, u_1, u_2, u_3, u_4 \in u\right\}, \tag{22}$$

where $u = \{u_1, u_2, u_3, u_4\}$ such that u_1, u_2, u_3, and u_4 are measurable with $0 \le u_1 \le 1$, $0 \le u_2 \le 1$, $0 \le u_3 \le 1$, and $0 \le u_4 \le 1$, for $t \in [0, t_f]$ is the control set.

6. Existence of an Optimal Control

Theorem 2. *There exists an optimal control set $(u_1^*, u_2^*, u_3^*, u_4^*) \in u$ with corresponding nonnegative states $(S_c, I_c, S_s, I_s, S_h, I_h, R_h)$ that minimize the objective functional $J(u_1(t), u_2(t), u_3(t), u_4(t))$.*

Proof. The positivity and uniform boundedness of the state variables as well as the controls on $[0, t_f]$ entail the existence of a minimizing sequence:

$$J(u_1^n(t), u_2^n(t), u_3^n(t), u_4^n(t)), \tag{23}$$

such that

$$\lim_{n\longrightarrow\infty} J(u_1^n(t), u_2^n(t), u_3^n(t), u_4^n(t)) = \inf_{(u_1^n(t), u_2^n(t), u_3^n(t), u_4^n(t))\in u} J(u_1^n(t), u_2^n(t), u_3^n(t), u_4^n(t)). \tag{24}$$

The boundedness of all the state and control variables implies that all the derivatives of the state variables are also bounded. If the corresponding sequence of state variables is denoted by $(S_c, I_c, S_s, I_s, S_h, I_h, R_h, B)$, then all state variables are Lipschitz continuous with the same Lipschitz constant. This implies that the sequence $(S_c, I_c, S_s, I_s, S_h, I_h, R_h)$ is uniformly equicontinuous in $[0, t_f]$. Following the approach in [44], the state sequence has a subsequence that converges uniformly to $(S_c, I_c, S_s, I_s, S_h, I_h, R_h, B)$ in $[0, t_f]$. In addition, we can establish that the control sequence $u^n = (S_c^n, I_c^n, S_s^n, I_s^n, S_h^n, I_h^n, R_h^n, B^n)$ has a subsequence that converges weakly in $L^2(0, t_f)$. Let $(u_1^*, u_2^*, u_3^*, u_4^*) \in u$ be such that $u_i^n \longrightarrow u_i^*$ weakly in $L^2(0, t_f)$ for $i = 1, 2, 3, 4$. Applying the lower semicontinuity of norms in weak L^2, we have

$$\left\|u_i^*\right\|_{L^2}^2 \leq \lim_{n\longrightarrow\infty} \inf \left\|u_i^n(t)\right\|_{L^2}^2, \quad i = 1,2,3,4. \tag{25}$$

This means that

$$J\left(u_1^*, u_2^*, u_3^*, u_4^*\right) \leq \lim_{n\longrightarrow\infty} \int_0^{t_f} \left(A_1 I_c^n + A_2 I_s^2 + A_3 I_h^n + A_4 B_4^n + \frac{B_1 u_1^n}{2} + \frac{B_2 u_2^n}{2} + \frac{B_3 u_3^n}{2} + \frac{B_4 u_4^n}{2}\right) \mathrm{d}t. \tag{26}$$

Thus, there exists a set of controls $(u_1^*, u_2^*, u_3^*, u_4^*)$ that minimizes our objective functional $J(u_1, u_2, u_3, u_4)$. □

7. Characterization of Optimal Control

In this section, we derive necessary conditions for an optimal control and formulate an optimality system that characterizes the optimal control using upper and lower bound technique. The necessary condition is that an optimal control problem must satisfy Pontryagin's maximum principle [45]. The principle converts system (1) and equation (21) into a problem of minimizing pointwise a Hamiltonian H, with respect to u_1, u_2, u_3, and u_4 defined by

$$\begin{aligned} H = {} & A_1 I_c + A_2 I_s + A_3 B + A_4 I_h + \frac{B_1 u_1^2}{2} + \frac{B_2 u_2^2}{2} + \frac{B_3 u_3^2}{2} + \frac{B_4 u_4^2}{2} \\ & + \lambda_{S_c}\left(\pi_c N_c - \left(\left(1-u_1\right)\left(\beta_c I_c + \alpha_c B\right) + \mu_c\right) S_c\right) \\ & + \lambda_{I_c}\left(\left(1-u_1\right)\left(\beta_c I_c + \alpha_c B\right) S_c - \left(\mu_c + u_2\right) I_c\right) \\ & + \lambda_{S_s}\left(\pi_s N_s - \left(\left(1-u_1\right)\left(\beta_s I_s + \alpha_s B\right) + \mu_s\right) S_s\right) \\ & + \lambda_{I_s}\left(\left(1-u_1\right)\left(\beta_s I_s + \alpha_s B\right) S_s - \left(\mu_s + u_2\right) I_s\right) \\ & + \lambda_B\left(\rho_c I_c + \rho_s I_s - \left(\varepsilon + u_3\tau\right) B\right) \\ & + \lambda_{S_h}\left(\pi_h N_h + \gamma R_h - \left(\left(1-u_4\right)\right.\right. \\ & \left.\left. \cdot \left(\beta_{hc} I_c + \beta_{hs} I_s + \beta_{hh} I_h + \alpha_h B\right) + \mu_h\right) S_h\right) \\ & + \lambda_{I_h}\left(\left(1-u_4\right)\left(\beta_{hc} I_c + \beta_{hs} I_s + \beta_{hh} I_h + \alpha_h B\right) S_h\right. \\ & \left. -\left(\sigma + \mu_h + d_h\right) I_h\right) \\ & + \lambda_{R_h}\left(\sigma I_h - \left(\gamma + \mu_h + d_h\right) R_h\right), \end{aligned} \tag{27}$$

where $\lambda_{S_c}, \lambda_{I_c}, \lambda_{S_s}, \lambda_{I_s}, \lambda_B, \lambda_{S_h}, \lambda_{I_h}$, and λ_{R_h} are the adjoint or costate variables.

Applying Pontryagin's maximum principle [45] and the existence result for the optimal control [46], we obtain the following.

Theorem 3. *For optimal tetra controls u_1^*, u_2^*, u_3^*, and u_4^* that minimizes $J(u_1, u_2, u_3, u_4)$ over u, there exist adjoint variables $\lambda_{S_c}, \lambda_{I_c}, \lambda_{S_s}, \lambda_{I_s}, \lambda_B, \lambda_{S_h}, \lambda_{I_h}$, and λ_{R_h}, satisfying*

$$\begin{aligned} \frac{\mathrm{d}\lambda_{S_c}}{\mathrm{d}t} &= \left(1-u_1\right)\left(\beta_c I_c + \alpha_c B\right)\left(\lambda_{S_c} - \lambda_{I_c}\right) + \mu_c \lambda_{S_c}, \\ \frac{\mathrm{d}\lambda_{I_c}}{\mathrm{d}t} &= -A_1 + \left(1-u_1\right)\left(\lambda_{S_c} - \lambda_{I_c}\right)\beta_c S_c + \lambda_{I_c}\left(\mu_c + u_2 d_c\right) \\ &\quad + \left(1-u_4\right)\left(\lambda_{S_h} - \lambda_{I_h}\right)\beta_{hc} S_h - \rho_c \lambda_B, \\ \frac{\mathrm{d}\lambda_{S_s}}{\mathrm{d}t} &= \left(1-u_1\right)\left(\beta_s I_s + \alpha_s B\right)\left(\lambda_{S_s} - \lambda_{I_s}\right) + \mu_s \lambda_{S_s}, \\ \frac{\mathrm{d}\lambda_{I_s}}{\mathrm{d}t} &= -A_2 + \left(1-u_1\right)\left(\lambda_{S_s} - \lambda_{I_s}\right)\beta_s S_s + \lambda_{I_s}\left(\mu_s + u_2 d_s\right) \\ &\quad + \left(1-u_4\right)\left(\lambda_{S_h} - \lambda_{I_h}\right)\beta_{hs} S_h - \lambda_B \rho_s, \\ \frac{\mathrm{d}\lambda_{S_h}}{\mathrm{d}t} &= \left(1-u_4\right)\left(\beta_{hc} I_c + \beta_{hs} I_s + \beta_{hh} I_h + \alpha_h B\right)\left(\lambda_{S_h} - \lambda_{I_h}\right) \\ &\quad + \mu_h \lambda_{S_h}, \\ \frac{\mathrm{d}\lambda_{I_h}}{\mathrm{d}t} &= -A_4 + \left(1-u_4\right)\left(\lambda_{S_h} - \lambda_{I_h}\right)\beta_{hh} S_h + \lambda_{I_h}\left(\sigma + \mu_h + d_h\right) \\ &\quad - \sigma \lambda_{R_h}, \\ \frac{\mathrm{d}\lambda_{R_h}}{\mathrm{d}t} &= \gamma\left(\lambda_{R_h} - \lambda_{S_h}\right) + \mu_h \lambda_{R_h}, \\ \frac{\mathrm{d}\lambda_B}{\mathrm{d}t} &= -A_3 + \left(1-u_1\right)\left(\lambda_{S_c} - \lambda_{I_c}\right)\alpha_c S_c \\ &\quad + \left(1-u_1\right)\left(\lambda_{S_s} - \lambda_{I_s}\right)\alpha_s S_s \\ &\quad + \left(1-u_4\right)\left(\lambda_{S_h} - \lambda_{I_h}\right)\alpha_h S_h + \lambda_B\left(\varepsilon + u_3\tau\right), \end{aligned} \tag{28}$$

with transversality conditions:

$$\lambda_{S_c}\left(t_f\right) = \lambda_{I_c}\left(t_f\right) = \lambda_{S_s}\left(t_f\right) = \lambda_{I_s}\left(t_f\right) = \lambda_B\left(t_f\right) = \lambda_{S_h}\left(t_f\right) = \lambda_{I_h}\left(t_f\right) = \lambda_{R_h}\left(t_f\right) = 0. \tag{29}$$

The following characterization holds on the interior of the control set u:

$$
\begin{aligned}
u_1^* &= \max\left\{0,\ \min\left(1, \frac{1}{B_1}\left((\beta_c I_c + \alpha_c B)\left(\lambda_{I_c} - \lambda_{S_c}\right)S_c + (\beta_s I_s + \alpha_s B)\left(\lambda_{I_s} - \lambda_{S_s}\right)S_s\right)\right)\right\},\\
u_2^* &= \max\left\{0,\ \min\left(1, \frac{1}{B_2}\left(d_c I_c \lambda_{I_c} + d_s I_s \lambda_{I_s}\right)S_c\right)\right\},\\
u_3^* &= \max\left\{0,\ \min\left(1, \frac{1}{B_3}\lambda_B B\right)\right\},\\
u_4^* &= \max\left\{0,\ \min\left(1, \frac{1}{B_4}\left(\beta_{hc} I_c + \beta_{hs} I_s + \beta_{hh} I_h + \alpha_h B\right)\left(\lambda_{I_h} - \lambda_{S_h}\right)S_h\right)\right\},
\end{aligned}
\tag{30}
$$

where λ_{S_c}, λ_{I_c}, λ_{S_s}, λ_{I_s}, λ_B, λ_{S_h}, λ_{I_h}, and λ_{R_h} are solutions of equation (29).

Proof. The form of adjoint (or costate) system (28) and transversality conditions (29) are standard results from Pontryagin's Maximum Principle [45]. To obtain the costate system (28), the partial derivatives of the Hamiltonian (H) equation (27) with respect to each state variable are computed as follows:

$$
\begin{aligned}
\frac{d\lambda_{S_c}}{dt} &= -\frac{\partial H}{\partial S_c}, \quad \lambda_{S_c}\left(t_f\right) = 0,\\
&\vdots\\
\frac{d\lambda_{R_h}}{dt} &= -\frac{\partial H}{\partial R_h}, \quad \lambda_{R_h}\left(t_f\right) = 0.
\end{aligned}
\tag{31}
$$

The optimality equation (30) is obtained by finding the partial derivative of the Hamiltonian equation (27) with respect to each control variable and solving for the optimal values of u_i^* where the derivative vanishes. That is, $(\partial H/\partial u_i) = 0$ for $i = 1, 2, 3, 4$.

Solving for u_i^* subject to the constraints gives the characterization equation (30). Next, we discuss the numerical solutions of the optimality system and the corresponding results of varying the optimal controls u_1, u_2, u_3, and u_4, the parameter choices, and the interpretations from various cases. □

8. Numerical Simulations

In this section, we analyze numerically the optimal control strategies for the brucellosis transmission in model system (27). The controls of interest are vaccination of susceptible ruminants, gradual culling of seropositive ruminants, environmental hygiene and sanitation, and personal protection in humans. The optimal control solution is obtained by solving the optimality system which consists of the state system (1) and the adjoint system (28). We start by solving the state equations with a guess for the controls over the simulated time using the fourth-order Runge–Kutta iterative scheme method. The adjoint equations are solved by the backward fourth-order Runge–Kutta scheme using the current iterations solutions of the state equations because of the transversality conditions (31). Furthermore, the controls are updated by using a convex combination of the previous controls and the value from the characterizations (30). This process is repeated and the iterations are stopped if the values of the unknowns at the previous iterations are very close to the ones at the present iteration [47]. Based on the fact that brucellosis is endemic in most of the sub-Saharan Africa countries and that one control cannot stop the disease transmission, we investigate the impacts of combining at least three control strategies in a period of six years. Moreover, the computation of real weights of the objective function is very involving and needs a lot of information. In view of the aforesaid, the weights of the objective function are theoretically chosen to be $A_1 = 15$, $A_2 = 20$, $A_3 = 5$, $A_4 = 10$, $B_1 = 15$, $B_2 = 10$, $B_3 = 10$, and $B_4 = 10$ just to concede the control strategies proposed in this paper, and the parameter values used are in Table 3. The initial state variables are chosen as $S_c(0) = 200, I_c(0) = 10, S_s(0) = 200, I_s(0) = 5, S_h(0) = 50, I_h(0) = 10, R_h(0) = 5$, and $B(0) = 100$.

The parameter values used in our computations are mainly from [3], a literature similar to this work.

8.1. Strategy A: Optimal Vaccination, Gradual Culling, and Environmental Sanitation. Under this strategy, the effectiveness of vaccination of ruminant control u_1, gradual culling of seropositive ruminants u_2, and environmental hygiene and sanitation u_3 are used to minimize the objective function J, whereas personal protection in humans control u_4 is set to zero. Figure 4 illustrates the trends of the infective classes.

Figure 4 shows that combination of the three control strategies leads to eradication of brucellosis from cattle in four years, small ruminants in two years, and humans in between two to three years. In case of no controls, the infective populations grow exponentially.

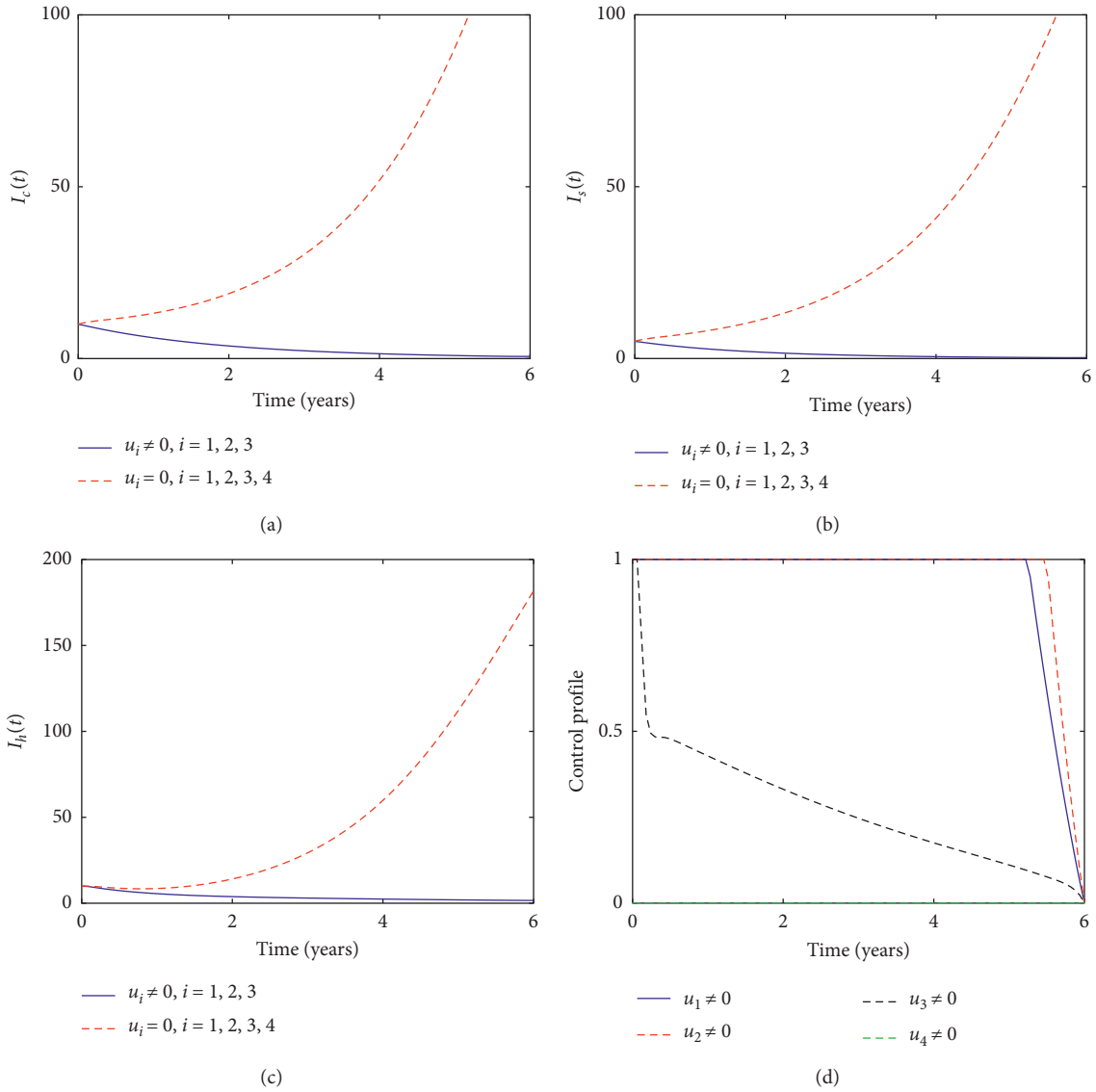

FIGURE 4: Dynamics of brucellosis with optimal vaccination, gradual culling of seropostive ruminants, and environmental hygiene and sanitation.

8.2. Strategy B: Optimal Vaccination, Gradual Culling, and Personal Protection. In this strategy, ruminant vaccination u_1, gradual culling of seropositive ruminants u_2, and personal protection in humans u_4 are used to optimize the objective function J while the environmental hygiene sanitation control u_3 is set to zero. Figure 5 illustrates the variations in the infective classes.

Figure 5 shows that the cattle population attains its disease equilibrium in less than four years, whereas the disease can be eradicated from the small ruminants and humans in less than two years if the combination of the three controls is applied. In case of no control, the infected populations grow exponentially.

8.3. Strategy C: Optimal Vaccination, Environmental Hygiene, and Personal Protection. In this strategy, ruminant vaccination control u_1, environmental sanitation u_3, and personal protection u_4 are used to optimize the objective function J while gradual culling of seropostive ruminants control u_2 is set to zero. Figure 6 illustrates the variations in the seropositive populations.

It can be seen from Figure 6 that the combination of the three control strategies leads to elimination of the infective humans and consequently a disease-free equilibrium is attained within a two years period. Furthermore, the small ruminant population attains its disease-free equilibrium point in five years and that of cattle will attain its equilibrium point in more than six years. In case of no controls, the number of infective individuals increases.

8.4. Strategy D: Optimal Gradual Culling, Environmental Hygiene, and Personal Protection. In this strategy, gradual culling of seropostive ruminants u_2, environmental hygiene and sanitation u_3, and personal protection u_4 are used to

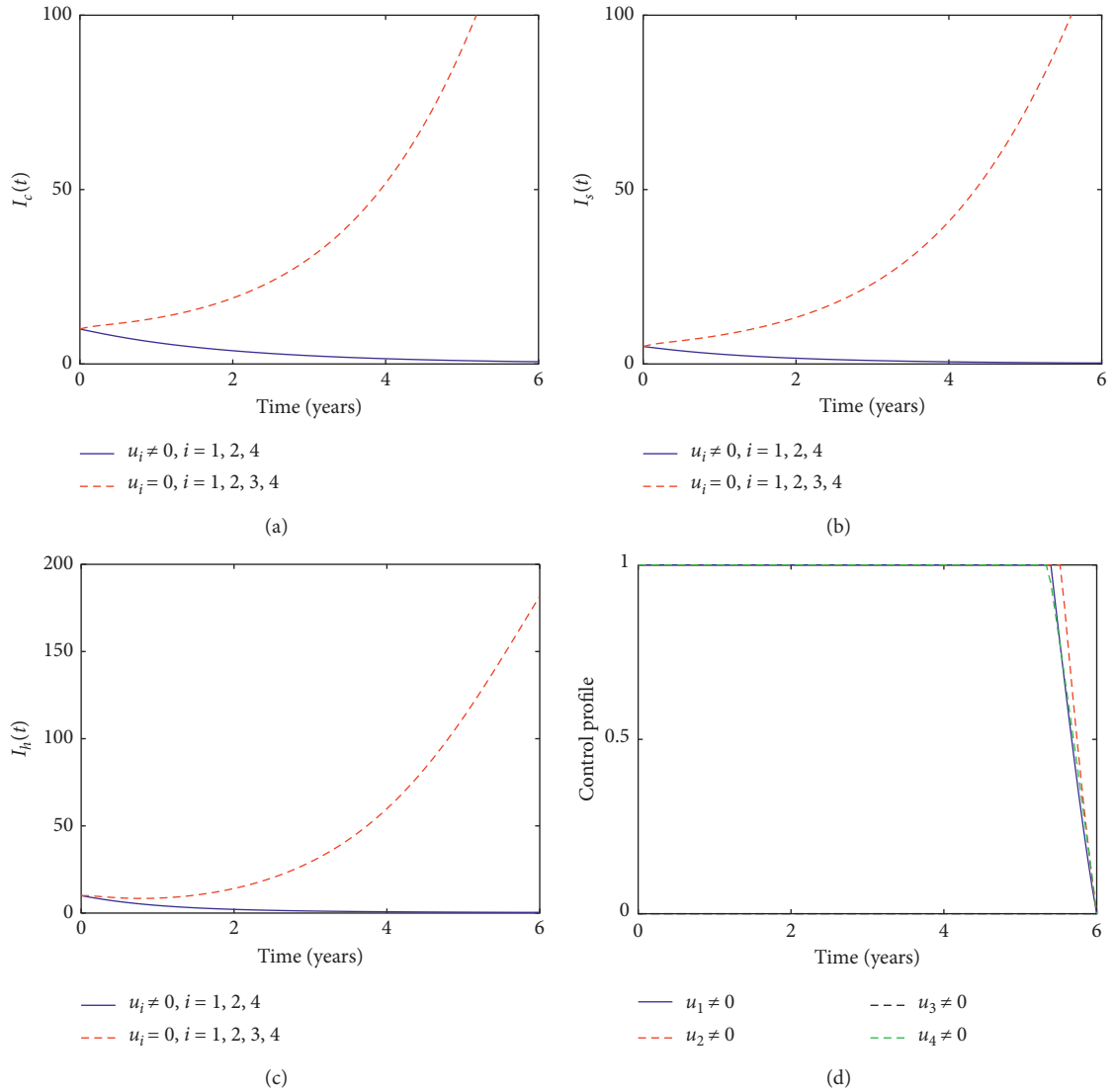

Figure 5: Dynamics of brucellosis with optimal vaccination, gradual culling of seropositive ruminants, and personal protection controls.

minimize the objective function J, whereas ruminants vaccination u_1 is set to zero. Figure 7 illustrates the variations in the seropositive populations.

It can be seen from Figure 7 that optimal implementation of gradual culling of seropostive ruminants, environmental hygiene, and personal protection reduces the number of infected human to zero in a period of less than two years, whereas the infected ruminants does not go to zero in a period of more than six years. This implies that implementation the three interventions under consideration does not make the ruminants population attain their disease-free equilibrium points. Thus, this strategy is not mathematically recommended.

8.5. Strategy E: Optimal Vaccination, Gradual Culling, Environmental Sanitation, and Personal Protection. With this strategy, the combination of the four control strategies under consideration, ruminants vaccination, u_1, gradual culling of seropositive ruminants, u_2, environmental hygiene and sanitation, u_3, and personal protection, u_4, are used to optimize the objective function J. Figure 8 illustrates the variations in the infective populations.

Figure 8 shows that due to the combination of the four control strategies, the number of infected small ruminants and humans decreases to zero in less than two years while that of infective cattle reduces to zero in less than four years. In case of no controls, the number of infective populations grows exponentially.

9. Cost-Effectiveness Analysis

In this section, the cost effectiveness of the control strategies A, B, C, D, and E is analyzed using the Incremental Cost-Effectiveness Ratio (ICER), as described in [48–51]. The choice of the method is based on the fact that it allows the comparison between the cost effectiveness of combination of at least two of the controls. In particular, we compare two

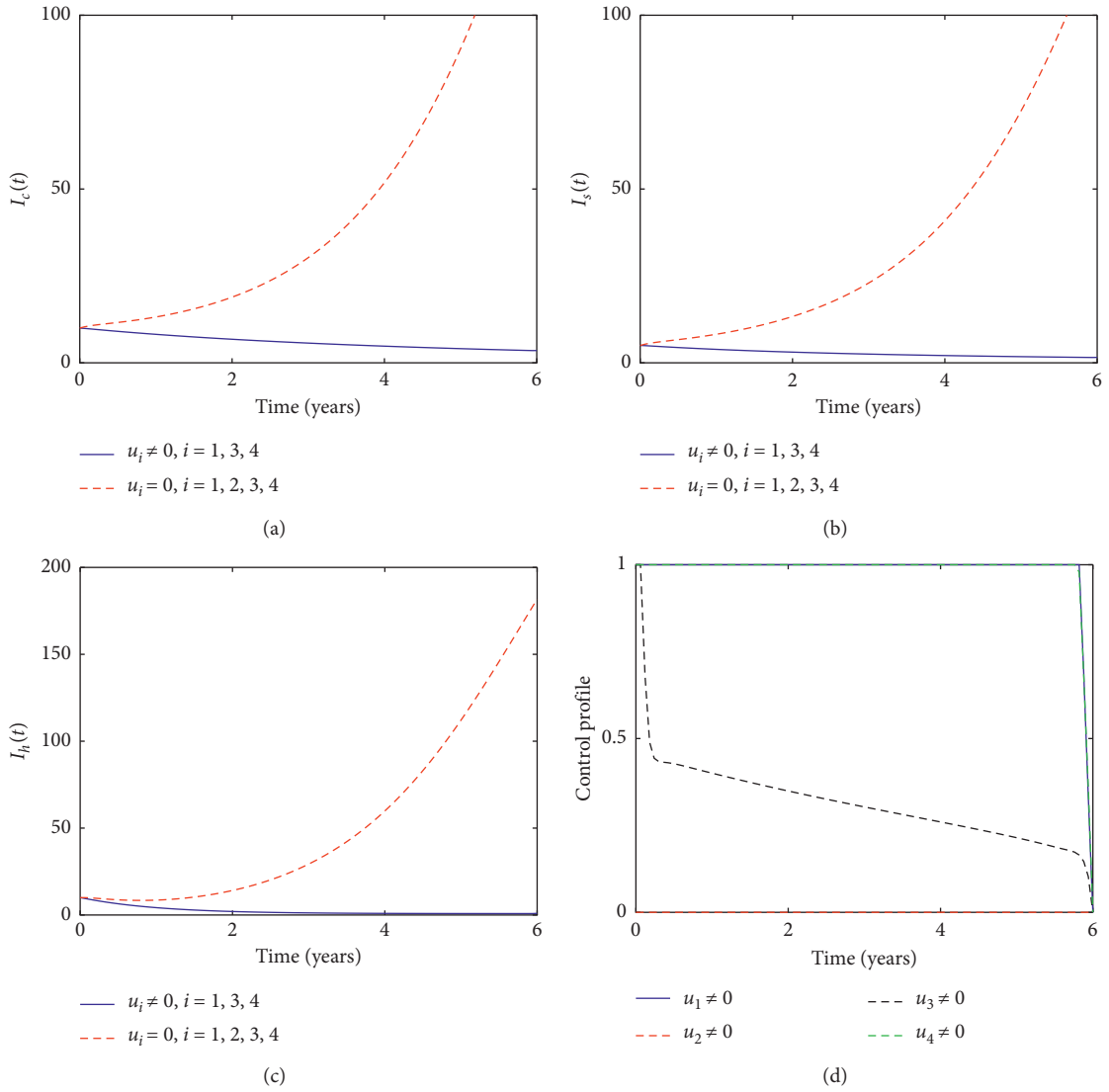

Figure 6: Dynamics of brucellosis with optimal vaccination, environmental hygiene, and personal protection controls.

competing intervention strategies incrementally; one intervention is being compared with the next less-effective alternative. ICER is defined by the difference in cost between two possible interventions divided by the difference in their outcome, given that they compete for the same resource. Mathematically,

$$\text{ICER for } X = \frac{\text{Cost of intervention } X - \text{Cost of intervention } Y}{\text{Effect of intervention } X - \text{Effect of intervention } Y}, \tag{32}$$

where X and Y are the two intervention strategies being compared in this case, and the effect or benefits in health status are measured in terms of quality-adjusted life years (QALYs) gained or lost. In this approach, alternatives that are more expensive and less effective are excluded. Following the numerical simulation results of model (1), we rank the five strategies in order of increasing effectiveness measured as total infections averted and compute the ICER for every two competing strategies, and the results are presented in Table 4.

From Table 4, we see that strategy D is the most expensive and less effective strategy; thus, we exclude it from the set of alternatives so it does not consume limited resources. The recalculated ICER for remaining four alternatives is in Table 5.

Table 5 shows that strategy C is the most expensive and less effective strategy; thus, we exclude it from the set of alternatives so it does not consume limited resources. Table 6 presents the recalculated ICER for remaining three alternatives.

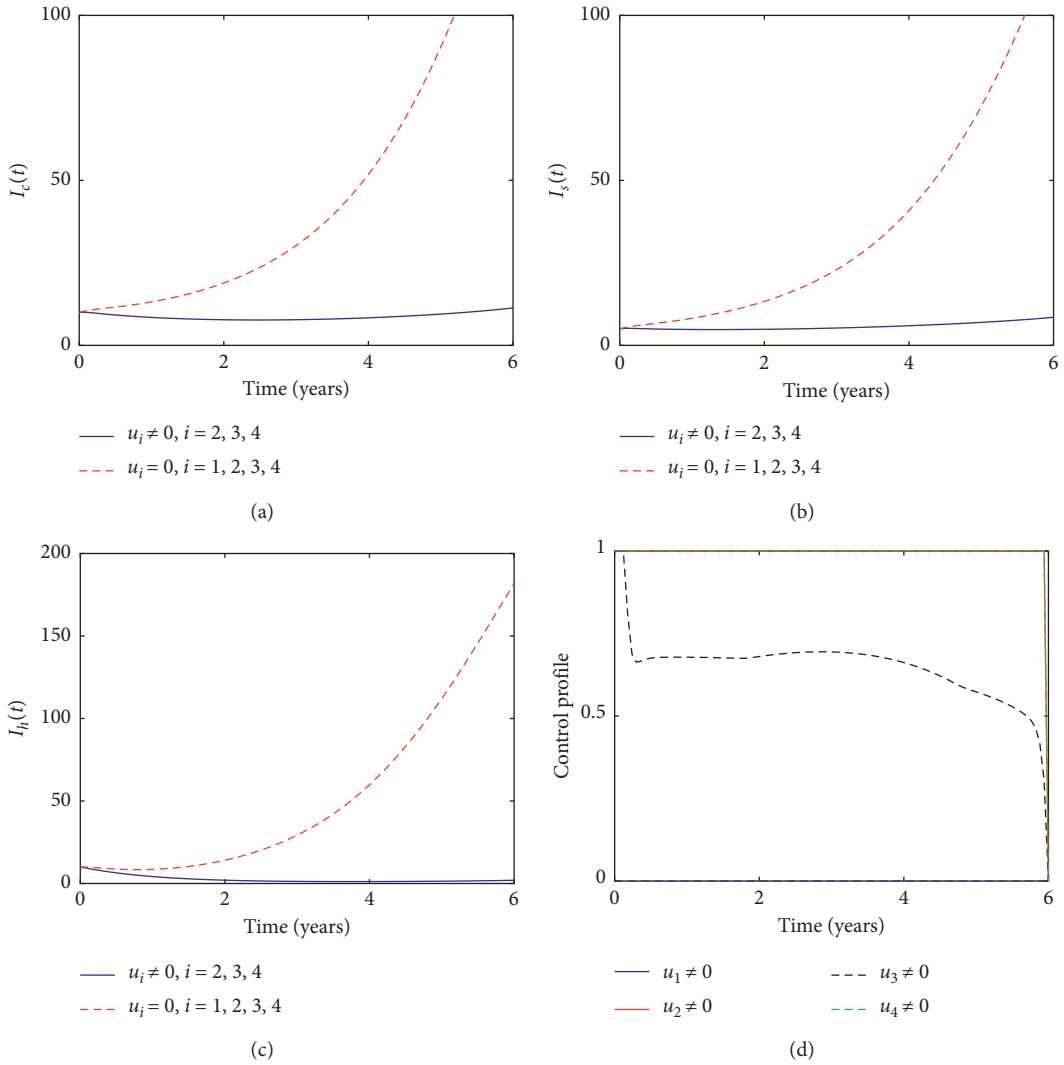

FIGURE 7: Dynamics of brucellosis with optimal gradual culling of seropostive ruminants, environmental sanitation, and personal protection controls.

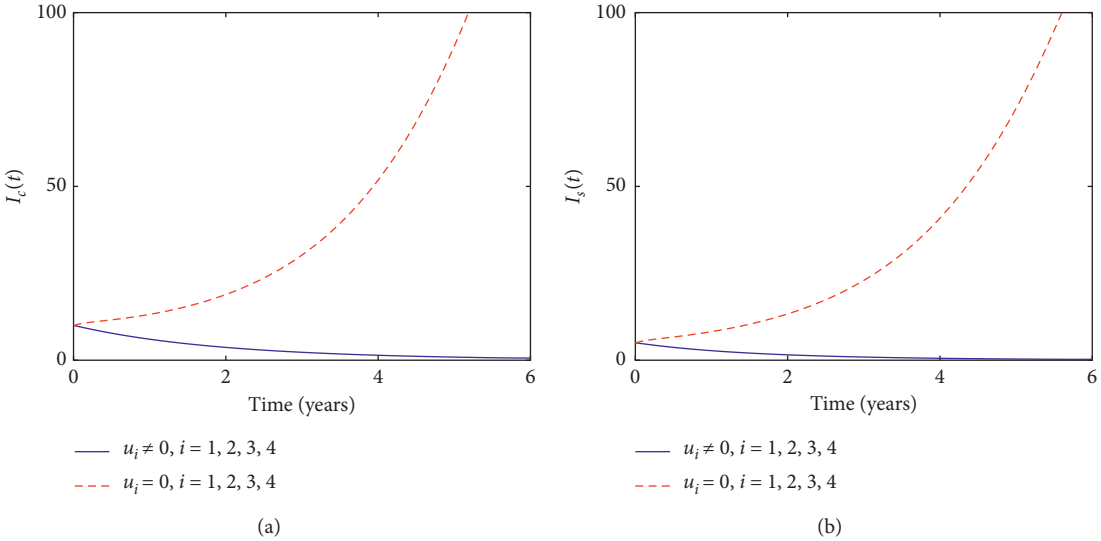

FIGURE 8: Continued.

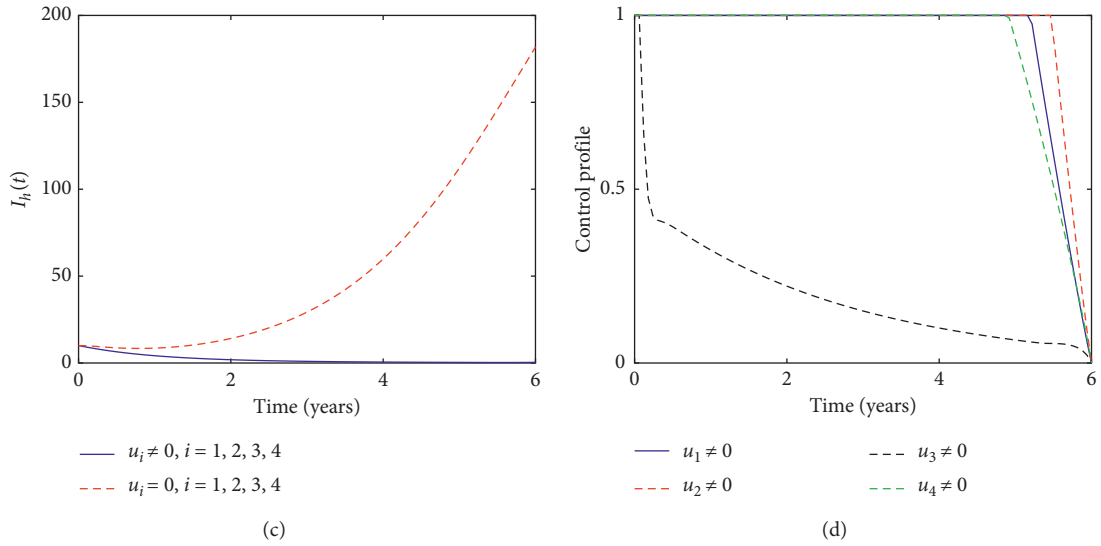

Figure 8: Dynamics of brucellosis with optimal vaccination, gradual culling of seropositive ruminants, environmental sanitation, and personal protection controls.

Table 4: ICER for alternative control strategies A, B, C, D, and E.

Strategy	Total infection averted	Total cost ($)	ICER
Strategy A	12953	4795.7	0.3702
Strategy B	19789	4368	−0.0625
Strategy D	20346	45535	73.9075
Strategy C	21409	13169	−30.4478
Strategy E	24832	4047	−2.6649

Table 5: ICER for alternative control strategies A, B, C, and E.

Strategy	Total infection averted	Total cost ($)	ICER
Strategy A	12953	4795.7	0.3702
Strategy B	19789	4368	−0.0625
Strategy C	21409	13169	5.4324
Strategy E	24832	4047	−2.6649

Table 6: ICER for alternative control strategies A, B, and E.

Strategy	Total infection averted	Total cost ($)	ICER
Strategy A	12953	4795.7	0.3702
Strategy B	19789	4368	−0.0625
Strategy E	24832	4047	−0.0638

The comparison between strategies A and B shows a cost saving of $0.0625 for strategy B over strategy A. The lower ICER for strategy B indicates that strategy A is strongly dominated; that is, strategy A is more costly and less effective than strategy B. Therefore, we exclude strategy A from the set of alternatives so it does not consume limited resources. The recalculated ICER is shown in Table 7.

Moreover, Table 7 shows a cost saving of $0.0638 for strategy E over strategy B. In this case, the incremental cost is

Table 7: ICER for alternative control strategies B and E.

Strategy	Total infection averted	Total cost ($)	ICER
Strategy B	19789	4368	0.2208
Strategy E	24832	4047	−0.0638

negative and the incremental effect is positive (south-east quadrant of the cost-effectiveness plane), and the intervention is unequivocally cost effective (it is dominant, achieving better outcomes at lower cost) [48–50]. The lower ICER for strategy E indicates that strategy B is more costly and less effective than strategy E; in other words, strategy E is more effective and saves money compared with the strategy B. Hence, strategy B is excluded from the set of alternatives so it does not consume limited resources. Thus, strategy E which is the combination of vaccination, gradual culling through slaughter of seropositive cattle and small ruminants, environmental sanitation, and personal protection in humans has the least ICER and therefore is more cost-effective strategy than all alternatives under consideration.

10. Conclusion

This paper aimed at formulating and analyzing a mathematical model for the impacts of different control options to the transmission dynamics of Brucellosis. We focused on livestock vaccination; gradual culling through slaughter of seropositive cattle and small ruminants; environmental hygiene and sanitation; and personal protection in humans. Pontryagin's Maximum Principle approach and incremental cost-effectiveness ratio were, respectively, used to analyze the optimal control problem and the cost effectiveness of the control strategies. Findings in both optimal control and cost-effectiveness analysis revealed that combination of vaccination, gradual culling of seropositive cattle and small ruminants, environmental hygiene, and personal protection in

humans is unequivocally best control strategy as it has high impact with lower cost of controlling the disease. It was revealed further that strategy B which is the combination of vaccination, gradual culling through slaughter of seropositive cattle and small ruminants, and personal protection in humans is the second cost-effective strategy, followed by strategy A which is the combination of vaccination, gradual culling of seropositive cattle and small ruminants, and environmental hygiene. Furthermore, strategy C which is the combination of vaccination of livestock, environmental hygiene, and personal protection in humans is less effective in controlling the disease while strategy D is the least among the alternatives and cannot be recommended for implementation as it has lower impact and higher cost. Critical analysis of the four control options showed that vaccination of susceptible livestock and gradual culling of seropostive cattle and small ruminants are the key parameter for any design of a control option. This paper recommends that, for effective and efficiency brucellosis transmission control, the combination of vaccination, gradual culling of seropositive cattle and small ruminants, environmental hygiene, and personal protection in humans should be adopted.

Data Availability

The data supporting the findings in the article were derived as follows. We used the set of parameter values mainly from Li et al. [3], an article similar to this work, while unavailable data, especially values of parameters, are estimated for the purpose of verifying results of the mathematical analyses of the model developed in the manuscript.

Conflicts of Interest

The authors declare no conflicts of interest regarding the publication of this paper.

Acknowledgments

Authors acknowledge the contributions from One Health and Tanzania Veterinary Association (TVA) for an opportunity to make a presentation in the "First One Health Conference, embedding the 37th TVA Scientific Conference, held on November 27th–29th, 2019, at Arusha International Conference Centre, Arusha-Tanzania" for comments that led to improvement of this work.

References

[1] WHO, "Brucellosis in humans and animals," 2018, http://www.who.int/csr/resources/publications/Brucellosis.pdf.

[2] F. P. Poester, L. E. Samartino, and R. L. Santos, "Pathogenesis and pathobiology of brucellosis in livestock," *Revue Scientifique et Technique de l'OIE*, vol. 32, no. 1, pp. 105–115, 2013.

[3] M.-T. Li, G.-Q. Sun, Y.-F. Wu, J. Zhang, and Z. Jin, "Transmission dynamics of a multi-group brucellosis model with mixed cross infection in public farm," *Applied Mathematics and Computation*, vol. 237, pp. 582–594, 2014.

[4] CFSPH, "Brucellosis brucella abortus," 2018, http://cfsph.iastate.edu/Factsheets/pdfs/brucellosis_abortus.pdf.

[5] E. Schelling, C. Diguimbaye, S. Daoud et al., "Brucellosis and Q-fever seroprevalences of nomadic pastoralists and their livestock in Chad," *Preventive Veterinary Medicine*, vol. 61, no. 4, pp. 279–293, 2003.

[6] R. A. Greenfield, D. A. Drevets, L. J. Machado, G. W. Voskuhl, P. Cornea, and M. S. Bronze, "Bacterial pathogens as biological weapons and agents of bioterrorism," *The American Journal of the Medical Sciences*, vol. 323, no. 6, pp. 299–315, 2002.

[7] J. Zhang, G. Sun, X. Sun et al., "Prediction and control of brucellosis transmission of dairy cattle in Zhejiang province, China," *PLoS One*, vol. 9, no. 11, Article ID e108592, 2014.

[8] F. Zhang, Z. Li, X. La et al., "Multiple-locus variable-number tandem-repeat analysis of Brucella isolates from patients in Xinjiang, China," *International Journal of Clinical and Experimental Medicine*, vol. 8, no. 9, pp. 15716–15723, 2015.

[9] B. E. Aïnseba, C. Benosman, and P. Magal, "A model for ovine brucellosis incorporating direct and indirect transmission," *Journal of Biological Dynamics*, vol. 4, no. 1, pp. 2–11, 2010.

[10] J. Zinsstag, F. Roth, D. Orkhon et al., "A model of animal-human brucellosis transmission in Mongolia," *Preventive Veterinary Medicine*, vol. 69, no. 1-2, pp. 77–95, 2005.

[11] M. N. Xavier, T. A. Paixao, A. B. den Hartigh, R. M. Tsolis, and R. L. Santos, "Pathogenesis of Brucella spp." *The Open Veterinary Science Journal*, vol. 4, no. 1, pp. 109–118, 2010.

[12] Medscape, "Brucellosis pathogenicity," 2018, https://emedicine.medscape.com/article/213430-overview.

[13] K. A. Franc, R. C. Krecek, B. N. Häsler, and A. M. Arenas-Gamboa, "Brucellosis remains a neglected disease in the developing world," *BMC Public Health*, vol. 18, no. 1, pp. 18–125, 2018.

[14] M. Ducrotoy, W. J. Bertu, G. Matope et al., "Brucellosis in Sub-Saharan Africa: current challenges for management, diagnosis and control," *Acta Tropica*, vol. 165, pp. 179–193, 2017.

[15] M. Yilma, G. Mamo, and B. Mammo, "Review on brucellosis sero-prevalence and ecology in livestock and human population of Ethiopia," *Achievements in the Life Sciences*, vol. 10, no. 1, pp. 80–86, 2016.

[16] A. S. Dean, L. Crump, H. Greter, E. Schelling, and J. Zinsstag, "Global burden of human brucellosis: a systematic review of disease frequency," *PLoS Neglected Tropical Diseases*, vol. 6, no. 10, pp. 1–9, 2012.

[17] CDC, *Brucellosis Signs and Symptoms*, CDC, Atlanta, GA, USA, 2018, https://www.cdc.gov/brucellosis/symptoms/index.html.

[18] K. John, J. Fitzpatrick, N. French et al., "Quantifying risk factors for human brucellosis in rural northern Tanzania," *PLoS One*, vol. 5, no. 4, Article ID e9968, 2010.

[19] G. Pappas, P. Papadimitriou, N. Akritidis, L. Christou, and E. V. Tsianos, "The new global map of human brucellosis," *The Lancet Infectious Diseases*, vol. 6, no. 2, pp. 91–99, 2006.

[20] G. Tumwine, E. Matovu, J. D. Kabasa, D. O. Owiny, and S. Majalija, "Human brucellosis: sero-prevalence and associated risk factors in agro-pastoral communities of Kiboga district, Central Uganda," *BMC Public Health*, vol. 15, no. 1, pp. 1–8, 2015.

[21] J. Kitaly, "Bovine brucellosis in Government parastatal and Ujamaa village dairy farms in central zone of Tanzania: assessment of Control measures in some farms," in *Proceedings of the 2nd Tanzania Veterinary Association Scientific Conference*, pp. 24–30, Arusha, Tanzania, December 1984.

[22] E. S. Swai and L. Schoonman, "Human brucellosis: seroprevalence and risk factors related to high risk occupational

groups in Tanga municipality, Tanzania," *Zoonoses and Public Health*, vol. 56, no. 4, pp. 183–187, 2009.

[23] M. Carugati, H. M. Biggs, M. J. Maze et al., "Incidence of human brucellosis in the Kilimanjaro region of Tanzania in the periods 2007-2008 and 2012–2014," *Transactions of The Royal Society of Tropical Medicine and Hygiene*, vol. 112, no. 3, pp. 136–143, 2018.

[24] G. M. Shirima, *The epidemiology of brucellosis in animals and humans in Arusha and Manyara regions in Tanzania*, Ph.D. thesis, University of Glasgow, Glasgow, Scotland, 2005.

[25] E. Swai and L. Schoonman, "A survey of zoonotic diseases in trade cattle slaughtered at Tanga city abattoir: a cause of public health concern," *Asian Pacific Journal of Tropical Biomedicine*, vol. 2, no. 1, pp. 55–60, 2012.

[26] A. G. Alhamada, I. Habib, A. Barnes, and I. Robertson, "Risk factors associated with brucella seropositivity in sheep and goats in Duhok province, Iraq," *Veterinary Sciences*, vol. 4, no. 65, pp. 1–9, 2017.

[27] N. Nyerere, L. S. Luboobi, S. C. Mpeshe, and G. M. Shirima, "Mathematical model for the infectiology of brucellosis with some control strategies," *New Trends in Mathematical Sciences*, vol. 7, no. 4, pp. 387–405, 2019.

[28] N. Nyerere, L. S. Luboobi, S. C. Mpeshe, and G. M. Shirima, "Mathematical model for brucellosis transmission dynamics in livestock and human populations," *Communications in Mathematical Biology and Neuroscience*, vol. 2020, no. 3, pp. 1–29, 2020.

[29] Q. Hou, X. Sun, J. Zhang, Y. Liu, Y. Wang, and Z. Jin, "Modeling the transmission dynamics of sheep brucellosis in inner Mongolia autonomous region, China," *Mathematical Biosciences*, vol. 242, no. 1, pp. 51–58, 2013.

[30] C. Li, Z.-G. Guo, and Z.-Y. Zhang, "Transmission dynamics of a brucellosis model: basic reproduction number and global analysis," *Chaos, Solitons & Fractals*, vol. 104, pp. 161–172, 2017.

[31] B. Nannyonga, G. G. Mwanga, and L. S. Luboobi, "An optimal control problem for ovine brucellosis with culling," *Journal of Biological Dynamics*, vol. 9, no. 1, pp. 198–214, 2015.

[32] P. O. Lolika, C. Modnak, and S. Mushayabasa, "On the dynamics of brucellosis infection in bison population with vertical transmission and culling," *Mathematical Biosciences*, vol. 305, pp. 42–54, 2018.

[33] F. Roth, J. Zinsstag, D. Orkhon et al., "Human health benefits from livestock vaccination for brucellosis: case study," *Bulletin of the World Health Organization*, vol. 81, pp. 867–876, 2003.

[34] O. Diekmann, J. A. P. Heesterbeek, and J. A. J. Metz, "On the definition and the computation of the basic reproduction ratio R_0 in models for infectious diseases in heterogeneous populations," *Journal of Mathematical Biology*, vol. 28, no. 4, pp. 365–382, 1990.

[35] O. Diekmann, J. A. P. Heesterbeek, and M. G. Roberts, "The construction of next-generation matrices for compartmental epidemic models," *Journal of the Royal Society Interface*, vol. 7, no. 47, pp. 873–885, 2010.

[36] D. Okuonghae and A. Korobeinikov, "Dynamics of tuberculosis: the effect of direct observation therapy strategy (DOTS) in Nigeria," *Mathematical Modelling of Natural Phenomena*, vol. 2, no. 1, pp. 113–128, 2007.

[37] A. Palanduz, S. Palanduz, K. Guler, and N. Guler, "Brucellosis in a mother and her young infant: probable transmission by breast milk," *International Journal of Infectious Diseases*, vol. 4, no. 1, pp. 1–55, 2000.

[38] M. J. Michael, *Brucellosis in Humans and Animals*, World Health Organization, Geneva, Switzerland, 2006.

[39] O. Mesner, K. Riesenberg, N. Biliar et al., "The many faces of human-to-human transmission of brucellosis: congenital infection and outbreak of nosocomial disease related to an unrecognized clinical case," *Clinical Infectious Diseases*, vol. 45, no. 12, pp. e135–e140, 2007.

[40] E. Meltzer, Y. Sidi, G. Smolen, M. Banai, S. Bardenstein, and E. Schwartz, "Sexually transmitted brucellosis in humans," *Clinical Infectious Diseases*, vol. 51, no. 2, pp. e12–e15, 2010.

[41] A. El-Sayed and W. Awad, "Brucellosis: evolution and expected comeback," *International Journal of Veterinary Science and Medicine*, vol. 6, no. 1, pp. s31–s35, 2018.

[42] F. F. Tuon, R. B. Gondolfo, and N. Cerchiari, "Human-to-human transmission of Brucella—a systematic review," *Tropical Medicine & International Health*, vol. 22, no. 5, pp. 539–546, 2017.

[43] M. Viana, G. M. Shirima, K. S. John et al., "Integrating serological and genetic data to quantify cross-species transmission: brucellosis as a case study," *Parasitology*, vol. 143, no. 7, pp. 821–834, 2016.

[44] D. L. Lukes, *Differential Equations: Classical to Controlled*, Vol. 162, Academic Press, vol.162, New York, NY, USA, 1982.

[45] L. S. Pontryagin, V. G. Boltyanskii, R. V. Gamkrelidze, and E. F. Mishchenko, *The Mathematical Theory of Optimal Processes*, Routledge, Abingdon, UK, 1962.

[46] W. H. Fleming and R. W. Rishel, *Deterministic and Stochastic Optimal Control,* vol. 1, Springer Science & Business Media, Berlin, Germany, 2012.

[47] S. Lenhart and J. T. Workman, *Optimal Control Applied to Biological Models*, CRC Press, London, UK, 2007.

[48] D. Hartwell, J. Jones, L. Baxter, and J. Shepherd, "Peginterferon alfa and ribavirin for chronic hepatitis C in patients eligible for shortened treatment, re-treatment or in HCV/HIV co-infection: a systematic review and economic evaluation," *Health Technology Assessment*, vol. 15, no. 17, pp. 1–210, 2011.

[49] R. M. Klok and M. J. Postma, "Four quadrants of the cost-effectiveness plane: some considerations on the south-west quadrant," *Expert Review of Pharmacoeconomics & Outcomes Research*, vol. 4, no. 6, pp. 599–601, 2004.

[50] P. A. McFarlane and A. M. Bayoumi, "Acceptance and rejection: cost-effectiveness and the working nephrologist," *Kidney International*, vol. 66, no. 5, pp. 1735–1741, 2004.

[51] K. O. Okosun, O. Rachid, and N. Marcus, "Optimal control strategies and cost-effectiveness analysis of a malaria model," *BioSystems*, vol. 111, no. 2, pp. 83–101, 2013.

Journal of Mathematics and Informatics
Vol. 19, 2020, 23-35
ISSN: 2349-0632 (P), 2349-0640 (online)
Published 21 July 2020
www.researchmathsci.org
DOI: http://dx.doi.org/10.22457/jmi.v19a04174

Journal of
Mathematics and Informatics

A Review of the Mathematical Models for Brucellosis Infectiology and Control Strategies

Nkuba Nyerere[1, 2*], Livingstone S. Luboobi[1, 3], Saul C. Mpeshe[4]* and *Gabriel M. Shirima[5]

[1]Department of Applied Mathematics and Computational Sciences, Nelson Mandela African Institution of Science and Technology, P.O. Box 447, Arusha, Tanzania.
e-mail: nyereren@nm-aist.ac.tz

[2]Department of Mathematics, Informatics and Computational Sciences, Sokoine University of Agriculture, P.O.Box 3038, Morogoro. e-mail: emmankuba@sua.ac.tz

[3]Institute of Mathematical Sciences, Strathmore University, PO Box 59857-00200, Nairobi, Kenya. e-mail: lluboobi@strathmore.edu

[4]Department of Mathematics, University of Iringa, P.O.Box 200, Iringa, Tanzania.
e-mail: mpesaul@yahoo.com

[5]Department of Global Health and Bio-Medical Sciences, Nelson Mandela African Institution of Science and Technology, P.O. Box 447, Arusha, Tanzania.
e-mail: gabriel.shirima@nm-aist.ac.tz
[*]Corresponding author

Received 2 June 2020; accepted 3 July 2020

Abstract. Brucellosis is a zoonotic bacterial infection that can be acquired by humans from infected animals' meat, urine, body fluids, aborted materials, unpasteurized milk, and milk products or contaminated environment. Mathematical models for infectious diseases have been used as important tools in providing useful information regarding the transmission and effectiveness of the available control strategies. In this paper, a review of the available compartmental mathematical models for Brucellosis was done. The main purpose was to assess their structure, populations involved, the available control strategies and suitability in predicting the disease incidence and prevalence in different settings. Diversities have been observed in the reviewed mathematical models; some models incorporated seasonal variations in a single animal population, some ignored the contributions of the contaminated environment while others considered the cattle or sheep population only. Most of the models reviewed have not considered the contribution of wild animals in the dynamics of Brucellosis. Some models do not match the real situation in most affected areas like sub-Saharan African region and Asian countries where wild animals, cattle and small ruminants share grazing areas and water points. Thus, to avoid unreliable results, this review reveals the need to affirm and incorporate wild animals, livestock, humans and seasonal weather parameters in the spread of Brucellosis and in planning for its controls.

Keywords: Brucellosis, infectiology, control strategies, mathematical models, compartmental models

AMS Mathematics Subject Classification (2010): 03H10

1. Introduction

Brucellosis is a disease caused by a number of species of bacteria collectively called *Brucella*. It is one of the most widespread human and livestock diseases acquired from infected animals or their products [1]. The disease is one of the highest priority animal diseases in different regions of the world. Brucellosis infects many species including livestock, wildlife, and humans. Most human infections are acquired through direct contact with infectious livestock or via indirect transmission by ingestion of unpasturized milk and milk products or through engaging in occupational activities. The disease has a wide range of impacts that include losses due to abortion, culling of infected animals, lost milk production, animal replacement costs, veterinary fees, and human illness- causing reduced work capacity.

The history of Brucellosis goes beyond the 1887 isolation and identification of *Brucella* melitensis and extends back to people's initial contact with animals [1, 2, 3]. The disease has been known by various names including Malta fever, Crimean fever, Bang's disease, Rock fever, Maltese fever, Gibraltar fever, Undulant fever, Mediterranean fever, or Gastric remittent [4,5]. It remains the most common and continually-reemerging zoonosis worldwide since 1884, and it is accountable for more than 500,000 new human cases annually [6]. Additionally, low infectious doses (10-100 bacterial cells), rapid transmission through different pathways, persistence in the environment, and treatment difficulties with antibiotics make *Brucella* a possible bioterrorism agent [5].

Control and eradication programmes based on various strategies have been successful in eliminating Brucellosis in several countries [7]. Strategies based on prevention of the spread between animals, monitoring of Brucellosis-free herds and zones, elimination of infected animals by test and slaughter, strict control of the movement of infected and suspected animals, mass immunization to reduce infection rate and supporting specific education and training programmes have all received attention in various countries [8, 9]. In addition, human treatment is given to cure or reduce symptoms duration, avert relapse, and avoid complications such as encephalitis, spondylitis, arthritis, endocarditis, sacroilitis, epididymoorchitis, and abortion [10]. However, the control or eradication of Brucellosis is highly dependent on national strategies, priorities, and policies.

The current review evaluates different Brucellosis models based on structure, various control interventions, and their effectiveness

2. Methodology

A literature search from Medline, Science Direct, OVID, PubMed, Research4Life, and Web of Science databases was conducted and analysis of the articles relevant to the study and written in English was done. The search was restricted to articles published from 2009 to 2019. To minimize the chance of missing important studies, manual search and sorting of the references of all articles found in our search including any potentially eligible studies that were found using Google Scholar were performed. The search keywords or MeSH were defined as: ("Brucellosis" OR "Brucella melitensis" OR

"Brucella abortus" OR "human brucellosis") AND ("mathematical model" OR "modeling" OR "mathematical approach" OR "deterministic model" OR "compartmental model"). Brucellosis studies which were conducted using compartmental models, available in full text, most recent in a series of articles with the same first authors, similar modeling structure and content, and those used to evaluate the potential impact of Brucellosis transmission control strategies on a population-based level were eligible for inclusion in the review. The initial number of returned articles from the searches was 125. Abstract of articles with compartmental models were retained for a detailed review and 20 were included in the list of references.

3. Mathematical models

A mathematical model is an illustration of a system using mathematical language and concepts; it is an essential tool for evaluating the spread and control of communicable diseases. Mathematical models are used to investigate and predict how communicable diseases advance, demonstrate the possible outcomes of an epidemic and advise public health interventions. Such models use some basic assumptions and mathematics to identify the parameters for various infectious diseases and gauge the effects of different interventions such as mass vaccination and education campaign programmes. They can also assist in decisions involving intervention(s) to be implemented and to what extent. Modeling of infectious diseases is a tool that has been used to study the spread of diseases, predicting outbreaks and appraising the control strategies of an epidemic.

In 1766, a trained physician Daniel Bernoulli performed the earliest mathematical modeling study on the spread of diseases. He developed a mathematical model to study smallpox mortalities in England and used the model to show that universal inoculation against the disease would increase life expectancy at birth by 3 years and 2 months [11]. In 1772, Lambert and Laplace improved Bernoulli's work by expanding the model to include age-dependent factors. Nevertheless, this research focus was not systematically developed until 1911 when a benchmark study by Ross established the modern mathematical epidemiology [12]. The law of mass action was then applied by William Hamer and Ronald Ross to explain the epidemic behaviour of measles and malaria respectively. Kermack-McKendrick and the Reed-Frost epidemic models of 1927 and 1928 respectively both described the association between immune, infected, and susceptible individuals in a population. The models successfully predicted the behaviour of outbreaks similar to recorded observations of many epidemics [13].

More importantly, the work by Ross, Kermack, and McKendrick addressed the use of mass-action incidence in disease transmission, signifying that the probability for a susceptible individual to be infected corresponds to the number of its interactions with infectious ones. Furthermore, their work establishes the compartmental deterministic epidemic modeling and predicted the critical fraction of susceptible individuals that must be exceeded in the population for an epidemic to occur depending on the transmission potential of an infection. Forty years after the reports by Ross, MacDonald extended Ross's model to clarify the malaria transmission process and proposed methods for eliminating the disease on an operational level. The significant contribution of MacDonald and Ross to the field through the use of computers made mathematical models for the dynamics and control of mosquito-transmitted pathogens to be branded as

Ross-MacDonald models [14]. Generally, there have been several different model compartment structures depending on the type of disease. Some possible classes of compartmental models are: susceptible-infectious (SI), susceptible-infectious-susceptible (SIS), susceptible-exposed-infectious (SEI), susceptible-exposed-infectious-susceptible (SEIS), susceptible-infectious-recovered (SIR), susceptible-infectious-recovered-susceptible (SIRS), susceptible-exposed-infectious-recovered (SEIR) and susceptible-exposed-infectious-recovered-susceptible (SEIRS) [15].

4. Brucellosis mathematical models

Amaku *et al*. [16] formulated a mathematical model to simulate Brucellosis dynamics in herds of female cattle and analyzed the effects of vaccination strategies. The model was based on statistics from some states of Brazil where surveys on serology were carried out and detected a prevalence rate higher than 2%. The findings showed that in areas with low immunization coverage (approximately 30%), the time required to lower the prevalence rate to 2%, would be approximately twice the time observed for higher coverage (approximately 90%). The study further predicted that, if the model parameters remain unchanged, it will take a decade to reduce the Brucellosis prevalence to 1 or 2% which is the adequate phase for the disease eradication. The intensification of female bovine vaccination efforts to achieve high vaccination coverage was recommended in this study.

Ainseba *et al.* [17] formulated and analyzed a susceptible-infected mathematical model for Brucellosis in the ovine population. In this model, both direct and indirect modes of disease transmission were considered. Susceptible individuals could directly contract *Brucella* from infected individuals through contact or indirectly due to the presence of virulent organisms in the environment. The net reproduction number was computed and used to analyze the global asymptotic behaviour of the model. Numerical simulations were performed to investigate the effect of a slaughtering policy. Findings from the study suggested that, in order to better understand the dynamics of the disease in ovine or any other animal population, incorporation of the age of infection and/or the chronological age is needed. However, the model formulated was too elementary to generalize the complex dynamics of the disease that involves wild animals, livestock, human and the environment.

Hou *et al*. [18] formulated a sheep to human Brucellosis transmission model that involved the human and sheep populations in Inner Mongolia, China. The model divided sheep population into susceptible, exposed and infectious while the human population was classified into susceptible, acute infection and chronic infection. The average bacterial load enough to cause infection on the host was defined as the infectious unit. Computation of the threshold number used in determination for the existence and stability of the equilibria was done. Numerical simulations and sensitivity analysis of the reproductive number were carried out using reported human Brucellosis data from the region. Findings showed that the disease could not be eliminated even if disinfection and immunization rates of adult sheep were 100%. The study further investigated and compared the effects of immunization, disinfection and elimination strategies. Findings showed that vaccination and disinfection of both adult and young sheep were effective and appropriate control strategies for Brucellosis control in Inner Mongolia. However, an assumption that the exposed and infectious sheep had the same infectivity and shedding

rates of *Brucella* to the environment through abortions or secretions makes the exposed class redundant. Similarly, the lack of data for human to human transmission was not a sufficient condition for this particular transmission route to be ignored.

Racloz *et al.* [19] performed a formal mathematical analysis of the Mongolia model by Zinsstag *et al.* [20] to examine different settings by which the number of latently infected, infectious animals remains stable. Although the need for more data was evident in order to have a better estimation of the threshold densities for the disease transmission in other regions of the world, the employed system of differential equations and the equilibrium conditions for the model were found to be reasonably robust. Demographic determinants for livestock were found to be the most important parameters for the disease persistence. The study further depicted that despite varying control efforts in pastoral areas, Brucellosis remains largely persistent worldwide. The study recommended for ecological considerations like sustaining ecosystem services when planning for the disease control strategies in pastoral settings. Improved governance, land reform, placing limitations on livestock stocking density, movement, and integrated social and economic development should be part and parcel of the plan. However, wild animals and the seasonal interactions between wild and domestic animals were not taken into account on the model formulation and analysis.

Li, Sun, Zhang, Jin, Sun, Wang, Huang and Zhang [21] presented a mathematical model to explore the effective control and preventive measures of Brucellosis transmission dynamics in Hinggan League of Inner Mongolia, China. The formulated model described the sheep-to-human and sheep-to-sheep spread of the disease. The sheep flock at any time was classified into basic ewes and other sheep, each of the classes was further divided into susceptible, recessive infected, quarantined seropositive infected and vaccinated subgroups while the human population was divided into susceptible, acute infections and chronic infections. The study indicated that susceptible sheep and human could acquire infections from polluted environment and recessive infected sheep. Numerical simulations for the study agreed with the 2001 to 2011 records of human Brucellosis incidences, and the trend of the disease incidences in was given. The reproduction number for the region was estimated to be 1.9789. The study demonstrated that a combination of detection and elimination, vaccination, and prohibition of mixed feeding between basic ewes and other sheep are useful in controlling the disease in the region. However, the model does not fit to the sub-Saharan Africa countries where cattle, small ruminants, and wild animals share grazing areas and water points. An assumption that recessive infected and quarantined seropositive infected sheep release the same quantity of *Brucella* organisms into the environment per unit time makes the quarantined class redundant. Thus, there is a need for combining the recessive infected and quarantined seropositive infected classes.

Kang *et al.* [22] developed SIR model to simulate the spread of Brucellosis within the cattle population in India. The formulated model was used to estimate the impact of test-and-slaughter, reduction of the transmission rate, and mass vaccination in controlling the spread of the disease. The epidemiological benefits of different rates of vaccination and decreased transmission were analyzed. Findings showed that test-and-slaughter is an effective strategy for eliminating and eradicating Brucellosis. However, socio-cultural restrictions prevents the culling of cattle in India. The model revealed

further that the reduction of Brucellosis transmission rates correspondingly lowered the stability and endemic levels of Brucellosis prevalence. Pulse vaccination initially lowered the prevalence rates but increased with the influx of new susceptible births. However, limitations in surveillance data acted as the major constraint of this study. In real practice, test and slaughter alone results in more financial losses than did eradication because the newborns are not protected. On the other hand, the model formulation was dictated by the available data and not the biology of the disease and so did not incorporate small ruminants, human population and the indirect route of disease transmission through the contaminated environment.

Nie *et el.* [23] described the spread of Brucellosis among dairy cattle in Jilin Province, China using a mathematical model. The dairy cattle population was classified into Susceptible, Exposed, and Infected while the bacterial compartment was included to capture the outside transferred amount of *Brucella*. The basic reproductive number was computed and used to prove the existence and global attraction of the equilibria. Parameter values for the system and prediction of infection numbers with time were estimated using 20 years Jilin province Brucellosis data. The findings from the study revealed that the disease would still persist in area for the next 30 years even if the existing measures were taken into account. Moreover, the combination of culling, sterilizing and minimization of the number of outer importing is the best control strategy for dairy cattle Brucellosis. However, the model did not consider the impact of small ruminants and weather variation on the disease spread.

Zhang *et al.* [4] presented a SEIV model to excavate the transmission of Brucellosis in Zhejiang Province in China. The formulated model fitted the real disease situation and predicted the disease tendency in the region. Assessment of the effectiveness of the control measures was done in dairy cows. Careful analysis of the model gave the following quantitative results: importation of dairy cows from northern areas limits control of the disease due to high fluctuation in the number of infectious dairy cows, and the rate of *Brucella* transmission from the environment to dairy cattle was greater than that from infectious dairy cattle to susceptible cattle. Brucellosis control strategies require consideration of seasonal parameters due to periodic nature under certain circumstances. Additionally, a combination of birth rate management and twice a week sterilization in infected regions best controls the disease in cows. Nevertheless, the model did not consider human and other animal populations.

Li, Sun, Wu, Zhang and Jin [24] proposed SEIRV multi-group model incorporating two-way transmissions between cattle and sheep in public farms. The influence of bidirectional infection resulting from mixed feeding of the two groups was investigated. Investigation and confirmation for the uniform existence of a unique positive equilibrium were done using the computed basic reproduction number. An endemic equilibrium of the model was proved to be globally attracting if the basic reproduction number is > 1. Sensitivity analysis of the infectious herds with different systems in terms of some parameter values was performed. Findings revealed that the disease cannot be eradicated if there is a two-way transmission between cattle and sheep; reproduction number been less than unity is not a sufficient condition for the disease eradication in the region. The study recommended that mixed feeding prohibition is the best control measure for Brucellosis elimination. However, the assumption that individuals at the latent stage and the one at the infectious stage have the same

transmission rate makes the exposed class redundant. In addition, the model did not incorporate the human population; a population that makes Brucellosis a public health concern.

Hou *et al*. [25] used Changling County of Jilin Province Brucellosis infection characteristics monitoring data to formulate a multi-stage model for the disease spread in sheep. Appertaining to the assumption that *Brucella* spread primarily causes disease in adult sheep and that young sheep infectivity is negligible, the sheep population was classified into young susceptible, susceptible adult or sexually mature, vaccinated, exposed and infectious classes. Basic reproductive number computation was done and the model dynamic properties were discussed. In terms of the embedded parameters, sensitivity analysis of the basic reproductive number was performed and found that the sheep birth, vaccination, and elimination rates for infectious sheep were important players in the disease transmission. Further investigation and comparison of the effects of sheep vaccination and culling strategies revealed that the two controls are effective and feasible for controlling Brucellosis in the region; however, the latter was more effective than the former. Nonetheless, the model did not consider the impact of the contaminated environment and human to human transmission in the dynamics of the disease.

Lou *et al*. [26] proposed a susceptible-exposed-infected-vaccinated (SEIV) Brucellosis model with periodicity in the rates of transmission. The impacts of seasonal disease transmission in livestock and human populations of Bayingolin Mongol Autonomous Prefecture of Xinjiang, China were investigated. Computation of the basic reproductive number was done and it was estimated to be 2.5524. Sensitivity analysis of the reproductive number and the new acute human Brucellosis cases for the model parameters demonstrated that livestock reduced birth rate, increased slaughter rate of seropositive livestock, increased immunization rates for susceptible livestock, and decreased loss rates of immunization efficacy are effective strategies for controlling the Brucellosis epidemic. The study predicted a continuous increase in the number of newly acute human Brucellosis and its maximum value was estimated to be 15325, which will be reached around the summer of 2023. However, this study did not consider the contribution of the contaminated environment in the disease transmission dynamics.

de Souza *et al*. [27] formulated a Brucellosis model for the purpose of measuring the impact of the combination of S19 and RB51 vaccines in reducing the disease prevalence. The model divided the cattle population into seven compartments namely: susceptible, vaccinated with the RB51 strain, primiparous latent carriers, vaccinated with the S19 strain, primiparous infectious cows, multiparous latent carriers, and multiparous infectious cows. The study concluded that the adoption of RB51 vaccination as a complement to S19 vaccination significantly reduces bovine Brucellosis prevalence in a short time. However, ignoring the contribution of small ruminants, wild animals, contaminated environment and the aspect of seasonality limits a better understanding of the disease transmission dynamics.

Li, Sun, Zhang and Jin [28] formulated a sheep and human Brucellosis dynamical model with direct and indirect transmission routes. The sheep population was grouped into basic ewes and other sheep and it was further divided into susceptible, recessive infected, quarantined seropositive infected and vaccinated subgroups while the human population was classified into susceptible, acute infections and chronic infections.

Recessive infected sheep and contaminated environment were the two main sources of infection for susceptible humans and sheep. It had been proved from this study that, Brucellosis extinction and persistence equilibria are globally attracting if and respectively. Nevertheless, this model did not consider goat and cattle populations which are mostly found in areas where sheep are kept.

Li, Guo and Zhang [29] presented a mathematical model incorporating indirect transmission routes to evaluate animal vaccination, elimination of infected animals, and environmental disinfection control strategies. The study used national human data from eleven China provinces that have a high number of Brucellosis cases to compare results for three different models. Potential possible disease outbreaks were investigated using the model with the best fit and standard incidence. It was found that the country's average reproduction number was relatively less than that of the province with high disease incidence, suggesting that indirect transmission of the disease was a more common route compared to direct transmission. The study concluded that Brucellosis in China could be controlled if infected animals elimination, environmental disinfection, and animal vaccination ware increased. The findings further suggested that the combination of infected animals' elimination, environmental disinfection, and animal vaccination is necessary for ensuring cost-effective Brucellosis control scheme. However, the important aspects of the disease control like personal protection in humans, and the impacts of seasonal weather variations were not captured in the model.

Tumwiine and Robert [30] presented a mathematical model depicting the conveyance of Brucellosis in the bovine herd. The model analysis was carried out to gain and establish the stability of the equilibria. A boundary parameter categorized as the basic reproduction number was calculated and the conditions under which bovine Brucellosis can be cleared in the cattle population were established. It was found out that if $R_0 < 1$, the infection can be eliminated in the cattle population or persists if $R_0 > 1$. Lyapunov function and Poincair´e-Bendixson theory were used to prove that the disease extinction and persistence equilibria are respectively globally asymptotic stable. Numerical simulation revealed that an increase in magnitude of treatment rate for infected cattle and reduction of contact rate between infectious cattle and susceptible or recovered cattle controls the disease. However, the formulated model can be improved by incorporating small ruminants and the aspect of seasonality that captures cattle calving season, temperature, humidity, soil salinity, and exposure of the bacteria to sunlight.

Zhou *et al*. [31] developed a multi-group model to explore the key factors, potential effects, characterize Brucellosis transmission, and prioritize control measures. Direct Lyapunov method and asymptotic autonomous systems theory were used to characterize the global threshold dynamics of the disease. The weighted sum method was used in the formulation of a multi-objective optimization problem, and it was converted to a scalar optimization problem of minimizing the total cost for control. Pontryagin's Maximum Principle was used to establish the existence and characterization of an optimal control problem. Model parameterization and computation of optimal control strategy for Inner Mongolia in China were done. The effects of health education on human, sheep recruitment, culling of infected sheep, and sheep vaccination to the dynamics and control of the disease were explored. The study revealed that Brucellosis would continue to increase in Inner Mongolia because the available controls were not working well. The controls recommended in this study are health education, sheep

vaccination and restriction of unregulated sheep breeding. However, the model did not consider the contribution of other ruminants and the impact of seasonal weather variations on the disease transmission.

Nepomuceno *et al*. [32] presented a network type of individual-based modeling as an alternative approach to compartmental models that are used in controlling bovine Brucellosis. Spatial aspects like migration between herds, heterogeneous populations, and control actions designated as pulse interventions were considered and implemented in the model. It was demonstrated that the mean-field behaviour of a compartmental model could be reproduced by an equivalent individual-based model. To enable the replication of the presented results, details of this process and flowcharts were provided. Real parameters from Sao Paulo state of Brazil herds were used to investigate three numerical examples in situations that explore meta-population, pulsed and continuous vaccination, and eradication effects. The analysis from this study depicted results which agreed with the expected disease behaviour.

Abatih *et al*. [33] presented a mathematical approach to analyze the transmission dynamics of Brucellosis among bison. Quantitative and qualitative analyses were used to show that the infection would disappear from the herd if $R_0 < 1$ and will persist otherwise. Results from Sobol method for global sensitivity analysis showed that recovery rate and loss of resistance rate were accountable for the high inconsistency in the expected number of infectious bison. Partial ranked correlation coefficients computation revealed that transmission coefficient, recovery rate, mortality rate, and density-dependent reduction in birth correlates highly negatively with the infective bison number while the calving rate and resistance loss rate highly correlates positively with the infectious bison number. Thus, measures to control the disease in bison should target at rising the size of mortality rate, recovery rate, and birth reduction density-dependent rate as well as decreasing calving rate and loss of resistance. To raise the accuracy of the expected number infectious bison, a precise estimate of the recovery rate and loss of resistance from experimental studies are needed. However, the recommendations from this study are socially and economically inapplicable.

Lolika *et al*. [34] introduced a framework for Brucellosis mathematical modeling that aimed at improving the quantitative understanding of the disease dynamics. In particular, the framework introduced which is an extension of the model by [33] was used to explore the impact of culling control and the influence of chronic individuals on the Brucellosis spread in the periodic or non-periodic environment. The model was analyzed to get insights on the epidemic and endemic behaviour of the disease using threshold dynamics described by the basic reproduction number. Culling at an optimal level in a periodic and non-periodic environment was explored using optimal control theory. However, this study did not incorporate the indirect transmission of the disease.

5. Summary

Mathematical models presented by [17, 25] investigated the transmission dynamics of Brucellosis in a population of sheep only while those presented by [4, 16, 22, 23, 27] focused on the dynamics of the disease in a population of cattle only. These models missed important aspects of the disease behaviour; Brucellosis is a zoonosis; the population of humans cannot be easily ignored when studying the disease dynamics. On

the other hand, the study by [34] adopting the study by [33] explored the impacts of various parameters accountable for transmission of the disease in a population of bison. However, the study is more theoretical as it considers a single population and does not show the effect of bison Brucellosis to other populations or the environment.

Furthermore, mathematical models by [18, 21, 28] were formulated to investigate the impact of various control strategies on sheep and human populations. The inclusion of humans, sheep and the contaminated environment in model and the incorporated control strategies provides a better understanding of Brucellosis dynamics compared to the ones with one or two populations. Nevertheless, the models could be improved by incorporating other ruminant populations and seasonality in the transmission of the disease. A mathematical model by [23] takes consideration of cattle and sheep populations and investigates the impact of mixed feeding and bidirectional infection between the two populations. This mathematical model is far better and can be improved more by including the human population and other domestic ruminants like goats so as to fit in most of the pastoral communities. Seasonal weather variation parameters and wild animals can also be incorporated so as to have a more realistic model. The [20] mathematical formulation adopted by [19] is also a better model as it includes sheep, goat and human populations, and it provides a better understanding of the disease dynamics as it incorporates most of the transmission key players. However, the model can be improved by incorporating the indirect route of transmission, seasonal weather parameters for disease dynamics and wild animals.

In terms of control strategies six of the mathematical models [4, 16, 17, 23, 27, 32] investigated the use of one control measure, five [4, 18, 22, 25, 26] explored the impact of the combination of two controls while four studies [21, 23, 29, 31] examined the impact of a combination of three control strategies in minimizing or elimination of the disease. The remaining studies aimed at providing potential information for Brucellosis spread. Based on the model structure and control strategies incorporated, the model by [29] fits in areas with mixed farming systems. However, it can be improved by considering personal protection in humans, wild animals, and seasonality. In addition, the mathematical model proposed by [18] and [25] are recommended for studying the disease in a single animal population and can also be improved by incorporating controls like personal protection, and environmental hygiene and sanitation.

6. Conclusions

Diversities have been observed in the reviewed mathematical models; some models incorporate seasonal variations in a single animal population, some ignored the contributions of the contaminated environment while others considered only the cattle or sheep population. Most of the models did not consider the contribution of wild animals and personal protection control in the dynamics of Brucellosis whereas few of them incorporated cattle and sheep only. In addition, some studies did not match the real situation for most Brucellosis endemic areas like sub-Saharan African region and Asian countries where wild animals, cattle and small ruminants share grazing areas and water points. In Brucellosis endemic areas, models with at least three populations and the combination of at least two control parameters works better. Generally, this review revealed that mathematical models regardless of their goodness cannot be applied everywhere; not all mathematical models fit every setting or group of animals. Some

models provide more insights on the disease dynamics and control in developed countries while others give a better understanding of the disease and control in developing countries. This review recommends that mathematical models by [20] and [29] though not perfect may be used in sub Saharan Africa and other areas where mixed farming is practiced.

Acknowledgements. Authors acknowledgments the financial support from African Development Bank (AfDB). Also, we are thankful to the referees for their valuable report for the improvement of the paper.

REFERENCES

1. H.V.Wyatt, Lessons from the history of brucellosis, *Journal of Maltese History*, 5(1) (2016) 75-84.
2. O.Akpinar, Historical perspective of brucellosis: a microbiological and epidemiological overview, *Le Infezioni in Medicina*, 24(1) (2016) 77-86.
3. M.J.Mutolo, L.L.Jenny, A.R.Buszek, T.W.Fenton and D.R.Foran, Osteological and molecular identification of brucellosis in ancient butrint, Albania, *American Journal of Physical Anthropology*, 147(2) (2016) 254-263.
4. J. Zhang, G.-Q.Sun, X.-D.Sun, Q.Hou, M.Li, B.Huang, H.Wang and Z.Jin. Prediction and control of brucellosis transmission of dairy cattle in zhejiang province, China. *Plos one*. 9(11): 1-13. 2014.
5. A.El-Sayed and W.Awad, Brucellosis: Evolution and expected comeback, *International Journal of Veterinary Science and Medicine*, 6(1) (2018) 31-35.
6. J. Godfroid, A.Cloeckaert, J.P.Liautard, S.Kohler, D.Fretin, K.Walravens, B.Garin-Bastuji and J.J.Letesson, From the discovery of the malta fever's agent to the discovery of a marine mammal reservoir, brucellosis has continuously been a re-emerging zoonosis, *Veterinary Research*, 36(3) (2005) 313-326.
7. WHO. Brucellosis. Fact sheet N173. *World Health Organization, Geneva, Switzerland*, 1997.
8. G.C.Bishop, P.P.Bosman and S.Herr, Bovine brucellosis, *Infectious Diseases of Livestock with Special Reference to Southern Africa*, 2 (1994) 1053-1066.
9. WHO. The Development of new/improved brucellosis vaccines: report of a WHO meeting, Geneva, Switzerland, 11-12 December 1997 (No. WHO/EMC/ZDI/98.14). Geneva: *World Health Organization*. 1998.
10. G.Pappas, P.Papadimitriou, N.Akritidis, L.Christou and E.V.Tsianos, The new global map of human brucellosis, *The Lancet Infectious Diseases*, 6(2) (2006) 91-99.
11. D.Bernoulli and S.Blower, An attempt at a new analysis of the mortality caused by smallpox and of the advantages of inoculation to prevent it, *Reviews in Medical Virology*, 14(5) (2004) 275-288.
12. C.I.Siettos and L.Russo, Mathematical modeling of infectious disease dynamics, *Virulence*, 4(4) (2013) 295-306.
13. F.Brauer and C.Castillo-Chavez, *Mathematical Models for Communicable Diseases.*, Vol. 84. SIAM. 2013.
14. D.L.Smith, K.E.Battle, S.I.Hay, C.M.Barker, T.W.F.Scott and E.McKenzie, Ross, macdonald, and a theory for the dynamics and control of mosquito-transmitted

pathogens. *PLoS pathogens*. 8(4): e1002588. doi:10.1371/journal.ppat.1002588. 2004.

15. H.W.Hethcote, A thousand and one epidemic models. In: *Frontiers in mathematical biology*. Springer. 1994, 504-515.
16. M.Amaku, R. Dias, J.Ferreira Neto and F.Ferreira, Mathematical modeling of bovine brucellosis control by vaccination, *Arquivo Brasileiro de Medicina Veterin´ariae Zootecnia*, 61 (2009) 135-141.
17. B.Ainseba, C.Benosman, and P.Magal, A model for ovine brucellosis incorporating direct and indirect transmission, *Journal of Biological Dynamics*, 4(1) (2010) 2-11.
18. Q.Hou, X.Sun, J.Zhang, Y.Liu, Y.Wang and Z.Jin, Modeling the transmission dynamics of sheep brucellosis in Inner Mongolia autonomous region, China, *Mathematical Biosciences*, 242(1) (2013) 51-58.
19. V.Racloz, E.Schelling, N.Chitnis, F.Roth and J.Zinsstag, Persistence of brucellosis in pastoral systems, *OIE Revue Scientifique et Technique*, 32(1) (2013) 61-70.
20. J.Zinsstag, F.Roth, D.Orkhon, G.Chimed-Ochir, M.Nansalmaa, J.Kolar and P.Vounatsou, A model of animal-human brucellosis transmission in Mongolia, *Preventive Veterinary Medicine*, 69 (1-2) (2005) 77-95.
21. M.Li, G.Sun, J.Zhang, Z.Jin, X.Sun, Y.M.Wang, B.Huang and Y.Zheng, Transmission dynamics and control for a brucellosis model in Hinggan League of Inner Mongolia, China, *Mathematical Bioscience and Engineering*, 11(5) (2014) 1115-1137.
22. G.J.Kang, L.Gunaseelan and K.M.Abbas, Epidemiological modeling of bovine brucellosis in India. In: *2014 IEEE International Conference on Big Data (Big Data). IEEE*. pp. 6-10, 2014.
23. J.Nie, G.-Q.Sun, X.-D.Sun, J.Zhang, N.Wang, Y.-M.Wang, C.-J.Shen, B.-X.Huang and Z.Jin, Modeling the transmission dynamics of dairy cattle brucellosis in jilin province, China, *Journal of Biological Systems*, 22(4) (2014) 533-554.
24. M.-T.Li, G.-Q.Sun, Y.-F.Wu, J. Zhang and Z.Jin, Transmission dynamics of a multi-group brucellosis model with mixed cross infection in public farm, *Applied Mathematics and Computation*, 237 (2014) 582-594.
25. Q.Hou and X.-D.Sun, Modeling sheep brucellosis transmission with a multi-stage model in changling county of jilin province, China, *Journal of Applied Mathematics and Computing*, 51(1-2) (2016) 227-244.
26. P.Lou, L.X.Zhang, J.Xu and K.Wang, Modelling seasonal brucellosis epidemics in bayingolin mongol autonomous prefecture of Xinjiang, China, 2010-2014, *BioMed Research International*, (2016) 1-17.
27. V.A.F.de Souza, J.S.F.Neto, M.Amaku, R.A.Dias, E.O.Telles, J.H.H.Grisi-Filho, M.B.Heinemann and F.Ferreira, Mathematical modeling of bovine brucellosis control using the rb51 vaccine, *Semina: Ciências Agrárias*, 37(5) (2016) 3767-3775.
28. M.-T.Li, G.-Q.Sun, W.-Y.Zhang and Z.Jin, Model-based evaluation of strategies to control brucellosis in China, *International Journal of Environmental Research and Public Health*, 14(3) (2017) 1-15.
29. C.Li, Z.-G.Guo and Z.-Y.Zhang, Transmission dynamics of a brucellosis model: Basic reproduction number and global analysis, *Chaos, Solitons & Fractals*, 104 (2017) 161-172.

30. J.Tumwiine and G.Robert, A mathematical model for treatment of bovine brucellosis in cattle population, *Journal of Mathematical Modeling*, 5(2) (2017) 137–152.
31. L.Zhou, M.Fan, Q.Hou, Z.Jin and X.Sun. Transmission dynamics and optimal control of brucellosis in Inner Mongolia of China, *Mathematical Biosciences and Engineering*, 15(2) (2018) 543-567.
32. E.G.Nepomuceno, A.M.Barbosa, M.X.Silva and M. Perc, Individual-based modelling and control of bovine brucellosis, *Royal Society Open Sscience*, 5(5) (2018) 180-200.
33. E.Abatih, L.Ron, N.Speybroeck, B.Williams and D.Berkvens, Mathematical analysis of the transmission dynamics of brucellosis among bison, *Mathematical Methods in the Applied Sciences*, 38(17) (2015) 3818-3832.
34. P.O.Lolika, C.Modnak and S.Mushayabasa, On the dynamics of brucellosis infection in bison population with vertical transmission and culling, *Mathematical Biosciences*, 305 (2018) 42-54.

Hindawi
Computational and Mathematical Methods in Medicine
Volume 2020, Article ID 8972063, 19 pages
https://doi.org/10.1155/2020/8972063

Research Article

Modeling the Impact of Seasonal Weather Variations on the Infectiology of Brucellosis

Nkuba Nyerere,[1,2] **Livingstone S. Luboobi**,[3] **Saul C. Mpeshe**,[4] **and Gabriel M. Shirima**[5]

[1]*Department of Applied Mathematics and Computational Sciences, Nelson Mandela African Institution of Science and Technology, P.O. Box 447, Arusha, Tanzania*
[2]*Department of Mathematics, Informatics and Computational Sciences, Sokoine University of Agriculture, P.O. Box 3038, Morogoro, Tanzania*
[3]*Institute of Mathematical Sciences, Strathmore University, P.O. Box 59857-00200, Nairobi, Kenya*
[4]*Department of Mathematics, University of Iringa, P.O. Box 200, Iringa, Tanzania*
[5]*Department of Global Health and Bio-Medical Sciences, Nelson Mandela African Institution of Science and Technology, P.O. Box 447, Arusha, Tanzania*

Correspondence should be addressed to Nkuba Nyerere; emmankuba@sua.ac.tz

Received 29 July 2020; Revised 3 October 2020; Accepted 7 October 2020; Published 17 October 2020

Academic Editor: Andrzej Kloczkowski

A deterministic mathematical model for brucellosis that incorporates seasonality on direct and indirect transmission parameters for domestic ruminants, wild animals, humans, and the environment was formulated and analyzed in this paper. Both analytical and numerical simulations are presented. From this study, the findings show that variations in seasonal weather have the great impact on the transmission dynamics of brucellosis in humans, livestock, and wild animals. Thus, in order for the disease to be controlled or eliminated, measures should be timely implemented upon the fluctuation in the transmission of the disease.

1. Introduction

Brucellosis is a bacterial zoonosis that causes potential loss of production in livestock and undulant fever in humans in many countries all over the world [1]. The infection is caused by the genus *Brucella* with *B. melitensis*, *B. suis*, and *B. abortus* being predominant in domestic animals and also infecting humans [2–4]. International organizations like the World Organisation for Animal Health (Office International des Epizooties (OIE)), the World Health Organization (WHO), and the Food and Agriculture Organization (FAO) identify brucellosis as one of the most prevalent zoonoses in the world alongside bovine tuberculosis and rabies [5].

In most parts of the developing world, brucellosis is endemic and leads to devastating losses in the livestock industry especially to smallholder keepers and to international market [6]. The disease results in huge financial losses by causing abortions, sterility, decreased milk production, veterinary fees, and cost of replacing animals. In many countries of sub-Saharan Africa, the control of the disease had proven to be a challenge because of different farming systems, low community awareness about the disease, poor health network systems, weak surveillance programmes, and limited vaccinations [7]. In animals, brucellosis is transmitted when a susceptible animal ingests contaminated materials such as pastures or discharges from infected animals while in humans, the bacteria are transmitted through ingestion of contaminated raw blood, meat, dairy products, and unpasteurized milk. Brucellosis is an occupational disease to abattoir workers, farmers, veterinarians, and laboratory personnel through direct contact with aborted materials and discharges, handling of suspected samples, and handling of livestock during deliveries [8]. Although traditionally *Brucella* species are host specific, recent studies revealed that cattle are also susceptible to *B. melitensis* [9–11].

Infected animals exhibit clinical signs like reduced fertility, late-term abortion, considerable drop in milk production, retained placenta, metritis, and hygromas in chronic cases in cattle [6, 12]. Symptoms in humans include headache,

weakness, continuous or intermittent fever, chills, joint pains, profuse sweats, weight loss, aches, and devastating complications that may lead to miscarriage during the first trimester in pregnant women. Endocarditis, bone abscesses, or testicular and neurological complications can also occur [1, 13]. Human brucellosis is debilitating and needs prolonged treatment using a combination of antibiotics [14]. Furthermore, the clinical signs of the disease in humans are not pathognomonic; hence, patients were clinically misdiagnosed with malaria, rheumatic fever, typhoid fever, elapsing fever, and joint diseases [15].

Globally, the burden of human brucellosis remains huge; more than 500,000 new cases per year are reported [8]. Brucellosis exists throughout the sub-Saharan African region, it is poorly understood with fluctuating records from one country to another, and its prevalence is still unclear [16]. In many parts of Tanzania, brucellosis is a highly prevalent disease. However, very limited data is available regarding its distribution, affected host species, and impact. In addition, it has been demonstrated that the cattle seroprevalence level in various production systems, zones, and regions varies from 1 to 30% while in humans, the average prevalence is from 1 to 5% [17]. A study by Carugati et al. [18] shows that brucellosis incidences are moderate in the northern part of Tanzania and that it is a common human health problem since it is endemic in the region. Human brucellosis cases have also been reported in parts of eastern, lake, and western regions of Tanzania with seroprevalences varying from 0.7 to 20.5% [19, 20].

The incidence and prevalence of most infectious diseases are directly linked to seasonal weather variations. The understanding of seasonal patterns in infectious disease occurrences dates back to the Hippocratic era [21]. The seasonal weather variations influence the dynamics of infectious diseases by affecting the host-pathogen interactions which alters the components of the reproduction number [22]. In particular, cold or wet seasons are associated with high disease incidences due to the abundance, survival, and virulence of pathogens and the fact that most people spend their time in poorly ventilated houses. On the other hand, warm or dry seasons are associated with decreased disease incidences due to increased outdoor activities and exposure of the pathogens to UV light. In addition, the survival of pathogens outside their hosts depends on other environmental factors such as humidity, salinity, temperature, and soil pH, abundance of vectors and nonhuman hosts, host immune function, and host behavior [23].

Mathematical models can give insight into how the mechanisms and strength of seasonality affect the persistence and spreading of communicable diseases. In this view, understanding the impact of seasonality and timing offers important intuitions on parasite-host system operation, how and when the parasite control measures should be applied, and the response of disease risks to anthropogenic climate change and patterns of seasonality.

Seasonal variations are exhibited in brucellosis incidences where a large number of new cases are expected in months with wet or dry seasons of the year in both developing and developed countries [19]. The disease incidence is higher during the wet season; breeding is synchronized for animals to give birth during the wet season when pastures are available. Pastoral and agropastoral settings depend on natural pastures. During this time, infected animals shed pathogens into the environment through birth fluids and tissues that contaminate pastures and the surroundings. In addition, during the wet season, it is anticipated that the cold weather favours survival of *Brucella* pathogens in the environment compared to the hot dry season hence influencing the transmission rate [24]. For instance, high transmission rates between domestic and wild animals are expected during the dry season due to sharing of pastures and water points, while the within-herd transmission is expected during the wet season due to a high birth rate and abortion storms [25]. According to the WHO [8], in countries with cold or temperate climates, there are notable seasonal variations in brucellosis incidences with most occurring cases in the summer and spring. This concurs with the peak period for parturitions and abortions in animals and consequently the highest level of exposure to other animals and people consuming their products or attending the animals. Seasonality in transmission dynamics of the disease is also attributed to seasonal livestock movements due to the availability of water and grasslands. This is the common practice in sub-Saharan Africa countries; for instance, during the dry seasons, 83.1% of the cattle owners in Northern Tanzania move their cattle away from homes for pasture and water needs [25]. This changes the disease dynamics since the concentration of animals is expected near water bodies and wildlife parks and increases the contact rates between susceptible and infected animals.

Brucella is a robust pathogen, and it can persevere outside and inside the mammalian hosts for a long time despite the unfriendly conditions; it remains in food for up to 15 months given adverse conditions such as acidity and temperature between 14°C and 11°C or for two to three days under 37°C. When *Brucella* is exposed directly to sunlight, it may survive for few hours while its survival in contaminated manure and aborted foeti is more than 2 months during the winter season [26]. Furthermore, in an ideal environment, the survival of *Brucella* spp. is reported to last up to 135 days [27]. Therefore, to estimate the impact of seasonality on brucellosis transmission in animals and humans using mathematical modeling becomes imperative to device timely interventions. Despite the fact that the WHO, FAO, and OIE efforts and interventions are available, brucellosis continues to pose great economic threats and it affects livelihoods and food security mostly in developing countries. Thus, there is need to assess the impact of the current control strategies if we are to control or eradicate the disease. So far, a few studies [28–34] analyzed the dynamics and spread of brucellosis in homogeneous/heterogeneous populations. However, none of these studies have considered the mathematical approach to analyze the impact of seasonal weather variations on the transmission of brucellosis in human, livestock, and wildlife populations. In this paper, the impacts of seasonal weather parameters on the transmission of brucellosis are studied using a mathematical model.

2. Model Formulation

A deterministic mathematical model that illustrates the transmission of brucellosis in humans and domestic and wild

animals is formulated and analyzed under this section. More importantly, in incorporating the variations on seasonal weather in both direct and indirect transmission routes of the disease, we follow the approach presented in [33, 35, 36]. The stimuli of seasonal variations on the direct transmission of brucellosis in domestic ruminants, humans, and wild animals are, respectively, modeled by the periodic continuous functions $\beta_a(t) = b_1(1 + a_1 \sin \omega t)$, $\beta_h(t) = b_2(1 + a_2 \sin \omega t)$, and $\beta_w(t) = b_3(1 + a_3 \sin \omega t)$ while the indirect transmission in the three populations is captured by $\alpha_a(t) = c_1(1 + r_1 \sin \omega t)$, $\alpha_h(t) = c_2(1 + r_2 \sin \omega t)$, and $\alpha_w(t) = c_3(1 + r_3 \sin \omega t)$, respectively.

Furthermore, we consider the pathogen shedding rate by the infective livestock and wild animals to be represented by the periodic functions of the form $\rho(t) = \rho_0(1 + \rho_1 \sin \omega t)$ and $\rho_w(t) = \rho_2(1 + \rho_3 \sin \omega t)$, respectively. The decaying rate of the pathogens in the environment is also represented by the periodic continuous function $\varepsilon(t) = \varepsilon_0(1 + \varepsilon_1 \sin \omega t)$. The constants b_1, b_2, b_3, c_1, c_2, c_3, ρ_0, ρ_2, and ε_0 are the baseline values of the parameters β_a, β_h, β_w, α_a, α_h, α_w, ρ_a, ρ_w, and ε, respectively, whereas $0 < a_1, a_2, a_3, r_1, r_2, r_3, \rho_1, \rho_3, \varepsilon_1 < 1$ are the strength of seasonal forcing in transmission (amplitudes of seasonal variations) for each of the seasonal parameters, and $\omega = \pi/6$ corresponds to a one-year period of time.

2.1. Model Assumptions. The following assumptions are considered in the formulation of the brucellosis model:

(i) Mixing of individuals in each population is homogeneous

(ii) Infected animals shed *Brucella* in the environment

(iii) Domestic and wild animals' seropositivity is lifelong

(iv) Immunized livestock cannot be infected unless their resistance to infection wanes

(v) The natural mortality rate in each of the species is constant

(vi) The birth rate for each population is greater than the natural mortality rate

The variables and parameter values per year incorporated in this model are summarized in Tables 1 and 2, respectively.

The interactions between humans, animals, and pathogens in the environment are shown in Figure 1, and the resulting model system is shown by equation (1).

$$\begin{cases} \dfrac{dV_a}{dt} &= \phi S_a - (\psi + \mu_a)V_a, \\ \dfrac{dS_a}{dt} &= \pi_a N_a + \psi V_a - (\beta_a(t)I_a + \alpha_a(t)B + \phi + \mu_a)S_a, \\ \dfrac{dI_a}{dt} &= (\beta_a(t)I_a + \alpha_a(t)B)S_a - (\mu_a + d)I_a, \\ \dfrac{dS_h}{dt} &= \pi_h N_h + \gamma R_h - (\beta_h(t)I_a + \beta_h I_h + \alpha_h(t)B + \mu_h)S_h, \\ \dfrac{dI_h}{dt} &= (\beta_h(t)I_a + \alpha_h(t)B)S_h - (\sigma + \mu_h)I_h, \\ \dfrac{dR_h}{dt} &= \sigma I_h - (\gamma + \mu_h)R_h, \\ \dfrac{dS_w}{dt} &= \pi_w N_w - (\beta_w(t)I_w + \alpha_w(t)B + \mu_w)S_w, \\ \dfrac{dI_w}{dt} &= (\beta_w I_w + \alpha_w(t)B) - \mu_w I_w, \\ \dfrac{dB}{dt} &= \rho(t)I_a + \rho_w(t)I_w - (\tau + \varepsilon(t))B. \end{cases} \tag{1}$$

2.2. Model Properties. In this section, we use the box invariance method proposed by [40] to assess the well-posedness of the model (1) (existence and feasibility of its solution). In other words, we investigate whether the solutions of system (1) that have nonnegative initial values remain nonnegative for all times $t \geq 0$. The compact form of system (1) can be expressed as

$$\frac{dX}{dt} = AX + F, \tag{2}$$

where $X = (V_a, S_a, I_a, S_h, I_h, R_h, S_w, I_w, B)$ and F is a column vector given by

$$F = (0, \pi_c N_c, 0, \pi_h N_h, 0, 0, \pi_w N_w, 0, 0)^T,$$

$$A = \begin{bmatrix} -(\psi + \mu_a) & \phi & 0 & 0 & 0 & 0 & 0 & 0 & 0 \\ \psi & -\lambda_1 & 0 & 0 & 0 & 0 & 0 & 0 & 0 \\ 0 & \lambda_1 & -(\mu_a + d(t)) & 0 & 0 & 0 & 0 & 0 & 0 \\ 0 & 0 & 0 & \lambda_2 + \mu_h & 0 & \gamma & 0 & 0 & 0 \\ 0 & 0 & 0 & \lambda_1 & -(\sigma + \mu_h) & 0 & 0 & 0 & 0 \\ 0 & 0 & 0 & 0 & \sigma & -(\gamma + \mu_h) & 0 & 0 & 0 \\ 0 & 0 & 0 & 0 & 0 & 0 & -(\lambda_3 + \mu_w) & 0 & 0 \\ 0 & 0 & 0 & 0 & 0 & 0 & \lambda_3 & -\mu_w & 0 \\ 0 & 0 & \rho & 0 & 0 & 0 & 0 & \rho_w & -\lambda \end{bmatrix}, \tag{3}$$

Table 1: Model variables.

Variable	Description
$S_h(t)$	Number of susceptible humans at time t
$I_h(t)$	Number of infected humans at time t
$R_h(t)$	Number of recovered humans at time t
$S_a(t)$	Number of susceptible animals at time t
$I_a(t)$	Number of infected animals at time t
$V_a(t)$	Number of vaccinated animals at time t
$B(t)$	Number of *Brucella* load per unit volume in the environment at time t

Table 2: Parameters of the model and their description.

Parameter	Description	Value	Source
π_a	Per-capita livestock birth rate	0.1	[37]
ϕ_a	Livestock vaccination rate	0.7	[37]
π_h	Per-capita human birth rate	0.02	[38]
σ	Human recovery rate	0.25	[37]
μ_h	Per-capita human natural death rate	0.02	[38]
ψ	Livestock vaccine efficacy waning rate	0.4	[31]
β_a	Within-livestock transmission rate	0.0011	[31]
d	Gradual culling of seropositive livestock	0.35	[31]
μ_a	Per-capita livestock natural mortality rate	0.25	[31]
π_w	Per-capita wild animal birth rate	0.08	[39]
β_w	Within-wild animal transmission rate	0.05	[39]
α_w	*Brucella* from B to wild animal transmission rate	0.00035	[3]
μ_w	Per-capita natural death rate of wild animals	0.07	[39]
α	*Brucella* from B to livestock transmission rate	0.00035	[3]
α_h	*Brucella* from B to human transmission rate	0.002	[37]
ρ	*Brucella* shedding rate of infected livestock	0.5	[37]
ρ_w	*Brucella* shedding rate of infected wild animals	15	[30]
β_h	Livestock to human transmission rate	0.0002	[37]
ε	Decaying rate of *Brucella* in the environment	8	[31]
τ	Environmental hygiene and sanitation rate	12	[3]

where

$$\begin{aligned}\lambda_a &= (\beta_a(t)I_a + \alpha(t)B + \phi + \mu_a),\\ \lambda_2 &= \beta_h(t)I_a + \beta_h(t)I_h + \alpha_h B,\\ \lambda_3 &= \beta_w(t)I_w + \alpha_w(t)B,\\ \lambda &= (\tau + \varepsilon(t)).\end{aligned} \tag{4}$$

It can be noticed that A is the Metzler matrix for all $X \in \mathbb{R}^9_+$. Therefore, based on the fact that $F \geq 0$, model (1) is positively invariant in $\mathbb{R}^9_+$. This implies that an arbitrary trajectory of the system starting in $\mathbb{R}^9_+$ forever remains in $\mathbb{R}^9_+$. In addition, F is Lipschitz continuous. Thus, a unique maximal solution exists, and so

$$\mathcal{D} = \{(V_a, S_a, I_a, S_h, I_h, R_h, S_w, I_w, B) \geq 0\} \in \mathbb{R}^9_+ \tag{5}$$

is the feasible region for the model (1). Thus, model (1) is epidemiologically and mathematically well-posed in the region $\mathcal{D}$.

2.3. Brucellosis-Free Equilibrium. The brucellosis-free equilibrium solution for system (1) is computed and found to be

$$\left(V_a^0, S_a^0, I_a^0, S_h^0, I_h^0, R_h^0, S_w^0, I_w^0, B^0\right) = \left(\frac{\phi\pi_a N_a}{\mu_a(\phi+\psi+\mu_a)}, \frac{(\psi+\mu_a)\pi_a N_a}{\mu_a(\phi+\psi+\mu_a)}, 0, \frac{\pi_h N_h}{\mu_h}, 0, 0, \frac{\pi_w N_w}{\mu_w}, 0, 0\right), \tag{6}$$

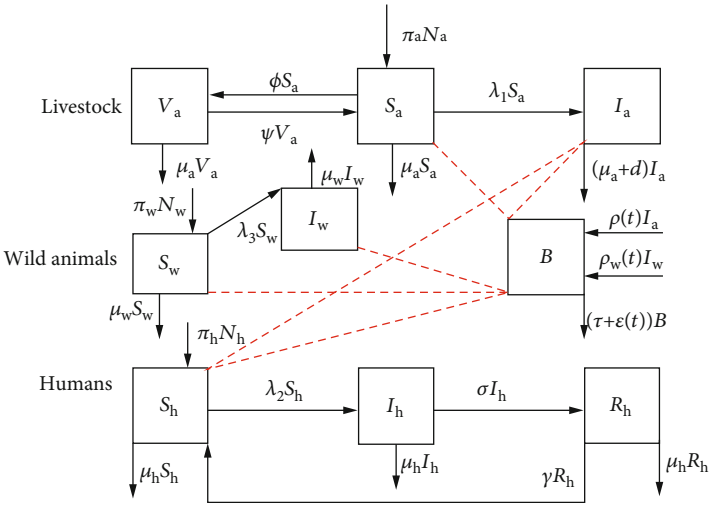

FIGURE 1: Flow diagram for brucellosis dynamics in animals, environment, and humans.

where N_a, N_h, and N_w are, respectively, the initial total populations of the livestock, humans, and wild animals.

2.4. The Reproduction Number. A heterogeneous population with individuals which can be grouped into n homogeneous compartments is considered in this section. Let $x = (x_1, \cdots, x_n)^T$, with $x_i \geq 0$, be the state of individuals in each compartment. It is assumed that the compartments can be divided into the following: infected designated as $i = 1, \cdots, m$ and uninfected designated as $i = m+1, \cdots, n$. We also define X_s to be the set of all disease-free states:

$$X_s = \{x \geq 0 : x_i = 0, \forall i = 1, \cdots, m\}. \tag{7}$$

Let $\mathcal{F}_i(t,x)$ be the input rate of newly infected individuals in the i^{th} compartment, $\mathcal{V}_i^+(t,x)$ be the input rate of individuals by other means (for example, births and immigrations), and $\mathcal{V}_i^-(t,x)$ be the rate of transfer of individuals out of compartment i (for example, deaths, recovery, and emigrations). Henceforth, the disease transmission model is governed by a nonautonomous ordinary differential system:

$$\frac{dx_i}{dt} = \mathcal{F}_i(t,x) - \mathcal{V}_i(t,x) \triangleq f_i(t,x), i = 1, \cdots, n, \tag{8}$$

where $\mathcal{V}_i(t,x) = \mathcal{V}_i^-(t,x) - \mathcal{V}_i^+(t,x)$.

Succeeding the approach by [41] and that of [42] for epidemic models, we look at conditions (A1)–(A7) for the brucellosis model. The model (1) is equivalent to periodic ordinary differential system (8), we can easily see that conditions (A1)–(A5) stated below are satisfied.

(A1) For each $1 \leq i \leq n$, the functions $\mathcal{F}_i(t,x)$, $\mathcal{V}_i^+(t,x)$, and $\mathcal{V}_i^-(t,x)$ are nonnegative and continuous on $\mathbb{R} \times \mathbb{R}_+^n$ and continuously differential with respect to x. This is based on the fact that each function denotes a directed nonnegative transfer of individuals

(A2) There is a real number $\omega > 0$ such that for each $1 \leq i \leq n$, the functions $\mathcal{F}_i(t,x)$, $\mathcal{V}_i^+(t,x)$, and $\mathcal{V}_i^-(t,x)$ are ω-periodic in t. This biologically describes a periodic environment due to seasonality

(A3) If $x_i = 0$, then $\mathcal{V}_i^-(t,x) = 0$. In particular, if $x \in X_s$, then $\mathcal{V}_i^-(t,x) = 0$ for $i = 1, \cdots, m$. That is, if a compartment is empty, then there is no transfer of individuals out of it

(A4) $\mathcal{F}_i = 0$ for $i > m$. This means that the infection incidence for uninfected compartments is zero

(A5) If $x \in X_s$, then $\mathcal{F}_i = \mathcal{V}_i^+ = 0$ for $i = 1, \cdots, m$. This implies that if the population is disease-free in the beginning, it will remain so

We know that model (8) has a disease-free periodic solution, so we define a 5×5 matrix for the nontransmitting compartments as

$$M(t) = \begin{bmatrix} -(\psi + \mu_a) & \phi & 0 & 0 & 0 \\ \psi & -(\phi + \mu_a) & 0 & 0 & 0 \\ 0 & 0 & -\mu_h & \gamma & 0 \\ 0 & 0 & 0 & -(\gamma + \mu_h) & 0 \\ 0 & 0 & 0 & 0 & -\mu_w \end{bmatrix}. \tag{9}$$

Let $\Phi_M(t)$ be the monodromy matrix of the linear ω-periodic system $dz/dt = M(t)z$. Then, $\rho(\Phi_M(\omega)) < 1$ implying that $E^0(t)$ is linearly asymptotically stable in the disease-free subspace X_s; that is,

(A6) $\rho(\Phi_M(\omega)) < 1$, where $\rho(\Phi_M(\omega))$ is the spectral radius of $\Phi_M(\omega)$, is satisfied

For convenience purposes and easy presentation of the results, we let C denote all continuous functions on the real line. If f is a periodic function in C, then we use $\bar{f}$ for the average value of the time interval $[0T]$ defined by

$$\bar{f} = \frac{1}{T}\int_0^T f(t)dt, \tag{10}$$

for continuous T periodic function $f(t)$. Inspired by the approach of [41, 43], we obtain

$$F = \begin{bmatrix} \frac{(\psi+\mu_a)\bar{\beta}_a(t)\pi_a N_a}{\mu_a(\phi+\psi+\mu_a)} & 0 & 0 & \frac{(\psi+\mu_a)\bar{\alpha}_a(t)\pi_a N_a}{\mu_a(\phi+\psi+\mu_a)} \\ \frac{\bar{\beta}_h(t)\pi_h N_h}{\mu_h} & \frac{\bar{\beta}_h(t)\pi_h N_h}{\mu_h} & 0 & \frac{\bar{\alpha}_h(t)\pi_h N_h}{\mu_h} \\ 0 & 0 & \frac{\bar{\beta}_w(t)\pi_w N_w}{\mu_w} & \frac{\bar{\alpha}_w(t)\pi_w N_w}{\mu_w} \\ \bar{\rho}_a(t) & 0 & \bar{\rho}_w(t) & 0 \end{bmatrix}, \tag{11}$$

$$V = \begin{bmatrix} \mu_a + d & 0 & 0 & 0 \\ 0 & \sigma + \mu_h & 0 & 0 \\ 0 & 0 & \mu_\omega & 0 \\ 0 & 0 & 0 & (\tau + \bar{\varepsilon}(t)) \end{bmatrix} \tag{12}$$

and observe that F is nonnegative and $(-V)$ is cooperative because its off-diagonal elements are nonnegative.

It follows that the effective reproductive number of the time-averaged autonomous system is

$$[R_e] = \frac{R_{11} + R_{33} + \sqrt{(R_{11} - R_{33})^2 + 4R_{13}R_{31}}}{2}, \tag{13}$$

where

$$\begin{aligned} R_{11} &= \frac{\left(\bar{\beta}_a(t)(\tau+\bar{\varepsilon}(t)) + \bar{\alpha}_a(t)\bar{\rho}(t)\right)(\psi+\mu_a)\pi_a N_a}{\mu_a(\phi+\psi+\mu_a)(\mu_a+d)(\tau+\bar{\varepsilon}(t))}, \\ R_{33} &= \frac{\left(\bar{\beta}_w(t)(\tau+\bar{\varepsilon}(t)) + \bar{\alpha}_w(t)\bar{\rho}_w(t)\right)(\psi+\mu_a)\pi_w N_w}{\mu_w^2(\tau+\bar{\varepsilon}(t))}, \\ R_{13} &= \frac{\bar{\alpha}_a(t)\bar{\rho}_w(t)(\psi+\mu_a)\pi_a N_a}{\mu_a\mu_w(\tau+\bar{\varepsilon}(t))(\phi+\psi+\mu_a)}, \\ R_{31} &= \frac{\bar{\alpha}_w(t)\rho(t)\pi_w N_w}{\mu_w(\mu_a+d)(\tau+\bar{\varepsilon}(t))}. \end{aligned} \tag{14}$$

Generally, the time-averaged effective reproduction number is computed as the dominant eigenvalue of FV^{-1} using the Maple package and is found to be

$$\rho\left(FV^{-1}\right) = [R_e] = \frac{1}{T}\int_0^T \frac{R_{11} + R_{33} + \sqrt{(R_{11} - R_{33})^2 + 4R_{13}R_{31}}}{2}\, ds. \tag{15}$$

If no interventions are administered, the time-averaged basic reproductive number for model system (1) is found to be

$$[R_0] = \frac{1}{T}\int_0^T \frac{R_{11}^0 + R_{33}^0 + \sqrt{\left(R_{11}^0 - R_{33}^0\right)^2 + 4R_{13}^0R_{31}^0}}{2}\, ds, \tag{16}$$

where

$$\begin{aligned} R_{11} &= \frac{\left(\bar{\beta}_a(t)\bar{\varepsilon}(t) + \bar{\alpha}_a(t)\bar{\rho}(t)\right)\pi_a N_a}{\mu_a^2\bar{\varepsilon}(t)}, \\ R_{33} &= \frac{\left(\bar{\beta}_w(t)\bar{\varepsilon}(t) + \bar{\alpha}_w(t)\bar{\rho}_w(t)\mu_a\right)\pi_w N_w}{\mu_w^2\bar{\varepsilon}(t)}, \\ R_{13} &= \frac{\bar{\alpha}_a(t)\bar{\rho}_w(t)\pi_a N_a}{\mu_a\mu_w\bar{\varepsilon}(t)}, \\ R_{31} &= \frac{\bar{\alpha}_w(t)\rho(t)\pi_w N_w}{\mu_w\mu_a\bar{\varepsilon}(t)}. \end{aligned} \tag{17}$$

$[R_0]$ may be interpreted as the average number of secondary cases arising from the introduction of a single infected person into a completely susceptible population at a random time of the year. The condition $[R_0] < 1$ is sufficient and necessary for long-term disease extinction. Furthermore, let $Y(t,s), t \geq s$, be the evolution operator of the linear ω-periodic system:

$$\frac{dy}{dt} = -V(t)y. \tag{18}$$

That is, for each $s \in \mathbb{R}$, the 4×4 matrix $Y(t,s)$ satisfies

$$\frac{d}{dt}Y(t,s) = -V(t)Y(t,s), \quad \forall t \geq s, Y(s,s) = I, \tag{19}$$

where I is a 4×4 identity matrix. Therefore, the monodromy matrix $\Phi_V(t)$ of (18) equals $Y(t,0), t \geq 0$. Thus, condition (A7) below is satisfied.

(A7) The internal evolution of individuals in the infectious compartments due to deaths and movements is dissipative and decays exponentially in many cases. This is because of loss of infective members from natural and disease-induced mortality. Thus, $\rho(\Phi_V(\omega)) < 1$

Based on the assumptions (A1)–(A7), we are now able to analyze the reproduction ratios for the epidemic model system (1). For this purpose, we always assume that the population is near the disease-free periodic state $E^0(t)$. By the standard theory of linear periodic systems [44], there exist $K > 0$ and $\alpha > 0$ such that

$$\|Y(t,s)\| \leq Ke^{-\alpha(t-s)}, \quad \forall t \geq s, s \in \mathbb{R}. \tag{20}$$

Consequently,

$$\|Y(t,t-a)F(t-a)\| \leq K\|F(t-a)\|e^{-\alpha a}, \quad \forall t \in \mathbb{R}, a \in [0,\infty). \tag{21}$$

In the computation of the basic reproduction number for the nonautonomous model system (1), we follow the method by [42]. Suppose $\Gamma(s)$ is the initial distribution of infectious individuals in this periodic environment; then, $F(s)\Gamma(s)$ is the rate of new infectious individuals produced by the infected individuals who were introduced at time s. $Y(t,s)F(s)\Gamma(s)$ represents the distribution of the newly infected at

time s and remains in the infected compartment at time $t \geq s$. It follows that the cumulative distribution of new infections at t produced by all infected $\Gamma(t)$ individuals introduced prior to $t = s$ is given by

$$\begin{aligned}\Psi(t) &= \int_{-\infty}^{t} Y(t,s)F(s)\Gamma(s)ds \\ &= \int_{0}^{\infty} Y(t,t-a)F(t,t-a)\Gamma(t-a)da, \quad \forall t \in \mathbb{R}, \Gamma \in C_\omega.\end{aligned} \tag{22}$$

Let C_ω be the ordered Banach space of all ω-periodic functions from $\mathbb{R}$ to $\mathbb{R}^n$, which is equipped with the maximum norm, $\|.\|_\infty$, and the positive cone $C_\omega^+ = \{\Gamma \in C_\omega \Gamma(t) \geq 0, t \in \mathbb{R}\}$. We define the linear operator $L : C_\omega C_\omega$ by

$$(L\Gamma)(t) = \int_{0}^{\infty} Y(t,t-a)F(t,t-a)\Gamma(t-a)da, \quad \forall t \in \mathbb{R}, \Gamma \in C_\omega, \tag{23}$$

where L is the next infection operator. Then, the basic reproduction number is given by

$$R_\omega = \rho(L), \tag{24}$$

where $\rho(L)$ is the spectral radius of L. By direct calculation, the evolution operator $Y(t,s)$ for the system (1) is found to be

$$Y(t,s) = \begin{bmatrix} e^{-(\mu_a+d)(t-s)} & 0 & 0 & 0 \\ 0 & e^{-(\sigma+\mu_h)(t-s)} & 0 & 0 \\ 0 & 0 & e^{-\mu_\omega(t-s)} & 0 \\ 0 & 0 & 0 & \bar{Y}(t,s) \end{bmatrix}, \tag{25}$$

with

$$\bar{Y}(t,s) = e^{-(\tau+\varepsilon_0)(t-s)+(6\varepsilon_0\varepsilon_1/\pi)(\cos(\pi t/6)-\cos(\pi s/6))}. \tag{26}$$

Motivated by [45], the next infection operator can be numerically evaluated as

$$\begin{aligned}(L\varphi)(t) &= \int_{0}^{\infty} Y(t,t-a)F(t,t-a)\Gamma(t-a)da \\ &= \int_{0}^{\omega} G(t,a)\Gamma(t-a)da,\end{aligned} \tag{27}$$

where

$$\begin{aligned}G(t,s) &\approx \sum_{k=0}^{M} Y(t,t-s-k\omega)F(t-s) \\ &\approx \sum_{k=0}^{M} \begin{bmatrix} m_{11} & 0 & 0 & m_{14} \\ m_{21} & m_{22} & 0 & m_{24} \\ 0 & 0 & m_{33} & m_{33} \\ m_{41} & 0 & m_{43} & 0 \end{bmatrix},\end{aligned} \tag{28}$$

for positive integers M which are large enough, and

$$\begin{cases} m_{11} = \dfrac{\beta_a(t-s)(\psi+\mu_a)\pi_a N_a}{\mu_a(\phi+\psi+\mu_a)} e^{-(\mu_a+d)(t-s)}, \\ m_{14} = \dfrac{\alpha_a(t-s)(\psi+\mu_a)\pi_a N_a}{\mu_a(\phi+\psi+\mu_a)} e^{-(\mu_a+d)(t-s)}, \\ m_{21} = \dfrac{\beta_h(t-s)\pi_h N_h}{\mu_h} e^{-(\sigma+\mu_a)(t-s)}, \\ m_{22} = \dfrac{\beta_h(t-s)\pi_h N_h}{\mu_h} e^{-(\sigma+\mu_a)(t-s)}, \\ m_{24} = \dfrac{\alpha_h(t-s)\pi_h N_h}{\mu_h} e^{-(\sigma+\mu_a)(t-s)}, \\ m_{33} = \dfrac{\beta_w(t-s)\pi_h N_h}{\mu_h} e^{-\omega(t-s)}, \\ m_{34} = \dfrac{\alpha_w(t-s)\pi_w N_w}{\mu_w} e^{-\omega(t-s)}, \\ m_{41} = \rho(t-s)e^{-(\tau+\varepsilon_0)(t-s)+(6\varepsilon_0\varepsilon_1/\pi)\left(\cos\left(\frac{\pi t}{6}\right)-\cos\left(\frac{\pi s}{6}\right)\right)}, \\ m_{43} = \rho_w(t-s)e^{-(\tau+\varepsilon_0)(t-s)+(6\varepsilon_0\varepsilon_1/\pi)\left(\cos\left(\frac{\pi t}{6}\right)-\cos\left(\frac{\pi s}{6}\right)\right)}. \end{cases} \tag{29}$$

2.5. Global Stability of the Brucellosis-Free Solution. In this section, we establish the conditions for global stability of a disease-free periodic solution.

Theorem 1. *The disease-free solution of system (1) is globally asymptotically stable if the basic reproduction number in $\mathcal{D}$ is less than one.*

Proof. Consider the matrix function:

$$F(t) - V(t) = \begin{bmatrix} \beta_a(t)S_a^0 - (\mu_a + d) & 0 & 0 & \alpha_a(t)S_a^0 \\ \dfrac{\beta_h(t)\pi_h N_h^0}{\mu_h} & \beta_h(t)S_h^0 - (\sigma+\mu_h) & 0 & \dfrac{\alpha_h(t)\pi_h N_h^0}{\mu_h} \\ 0 & 0 & \beta_w(t)S_w^0 - \mu_w & \dfrac{\alpha_w(t)\pi_w N_w}{\mu_w} \\ \rho(t) & 0 & \rho_w(t) & -(\tau+\varepsilon(t)) \end{bmatrix}. \tag{30}$$

We verify that matrix function (30) is continuous, cooperative, irreducible, and ω-periodic. Let $\Phi_{(F-V)(.)}(t)$ be the

fundamental solution matrix of the linear ordinary differential system:

$$\dot{x} = [F(t) - V(t)]x, \tag{31}$$

and $\rho(\Phi_{(F-V)(.)}(\omega))$ be the dominant eigenvalue of $\Phi_{(F-V)(.)}(\omega)$. From Theorem 2.2 in [42], we have $R_0 < 1$ if and only if $\rho(\Phi_{(F-V)(.)}(\omega)) < 1$.

Lemma 2. *Let $v = 1/\omega ln\rho(\Phi_{(F-V)(.)}(\omega))$. Then, there exists a positive ω-periodic function $v(t)$ such that $e^{vt}v(t)$ is a solution to equation (31).*

From the nondisease transmitting equations of system (1), we obtain the following:

$$\begin{aligned} V_a(t) &\leq \frac{\phi\pi_a N_a}{\mu_a(\phi+\psi+\mu_a)} \triangleq V_a^0, \\ S_a(t) &\leq \frac{(\psi+\mu_a)\pi_a N_a}{\mu_a(\phi+\psi+\mu_a)} \triangleq S_a^0, \\ S_h(t) &\leq \frac{\pi_h N_h}{\mu_h} \triangleq S_h^0, \\ S_\omega(t) &\leq \frac{\pi_w N_w}{\mu_w} \triangleq S_w^0. \end{aligned} \tag{32}$$

Again, from the infectious and recovered classes of system (1), we have the following:

$$\frac{d}{dt}\begin{bmatrix} I_a(t) \\ I_h(t) \\ I_w(t) \\ B(t) \end{bmatrix} \leq (F-V)\begin{bmatrix} I_a(t) \\ I_h(t) \\ I_w(t) \\ B(t) \end{bmatrix}. \tag{33}$$

Based on Lemma 2, there exists $v(t)$ such that $x(t) = (\bar{I}_{\mathrm{a}}(t), \bar{I}_{\mathrm{h}}(t), \bar{I}_{\mathrm{w}}(t), \bar{B}(t)) = v(t)e^{vt}$ is a solution to equation (31) with $v = 1/\omega ln\rho(\Phi_{(F-V)(.)})$.

Based on the fact that $R_0 < 1$, we have $\rho(\Phi_{(F-V)(.)}) < 1$ and $v < 0$. Thus,

$$(I_{\mathrm{a}}(t), I_{\mathrm{h}}(t), I_{\mathrm{w}}(t), B(t)) \leq \left(\bar{I}_{\mathrm{a}}(t), \bar{I}_{\mathrm{h}}(t), \bar{I}_{\mathrm{w}}(t), \bar{B}(t)\right), \tag{34}$$

when t is very large which would imply that

$$\lim_{t\to\infty} I_{\mathrm{a}}(t) = \lim_{t\to\infty} I_{\mathrm{h}}(t) = \lim_{t\to\infty} I_{\mathrm{w}}(t) = \lim_{t\to\infty} B(t) = 0. \tag{35}$$

Moreover, as $t \longrightarrow \infty$, we have

$$\frac{d}{dt}(V_{\mathrm{a}} + S_{\mathrm{a}}) \longrightarrow \pi_{\mathrm{a}}N_{\mathrm{a}} - \mu_{\mathrm{a}}(V_{\mathrm{a}} + S_{\mathrm{a}}), \tag{36}$$

which implies

$$\begin{aligned} \frac{dV_{\mathrm{a}}}{dt} &\longrightarrow \phi\left(\frac{\pi_{\mathrm{a}}N_{\mathrm{a}}}{\mu_{\mathrm{a}}} - V_{\mathrm{a}}\right) - (\psi+\mu_{\mathrm{a}})V_{\mathrm{a}} \\ &= \frac{\psi\pi_{\mathrm{a}}N_{\mathrm{a}}}{\mu_{\mathrm{a}}} - (\phi+\psi+\mu_{\mathrm{a}})V_{\mathrm{a}}, \end{aligned} \tag{37}$$

$$\text{or } \frac{\phi\pi_{\mathrm{a}}N_{\mathrm{a}}}{\mu_{\mathrm{a}}(\phi+\psi+\mu_{\mathrm{a}})} = V_{\mathrm{a}}^0, \tag{38}$$

which leads to

$$S_{\mathrm{a}}(t) \longrightarrow \frac{\pi_{\mathrm{a}}N_{\mathrm{a}}}{\mu_{\mathrm{a}}} - V_{\mathrm{a}}^0 = \frac{(\psi+\mu_{\mathrm{a}})\pi_{\mathrm{a}}N_{\mathrm{a}}}{\mu_{\mathrm{a}}(\pi+\psi+\mu_{\mathrm{a}})} = S_{\mathrm{a}}^0. \tag{39}$$

Again,

$$\begin{aligned} \frac{dS_{\mathrm{h}}}{dt} &\longrightarrow \pi_{\mathrm{h}}N_{\mathrm{h}} - \mu_{\mathrm{h}}S_{\mathrm{h}}, \\ \frac{dS_{\mathrm{w}}}{dt} &\longrightarrow \pi_{\mathrm{w}}N_{\mathrm{w}} - \mu_{\mathrm{w}}S_{\mathrm{w}}, \end{aligned} \tag{40}$$

which gives

$$\begin{aligned} S_{\mathrm{h}}^0 &= \frac{\pi_{\mathrm{h}}N_{\mathrm{h}}}{\mu_{\mathrm{h}}}, \\ S_{\mathrm{w}}^0 &= \frac{\pi_{\mathrm{w}}N_{\mathrm{w}}}{\mu_{\mathrm{w}}}. \end{aligned} \tag{41}$$

Therefore,

$$\lim_{t\to\infty} x(t) = \left(V_{\mathrm{a}}^0, S_{\mathrm{a}}^0, 0, S_{\mathrm{h}}^0, 0, 0, S_{\mathrm{w}}^0, 0, 0\right), \tag{42}$$

for each solution $x(t)$ in system (1).

2.6. Endemic Equilibrium Solution. This section is aimed at investigating the behavior of model system (1) when $R_0 > 1$. We show that if $R_0 > 1$, brucellosis infection persists in the animal and human populations and there exists a positive periodic solution. Following the approach in [46, 47], we define

$$\mathcal{X} = \mathbb{R}_+^9 ; \mathcal{X}_0 = \mathbb{R}_+^4 \times \mathrm{Int}(\mathbb{R}_+)^5 ; \partial\mathcal{X}_0 = \mathcal{X} \setminus \mathcal{X}_0. \tag{43}$$

Let $L : \mathcal{X} \longrightarrow \mathcal{X}$ be the Poncaré map associated with model system (1) such that $\mathcal{P}(x_0) = u(\omega, x_0)\forall x_0 \in \mathcal{X}$, where $u(t, x_0)$ denotes a unique solution of the system with $u(0, x_0) = x_0$.

Definition 3. The solutions of the model system (1) are said to be uniformly persistent if there exists some $\xi > 0$ such

that

$$\begin{aligned}&\lim_{t\to\infty}\operatorname{Inf}V_{\mathrm{a}}(t)>\xi,\ \lim_{t\to\infty}\operatorname{Inf}S_{\mathrm{a}}(t)>\xi,\ \lim_{t\to\infty}\operatorname{Inf}I_{\mathrm{a}}(t)>\xi,\\&\lim_{t\to\infty}\operatorname{Inf}S_{\mathrm{h}}(t)>\xi,\ \lim_{t\to\infty}\operatorname{Inf}I_{\mathrm{h}}(t)>\xi,\ \lim_{t\to\infty}\operatorname{Inf}R_{\mathrm{h}}(t)>\xi,\\&\lim_{t\to\infty}\operatorname{Inf}S_{\mathrm{w}}(t)>\xi,\ \lim_{t\to\infty}\operatorname{Inf}I_{\mathrm{w}}(t)>\xi,\ \lim_{t\to\infty}\operatorname{Inf}B(t)>\xi,\end{aligned}\tag{44}$$

whenever

$$\begin{aligned}&V_{\mathrm{a}}(0)>0, S_{\mathrm{a}}(0)>0, I_{\mathrm{a}}(0)>0, S_{\mathrm{h}}(0)>0, I_{\mathrm{h}}(0)\\&\quad>0, R_{\mathrm{h}}(0)>0, S_{\mathrm{w}}(0)>0, I_{\mathrm{w}}(0)>0, B(0)>0.\end{aligned}\tag{45}$$

Theorem 4. *The solutions of the model system (1) are uniformly persistent, and the system admits at least one positive ω-periodic solution if $R_0 > 1$.*

Proof. We define

$$\begin{aligned}H_{\partial}=\{&(V_{\mathrm{a}}(0),S_{\mathrm{a}}(0),I_{\mathrm{a}}(0),S_{\mathrm{h}}(0),I_{\mathrm{h}}(0),R_{\mathrm{h}}(0),S_{\mathrm{w}}(0),I_{\mathrm{w}}(0),B(0))\\&\in\partial\mathscr{X}_0:\mathscr{P}^m(V_{\mathrm{a}}(0),S_{\mathrm{a}}(0),I_{\mathrm{a}}(0),S_{\mathrm{h}}(0),I_{\mathrm{h}}(0),R_{\mathrm{h}}(0),S_{\mathrm{w}}(0),I_{\mathrm{w}}(0),B(0))\in\partial X_0,\quad\forall m\geq 0\},\\\tilde{H}=\{&(V_{\mathrm{a}}(0),S_{\mathrm{a}}(0),0,S_{\mathrm{h}}(0),0,0,S_{\mathrm{w}}(0),0,0):\ V_{\mathrm{a}}(0)\\&\geq 0,S_{\mathrm{a}}(0)\geq 0,S_{\mathrm{h}}(0)\geq 0,S_{\mathrm{w}}(0)\geq 0\}.\end{aligned}\tag{46}$$

It is evident that $\tilde{H}_{\partial}\subseteq H_{\partial}$.

We first show that $H_{\partial}=\tilde{H}_{\partial}$. Consider the initial values:

$$(V_{\mathrm{a}}(0),S_{\mathrm{a}}(0),I_{\mathrm{a}}(0),S_{\mathrm{h}}(0),I_{\mathrm{h}}(0),R_{\mathrm{h}}(0),S_{\mathrm{w}}(0),I_{\mathrm{w}}(0),B(0))\in\partial\mathscr{X}_0\tilde{H}.\tag{47}$$

If $I_{\mathrm{a}}(0)=0$, $I_{\mathrm{h}}(0)$, $I_{\mathrm{w}}(0)=0$, and $B(0)>0$, then based on the fact that there is a recruitment rate for susceptible individuals, we have $I_{\mathrm{a}}{}'>0$. Similarly, if $I_{\mathrm{w}}(0)=0$, $I_{\mathrm{h}}(0)$, $B(0)=0$, and $I_{\mathrm{a}}(0)>0$, then $B'(0)>0$, $I_{\mathrm{a}}(0)=0$, $I_{\mathrm{h}}(0)$, $I_{\mathrm{w}}(0)=0$, and $B(0)>0$, and if $I_{\mathrm{a}}(0)=0$, $I_{\mathrm{h}}(0)$, $B(0)=0$, and $I_{\mathrm{w}}(0)>0$, then $B'(0)>0$. It follows that $(V_{\mathrm{a}}(t),S_{\mathrm{a}}(t),I_{\mathrm{a}}(t),S_{\mathrm{h}}(t),I_{\mathrm{h}}(t),R_{\mathrm{h}}(t),S_{\mathrm{w}}(t),I_{\mathrm{w}}(t),B(t))\notin\partial\mathscr{X}_0$ for $0<t\ll 1$. The positive invariance of X_0 implies that $H_{\partial}=\tilde{H}_{\partial}$.

Again, if we consider the fixed point:

$$H_0=\left(\frac{\phi\pi_{\mathrm{a}}N_{\mathrm{a}}}{\mu_{\mathrm{a}}(\phi+\psi+\mu_{\mathrm{a}})},\frac{(\psi+\mu_{\mathrm{a}})\pi_{\mathrm{a}}N_{\mathrm{a}}}{\mu_{\mathrm{a}}(\phi+\psi+\mu_{\mathrm{a}})},0,\frac{\pi_{\mathrm{h}}N_{\mathrm{h}}}{\mu_{\mathrm{h}}},0,\frac{\pi_{\mathrm{w}}N_{\mathrm{w}}}{\mu_{\mathrm{w}}},0,0\right),\tag{48}$$

we define

$$W^S(H_0)=\{x_0:L^m(x_0)\longrightarrow H_0,x\longrightarrow\infty\}.\tag{49}$$

It can be deduced from system (1) that if $I_{\mathrm{a}}=I_{\mathrm{h}}=I_{\mathrm{w}}=B=0$ and $t\longrightarrow\infty$,

$$\begin{aligned}V_{\mathrm{a}}(t)&\longrightarrow V_{\mathrm{a}}^0=\frac{\phi\pi_{\mathrm{a}}N_{\mathrm{a}}}{\mu_{\mathrm{a}}(\phi+\psi+\mu_{\mathrm{a}})},\\S_{\mathrm{a}}(t)&\longrightarrow S_a^0\frac{(\psi+\mu_{\mathrm{a}})\pi_{\mathrm{a}}N_{\mathrm{a}}}{\mu_{\mathrm{a}}(\phi+\psi+\mu_{\mathrm{a}})},\\S_{\mathrm{h}}(t)&\longrightarrow S_{\mathrm{h}}^0=\frac{\pi_{\mathrm{h}}N_{\mathrm{h}}}{\mu_{\mathrm{h}}},\\S_{\mathrm{w}}(t)&\longrightarrow S_{\mathrm{w}}^0=\frac{\pi_{\mathrm{w}}N_{\mathrm{w}}}{\mu_{\mathrm{w}}}.\end{aligned}\tag{50}$$

We prove that $W^S(H_0)\cap\mathscr{X}_0=\varnothing$.

Let $\|.\|$ denote a norm on $\mathbb{R}_+^9$. Based on the continuity of solutions with respect to the initial conditions, for every $\varepsilon>0$, there exists $\delta>0$ but small such that for all

$$\begin{aligned}&(V_{\mathrm{a}}(0),S_{\mathrm{a}}(0),I_{\mathrm{a}}(0),S_{\mathrm{h}}(0),I_{\mathrm{h}}(0),R_{\mathrm{h}}(0),S_{\mathrm{w}}\\&\cdot(0),I_{\mathrm{w}}(0),B(0))\in\partial\mathscr{X}_0,\end{aligned}\tag{51}$$

with

$$\begin{aligned}&\|(V_{\mathrm{a}}(0),S_{\mathrm{a}}(0),I_{\mathrm{a}}(0),S_{\mathrm{h}}(0),I_{\mathrm{h}}(0),R_{\mathrm{h}}(0),S_{\mathrm{w}}\\&\cdot(0),I_{\mathrm{w}}(0),B(0))-H_0\|\leq\delta,\end{aligned}\tag{52}$$

we have

$$\begin{aligned}&\|u(t,(V_{\mathrm{a}}(0),S_{\mathrm{a}}(0),I_{\mathrm{a}}(0),S_{\mathrm{h}}(0),I_{\mathrm{h}}(0),R_{\mathrm{h}}(0),S_{\mathrm{w}}(0),I_{\mathrm{w}}(0),B(0)))\\&\quad-u(t,H_0)\|\leq\varepsilon,\quad\forall t\in[0,\omega].\end{aligned}\tag{53}$$

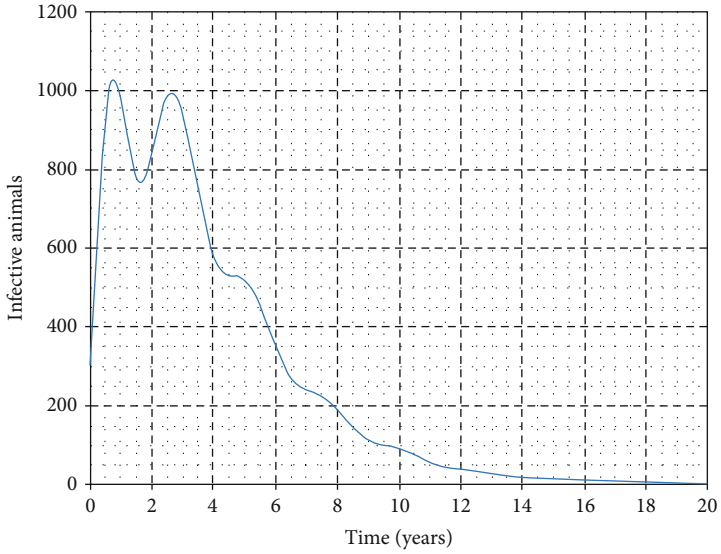

(a)

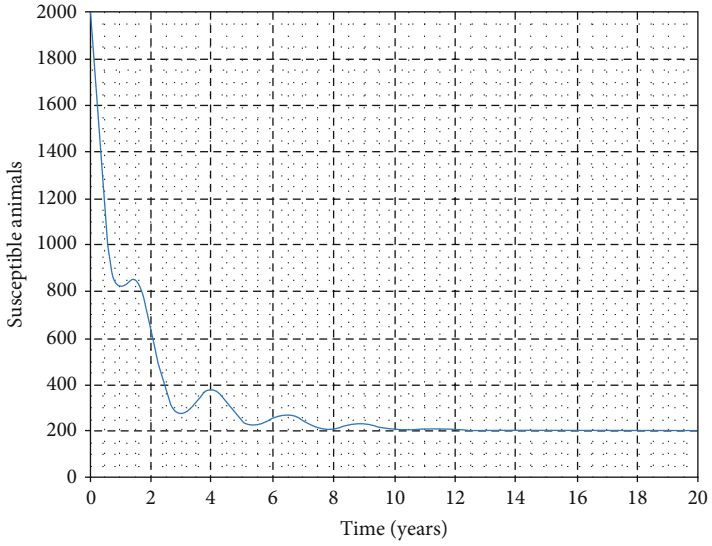

(b)

Figure 2: Seasonal variations in the number of infective and susceptible animals.

So we claim that

$$\lim_{t\to\infty} \sup \|(V_a(0), S_a(0), I_a(0), S_h(0), I_h(0), R_h(0), S_w(0), I_w(0), B(0)) - H_0\| \geq \delta, \quad \forall (V_a(0), S_a(0), I_a(0), S_h(0), I_h(0), R_h(0), S_w(0), I_w(0), B(0)) \in \mathcal{X}_0 \tag{54}$$

and prove by contradiction as follows:

Suppose

$$\lim_{t\to\infty} \sup \|(V_a(0), S_a(0), I_a(0), S_h(0), I_h(0), R_h(0), S_w \cdot (0), I_w(0), B(0)) - H_0\| < \delta, \tag{55}$$

for some

$$(V_a(0), S_a(0), I_a(0), S_h(0), I_h(0), R_h(0), S_w \cdot (0), I_w(0), B(0)) \in \mathcal{X}_0. \tag{56}$$

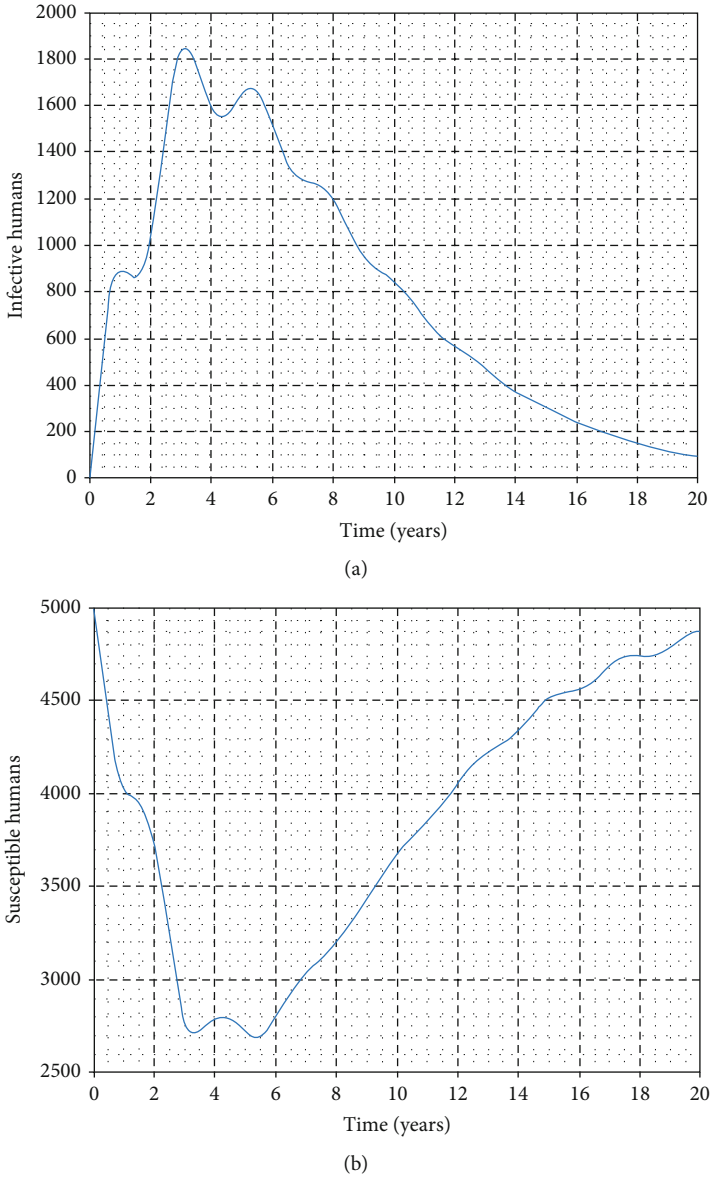

Figure 3: Seasonal variations in the number of infective and susceptible humans.

In addition, we assume without loss of generality that

$$\mathscr{P}^m \| (V_a(0), S_a(0), I_a(0), S_h(0), I_h(0), R_h(0), S_w(0), I_w(0), B(0)) - H_0 \| < \delta, \quad \forall m \geq 0. \tag{57}$$

Therefore, $\forall t \in [0, \omega]$, $m \geq 0$, we have

$$\| u(t, (V_a(0), S_a(0), I_a(0), S_h(0), I_h(0), R_h(0), S_w(0), I_w(0), B(0))) - u(t, H_0) \| \leq \varepsilon. \tag{58}$$

Furthermore, for any nonnegative t, we can write $t = t_0 + n\omega$ with $t_0 \in [0, \omega]$ and n being the greatest integer less than or equal to t/ω. Then, we get

$$\| u(t, (V_a(0), S_a(0), I_a(0), S_h(0), I_h(0), R_h(0), S_w(0), I_w(0), B(0))) - u(t, H_0) \| = \| u(t_0, (V_a(0), S_a(0), I_a(0), S_h(0), I_h(0), R_h(0), S_w(0), I_w(0), B(0))) - u(t_0, H_0) \| \leq \varepsilon, \tag{59}$$

for any $t > 0$.

Let

$$(V_a(t), S_a(t), I_a(t), S_h(t), I_h(t), R_h(t), S_w(t), I_w(t), B(t)) = (V_a(0), S_a(0), I_a(0), S_h(0), I_h(0), R_h(0), S_w(0), I_w(0), B(0)). \tag{60}$$

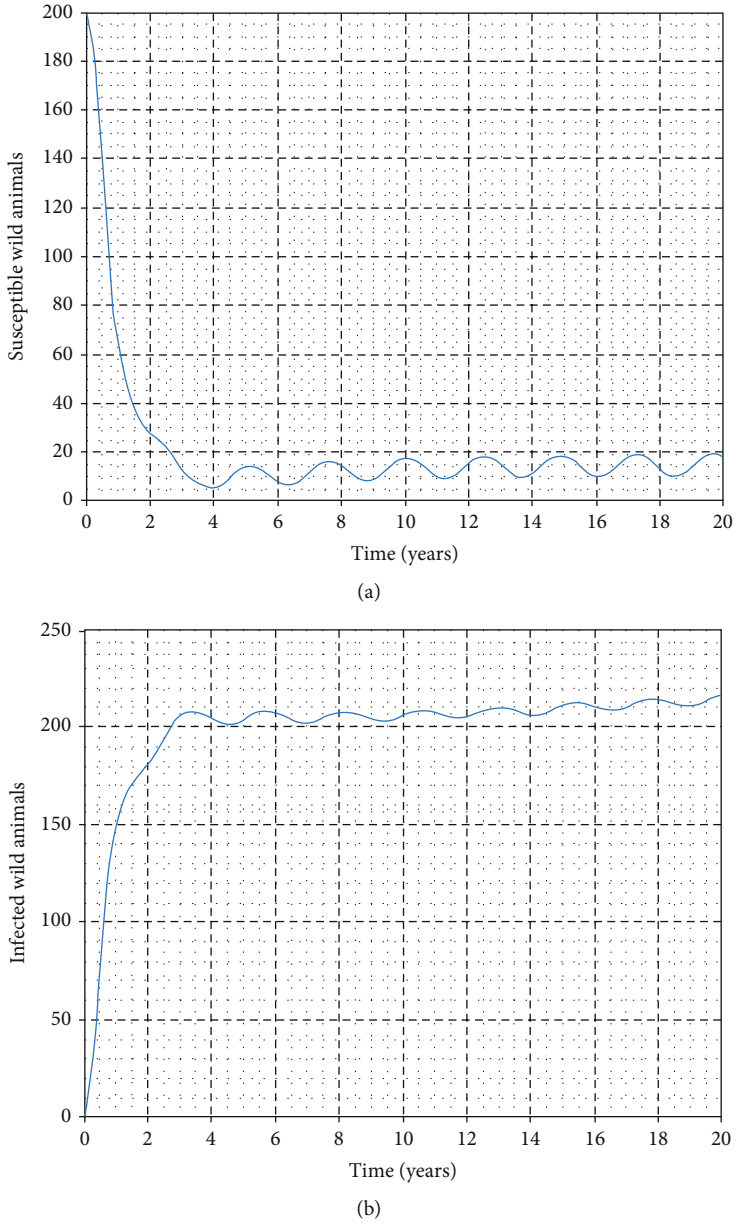

Figure 4: Seasonal variations in the number of infective and susceptible wild animals.

It follows that

$$\begin{aligned}
&\frac{\phi\pi_a N_a}{\mu_a(\phi+\psi+\mu_a)} - \varepsilon < V_a(t) < \frac{\phi\pi_a N_a}{\mu_a(\phi+\psi+\mu_a)} + \varepsilon, \frac{(\psi+\mu_a)\pi_a N_a}{\mu_a(\phi+\psi+\mu_a)} \\
&\quad - \varepsilon < S_a(t) < \frac{(\psi+\mu_a)\pi_a N_a}{\mu_a(\phi+\psi+\mu_a)} + \varepsilon, \frac{\pi_h N_h}{\mu_h} \\
&\quad - \varepsilon < S_h(t) < \frac{\pi_h N_h}{\mu_h}, \frac{\pi_w N_w}{\mu_w} - \varepsilon < S_w(t) \\
&\quad < \frac{\pi_w N_w}{\mu_w}, 0 < I_a(t) < \varepsilon, 0 < I_h(t) < \varepsilon, 0 \\
&\quad < I_w(t) < \varepsilon, 0 < B(t) < \varepsilon.
\end{aligned} \tag{61}$$

Then, we have

$$\begin{aligned}
\frac{dI_a}{dt} &= (\beta_1(t)I_a + \alpha_1(t)B)S_a - (\mu_a + d)I_a \\
&\geq (\beta_1(t)I_a + \alpha_1(t)B)\left(\frac{(\psi+\mu_a)\pi_a N_a}{\mu_a(\phi+\psi+\mu_a)} - \varepsilon\right) - (\mu_a + d)I_a \\
&= (\beta_1(t)I_a + \alpha_1(t)B)\left(\frac{(\psi+\mu_a)\pi_a N_a}{\mu_a(\phi+\psi+\mu_a)}\right) - (\mu_a + d)I_a \\
&\quad - \varepsilon(\beta_1(t)I_a + \alpha_1(t)B).
\end{aligned} \tag{62}$$

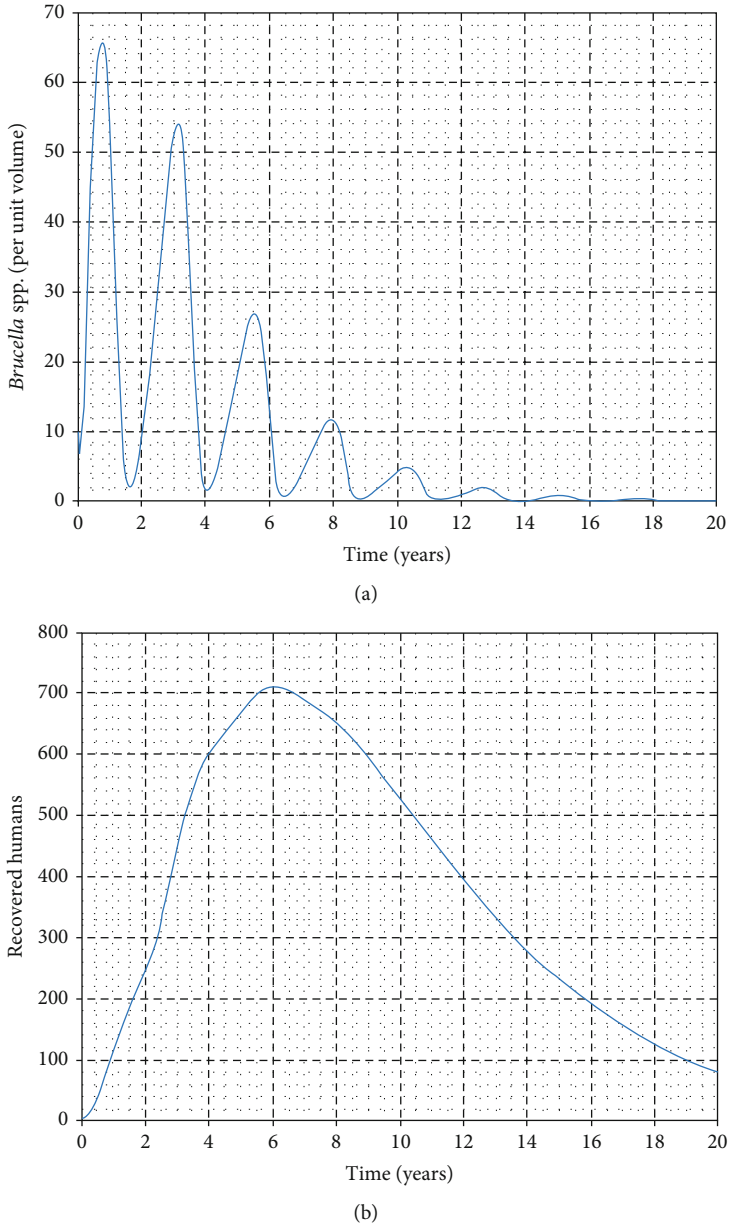

Figure 5: Variations in the effective reproduction number with respect to changes in environmental hygiene and human treatment.

Similarly,

$$\begin{aligned}\frac{dI_h}{dt} &\geq (\beta_2(t)I_h + \alpha_2(t)B)\left(\frac{\pi_h N_h}{\mu_h}\right) - (\sigma + \mu_h)I_h \\ &\quad - \varepsilon(\beta_2(t)I_h + \alpha_2(t)B), \\ \frac{dI_w}{dt} &\geq (\beta_w(t)I_w + \alpha_w(t)B)\left(\frac{\pi_w N_w}{\mu_w}\right) - \mu_w I_w \\ &\quad - \varepsilon(\beta_w(t)I_w + \alpha_w(t)B).\end{aligned} \tag{63}$$

Thus, we obtain

$$\frac{d}{dt}\begin{bmatrix} I_a(t) \\ I_h(t) \\ I_w(t) \\ B(t) \end{bmatrix} \geq (F - V - \varepsilon K)\begin{bmatrix} I_a(t) \\ I_h(t) \\ I_w(t) \\ B(t) \end{bmatrix}. \tag{64}$$

But $R_0 > 1$ if and only if $\rho(\Phi_{(F-V)(.)}) > 1$. Thus, for $\varepsilon > 0$ whenever small, we have $\rho(\Phi_{(F-V)(.)}) > 1$. Using Lemma 2 and the comparison principle, we get

$$\lim_{t\to\infty} I_a(t) = \lim_{t\to\infty} I_h(t) = \lim_{t\to\infty} I_w(t) = \lim_{t\to\infty} B(t) = \infty, \tag{65}$$

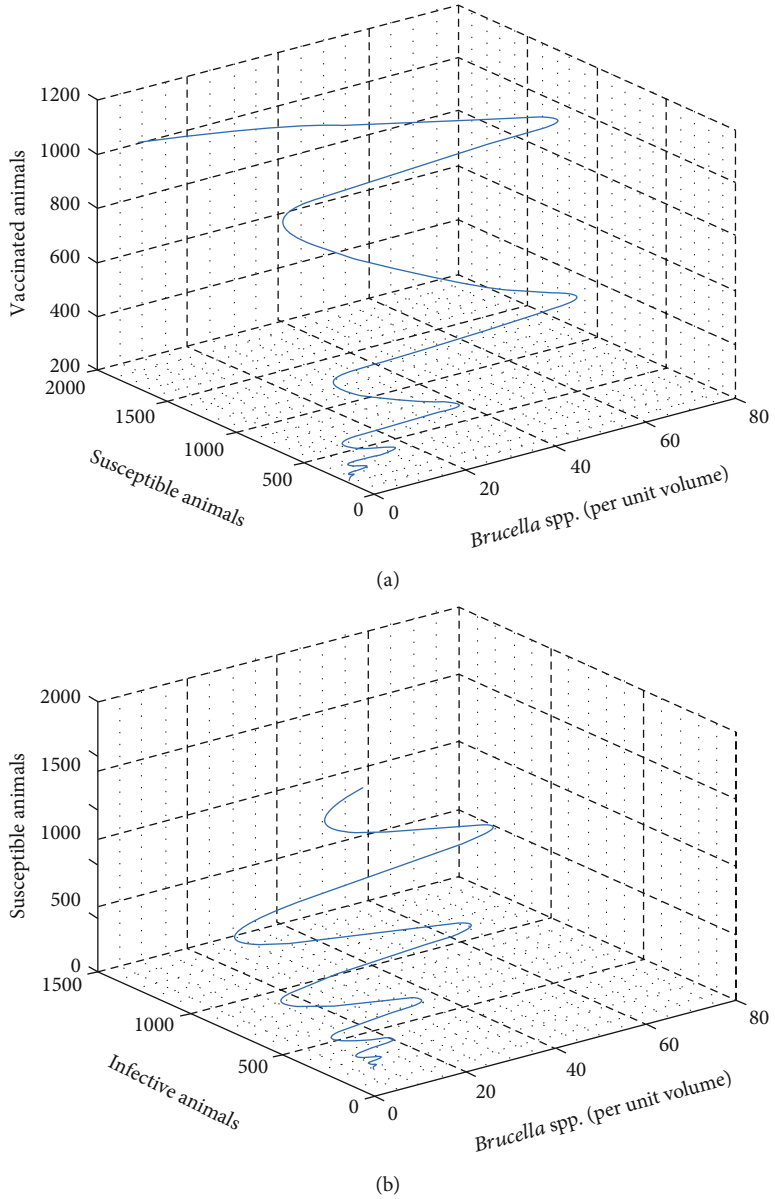

Figure 6: Relationship between *Brucella* spp. and susceptible and infected subpopulations.

which contradicts our original assumption.

Thus, H_0 is acyclic in H_{∂}, and $\mathcal{P}$ is uniformly persistent with respect to $(\mathcal{X}_0, \partial\mathcal{X}_0)$, which implies the uniform persistence of the solutions to the original system [47]. Consequently, the Poincaré map p has a fixed point:

$$\left(\bar{V}_a(0), \bar{S}_a(0), \bar{I}_a(0), \bar{S}_h(0), \bar{I}_h(0), \bar{S}_w(0), \bar{I}_w(0), \bar{B}(0)\right) \in \mathcal{X}_0, \tag{66}$$

with $V_a(0), S_a(0), S_h(0), S_w(0) \neq 0$. Thus,

$$\left(\bar{V}_a(0), \bar{S}_a(0), \bar{I}_a(0), \bar{S}_h(0), \bar{I}_h(0), \bar{S}_w(0), \bar{I}_w(0), \bar{B}(0)\right) \in \mathrm{Int}(\mathbb{R}_+)^9, \tag{67}$$

and

$$\left(\tilde{V}_a(0), \tilde{S}_a(0), \tilde{I}_a(0), \tilde{S}_h(0), \tilde{I}_h(0), \tilde{S}_w(0), \bar{I}_w(0), \tilde{B}(0)\right) = u\left(t, \left(\tilde{V}_a(0), \tilde{S}_a(0), \tilde{I}_a(0), \tilde{S}_h(0), \tilde{I}_h(0), \tilde{S}_w(0), \bar{I}_w(0), \tilde{B}(0)\right)\right) \tag{68}$$

is a positive ω-periodic solution of the system.

3. Numerical Simulations

In this part, we perform numerical simulations for model system (1) for the purpose of verifying some of the analytical findings. The baseline parameter values used in our computations are mainly from literature similar to this work, and

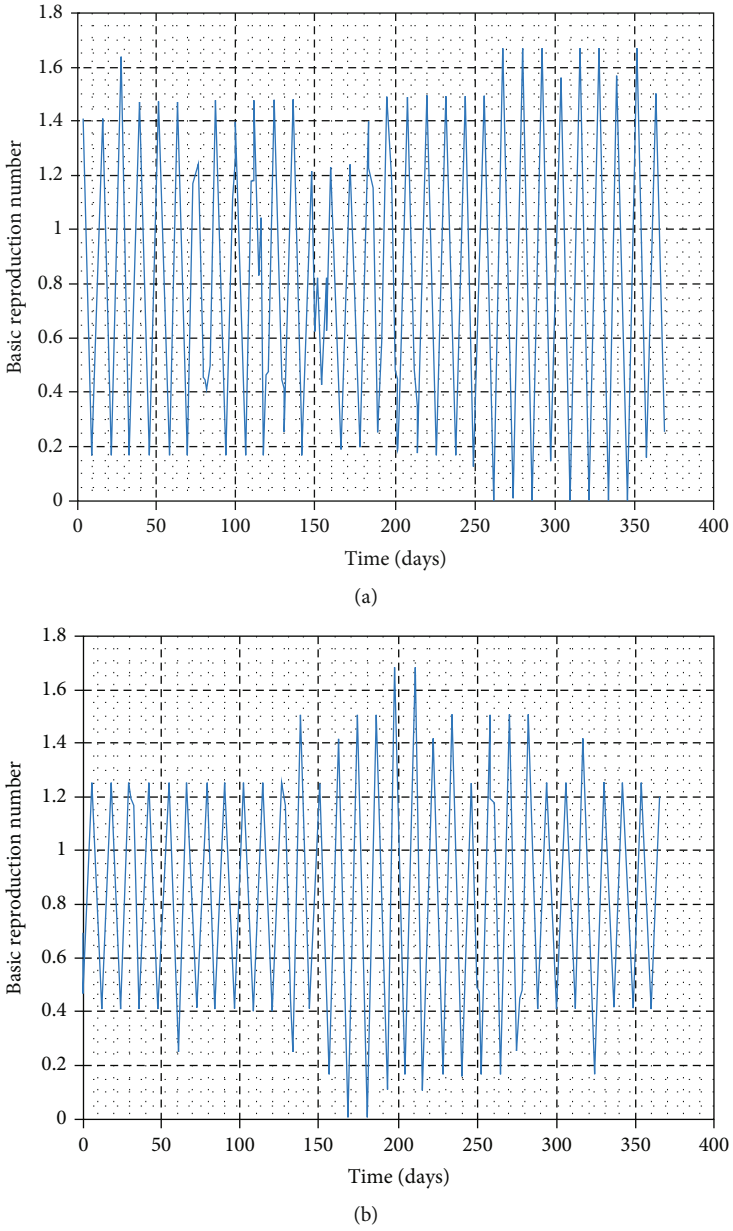

Figure 7: Variations in the effective reproduction number with seasonal changes in temperature for the year 1979 in Mpwapwa District, Dodoma.

unavailable parameter values are assumed for illustration. The parameter descriptions and values per year are shown in Table 2. Figures 2–5 illustrate the variations in human, wild animal, and livestock subpopulations while Figure 6 shows the existence of a globally stable disease-free periodic solution. Additionally, Figures 7–9 highlight the impact of temperature variations on the transmission dynamics of brucellosis. Figure 2 shows that the number of infective livestock decreases seasonally with an increase in time while Figure 2(a) illustrates a decrease in the susceptible animal subpopulation as time increases. The decrease in the number of infective livestock is due to proper implementation of vaccination and gradual culling of seropositive animals as control strategies. On the other hand, the sharp decrease in the susceptible animal subpopulation can be associated with the large number of infective animals and consequently high transmission rate in less than a one-year period of time while the gradual decrease in the next two years is due to vaccination programmes and decreased infection rate. Figure 3 shows a strong relationship between the number of infective and susceptible humans. For instance, at $t = 0$, $S_a = 5000$ and $I_a = 0$ while at $t = 3$, $S_a = 2555$ and $I_a = 1850$. The seasonal increase in the individuals in Figure 3(a) is associated with the low human treatment rate and poor control of the disease from infective livestock as well as contaminated environment. Besides, the decrease in the number of susceptible

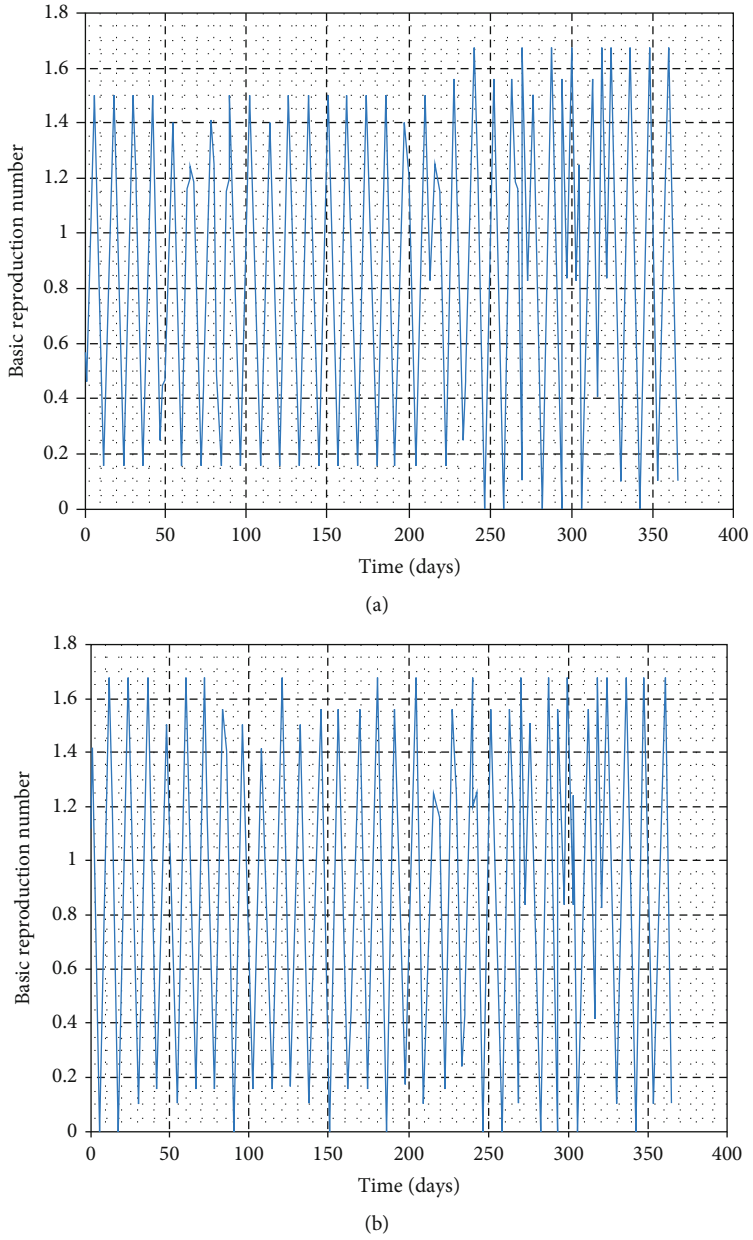

Figure 8: Variations in the effective reproduction number with seasonal changes in temperature for the year 2014 in Ngorongoro District, Arusha.

humans in Figure 3(b) is due to the high transmission rate from both infective animals and their products while the increase may be associated with proper implementation of the control strategies such as environmental hygiene, animal vaccination, and gradual culling of seropositive animals [24]. Figure 4 shows that the number of susceptible wild animals decreases with the increase in infective wild animals. In particular, the introduction of 200 susceptible wild animals in the contaminated environment produces more than 200 infective wild animals. This is based on the fact that both infective and susceptible animals have free movements and interactions within their parks. Besides, lack of wild animal brucellosis control measures and the fact that the disease does not kill keep the number of infected wild animals seasonally increasing. This implies that, in order to control the transmission dynamics of brucellosis in livestock and humans, interactions between domestic and wild animals should be restricted. Figure 5(a) shows that the number of *Brucella* bacteria in the environment decreases seasonally as the time increases while Figure 5(b) illustrates the variations in the number of recovered humans with respect to increase in time. These variations are associated with the regular implementation of the control strategies like environment hygiene and sanitation, human treatment, and gradual culling of infective animals. Furthermore, the recovered human population in the first six years increases due to effective treatment of the infective animals, and its decrease is associated with the decrease in the number of infected humans as

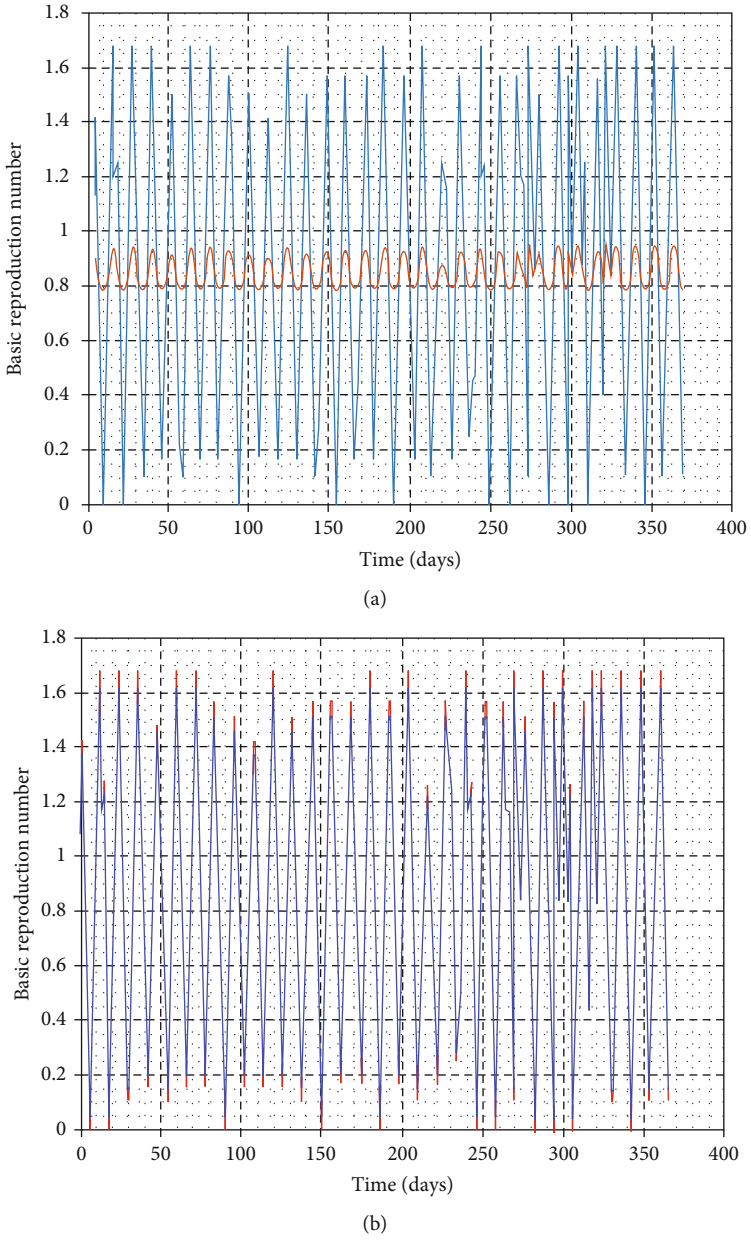

Figure 9: Variations in the effective reproduction number with seasonal changes in temperature for the year 2014 in Ngorongoro District, Arusha.

well as proper control of the disease from livestock and their products. Figure 6 shows the existence of a stable periodic solution between the animal subpopulations and the number of *Brucella* bacteria in the environment. Figure 7(a) shows the seasonal variations in the effective reproductive number with respect to maximum daily temperature while Figure 7(b) illustrates the changes in the effective reproduction number with respect to seasonal variations in minimum daily temperature. Figure 8(a) illustrates the variations in the effective reproduction number versus maximum daily temperature while Figure 8(b) depicts the changes in the effective reproduction number with respect to seasonal variations in minimum daily temperature. Figure 9 presents the comparison between direct and indirect routes of brucellosis transmission. In particular, high strength of seasonal forcing shown in Figure 9(a) is due to seasonality in both direct and indirect routes of disease transmission while the curve with low amplitude shows the impact of lack of seasonality on the direct disease transmission. Moreover, Figure 9(b) indicates that seasonality in direct transmission has a significant contribution to the brucellosis transmission than that in indirect transmission; the graph in red is for seasonality in both direct and indirect transmission while the one in blue is for seasonality in both.

Generally, findings from this study advocate that, when the weather condition favours the increase in the transmission rates of brucellosis in livestock, humans, wild animals, and the environment, the incidence of the disease

increases significantly and vice versa. This implies that in order to effectively prevent, control, eliminate, or eradicate brucellosis from the community, measures should be timely taken in accordance with the fluctuation in the disease transmission rates as a result of daily temperature variations. Thus, to avoid underestimation or overestimation of the resources when dealing with brucellosis, the aspect of seasonal weather variation should be taken into account when planning for prevention, control, elimination, or eradication of brucellosis infections.

Data Availability

The data supporting the findings in the article were derived as follows: We used the set of parameter values mainly from articles similar to this work, while unavailable data, especially values of parameters, were estimated for the purpose of verifying results of the mathematical analyses of the models developed in the manuscript.

Conflicts of Interest

The authors declare no conflict of interest regarding the publication of this paper.

References

[1] A. S. Dean, L. Crump, H. Greter, E. Schelling, and J. Zinsstag, "Global burden of human brucellosis: a systematic review of disease frequency," *PLoS Neglected Tropical Diseases*, vol. 6, no. 10, article e1865, 2012.

[2] F. P. Poester, L. E. Samartino, and R. L. Santos, "Pathogenesis and pathobiology of brucellosis in livestock," *Revue Scientifique et Technique*, vol. 32, no. 1, pp. 105–115, 2013.

[3] M. Li, G. Sun, Y. Wu, J. Zhang, and Z. Jin, "Transmission dynamics of a multi-group brucellosis model with mixed cross infection in public farm," *Applied Mathematics and Computation*, vol. 237, pp. 582–594, 2014.

[4] CFSPH, "Brucellosis Brucella abortus," 2008, http://cfsph.iastate.edu/Factsheets/pdfs/brucellosis_abortus.pdf.

[5] E. Schelling, C. Diguimbaye, S. Daoud et al., "Brucellosis and Q-fever seroprevalences of nomadic pastoralists and their livestock in Chad," *Preventive Veterinary Medicine*, vol. 61, no. 4, pp. 279–293, 2003.

[6] K. A. Franc, R. C. Krecek, B. N. Häsler, and A. M. Arenas-Gamboa, "Brucellosis remains a neglected disease in the developing world: a call for interdisciplinary action," *BMC Public Health*, vol. 18, no. 1, p. 125, 2018.

[7] G. Pappas, P. Papadimitriou, N. Akritidis, L. Christou, and E. V. Tsianos, "The new global map of human brucellosis," *The Lancet Infectious Diseases*, vol. 6, no. 2, pp. 91–99, 2006.

[8] WHO, "Brucellosis in humans and animals," 2018, http://www.who.int/csr/resources/publications/Brucellosis.pdf.

[9] I. I. Musallam, M. Abo-Shehada, M. Omar, and J. Guitian, "Cross-sectional study of brucellosis in Jordan: prevalence, risk factors and spatial distribution in small ruminants and cattle," *Preventive Veterinary Medicine*, vol. 118, no. 4, pp. 387–396, 2015.

[10] M. Ducrotoy, W. J. Bertu, G. Matope et al., "Brucellosis in sub-Saharan Africa: current challenges for management, diagnosis and control," *Acta Tropica*, vol. 165, pp. 179–193, 2017.

[11] Medscape, "Brucellosis pathogenicity," 2018, https://emedicine.medscape.com/article/213430-overview.

[12] M. Yilma, G. Mamo, and B. Mammo, "Review on brucellosis sero-prevalence and ecology in livestock and human population of Ethiopia," *Achievements in the Life Sciences*, vol. 10, no. 1, pp. 80–86, 2016.

[13] CDC, "Brucellosis signs and symptoms," 2018, https://www.cdc.gov/brucellosis/symptoms/index.html.

[14] K. John, J. Fitzpatrick, N. French et al., "Quantifying risk factors for human brucellosis in rural northern Tanzania," *PLoS One*, vol. 5, no. 4, pp. 1–6, 2010.

[15] E. M. Galinska and J. Zagórski, "Brucellosis in humans-etiology, diagnostics, clinical forms," *Annals of agricultural and environmental medicine*, vol. 20, no. 2, pp. 233–238, 2013.

[16] G. Tumwine, E. Matovu, J. D. Kabasa, D. O. Owiny, and S. Majalija, "Human brucellosis: sero-prevalence and associated risk factors in agro-pastoral communities of Kiboga District, Central Uganda," *BMC Public Health*, vol. 15, no. 1, 2015.

[17] E. S. Swai and L. Schoonman, "Human brucellosis: seroprevalence and risk factors related to high risk occupational groups in Tanga Municipality, Tanzania," *Zoonoses and Public Health*, vol. 56, no. 4, pp. 183–187, 2009.

[18] M. Carugati, H. M. Biggs, M. J. Maze et al., "Incidence of human brucellosis in the Kilimanjaro Region of Tanzania in the periods 2007–2008 and 2012–2014," *Transactions of The Royal Society of Tropical Medicine and Hygiene*, vol. 112, no. 3, pp. 136–143, 2018.

[19] G. M. Shirima, *The epidemiology of brucellosis in animals and humans in Arusha and Manyara regions in Tanzania, [Ph.D. thesis]*, University of Glasgow, 2005.

[20] E. S. Swai and L. Schoonman, "A survey of zoonotic diseases in trade cattle slaughtered at Tanga City abattoir: a cause of public health concern," *Asian Pacific Journal of Tropical Biomedicine*, vol. 2, no. 1, pp. 55–60, 2012.

[21] A. Fares, "Seasonality of tuberculosis," *Journal of Global Infectious Diseases*, vol. 3, no. 1, pp. 46–55, 2011.

[22] S. Altizer, A. Dobson, P. Hosseini, P. Hudson, M. Pascual, and P. Rohani, "Seasonality and the dynamics of infectious diseases," *Ecology Letters*, vol. 9, no. 4, pp. 467–484, 2006.

[23] N. C. Grassly and C. Fraser, "Seasonal infectious disease epidemiology," *Proceedings of the Royal Society B: Biological Sciences*, vol. 273, no. 1600, pp. 2541–2550, 2006.

[24] G. M. Shirima, S. N. Masola, O. N. Malangu, and B. A. Schumaker, "Outbreak investigation and control case report of brucellosis: experience from livestock research centre, Mpwapwa, Tanzania," *Onderstepoort Journal of Veterinary Research*, vol. 81, no. 1, 2014.

[25] E. G. Kimaro, J. A. L. M. L. Toribio, P. Gwakisa, and S. M. Mor, "Occurrence of trypanosome infections in cattle in relation to season, livestock movement and management practices of Maasai pastoralists in Northern Tanzania," *Veterinary Parasitology: Regional Studies and Reports*, vol. 12, pp. 91–98, 2018.

[26] N. E. Lucero, M. Tenenbaum, N. R. Jacob, G. I. Escobar, P. Groussaud, and A. M. Whatmore, "Application of variable number of tandem repeats typing to describe familial outbreaks of brucellosis in Argentina," *Journal of Medical Microbiology*, vol. 59, no. 6, pp. 648–652, 2010.

[27] K. Aune, J. C. Rhyan, R. Russell, T. J. Roffe, and B. Corso, "Environmental persistence of Brucella abortusin the Greater Yellowstone Area," *The Journal of Wildlife Management*, vol. 76, no. 2, pp. 253–261, 2012.

[28] J. Zinsstag, F. Roth, D. Orkhon et al., "A model of animal–human brucellosis transmission in Mongolia," *Preventive Veterinary Medicine*, vol. 69, no. 1–2, pp. 77–95, 2005.

[29] A. G. Alhamada, I. Habib, A. Barnes, and I. Robertson, "Risk factors associated with brucella seropositivity in sheep and goats in Duhok Province, Iraq," *Veterinary sciences*, vol. 4, no. 65, pp. 1–9, 2017.

[30] Q. Hou, X. Sun, J. Zhang, Y. Liu, Y. Wang, and Z. Jin, "Modeling the transmission dynamics of sheep brucellosis in Inner Mongolia Autonomous Region, China," *Mathematical Biosciences*, vol. 242, no. 1, pp. 51–58, 2013.

[31] C. Li, Z. Guo, and Z. Zhang, "Transmission dynamics of a brucellosis model: basic reproduction number and global analysis," *Chaos, Solitons & Fractals*, vol. 104, pp. 161–172, 2017.

[32] B. Nannyonga, G. G. Mwanga, and L. S. Luboobi, "An optimal control problem for ovine brucellosis with culling," *Journal of Biological Dynamics*, vol. 9, no. 1, pp. 198–214, 2015.

[33] P. O. Lolika, C. Modnak, and S. Mushayabasa, "On the dynamics of brucellosis infection in bison population with vertical transmission and culling," *Mathematical Biosciences*, vol. 305, pp. 42–54, 2018.

[34] F. Roth, J. Zinsstag, D. Orkhon et al., "Human health benefits from livestock vaccination for brucellosis: case study," *Bulletin of the World Health Organization*, vol. 81, no. 12, pp. 867–876, 2003.

[35] R. C. Ngeleja, L. S. Luboobi, and Y. Nkansah-Gyekye, "The effect of seasonal weather variation on the dynamics of the plague disease," *International Journal of Mathematics and Mathematical Sciences*, vol. 2017, 25 pages, 2017.

[36] R. C. Ngeleja, L. S. Luboobi, and Y. Nkansah-Gyekye, "Plague disease model with weather seasonality," *Mathematical Biosciences*, vol. 302, pp. 80–99, 2018.

[37] N. Nyerere, L. S. Luboobi, S. C. Mpeshe, and G. M. Shirima, "Mathematical model for the infectiology of brucellosis with some control strategies," *New Trends in Mathematical Sciences*, vol. 4, no. 7, pp. 387–405, 2019.

[38] N. Nyerere, A. X. Matofali, S. C. Mpeshe, and S. Edward, "Modeling the impact of vertical transmission in vectors on the dynamics of dengue fever," *World Journal of Modelling and Simulation*, vol. 13, no. 3, pp. 219–227, 2017.

[39] E. Abatih, L. Ron, N. Speybroeck, B. Williams, and D. Berkvens, "Mathematical analysis of the transmission dynamics of brucellosis among bison," *Mathematical Methods in the Applied Sciences*, vol. 38, no. 17, pp. 3818–3832, 2015.

[40] A. Abate, A. Tiwari, and S. Sastry, "Box invariance in biologically-inspired dynamical systems," *Automatica*, vol. 45, no. 7, pp. 1601–1610, 2009.

[41] P. van den Driessche and J. Watmough, "Reproduction numbers and sub-threshold endemic equilibria for compartmental models of disease transmission," *Mathematical Biosciences*, vol. 180, no. 1-2, pp. 29–48, 2002.

[42] W. Wang and X.-Q. Zhao, "Threshold dynamics for compartmental epidemic models in periodic environments," *Journal of Dynamics and Differential Equations*, vol. 20, no. 3, pp. 699–717, 2008.

[43] O. Diekmann, J. A. P. Heesterbeek, and M. G. Roberts, "The construction of next-generation matrices for compartmental epidemic models," *Journal of the Royal Society Interface*, vol. 7, no. 47, pp. 873–885, 2010.

[44] J. K. Hale, *Ordinary differential equations*, Brown Univ. Providence RI Div. of Applied Mathematics, 1969.

[45] D. Posny and J. Wang, "Computing the basic reproductive numbers for epidemiological models in nonhomogeneous environments," *Applied Mathematics and Computation*, vol. 242, pp. 473–490, 2014.

[46] X. Q. Zhao, "Uniform persistence in processes with application to nonautonomous competitive models," *Journal of Mathematical Analysis and Applications*, vol. 258, no. 1, pp. 87–101, 2001.

[47] X. Q. Zhao, J. Borwein, and P. Borwein, *Dynamical Systems in Population Biology*, Springer, New York, 2003.

POSTER PRESENTATION

Optimal Control Strategies for the Infectiology of Brucellosis

Nkuba Nyerere[1,2] , Livingstone S. Luboobi[3], Saul C. Mpeshe[4], and Gabriel M. Shirima[5]

[1]Department of Applied Mathematics and Computational Sciences, Nelson Mandela African Institution of Science and Technology, P. O. Box 447, Arusha, Tanzania

[2]Department of Mathematics, Informatics and Computational Sciences, Sokoine University of Agriculture, P. O. Box 3038,Morogoro, Tanzania

[3]Institute of Mathematical Sciences, Strathmore University, P. O. Box 59857-00200, Nairobi, Kenya

[4]Department of Mathematics, University of Iringa, P. O. Box 200, Iringa, Tanzania [5]Department of Global Health and Bio-Medical Sciences,

Nelson Mandela African Institution of Science and Technology, P. O. Box 447, Arusha, Tanzania

**Tel : +255-767-994-591; E-mail: nyererer@nm-aist.ac.tz*

Abstract

The impacts of controls of livestock vaccination, gradual culling of seropositive cattle and small ruminants, environmental hygiene, and personal protection in humans on the transmission dynamics of Brucellosis are invested with the aid of a mathematical model. The aim is to minimize the spread of Brucellosis in the community and the costs of control strategies. Findings showed that the combination of livestock vaccination, gradual culling through slaughter, environmental sanitation, and personal protection in humans has high impact and lower cost of prevention.

Introduction

Brucellosis is a zoonotic infection caused by Gram-negative bacteria of genus *Brucella*. The disease is of public health, veterinary, and economic significance in most of the developed and developing countries. Direct contact between susceptible and infective animals or their contaminated products are the two major routes of the disease transmission. The global incidence of human brucellosis is over 500,000 new cases per year. Therefore it is becoming essential to find a viable alternatives to minimize the prevalence of the disease. In this paper, the dynamics and cost-effectiveness of the control strategies for brucellosis using mathematical models are rigorously studied.

Model Formulation

A mathematical model for the transmission dynamics of Brucellosis incorporating the time-dependent controls to some parameters is formulated and analysed. The human population is divided into Susceptible (S), Infectious (I_h), and Recovered (R) while the cattle and small ruminants populations are divided in susceptible and infectious subclasses. A time-dependent variable $u_1(t)$ is introduced as a control that aims at reducing the number of susceptible animals in the herds and consequently to reduce the Brucellosis transmission. Based on the fact that there is neither disease-induced deaths nor treatment for infected ruminants, we introduced $u_2(t)$, a control variable that measures the efficiency of gradual culling of seropositive animals.. To reduce or eliminate the number of *Brucella* in the environment, the control variable $u_3(t)$ is introduced as the measure of effectiveness of environmental hygiene. A time-dependent control variable $u_4(t)$ was introduced in the model as the measure of the effectiveness of personal protection in humans. The details for the model formulation and analysis are in Nyerere *et al.* (2020).

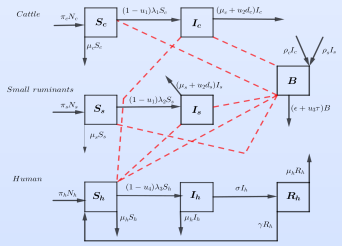

Figure 1:A Flowchart for the dynamics of Brucellosis

Results

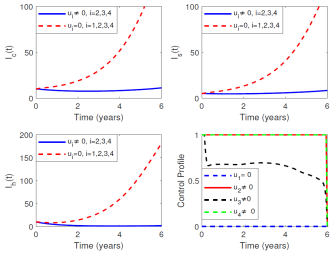

Figure 2: Dynamics of brucellosis with optimal gradual culling of seropostive ruminants, environmental sanitation, and personal protection controls.

Figure 2 shows that optimal implementation of gradual culling of seropostive ruminants, environmental hygiene, and personal protection reduces the number of infected human to zero in a period of less than two years, whereas the infected ruminants does not go to zero in a period of more than six years. This implies that implementation the three interventions under consideration does not make the ruminants population attain their disease free equilibrium points. &us, this strategy is not mathematically recommended.

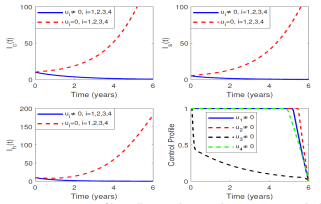

Figure 3: Dynamics of brucellosis with optimal vaccination, gradual culling of seropositive ruminants, environmental sanitation, and personal protection controls.

Figure 3 shows that due to the combination of the four control strategies, the number of infected small ruminants and humans decreases to zero in less than two years while that of infective cattle reduces to zero in less than four years. In case of no controls, the number of infective populations grows exponentially.

Conclusion

This paper aimed at formulating and analysing a mathematical model for the impacts of different control options to the transmission dynamics of Brucellosis. We focused on livestock vaccination; gradual culling through slaughter of seropositive cattle and small ruminants; environmental hygiene and sanitation; and personal protection in humans. Pontryagin's Maximum Principle approach and incremental cost-effectiveness ratio were, respectively, used to analyze the optimal control problem and the cost effectiveness of the control strategies. Findings in both optimal control and cost-effectiveness analysis revealed that combination of vaccination, gradual culling of seropositive cattle and small ruminants, environmental hygiene, and personal protection in humans is unequivocally best control strategy as it has high impact with lower cost of controlling the disease.

Reference

Nyerere,N., Luboobi , L.S., Mpeshe S, C., & Shirima, G. M. (2020), Optimal Control Strategies for the Infectiology of Brucellosis. *International Journal of Mathematics and Mathematical Sciences, 2020, 1-17*